



THE UNIVERSITY *of* EDINBURGH

This thesis has been submitted in fulfilment of the requirements for a postgraduate degree (e.g. PhD, MPhil, DClinPsychol) at the University of Edinburgh. Please note the following terms and conditions of use:

This work is protected by copyright and other intellectual property rights, which are retained by the thesis author, unless otherwise stated.

A copy can be downloaded for personal non-commercial research or study, without prior permission or charge.

This thesis cannot be reproduced or quoted extensively from without first obtaining permission in writing from the author.

The content must not be changed in any way or sold commercially in any format or medium without the formal permission of the author.

When referring to this work, full bibliographic details including the author, title, awarding institution and date of the thesis must be given.

Statistical modelling and analysis
of the infection dynamics
of PRRSV *in vivo* infections

Zeenath Ul Islam



Doctor of Philosophy
University of Edinburgh

2016



Contents

Declaration.....	I
Acknowledgements	II
Sonnet 1.....	III
Lay Summary	IV
Abstract.....	1
Chapter 1 Introduction	3
1.0 Porcine Reproductive and Respiratory Syndrome prevalence and related economic losses	3
1.1 Mode of infection and the host response to infection	4
1.1.1 Viraemia data	5
1.1.2 Cytokine data	5
1.1.3 Neutralising antibody data	6
1.1.4 Genotyping.....	6
1.2 Genetic variability in the host for PRRS.....	8
1.2.1 Evidence for genetic variation in host resistance to PRRSV	8
1.2.2 The PRRS Host Genetic consortium (PHGC) PRRSV trials.....	6
1.2.3 Previous findings for the PHGC nursery pigs PRRSV challenge data relevant for this thesis: The WUR “resistance” genotype.....	9
1.3 The “persistent” nature of a PRRSV infection	10
1.4 PRRSV viraemia profiles and inter host variation.....	11
1.5 Genetic diversity of the PRRS virus	12
1.5.1 The PRRS virus structure.....	12
1.5.2 PRRS virus strains	13
1.5.3 North American PRRSV isolates.....	14
1.6 Immune responses to PRRSV infection.....	14
a) Innate Immune Responses	14
b) Adaptive Immune Responses	16
c) Antibodies	17
1.7 Mathematical modelling of within-host virus infection dynamics	20
1.7.1 Statistical modelling and inference approaches adopted in this thesis.....	20
1.7.2 Linear and non-linear mixed models	21

1.7.3 Repeated measures models	23
1.7.4 Curve fitting	23
a) Spline functions	23
b) Mathematical functions with biological interpretation.....	24
1.7.5 Bayesian inference	25
1.8 Thesis outline	26
Chapter 2 Examining PRRS viraemia profiles of pigs from an experimental challenge: a repeated measures and mixed modelling approach.....	40
2.0 Introduction.....	40
2.1 Materials and Methods.....	42
2.1.1 The Experimental data	42
2.1.2 Classifying bimodal profiles and subdividing the viraemia dataset .	43
2.1.3 Statistical analysis	44
2.2 Results.....	47
2.2.1 Qualitative assessment and univariate statistics of the longitudinal PRRS viraemia data	47
2.2.2 Repeated measures model of PRRS viraemia.....	50
2.2.3 Fitting the linearized Wood's function for modelling viraemia profiles	60
2.3 Discussion	72
Chapter 3 Quantitative analysis of Porcine Reproductive and Respiratory Syndrome (PRRS) viraemia profiles from experimental infection: a Bayesian statistical modelling approach.....	79
3.0 Introduction.....	79
3.1 Conclusion	94
Chapter 4 Exploring the relationship of PRRS viraemia profiles with longitudinal cytokine expression	95
4.0 Introduction.....	95
4.1 Materials and Methods.....	98
4.1.1 Experimental data	98
4.1.2 Smoothing and classification of viraemia and cytokine profiles and classification of nAb response	100
4.1.3 Statistical Analysis.....	104
4.1.4 Associations between cytokine responsiveness and nAb cross protection with viral profile class, WUR genotype and genetic background	105

4.1.5 The association between viraemia and cytokine responses	106
4.2 Results.....	108
4.2.1 Qualitative assessment of cytokine profiles and classification into cytokine response categories.....	108
4.2.2 Associations between cytokines and factors affecting cytokine response over time	110
4.2.3 Cytokine responsiveness and the association with viral profile class, WUR genotype and genetic background	119
4.2.4 Associations between viraemia and cytokine responses.....	129
4.3 Discussion	135
Chapter 5 Discussion	150
5.0 Summary of the novel findings of this thesis and their implications.....	150
5.0.1 The Wood's model.....	151
5.0.2 Review and comparison of the statistical modelling and inferences employed	152
5.0.3 Statistical categorization of pigs: viraemia profiles	154
5.0.4 Influential effects on the viraemia profiles	156
5.0.5 The relationship between the viraemia and the immune response measures	158
5.1 Further implications	160
5.1.1 Genetic selection for host resistance to PRRSV infection.....	165
5.1.2 Process based mathematical modelling of PRRSV infection	165
5.1.3 Epidemiological consequences of infection.....	166
5.1.4 Sequencing the virus from rebound, persistent and cleared pigs to understand viraemia profile variation	167
5.2 Limitations	167
5.2.1 Viraemia and the immune responses: could different underlying immune responses result in similar observed viraemia?.....	167
5.2.2 Challenge and strain specific conditions.....	169
5.2.3 Weight gain and tolerance to infection	170
5.3 Conclusions.....	170
Appendices	181
Appendix 1 The effect of the removal of bimodal profiles on the linearized Wood's model curves from Chapter 3	181
Appendix 2 KS06 Wood's and Extended Wood's model residuals	183
Appendix 2b Breadth of nAb and WUR genotype	183

Appendix 3 Comparison of host genetic factors influencing piglet response to infection
with two different isolates of Porcine Reproductive and Respiratory Syndrome Virus
suggests selection for reduced susceptibility to PRRSV infection

is feasible across isolates 187

List of Figures

Figure 1.1 The PRRS virion: showing the structure of the small enveloped virus with a nucleocapsid core and the major and minor proteins.....	13
Figure 2.1 Viraemia profiles from a PRRSV challenge at 0dpi with either PRRSV isolate NVSL or KS06.....	41
Figure 2.2 Boxplots of the viraemia data from the PHGC trials.	47
Figure 2.3 The model residuals from fitting the final repeated measures model to the full dataset 1 and the reduced dataset 2	51
Figure 2.4 Comparison of the least square mean estimates obtained from fitting the repeated measures model to both datasets	53
Figure 2.5 Comparison of the LSMs from dataset 1 and dataset 2 for each WUR genotype	55
Figure 2.6 The least square mean estimates for each genetic background at each observation of the PRRSV challenge experiment	56
Figure 2.7 Comparison of LSM estimates for different genetic background from dataset 1 (solid lines) and 2 (dashed lines).....	57
Figure 2.8 The LSMs for each trial fitting the repeated measures model with trial substituted for genetic background to dataset 1	58
Figure 2.9 Comparison of the LSMs for each trial from fitting the repeated measures model with trial substituted for genetic background to dataset 1(lines) and dataset 2(dashed lines).....	60
Figure 2.10 Individual Wood's model fits (black solid line) to the \log_{10} viraemia data (blue crosses)	62
Figure 2.11 Plot of the residuals from fitting the final linearized Wood's model	63
Figure 2.12 Estimated viraemia curves obtained from LSM parameter estimates obtained when fitting the final linearized Wood's model	64
Figure 2.13 Predicted viraemia profiles estimated by the linearised Wood's model (lines), together with the estimates produced by the repeated measures models (green and blue points with confidence limits)	66
Figure 2.14 Wood's model predictions for WUR genotypes.	67
Figure 2.15 Wood's model predictions for each genetic background (lines) together with the corresponding estimated LSM viraemia at the observation times obtained from repeated measures model (asterisks).. ..	69

Figure 2.15 Wood's model predictions for each genetic background (lines) together with the corresponding estimated LSM viraemia at the observation times obtained from repeated measures model (asterisks).. ..	70
Figure 2.16 Wood's model predictions for each trial (lines) and corresponding LSM viraemia estimates obtained from the repeated measures models (asterisks).	65
Figure 4.1 A typical viraemia profile with the derived variables from the Woods model annotated.....	101
Figure 4.2 Typical CCL2 cytokine profile obtained from cubic spline fitting with the derived variables annotated.....	103
Figure 4.3 Individual cytokine cubic spline curves for the measured cytokines....	109
Figure 4.4 The effect of genetic background on cytokine profiles.....	116
Figure 4.5 The effect of viral class on the cytokine profile.....	117
Figure 4.6 The effect of WUR on the cytokine profile.....	118
Figure 4.7 The distribution of responder and non-responders for each cytokine by viraemia class.....	123
Figure 4.8 The distribution of responder and non-responders for each cytokine by genetic background.....	124
Figure 4.9 The distribution of responder and non-responders for each cytokine according to WUR genotype.....	125

List of Tables

Table 1.1 Animal composition across the PHGC trials	7
Table 2.1 Animal composition across the PHGC trials	38
Table 2.2 Two longitudinal PRRS viraemia datasets used in this statistical analysis	40
Table 2.3 The distribution of the WUR genotype across the PHGC trials.....	44
Table 2.4 The frequency of bimodal profiles across the PHGC trials.....	45
Table 2.5 The frequency of the WUR genotypes across uni and bimodal viral profiles....	50
Table 2.6 The least square mean estimates (standard error of the mean) for each PRRSV isolate from fitting the repeated measures model to dataset 1... ..	52
Table 2.7 The least square mean estimates for each PRRSV isolate from fitting the repeated measures model to dataset 2.	53
Table 2.8 The LSMs for each WUR genotype from fitting the repeated measures model to dataset 1.	54
Table 2.9 The least square mean estimates for each WUR genotype, from fitting the repeated measures model to dataset 2..	55
Table 4.1 Animal composition across a subset of the PHGC trials used for studying the cytokine profiles and nAb cross protection.	98
Table 4.2 The viraemia measures generated from the Wood's model fitting to viraemia profiles	101
Table 4.3 Cytokine measures associated with IL-8 generated from cubic spline fitting	102
Table 4.4 The number of cleared, persistent and rebound individuals in the cytokine dataset	108
Table 4.5 Pearson correlations of pairwise log ₁₀ cytokine concentration area under the curves above the baseline response (AAUC).....	111
Table 4.6 A selection of the final multiple regression models for testing the associations between cytokines.....	112
Table 4.7 Summary of the significant effects in the repeated measures models for longitudinal cytokine profiles	114

Table 4.8 The distribution of responders and non-responders for each cytokine	120
Table 4.9 The number and percentage of responders for each cytokine according to viraemia class, genetic background and WUR genotype.....	121
Table 4.10 The pooled cytokine response classes	126
Table 4.11 Summary of the distribution of the breadth of cytokine response for viral profile class, genetic background and WUR genotype	127
Table 4.12 Odds ratios for the breadth of cytokine response	129
Table 4.13 Pearson correlations of pairwise cytokine AAUC and viraemia AUC at 4, 21 and 35dpi (denoted as I4, I21 and I35, respectively)	129
Table 4.14 Goodness of fit statistics for the final mixed model exploring the association between cytokine measures and the rate of post viraemia peak decline captured by the Woods parameter C1	130
Table 4.15 The final mixed models when the viraemia traits were the response variables and the cytokines where the potential predictors	132
Table 4.16 The final mixed models when cytokines were the response variables and the viraemia traits were the potential predictors	134

List of Abbreviations

AUC: area under the curve

NVSL: NVSL-97-7895 north American PRRS isolate

KS06: KS-2006-72109 north American PRRS isolate

ORFs: open reading frames

GPs: glycoproteins

PAM: pulmonary alveolar macrophage

PRRSV: porcine reproductive and respiratory syndrome virus

PHGC: PRRS host genetic consortium

nAb: neutralising antibodies

NK: natural killer cell

IL- : interleukin

Declaration

I declare that this thesis was composed by myself, that the work contained herein is my own except where explicitly stated otherwise in the text, and that this work has not been submitted for any other degree or professional qualification except as specified.

A handwritten signature in black ink, appearing to read 'Zeenath Ul Islam', written in a cursive style.

Signed:

Zeenath Ul Islam

Date: 23/05/16

Acknowledgements

I would like to thank my supervisors Andrea Doeschl-Wilson, the late Steve Bishop, and Georgios Banos for all their valuable expertise, excellent supervision and support throughout my PhD. I would also like to thank Nick Savill for his insights into Bayesian model fitting and the use of the model fitting program which was used in Chapter 3. I would like to thank my collaborators Joan Lunney, Bob Rowland, Jack Dekkers, and Andrew Hess firstly for their creative thought provoking discussions and secondly for their technical expertise and insights into PRRSV infection or quantitative genetics. This thesis would not have been possible without all of them.

I would also like to thank all the members of the Roslin Institute “Epi group” and “Wilson lab” for their stimulating group discussions. Specifically I would like to thank Osvaldo Anacleto and Helen Brown for their statistical expertise and I would like to thank Natacha Go for her insights into modelling PRRSV infection dynamics.

This PhD was funded by the Genome Canada. I would like to thank the PHGC project for providing the data analysed in this thesis.

Last but not least, I would like to thank my family and friends who have supported me throughout my PhD.

Sonnet 1

How can I then return a model right,
That am debarr'd the benefit to know?
When viral rule is not eased by night,
But day by night and night by day, in vivo?

And the virus a foe to the host reign,
Do in consent up-regulate macrophage inside,
The host by toil, immune system complain,
How far I toil, you still further do divide.

So then the host is not lame, poor, nor despised,
Whilst that CCL2 doth substance give,
That virus in thy abundance am sufficed
And by in host with all glory live

But daily post infection in host for no longer,
For cytokine doth make the immunity stronger.

Z. U. Islam

Lay Summary

Infectious respiratory viral diseases can have potentially devastating impacts upon animal health, welfare and production traits and thus cause considerable economic losses to the industry. Developing effective control measures can be challenging due to the complexity of the underlying immune mechanisms involved and numerous potential influential factors in the course of an infection. In the age of “Big Data” we can harness the power of multiple repeated measurements from large *in-vivo* virus challenge experiments to exploit a rich wealth of information about the underlying processes of a biological system. The insights gained from a data-driven statistical modelling approach can be then used to develop and inform a wide range of hypothesis surrounding infection duration, variation, clearance rates and the related immune processes all of which can inform future studies and aid the development of new disease control measures.

In this thesis we are primarily concerned with gaining insights into the within-host dynamics of a specific virus infection (PRRSV) using a data-driven statistical modelling approach. Porcine reproductive and respiratory syndrome (PRRS) is one of the most economically significant viral diseases facing the global swine industry. Sequential measures of the level of the virus within a host following infection, i.e. longitudinal viraemia profiles, reflect the severity and progression of infection within the host and provide crucial information for subsequent disease control measures.

We analyse the largest longitudinal PRRS viraemia dataset from an in-vivo experiment, and corresponding immune measures in the form of cytokines and neutralising antibodies. We provide a suitable mathematical description of all viraemia profiles with biologically meaningful parameters for quantitative analysis of profile characteristics.

In the experimental study of this thesis pigs were challenged with one of two PRRSV strains. In Chapter 2 we derive a statistical description of the temporal changes in viraemia and determine the influence of diverse factors on the viraemia profiles. The typical time trends of the viraemia profiles were a rise to a peak followed by a period of decline with dynamics and magnitude influenced by the virus strain. Both uni and bimodal viraemia profiles were observed.

The Wood’s model, a mathematical function, appeared to be a suitable candidate model for the data associated with uni-modal profiles. Furthermore the Wood’s model captured the time trends concisely in only three model parameters which also had a biological relevance.

The longitudinal viraemia measures revealed substantial differences in the viraemia profiles between hosts infected with the same PRRSV challenge dose. In Chapter 3 we provide a suitable mathematical description of all viraemia profiles with biologically meaningful parameters for quantitative analysis of profile characteristics. The Wood’s function and a biphasic extended Wood’s function were used to model the viraemia data. Three viraemic categories emerged: cleared (uni-modal and below detection within 42 days post infection(dpi)), persistent (transient experimental persistence over 42 dpi) and rebound (biphasic within 42 dpi).

The variation of outcomes observed following PRRSV infection are most likely a consequence of the complex set of interactions between the virus and the host’s immune response. In Chapter 3 and 4 we explored the association between the observed PRRS viraemia profile characteristics and the corresponding measures of the immune response in the form of: neutralising antibody (nAb) cross protection data (Chapter 3) and longitudinal cytokine profiles (Chapter 4). Cytokines are a large group of proteins secreted by cells of the immune system that mediate many of the processes of these

cells. Numerous cytokines have been reported to influence responses of pigs to PRRSV infection. Cytokines don't act in isolation and their responses are transient. In Chapter 4, we determined the typical features and time trends of each cytokine profile, examine the associations between the cytokines, and characterise the cytokine response. We characterised the responsiveness for each pig of across all seven cytokines in this study and examined the impact of various effects on the breadth of cytokine response. We then determined the associations between viraemia and the ensuing cytokine measures and the cytokines and the ensuing viraemia measures. We assessed whether the strength of the serum cytokine response was associated with the rate of the serum viraemia decline.

In conclusion, this study provides novel insights into the nature and degree of variation of hosts' responses to infection as well as new informative traits for subsequent genetic and modelling studies.

Abstract

Porcine reproductive and respiratory syndrome (PRRS) is one of the most economically significant viral diseases facing the global swine industry. Viraemia profiles of PRRS virus challenged pigs reflect the severity and progression of infection within the host and provide crucial information for subsequent control measures. In this thesis we analyse the largest longitudinal PRRS viraemia dataset from an in-vivo experiment, and corresponding immune measures in the form of cytokine data and neutralising antibodies. In the PRRS Host Genetic Consortium (PHGC) trials, pigs were challenged with one of two PRRSV isolates (NVSL and KS06, respectively).

In Chapter 2 we derive a statistical description of the temporal changes in viraemia and determine the influence of diverse factors (e.g. PRRSV strain, pig genetic background, resistance genotype, etc.) on viraemia profiles. The well-established methodology of linear mixed modelling with a repeated measures model and fitting a linearized Wood's function, a gamma-type function, is applied to the viraemia dataset. The virus isolate had a significant impact on the viraemia profiles which was captured by statistically significant differences in model parameters via both statistical methods. The more virulent NVSL isolate had higher early viraemia predictions and a faster rate of decline than KS06. In line with previous studies the WUR "resistance" genotype, associated with lower AUC viraemia found in previous studies, also resulted in lower viraemia predictions in the statistical models. The typical time trends of the viraemia profiles were a rise to a peak followed by a period of decline with dynamics and magnitude influenced by the virus isolate. Both uni and bimodal viraemia profiles were observed.

The Wood's model appeared a suitable candidate model for the data associated with uni-modal profiles and captured the time trends concisely in only three model parameters which also had a biological relevance. Overall the best fitting Wood's model ($y=at^be^{-ct}$) was when there was a random effect in Wood's parameters b and c . Bimodal profiles significantly reduced the model fit, particularly in the later phase of infection resulting in large model residuals. However bimodal profiles did not impact upon the significance of the differences between the LSM repeated measures estimates nor the LSM linearized Wood's model parameter estimates.

The longitudinal viraemia measures from the PRRSV challenge experiment revealed substantial differences in the viraemia profiles between hosts infected with the same PRRSV challenge dose, pointing to considerable variation in the host response to PRRSV infections. In Chapter 3 we provide a suitable mathematical description of all viraemia profiles with biologically meaningful parameters for quantitative analysis of profile characteristics. The Wood's function and a biphasic extended Wood's function were fit to the individual profiles using Bayesian inference with a likelihood framework in Chapter 3. Using maximum likelihood inference and numerous fit criteria, we

established that the broad spectrum of viraemia trends could be adequately represented by either uni- or biphasic Wood's functions. Three viraemic categories emerged: cleared (uni-modal and below detection within 42 days post infection(dpi)), persistent (transient experimental persistence over 42 dpi) and rebound (biphasic within 42 dpi). The convenient biological interpretation of the model parameters estimates, allowed us not only to quantify inter-host variation, but also to establish common viraemia curve characteristics and their predictability. The convenient biological interpretation of the model parameters estimates, allowed us not only to quantify inter-host variation, but also to establish common viraemia curve characteristics and their predictability, which were utilized in subsequent quantitative genetic analyses to identify genomic regions associated with these new resistance traits. The Bayesian approach for curve fitting in Chapter 3 led to better model fits than the classical linear mixed models approach of Chapter 2.

Furthermore in Chapter 4 we explored the association between the observed PRRS viraemia profile characteristics and the corresponding measures of the immune response in the form of: neutralising antibody (nAb) cross protection data and longitudinal cytokine profiles. Statistical analysis of the profile characteristics revealed that persistent profiles were distinguishable already within the first 21 dpi, whereas it is not possible to predict the onset of viraemia rebound. Analysis of the neutralizing antibody (nAb) data indicated that there was a ubiquitous strong response to the homologous PRRSV challenge, but high variability in the range of cross-protection of the nAbs. Persistent pigs were found to have a significantly higher nAb cross-protectivity than pigs that either cleared viraemia or experienced rebound within 42 dpi.

We determined the typical features and time trends of each cytokine profile, examined the associations between cytokines, and characterised the cytokine response. A stronger association was found in the direction of cytokines driving the ensuing viraemia characteristics as opposed to vice versa. It was found that viraemia class differences were best captured in the anti-viral cytokine IFNA and also the chemokine CCL2, furthermore these key cytokines were the most strongly associated with viraemia measures. The breadth of the cytokine responsiveness was associated with viral profile class and genetic background but not the WUR genotype.

The statistical categorization of pigs from each PHGC trial through model fitting provides a critical basis for the generation of new desirable host phenotypes, and of potential use in the genetic selection of pigs with favourable infection traits. Our study provides novel insights into the nature and degree of variation of hosts' responses to infection as well as new informative traits for subsequent genetic and modelling studies

Chapter 1. Introduction

Infectious respiratory viral diseases can have potentially devastating impacts upon animal health, welfare and production traits and thus cause considerable economic losses to the livestock industry. Developing effective control measures can be challenging due to the complexity of the underlying immune mechanisms involved and numerous potential influential factors during the course of an infection. Thanks to recent developments in bio-technology we can harness the power of multiple repeated measurements from large *in vivo* virus challenge experiments to exploit a wealth of information about the underlying processes affecting host response to infection. The insights gained from a data-driven statistical modelling approach can be then used to develop and inform a wide range of hypothesis surrounding infection duration, variation, clearance rates and the related immune processes all of which can inform future studies and aid the development of new disease control measures.

In this thesis we are primarily concerned with gaining insights into the within-host dynamics of a specific virus infection using a data-driven statistical modelling approach. We begin with a review of the particular virus in question and the associated knowledge gaps addressed in this thesis, followed - by an outline of the experimental protocol and data generated, and conclude with an outline of the statistical approaches adopted thus providing an outlook for the subsequent thesis Chapters.

The main goal of this study is to gain a deeper insight into the within-host dynamics of a Porcine Reproductive and Respiratory Syndrome Virus (PRRSV) infection; knowledge that can be exploited to improve the current disease control mechanisms and aid the development of process based-mathematical models and genetic analysis of the host response to infection for the development of genetic disease control strategies.

1.0 Porcine Reproductive and Respiratory Syndrome prevalence and related economic losses

Respiratory diseases in pigs are arguably currently the most important health concern for swine producers[1]. PRRSV is currently one of the most economically important infectious viral diseases in swine with a global spread[2]. It was first recognised in the United States of America in 1989 and in Japan in 1989, and by 1990 it had been isolated in Germany. PRRS reportedly costs U.S. swine producers more than \$560 million annually [3-6]. There are two related but genetically distinguishable strains: Type 1, predominating in Europe and known also as the European strain, and Type 2, mostly found in North or South America and Asia, also known as the North American strain. The development of the virulent and highly pathogenic Type 2 PRRSV variants, spreading throughout

Asia highlight the need to advance effective interventions to prevent PRRSV pathology, mortality and production losses [7-9].

Infection with PRRSV results in viraemia and virus replication in multiple organs within the host; the targets for replication are macrophages in various tissues, primarily the lung but also in lymph nodes, spleen, placenta and umbilical cord [10-12]. PRRSV targets a subpopulation of macrophages, in the lung and other tissues, that have reached a state of differentiation rendering them permissive to the virus; causing cell apoptosis to infected cells and a large proportion of uninfected neighbouring macrophages [13]. The virus uses several evasion strategies to thwart the unsuspecting innate and acquired immunity, such as interference with antigen presentation, antibody-mediated enhancement, reduced cell surface expression of viral proteins and shielding of neutralizing epitopes [14]. The immune responses elicited during a PRRSV infection are reviewed in more detail below.

PRRS reduces reproductive performance in breeding animals and increases respiratory problems in animals of all ages, leading to impaired growth in young piglets and, in some cases, mortality [3,15,16]. PRRSV infected sows have increased rates of abortions, stillbirths, mummifications, and give birth to weak piglets with chronic respiratory problems. It can take weeks, even months, for pigs to clear this RNA virus, which evolves and adapts quickly to new environmental challenges, vaccines or medication [17]. Within the swine production system, PRRSV infection predominantly exists as a subclinical infection, often as a co-factor in various polymicrobial disease syndromes [1]. PRRSV infected pigs are susceptible to secondary infections such as pneumonia and postweaning multisystemic wasting syndrome (PMWS) caused by infection with the Porcine Circovirus Type 2 (PCV2) [5,18-20].

1.1 Mode of infection and the host response to infection

This PhD project uses data from the nursery pig infection model of the PHGC trials to assess resistance or susceptibility of growing pigs to primary PRRSV infection. To date, 15 groups of ~200 crossbred pigs from high health farms have been donated by commercial sources. After acclimatisation, the pigs were infected with one of two PRRSV isolates (NVSL or KS06) in a biosecure facility and followed for 42 days post infection (dpi). Blood samples were collected at 0, 4, 7, 10, 14, 21, 28, 35 and 42 dpi for serum and whole blood RNA gene expression analyses; weekly weights were recorded for growth traits [21].

For each trial one company was requested to provide 200 pigs at weaning from PRRSV negative (PRRSV-), *Mycoplasma hyopneumoniae*-, and swine influenza virus- farms, and if possible from porcine circovirus type 2 (PCV2) free farms. Pigs could be from vaccinated sows since maternal antibody prevents them from becoming infected with PCV2. PRRSV affects growing pigs; the pigs in this experiment are post-weaning, hence the impact of maternal immunity has been removed as a

factor impacting upon the experimental results. The impact of PCV2 was not included in the modelling of this thesis since the pigs were from high health farms free from PCV2.

The source populations were crossbred commercial pigs with complete parentage and pedigree records. The animal composition of the full dataset is outlined in Table 1.1. There was no pre-selection of sires for disease traits. Pigs (~200/trial) were transported to the biosecure Kansas State University testing facility at weaning. After arrival pigs were treated with broad spectrum antibiotics for 1 week, to prevent expression of other organisms. After the 7 day acclimation period, pigs were challenged both intramuscularly and intranasally with PRRSV and followed for 42 days post infection (dpi). Infection in the PHGC trials of this thesis was in line with the protocols of other challenge studies, such as [22,23], in which both simultaneous intranasal and intramuscular PRRSV challenges were used at 0dpi. It is important to note that the mode of infection via intranasal or intramuscular routes adopted in a challenge study could potentially induce distinct responses in the host. The route of infection has been found to be reflected in observed differences in the levels of the virus in the plasma, ability to detect the virus, and the levels and consequently ability to detect virus neutralising antibodies in the plasma [24] [25,26], thus care needs to be taken when comparing the inferences made with other challenge studies in which only one of the mode of infection was adopted. In this study it is assumed that the observed response is due to the primary infection. However one cannot exclude the potential hypothesis that co-infection could occur between the pigs due to the shared pen structure. Pigs were weighed weekly for growth data. Pigs were killed at 42 dpi and tonsils collected for viral persistence and ears for genomic DNA. Across the trials infected with NVSL, 12% of pigs had died or were euthanized for humane reasons before 42 dpi. Mortality rate was similar in the KS06 trials, with 9% pigs dying or euthanized before 42 dpi across the five trials. Dead pigs were necropsied and subsequent gross and microscopic pathology by a board-certified pathologist identified PRRS associated disease as the major source of mortality, except for trial 6. Death loss was high in trial 6 (46% by day 42), due to secondary bacterial infections, as identified by pathology, including *Escherichia coli*, *Streptococcus suis*, *Staphylococcus aureus*, and *Mycoplasma hyopneumoniae*.

1.1.1 Viraemia data: Blood samples were collected immediately before infection (0 dpi) and at 4, 7, 11, 14, 19/21, 28, 35, 40/42 dpi and the level of PRRS viraemia was measured using a semi-quantitative TaqMan PCR assay for PRRSV RNA. The viraemia quantity data from RT-PCR was transformed on the logarithmic scale to the base 10. Due to the sensitivity of RT-PCR the threshold of detection was set at 1 units on the log₁₀ scale [27].

1.1.2 Cytokine data: Longitudinal cytokine measures were also taken from serum. Cytokine data from serum collected at 0, 4, 7, 10, 14, 21, 28, 35, 42dpi was obtained for 228 randomly chosen individuals from the three PHGC trials 3, 5, and 7 (with cytokine data from 35, 77, and 117 pigs in each trial

respectively) using Fluorescent Microsphere Immunoassay (FMIA) outlined in [28] and [22]. The FMIA Luminex multiplex swine cytokine assay provided simultaneous quantitative measures of the concentration of four innate (IL-1b, IL-8, IFNA, IL-12), two regulatory (IL-10) and Th2 (IL-4) cytokines and a chemokine (CCL2) at each time point of the infection. There was no successful assay for IFN-gamma as the monoclonal antibody that made the assay is no longer available. Trial 7 had missing values at 42dpi and Trial 3 had no observations for IL-1b. The \log_{10} transformation of the cytokine observations were used to normalise the data. The recent development of FMIA allows for the reliable and effective simultaneous quantification of multiple cytokines in porcine sera [28]. FMIA is a relatively new method of cytokine detection for PRRSV and has only been used in one previous study[22]. Serum measurements were used in this PRRSV challenge study as they allowed for multiple repeated measures and were less labour intensive due to the scale of the PRRSV challenge experiment conducted. The limitations of inference from serum data as opposed to measures taken at the site of infection is included in the discussion Chapter of this thesis.

1.1.3 Neutralising antibodies (nAbs) data: nAb data from serum collected at 42dpi was obtained for 490 individuals from the first three PHGC infection trials using a virus neutralization assay as outlined in [29]. Serum neutralising assays were conducted to examine the presence of cytopathic effects on the homologous PRRSV strain as used in the *in-vivo* challenge experiment (NVSL-7985 denoted henceforth as NVSL) and three additional PRRSV isolates: KS06-72109 (KS06), P-129 and VR-2332 (VR). These type 2 PRRSV isolates were chosen for genetic differences based on viral ORF5 sequence. Excluding the relatedness between P129 and NVSL (95%), nucleotide comparisons within ORF5 show that the PRRSV isolates differed from each other by 10% or greater. Each serum sample was reacted with the panel of four type 2 viral isolates, where the NVSL isolate served as the homologous virus in the serum neutralisation assays. Serum samples were considered positive for PRRSV nAb at a titre of eight or higher.

1.1.4 Genotyping: Ear tissue was collected from all pigs for DNA isolation. Tissues or DNA samples for trials 1-10 were genotyped with Illumina's Porcine SNP60 Beadchip v1 (San Diego, California) at GeneSeek Inc. (Lincoln, Nebraska) and samples from trials 11-15 were genotyped with Illumina's Porcine SNP60 Beadchip v2 (San Diego, California) at Livestock Gentec Delta Genomics (Edmonton, Alberta). Only SNPs that were included on both versions of the Illumina's Porcine SNP60 Beadchip were used in this study. SNPs were removed if they were fixed within a breed, or if they were unmapped or mapped to a sex chromosome in build 10.2 of the swine genome (<http://www.ncbi.nlm.nih.gov/genome/guide/pig/>, accessed August 13, 2015); this left 48,164 SNPs. Missing genotypes were assigned the average genotype (on 0,1,2 scale) for animals in that trial for that SNP. Both sera and ABI Tempus tubes for later RNA analyses were collected at all sampling times.

PRRS Virus Isolate	Trial Number	Number of Animals	Breed Cross ¹	Genetic Background ²
NVSL-97-7895 (NVSL)	1	188	LW x LR	1
	2	190	LW x LR	1
	3	184	LW x LR	1
	4	191	Duroc x LW/LR	2
	5	182	Duroc x LR/LW	3
	6	109	LR x LR	4
	7	186	Pietran x LW/LR	5
	8	158	Duroc x LW/LR	6
	9	200	Yorkshires	10
	15	166	Pietran x LW	7
	Total	1554	-	1-7, 10
KS-2006-72109 (KS06)	10	184	Pietran x LW	7
	11	177	LW x LR	1
	12	146	LR x LW	8
	13	173	Duroc x LW/LR	9
	14	165	Duroc x LR/LW	3
	Total	672	-	1,3,7,8,9

Table 1.1 Animal composition across the PHGC trials. ¹LW = Large White; LR = Landrace.

²Genetic background is defined as pigs from the same breeding company and the same breed cross.

1.2 Genetic variability in the host for PRRS

Numerous PRRSV in-vivo and in-vitro studies point to breed differences in the response to infection; which suggest that there is a host genetic component in the host resistance to infection [16,21,27,30-39].

1.2.1 Evidence for genetic variation in host resistance to PRRSV

Evidence for the host genetic impact on PRRSV infection was found in early studies which observed that different pig breeds were associated with different numbers of lung lesions [36] and rates of abortions (in sows) [37]. Breed differences have since been found in serum viraemia and IL-8 expression [40]. Reiner et al.[41] observed that Pietrain pigs infected with an attenuated PRRSV strain had longer viraemia lasting until 72 days post infection (dpi), and a less efficient antibody production than Miniature pigs whose viraemia only lasted up to 35dpi. Furthermore there appeared to be a minor heritable component to PRRSV resistance [42]. *In vitro* studies indicated that macrophage responses were related to breed [31,32] and reduced viral replication was observed for Landrace pigs compared to other breeds [38]. Most recently, genetic markers associated with host resistance have been identified for NVSL infected pigs of genetic backgrounds 1-3 as outlined further below.

1.2.1 The PRRS Host Genetic Consortium (PHGC) PRRSV infection trials

The work presented in this thesis is part of a wider project of the PRRS Host Genetic Consortium called “Application of Genomics to Improve Swine Health and Welfare” (funded by Genome Canada). Genetic selection of pigs that are less susceptible to PRRS is an attractive method to improve the swine herd health status. The overall goal of the PRRS Host Genetics Consortium (PHGC) is to exploit state-of-the art genomic technologies to breed healthier pigs with improved resistance to PRRSV infection. Previous studies have provided evidence for a host-genetic component in the effectiveness of responding to and clearing a PRRSV infection [15,31,32,36,43]. However, in order to harness genetic variation in host response to PRRSV infections for genetic disease control strategies, large datasets containing records of thousands of infected animals are required. Furthermore, deep phenotypes for a sufficiently large number of animals are required for identifying the genetic loci and pathways that are responsible for the genetic control of PRRSV infection responses [21]. The PHGC was created to produce the necessary data for genetic analysis of pigs’ responses to PRRSV infections. In the PHGC PRRSV challenge trials pigs were infected with one of two north American PRRSV isolates (NVSL or KS06).

The main objectives for the PHGC are to:

- 1) Use genotyping and phenotyping tools to determine if there are host genes that control resistance/susceptibility to PRRSV infection

- 2) Verify genetic variation in response to PRRSV, via improved health, survivability and growth.
- 3) Identify relative importance of different phenotypic traits, and their heritability, that predict response to PRRSV infection.

The data analysed in this thesis was obtained from the PRRS Host Genetic Consortium (PHGC) trials, which is the largest PRRSV in-vivo challenge study to date. The PHGC carried out various challenge studies including pregnant sows and growing piglets. In this thesis we consider data from the growing piglet PRRSV challenges only.

1.2.3 Previous findings for the PHGC nursery pig PRRSV challenge data relevant for this thesis: The WUR ‘resistance’ genotype

Previous studies using multiple contemporary North American crossbred weaned piglets experimentally infected with the NVSL-97-7895 (NVSL) isolate of PRRSV identified heritable genetic components to the area under the curve (AUC) of the viraemia profile, up to 21dpi, and weight gain, and found an association between the single nucleotide polymorphism (SNP) WUR10000125 (henceforth referred to as WUR) on chromosome 4 and these two host response traits [27,33,35,44,45]. Thus the WUR genotype used in this thesis refers to the presence or absence of the favourable B-allele strongly associated with cumulative viraemia (viraemia AUC 0-21dpi). The WUR SNP was found to act in a dominant manner irrespective of whether the favorable B allele is inherited from the sire or dam [44].

While the WUR genotype does appear to play a significant role in host response to PRRSV infection, there is a substantial polygenic portion to viraemia: the WUR genotype only explained 13% of the total genetic variance in the AUC of viraemia [33,45,46]. GBP5 is the relevant candidate gene in the region of the WUR SNP. GBP5 plays a role in the innate immune response during infection; interacting with the inflammasome NLRP3 which is a multi-protein complex that acts as a sensor for pathogen associated damage and is associated with the cleavage of some pro-inflammatory cytokines [47,48]. Animals that have the AA genotype do not produce functional GBP5 [49].

The effect of the WUR genotype on piglet response to infection has only been validated on NVSL infected piglets. It is currently unknown whether the host genetics influencing response to PRRSV infection is consistent across all North American PRRSV isolates. Also, the WUR genotype is associated with infection data from the primary phase of infection (0-21dpi). It would be interesting to assess the impact, if any, it has on the full viraemia profiles (0-42dpi). Furthermore the impact on or association between the WUR genotype and the longitudinal cytokine expression profiles or the breadth of the neutralizing antibody (nAb) response has not yet been determined. Furthermore,

variation in host response has only been quantified in terms of cumulative viraemia (AUC 0-21dpi); it has not been fully specified how the viraemia profiles differ over time.

1.3 The “persistent” nature of a PRRSV infection

The etiologic agent, PRRSV, is an enveloped, positive-stranded RNA virus, which belongs to the order Nidovirales, of the family Arteriviridae (arteriviruses are reviewed in [50]). Arteriviruses possess several characteristic properties related to viral pathogenesis such as: cytopathic replication in macrophages, the capacity to establish a persistent infection, and the ability to cause severe disease [51].

One of the most significant challenges facing the eradication of the disease is the persistent nature of the PRRSV virus, which may persist within the host for several weeks or months, in some cases maintaining a sub-clinical lifetime persistence [51,52]. By definition, PRRSV is not a “persistent” virus, however given the average lifetime of a production pig being approximately 180 days, PRRSV infection can be regarded as “life-long” [39].

The causes for persistence are not fully understood, however it could be due to a combination of factors such as: the complex virion structure that possesses a heavily glycosylated surface, the focus of the humoral response on the non- surface proteins, antigenic and genetic drift, and the subversion of interferon gene induction [21,39,53,54]. If the persistently PRRSV infected individuals also remain infectious, they could potentially drive the epidemiological dynamics of the disease within the population through perpetuating the cycle of transmission to susceptible animals [55].

During an infection PRRSV may avoid the host immune response, possibly escaping the humoral immune response by localizing to certain tissues. Previous research has identified that the tonsils are a primary source of viral persistence [56,57]. This may be due to an abundance of memory B-cells in the tonsil, but the lack of effector, plasma-producing, B-cells [58]. An abundance of PRRSV in tonsils may result in a cyclical reappearance of circulating virus in the serum. If the ability of the virus to localize to tissue to escape immune response differs between isolates, this will be reflected in the tonsil viraemia levels. Suppression of the innate system during a PRRSV infection could also be responsible for the persistent or prolonged viraemia profiles. It has been reported that PRRSV can suppress phagocytosing activity, the expression of innate cytokines and alter their expression patterns [14,17].

The host immune response mechanisms and genetics associated with variation in PRRS viraemia clearance have not been fully determined. The quantification of inter-host viraemia variation, the rate of viral clearance, and the statistical categorization of “persistently” infected pigs following challenge

would enable the possible host genetic contribution to “persistence” or inefficient clearance of PRRSV to be determined.

1.4 PRRSV viraemia profiles and inter-host variation

Viraemia profiles of *in-vivo* experimentally PRRSV challenged pigs are valuable indicators of the severity and progression of the infection in the host, and thus provide crucial information for the required subsequent disease control measures [59]. The course of a typical PRRSV infection is characterised by an acute viraemic stage lasting approximately 4 weeks followed by a stage characterised by low levels and eventual resolution of viraemia [2,39,60,61]. Previous studies suggest that in the majority of animals viraemia reaches undetectable levels typically by 4-6 weeks, although the virus may still be isolated months later in the lymphoid tissues [62,63].

In a study involving two different breed crosses, pigs were categorized into high or low disease burden [64]. Viraemia differences were observed between different pig lines; pointing to genetic variation in responses to infection. High viraemia was associated with a high immune response, and low viraemia was associated with low or no changes in immune gene expression compared to the uninfected controls [64].

PRRSV challenge experiments with longitudinal viraemia measures reveal substantial differences in the viraemia profiles between hosts infected with the same PRRSV challenge dose, pointing to considerable variation in the host response to PRRSV infections. For example, numerous studies have shown breed differences in viraemia levels and duration and also in antibody production [30,40,59,64]. Reiner et al.[41] observed that Pietrain pigs infected with an attenuated PRRSV strain had longer viraemia lasting until 72 days post infection (dpi), and a less efficient antibody production than Miniature pigs whose viraemia only lasted up to 35dpi. Viraemia was classified as persistent in Pietrain pigs, however the profiles revealed both uni- and biphasic curves which could be a manifestation of viraemia reactivation from the original infection within the host or reinfection between the pigs [65]. In a more recent PRRSV infection study persistently infected pigs were defined as having positive serum viraemia levels by 28dpi [66]. Furthermore persistence was associated with lower serum levels of the cytokine IL-8 [66].

Using longitudinal viraemia records from a subset of data used in this thesis, Boddicker et al. [27] reported substantial differences between individual viraemia profiles and cumulative viraemia (viraemia AUC 0-21dpi). Furthermore, based on visual inspection, they classified pigs into two categories, i.e. non-rebounders and rebounders, characterised by mono- and bi-phasic serum viral profiles, respectively. The underlying causes for this rebound phenomenon are currently not understood. It is not known whether rebound occurs across all PHGC trials, PRRSV isolates or genetic backgrounds. Furthermore it is not known whether the viraemia rebound trend is captured in

immune response measures such as the longitudinal cytokine expression, responsiveness in cytokines or the breadth of the nAb response. The statistical categorization of viraemia profiles pigs from a PRRSV infection could provide a critical basis for the selection of pigs with favourable infection traits. Rebound could be important from an epidemiological perspective since animals in the same pen could potentially transfer quasispecies between each other, whereby a quasispecies from one pig could be transferred to another pig and cause reinfection and viral rebound [67]. The underlying mechanisms behind the observed viral rebound have not yet been fully determined. The association between longitudinal viraemia variation and the longitudinal cytokine expression has not been explored in previous studies. Determining the key cytokines associated with specific viraemia trends, such as rebound or persistence, could provide insight into the underlying mechanisms behind the observed inter-host variation following infection.

1.5 Genetic diversity of the PRRS virus

One hallmark of the PRRS virus is its high genetic diversity due to its fast mutation rate, resulting in continuous emergence of new quasi-species that may evade the host's immune system [68,69]. PRRSV has a high mutation rate estimated at $4.7\text{--}9.8 \times 10^{-2}$ nucleotides/year which was the highest reported for an RNA virus [70]. This high mutation rate causes within-animal variation in the PRRSV genome [67], with each variant termed a quasispecies. These rapid mutation rates and antigenic variability of the PRRS virus are partly responsible for the limited success in past efforts to contain PRRS and have encumbered efforts to produce vaccines that provide protection across different PRRSV isolates [71]. PRRSV evolves continuously in infected pigs, with different genes of the viral genome undergoing various degrees of change [55]. Although the mechanism(s) by which the virus persists in the host are not fully understood, the high degree of genetic and antigenic variability that characterizes PRRSV isolates are thought to play a fundamental role in viral persistence. Indeed, persistence in the host and viral diversity could be two manifestations of the same function [55].

1.5.1 The PRRS virus structure

The PRRS virion appears to be an oval-shaped particle as shown in Figure 1.1. The PRRSV genome RNA is approximately 15 kb in length and contains 11 known open reading frames (ORFs). The viral genome RNA is packed by nucleocapsid proteins. Surrounding the nucleocapsid are surface glycoproteins (GPs) and membrane proteins to form the virion particles. The structural proteins GP5, M and N are needed for both virion formation and infectivity, whilst the proteins GP2, GP3 and GP4 are needed for infectivity [51]. The link between ORF 5 and GP5 has been explored in previous studies [72, 53, 73]; ORF 5 is encoded by GP5 [53]. The structure and composition of the virion are reviewed in detail elsewhere [53, 54], but for the sake of our study we are broadly concerned with the

structural proteins in relation to their implications in the host's immune response against infection such as the antibody response in section 1.7c below.

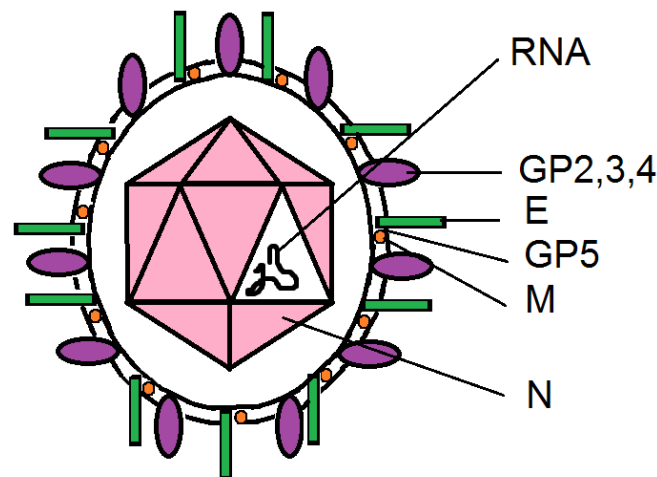


Figure 1.1 The PRRS virion: showing the structure of the small enveloped virus with a nucleocapsid core and the major and minor proteins.[74]

1.5.2 PRRS virus strains

The different PRRSV strains include: Type 1 also known as the European strain, Type 2 also known as the North American PRRSV strain, and a subset of Type 2 known as highly pathogenic PRRSV (HP PRRSV) found in Asia [2]. It was found that a Type 1 virus (Lelystad) and Type 2 virus (VR-2332) shared 55-70% nucleotide identity [75]. There is also evidence for differences in the immune responses following infection with different PRRSV strains [2,76-78]; since GP5, the major envelope protein typically involved in nAb induction and cross-protection is highly variable between Type 1 and 2, with only 50-55% identity between the two genotypes [14]. Typically the Type 2 PRRSV infection results in a higher peak viraemia load, higher respiratory and reproductive virulence and a higher evolution rate [68,76,78-80]; with the HP PRRSV infections resulting in 20% mortality in pigs of all ages and leading to the severest respiratory pathology [7]. ORF 5 homology between European field strains and 2 vaccine strains is <64% with the North American live vaccine [81].

The association between the longitudinal viraemia and longitudinal cytokine trends or nAb cross protection has not been determined for NVSL or KS06 infections, used in the PHGC challenge trials. The PRRSV virus type differences impact upon the viraemia and immune response measures following infection and thus the findings following the infection with one PRRS virus type may not be indicative of the findings following the infection with another PRRS virus type. The main focus of this thesis is *in vivo* infection with North American PRRSV isolates; the viraemia, cytokine and nAb trends found in this study are thus likely to be Type 2 specific trends.

1.5.3 North American PRRSV isolates

In this thesis we analysed infection data from two distinct North American PRRSV isolates: NVSL-97-7895 (NVSL) and KS-2006-72109 (KS06). Both are Type 2 strains, but NVSL is a highly virulent PRRSV isolate [82], while the more contemporary KS06 isolate is less virulent. NVSL and KS06 are 89% similar at the GP5 nucleotide sequence level [23]. PRRSV glycoprotein 5 (GP5) is a major envelope protein, that plays a vital role in the virion's formation and infectivity, and harbors a major neutralizing epitope [83]. This gene is often used to assess genetic differences between PRRSV isolates and is suggestive of differences in virulence between isolates [84]. Variation in GP5 impacts the pig's ability to produce neutralizing antibodies, which may not be protective against different isolates [84,85]. NVSL and KS06 were isolated from different geographic regions nearly ten years apart, and are 89% similar at the GP5 nucleotide sequence level. Molecular phylogeny clustered these viruses into two distinct branches [23].

1.6 Immune responses to a PRRSV infection

The variation of outcomes observed following a PRRSV infection are a consequence of the complex set of interactions between the virus and the host's immune response. Typically PRRSV elicits weak innate and adaptive immune responses, associated with immune modulation, but induces a strong immunosuppressive response, resulting in delayed onset of a Th1 immune response [80,86-88]. Below we briefly review the current understanding of the immune responses to a PRRSV infection relevant to this thesis (i.e. we focus on implications for viraemia, cytokines and neutralising antibodies (nAbs)).

a) Innate Immune Responses

The first line of defence in a viral infection is the innate immune response; comprising of physical barriers, chemical barriers and immune cells such as macrophages, dendritic cells and natural killer (NK) cells as well as cytokines. The latter are a large group of proteins, peptides or glycoproteins secreted by cells of the innate and adaptive immune systems that mediate many of the processes of these cells [89]. Their functions fall into three broad categories of (i) pro-inflammatory cytokines, which amplify the recruitment of innate cells to the site of infection, (ii) antiviral cytokines, which inhibit the infection of cells and the viral replication, and (iii) immune-regulatory cytokines, which orientate the adaptive response. Numerous cytokines have been reported to influence responses of pigs to PRRSV infection [22,66,87,90-94]. Cytokines don't act in isolation and their responses are transient [95].

Infection with PRRSV results in a weak induction of the innate immune response; in vitro studies on pulmonary alveolar macrophages (PAMs) have shown that PRRSV infection results in the

downregulation of IFNA (interferon alpha), and TNF-A (tumour necrosis factor alpha) and increased production of IL-1; it can thus be hypothesised that these responses could be responsible for resulting in an influx of macrophages at the site of infection, if replicated in *in vivo* conditions, this hypothesised increase in the number of potentially susceptible cells in the infected tissues could thus be a driving factor in the dynamics of a PRRSV infection [18,92,96]. The low levels of TNF-A and IFNA contribute to the high permissiveness of the target cells and the high virus replication rate.

The quantity of innate cytokines secreted in PRRSV-infected pigs is strain dependent, significantly lower compared to that associated with other viral infections, and leads to the delayed activation and dampened adaptive immunity [92]. PRRSV infection typically results in low levels of innate antiviral cytokines [2], however previous studies have established that the anti-viral cytokines IFNA, IFN-gamma, and TNF-A play a key role in the clearance of PRRS viraemia [14,66,97,98]. There are conflicting reports on IFNA expression following PRRSV infection: the North American PRRS virus can inhibit type-1 interferon production [99], or lead to no significant increases in expression following PRRSV infection [28,90]. Conversely isolate dependent increases in IFNA expression have also been observed [22,100-102]. TNF-A response to PRRSV infection is variable, often weak, and also strain dependent [78,98]. Known cytokines with immune-regulatory roles in PRRSV infection include: IL-12, IFN-gamma, IL-6, IL-4, TGF- β (transforming growth factor beta), and IL-10 [2,71,80,97,103]. Reduced NK (natural killer) cell cytotoxicity was associated with increased plasma concentrations of IL-4, IL-10 and IL-12 [101]. NK cell function regulation during PRRSV infections is coordinated by multiple cytokines: IFN-A/B, IL-12, and IL-15 [104]. Reduced NK cell activity was found in pigs with low levels of IFNA secretion [86,94,105].

Secretion of serum IL-8, IL-1 β and IFN-gamma have been found to be correlated to virus level accounting for ~84% of the observed variation [66]. IL-10 has an immune-modulatory role acting as a potent suppressor of macrophage functions [106] and the activator of antigen presenting cells through toll like receptors (TLRs) [107]. There are conflicting reports on whether PRRSV infection elicits an up-regulation of IL-10 expression [88,91,108,109] or no significant response [110,111]. Generally the role of IL-12 is typically that of activating NK cells and inducing CD4 T-cell differentiation in other species [106]. However both *in vivo* and *in vitro* treatment with IL-12 was capable of significantly reducing PRRSV titres in PAMs or in the lungs and blood [112]. IL-12 positive cells have been detected in the lung as early as 1 day post infection (dpi) with a peak at 5dpi, which suggests IL-12 expression also plays a role in pulmonary defence mechanisms against PRRSV in pigs [113].

b) Adaptive Immune Responses

The main aim of the adaptive immune response, cells and related processes is the pathogen specific elimination and prevention of pathogen growth. The adaptive immune response consists of pathogen specific clearance mechanisms comprised of highly specialised cells and systems that appear later than the innate immune response such as: the cellular response, the regulatory response and the antibody response (outlined below). The adaptive immune response is often considered the key system for the successful resolution of the infection in numerous infections and is triggered by a pathogen which successfully evades the innate immune response and hence appears at a later time than the innate response.

In many species IL-4 is a cytokine of the adaptive immune response with the principle cellular sources from CD4⁺ T cells and mast cells, targeting B cells (causing isotype switching), T cells (causing differentiation and proliferation), and Mast cells (causing proliferation)[89]. However the role of IL-4 is species dependent and in swine IL-4 is not a stimulatory factor for porcine B cells, instead it blocks antibody and IL-6 secretion and suppresses the antigen-stimulated proliferation of B cells [114]. Following a PRRSV infection IL-4 is up-regulated and appears to have some immune-modulatory consequences [101]. One study reports that swine IL-4 markedly enhanced the protective immune response of pigs and improved the efficacy of a modified live vaccine in preventing PRRS disease and resulted in a higher antibody titre, higher sera neutralizing efficacy, higher ratio of CD3⁺CD4⁺/CD3⁺CD8⁺ T lymphocytes, and lower virus loads in peripheral blood [115].

Cellular response: IFN-gamma is a regulator of the adaptive immune response [92] and appears 2-4 weeks post (PRRSV) infection. The cellular (i.e. T-cell response) to PRRSV is weak and delayed when contrasted to the peak viraemia which typically occurs between 7-9 dpi. The transient T-cell response is: variable, appears uncorrelated to the level of the virus, is detected between 4-12 weeks post infection, and remains detectable up to 3 months post infection [116]. T cells thus appear to play a secondary role in PRRS virus clearance [95]. Furthermore there was no correlation between tissue viral levels and the number of PRRSV-specific T-cells [116]. Long term persistence, discussed earlier, of the virus could be due to the ineffective cellular response against PRRSV. Conversely pigs were protected against PRRS viraemia by a live attenuated PRRSV vaccine which elicited a response with high titers of cytotoxic T cells[14]. The cellular response has the potential to be effective but may not be activated to the correct strength in hosts where the levels of viraemia remain high over time and are able to persist. However increasing the cytotoxic T cells may not significantly improve infection clearance and they remain difficult to observe both in vitro and in vivo [117]. Cytotoxic T cells and Th1 cells (T helper cells) are IFN-gamma (interferon gamma) producing cells. During a PRRSV infection the IFN-gamma levels are typically low whilst IL-10, which is produced by Th2 cells (T helper cells) and Tregs (regulatory T cells), is typically high. This immunosuppressive

cytokine, IL-10, inhibits functions of the innate, adaptive and in particular the cellular adaptive response thus indicating that PRRSV is capable of shifting the immune response towards a less effective Th2-mediated immune response. However, this may not always be observed due to inter-host variation in the synthesis of IFN-gamma. Furthermore the ability of PRRSV strains to induce protective immunity could also be dependent on their ability to induce a strong cellular immune response[71].

Regulatory response: PRRSV infection evades the host immunity through promotion of a strong immunosuppressive response, and a delayed onset of the Th1 immune response [80,86-88]. The N protein up-regulates the number of Foxp3+ T-regulatory cells (Tregs) and the IL-10 production [118]. Despite recent studies on the role of the Tregs (regulatory T cells) there are still limited results on the role of the Tregs during a PRRSV infection. However, TGF β -dependent induction of Tregs by PRRSV-infected dendritic cells has been observed and the infection of dendritic cells appears to be adequate to induce Tregs [119]. A study using an experimental infection of a North American PRRSV isolate induced Tregs from 28dpi, furthermore the Treg concentration and the viraemia were found to be positively correlated (for Type 2 infection) [120]. There appear to be strain differences between the North American and the European types in their ability to generate Tregs; the Tregs induced by the North American strain more strongly impair the host immune response than the European strain [119,121]. The exploitation of Tregs has been shown to be related to persistence in other arterivirus infections [122]. Tregs inhibit immune functions and could contribute to delayed viraemia clearance and thus the persistence of PRRSV in young pigs could be the result of an active regulatory response [71]. However the roles of Tregs, their ability to suppress antiviral immunity, and facilitate establishment of PRRSV or the effect of PRRSV infection on CD8+ T-cell frequencies has not yet been fully determined [2].

c) Antibodies

Variation is the hallmark of a PRRSV infection in both the host and the virus; high levels of genetic and antigenic variability are typically observed between different PRRSV isolates [71]. Antibody responses can be categorized into a neutralizing antibody response, where the antibody directly inhibits the function of the virus in some way [123] and non-neutralizing antibody response, where the antibody binds to the virus in order to tag it for virolysis or viral clearance via phagocytosis [124]. Following infection, the earliest and strongest antibody response is a non-neutralizing (IgG) response against the virus nucleocapsid (N) protein [125]. Virus neutralizing antibodies are typically weak and delayed during PRRSV infection but once an antibody is produced that successfully neutralizes the virus, this response is effective [123].

Understanding the host's ability to mount a non-neutralizing PRRSV-specific antibody response, such as PRRSV N-protein specific IgG, may afford a better understanding of host response to PRRSV

infection that is not specific to the isolate of PRRSV. One hypothesis is that the breadth and magnitude of the nAb (neutralizing antibody) response could have a host genetic component. Genetic improvement that enhances the response to vaccination creates the opportunity to bring the production pig closer to the vaccine that has remained so elusive for PRRS. Development of an effective PRRSV vaccine has been widely unsuccessful because they lack cross protection against different PRRSV strains [71]. Selecting pigs that are resistant to a broad selection of currently circulating PRRSV field isolates could be a successful disease control measure [126,127]; in order for this to be achieved the nAb cross-protection for pigs would need to be determined. The characterization of the breadth of the nAb response has not been conducted in previous studies.

The majority of the antibody response during infection is primarily directed against viral proteins and is not associated with virus neutralization. Antibodies with PRRSV-neutralising activity usually appear from 14-28 days post infection (dpi), when the virus levels already appear to have declined [20], and are correlated with the reduction of PRRSV in the lung and the peripheral blood [95]. There appear to be conflicting reports on the significance of neutralizing antibodies in anti-PRRSV protection [128]. The causes for the delayed production of nAbs have not been fully determined, however current potential hypothesis include:

1. Glycan shielding [84]
2. Decoy epitopes in GP5 [129]
3. Antibody dependent enhancement of viral entry into target cells [130]
4. Suppression of the innate immune response (reviewed below)[131]
5. Modulation of B cell repertoire development [117].

Virulent field isolates have been found to cause longer and more elevated viraemia profiles, and can induce a faster and more intense humoral response [132]. Antibody differences could be a reflection of the genetic differences between the PRRSV isolates. The anti-N protein antibodies appear within one week of infection [103], and can remain uncorrelated with protection against the virus [128,133], whilst a strong antibody response is also made against nsp (non-structural protein) [134,135].

Following infection the antibody response against the major surface component, the GP5-M heterodimer, is weak and delayed with some animals even failing to make a detectable antibody response against GP5 [14,136]. However it is important to note that even without the development of neutralising antibodies (nAb) viraemia resolution can occur in a PRRSV infection [17,97,137], thus the importance of the humoral response in PRRS viral clearance remains unclear. Furthermore it is important to note that PRRSV infection is not fully immunosuppressive. When antibody dependent enhancement occurs in, for example, Dengue fever then a later reinfection with a different serotype leads to a highly severe disease [138]. The same phenomenon is not observed in the infections of North American PRRSV isolates. However, the delayed production of virus neutralising antibodies

and long-term virus persistence indicates the reliance on cell-mediated immunity to clear the virus [139,140].

Currently modified live vaccinations for PRRSV can provide protection against the homologous strain, however work needs to be continued to develop a vaccine that provides adequate cross protective immunity against a wide range of strains that would be observed in field conditions [141]. Intramuscular PRRSV vaccination with a modified live virus induces a virus specific T cell response in pigs, but work needs to be done to improve the strength cross-protective immunity against challenge strains. In a recent study the route of immunisation was found to be a contributing factor in the protective impact of a modified live vaccine during a PRRSV challenge with a heterologous PRRSV strain [24]. The study showed that intramuscularly vaccinated pigs had greater numbers of RNA copies of the virus at 14 and 26 days post vaccination (dpv) than intranasally vaccinated pigs. At 26 dpv intramuscularly vaccinated pigs had increased levels of CD4 and CD8 T cells, and at 14 dpi increased levels of IFN- γ ⁺ total lymphocytes, NK, CD4, CD8 and $\gamma\delta$ T cells. Intramuscularly vaccinated pigs also had detectable nAb titres against the vaccine and challenged virus which is indicative of immune competence and could potentially be utilised in future vaccine development.

Microarray studies have the potential to obtain a deeper understanding of the molecular differences related to high or low immune competence and disease resistance for a PRRSV infection. In a recent study from the PHGC consortium the associations of gene expression with weight gain and viral load phenotypes were investigated. The effect of the single nucleotide polymorphism (SNP) marker WUR10000125 (WUR) on the porcine 60 K SNP chip on the expression in whole blood indicated that there are molecular differences in blood RNA patterns between pigs with high or low disease resistance (i.e. high or low viral load and weight gain) or with a different WUR genotype following PRRSV infection[142]. Furthermore it has been found that gene expression patterns are different between the WUR genotypes. The presence of the desirable allele (B allele) associated with the traits of weight gain and reduced cumulative viral load is associated with the presence of an intact as opposed to truncated GBP5 protein which enables the pigs to successfully inhibit viral entry and replication[143].

The majority of studies of the immune response to PRRSV do not use longitudinal data with several repeated measures. Furthermore it is not fully known how time trends in viraemia are captured in the time trends of cytokine expression following infection. The responsiveness in cytokines over the full time course of infections (0-42dpi), and the association between host genetics, the WUR genotype or viraemia trends has not been determined in previous studies. The key cytokines associated, and the timings of the strongest associations, with the viraemia measures and profiles have not been fully explored in previous studies; neither has the rate of viraemia decline and its' relationship with the strength of cytokine response been fully determined. Finally the association between the variation in

the time trends of PRRSV viraemia profiles following infection and the breadth of the nAb cross-protection is yet to be explored.

1.7 Mathematical modelling of within-host virus infection dynamics

Mathematical modelling is the representation of a system or process that allows for investigation of its' properties and, in some cases, make predictions about future outcomes using the language of mathematics. The dynamics between a host's immune system and the virus involve numerous factors and hence the principles governing the infection dynamics and outcome need more than just verbal or graphical reasoning. Mathematical models can be useful tools to represent and explore the within-host dynamics of infection. There are two distinct types of mathematical modelling approaches: process-based mechanistic mathematical modelling or a data driven statistical modelling approach.

Process based mathematical modelling is an alternative approach to exploring hypotheses surrounding the within host dynamics of viral infections. Systems of ODEs have been used to represent the various components of within host dynamics of virus infections such as HIV [144-149], influenza [150-152] and more recently PRRSV [153,154].

In this thesis, we adopt a statistical modelling approach to the data generated by the PHGC PRRSV infection trials in order to address knowledge gaps in terms of PRRSV viraemia and cytokine responses. The insights gained in our study could be used to inform, parameterise and validate future within-host PRRSV infection process-based dynamic mathematical models. A statistical modelling approach is a logical place to start when presented with experimental data such as the longitudinal measures from *in-vivo* PRRSV challenge experiments.

1.7.1 Statistical modelling and inference approaches adopted in this thesis

Statistical models establish relationships or patterns between measured quantities such as, for example, viraemia and cytokine responses over time. Firstly statistical models can allow the filtering out of noise whilst retaining the relevant features of inherently noisy biological data. Using statistical modelling we can obtain estimates for the mean response and assess factors influencing the variation on the response.

Secondly, the use of statistical inference allows the statistical relationships between different data to be determined. The main aim of the inference approach is to fit appropriate mathematical functions to data and to estimate the best function parameters. Mathematical functions with parameters that have a biological relevance are ideal candidates for statistical modelling and inference as the significant effects on the fitted model parameters can be related to the underlying biology of the system.

In this thesis we analyse both continuous data (viraemia and cytokine measures), and discrete data (nAb cross-protection and the breadth of the cytokine response). Longitudinal viraemia and cytokine measures are analysed and the time trends and associations between them are explored; whilst cross-sectional data such as the viraemia profile classes and WUR genotypes is also included in the analysis.

Statistical models are used to filter out biological noise from the data, to quantify the mean and the variation in response profiles and underlying factors responsible for the observed variation and to establish relationships between quantities over time.

1.7.2 Linear and non-linear mixed models: Mixed models are a well-established statistical modelling methodology, that allows for the inclusion of both fixed and random effects that could potentially influence the response variables [155-160]. A mixed model can be linear or non-linear. Fixed effects occur in a model when the levels of an effect constitute the entire population[161]; in this thesis, for example, the virus strain, WUR genotype, genetic background and trial are all potential fixed effects that could impact upon the viraemia. Significance of fixed effects in the model can be determined according to the F-test at the 95% significance level [161]. A random effect is modelled when conclusions are to be drawn about the population from which the observed units were taken, rather than about the particular units themselves [162]; in this thesis the effect of pig, or pen, were potential random effects in the model. The significance of random effects can be determined by the likelihood ratio test (LRT) at the 95% significance level. In summary, fixed effects have levels that are of primary interest and would be used again if the experiment were repeated, whilst random effects have levels that can be considered as a random selection from a much larger set of levels [163]. The standard linear mixed model is represented by the following equations:

$$Y = X_b b + Zu + \varepsilon \quad (1)$$

$$u \sim N(0, G)$$

$$\varepsilon \sim N(0, R)$$

Where: Y is the vector of the response variables (e.g. viraemia or cytokine), b is the vector of fixed effects, u is the vector of random effects, and ε is the vector of the residual effects. The matrices X_b , and Z are incidence matrices assigning individuals to their corresponding effects. G and R are the covariance matrices for the random effects and the random errors, respectively. It is generally assumed that the covariance between random effects and errors is zero.

Mixed models can be applied to both, cross-sectional or longitudinal data with continuous or discrete predictors. They allow for great flexibility in the covariance structures, e.g. by allowing for serial correlation between consecutive observations along a longitudinal viraemia or cytokine profile[164].

In this thesis, linear mixed models were used to analyse the viraemia and cytokine responses of the PRRSV infected pigs over time and in relation to each other.

In this thesis, linear mixed models were implemented using PROC MIXED in SAS. The MIXED procedure estimates parameters by likelihood or moment- based techniques[161] . In this thesis the default fitting method was used i.e. maximizing the restricted likelihood of the data under the assumption that the data are normally distributed and any missing data are missing at random.

The linear mixed modelling framework was adopted in Chapters 2 & 4 of this thesis. Whereas Chapter 2 implemented linear mixed models to identify influencing factors determining the PRRS viraemia profiles, in Chapter 4 mixed models were applied for multiple regression. These were used to determine the statistically significant associations between viraemia measures and their preceding cytokine viraemia measures, i.e. using viraemia measures as the response variables and the preceding cytokine measures as the potential predictors, and *vice versa*.

To perform multiple regression, additional covariates representing potential predictors were added to the null model (equation (1)) for testing the associations between viraemia and cytokine and vice versa:

$$Y = X_b b + X_c c + Zu + \varepsilon \quad (2)$$

Where in addition to the terms defined in equation (1), c is the vector of fixed effects for the additional covariates, the matrix X_c is the incidence matrix assigning individuals to their corresponding additional fixed effects.

Mixed models were also used to perform logistic regression to obtain odds ratios associated with discrete data in order to determine the association of nAb cross protection (broad or narrow) and cytokine responsiveness (high responsiveness or low) with viral profile class, WUR and genetic background. Logistic regression was implemented using PROC GLIMMIX in SAS 9.3, which allows for the inclusion of both fixed and random effects included in the model. For analysis of categorical data a generalized linear mixed model (GLMM) was applied with a logit link function:

$$E[Y|u] = g^{-1}(Xb + Zu) \quad (3)$$

Where Y is the vector of the response variable, b is the vector of fixed effects, u is the vector of random effects and g^{-1} is the inverse logit link function.

The logit link function is a standard link function and is defined as follows:

$$g(p) = \ln\left(\frac{p}{1-p}\right) \quad (4)$$

Unless stated otherwise, residual errors were assumed to be independently normally distributed. However, models that included repeated measurements serial correlations between consecutive measures were implemented in the residual error structure.

Non-linear mixed models can also be implemented in SAS using PROC NLMIXED, however it was not used in this thesis due to a failure to converge with the inclusion of fixed effects when applied to the viraemia data. Mixed models can also be implemented in Bayesian framework however this approach was not adopted in this thesis.

1.7.3 Repeated measures models

The response variable in this PRRSV experiment was measured at different time points between 0-42dpi thus a further modification to the linear mixed models framework described above was adopted for “repeated measures” modelling in Chapter 2 and 4. In this thesis repeated measure models are mixed models implemented using the mixed modelling framework in SAS in which time is included as a fixed effect and the serial correlation was represented by specifying a correlation structure in the residuals.

1.7.4 Curve fitting

For the analysis of the longitudinal viraemia and cytokine measures two types of curve fitting approaches were adopted: spline functions and established mathematical functions with few parameters with a related biological meaning.

a) Spline functions: are defined as piecewise polynomial functions, of degree n , the pieces join at “knots” whose location and number can be specified in programs such as MATLAB[165]. Splines have the flexibility to capture disjointed time trends [165]. Splines are a useful and convenient statistical tool for expressing the relationship between measured traits due to their flexibility and ability to adjust well to the data [166]. For example in previous animal science studies splines have been used, and are not limited, to: expressing the relationship between the body area and the live weight of pigs before conducting mixed models analysis[167], estimating of genetic parameters for lactation [168], and the genetic evaluation of growth in beef cattle [169]. Polynomials with a high degree of mathematical complexity often provide a good empirical fit to a set of data [170]. Splines are particularly useful tool for cleaning noise from the observational data or determining the role of influencing factors at different stages of the spline. In Chapter 4 splines are used to filter noise from the longitudinal cytokine profiles. The limitation in the spline approach, however, is that this method doesn’t lend itself for the extraction of fitted parameters that specify physical properties of the biological system, which would be important for the understanding the dynamics of PRRSV infection.

Hence in the next section the curve fitting approach in which parameter estimates with a biological interpretation for the quantitative assessment of viraemia profile characteristics is outlined.

b) Mathematical functions with biological interpretation: Numerous previous studies have used non-linear mathematical functions for the quantitative analysis of growth, weight gain and lactation [160,171-182] . Non-linear functions have been used to describe the temporal evolution of measured quantities to assess individual patterns (such as in milk yield [171]) and quantify inter-host variation for subsequent genetic analysis [168,174].

The Wood's curve, an incomplete gamma function often used to model lactation yield in dairy cattle [172-174], will be used to describe viraemia profiles in this thesis:

$$Y(t) = a_1 t^{b_1} e^{-c_1 t}$$

where $Y(t)$ is serum viraemia on the \log_{10} scale at time t dpi, a_1 impacts the magnitude of all points on the curve, b_1 is an indicator of the initial rate of increase to peak viraemia, c_1 is an indicator of the rate of decline after the peak and dominates the viraemia profile at the later stages of infection. Using the piglet specific curve parameters estimates, \widehat{a}_1 , \widehat{b}_1 , and \widehat{c}_1 , a fitted viraemia value can be estimated for each piglet for each time point ($\widehat{Y}(t)$).

Derived phenotypes can be generated from the Wood's model and are outlined below. The area under the Wood's curve (AUC) up to each observation, (e.g 0-21dpi), was given by the definite integral:

$$I_{21} = \int_0^{21} \widehat{a}_1 t^{\widehat{b}_1} e^{-\widehat{c}_1 t} dt$$

The viraemia AUC is a measure of both the level of viraemia and the extent to which viraemia is maintained. The range 0-21 dpi is presented above but I4, I7, ..., I35,42 can also be obtained to explore different phases of the infection. Previous analyses on the PHGC trials 1-8 fitted a Loess curve through viraemia and integrated to get area under the curve from 0-21 dpi [33,45,46]. In Appendix 4 the results from these two approaches for the AUC will be compared.

The time to peak of the curve (T_{max}), derived by setting the first derivative of the Wood's equation to zero and solving for t , resulting in:

$$T_{max} = \frac{\widehat{b}_1}{\widehat{c}_1}$$

The value of the peak viraemia (V_{max}), which was calculated by setting $t = T_{max}$ in the Wood's equation:

$$V_{\max} = \hat{a}_1 \left(\frac{\hat{b}_1}{\hat{c}_1} \right)^{\hat{b}_1} e^{-\hat{b}_1}$$

When used for modelling viraemia the terms T_{\max} and V_{\max} are related to the host's ability to respond during the replication-dominant phase of early PRRSV infection [183]. V_{\max} is reached when the rate of virus clearance from serum is equal to the number of virus particles released into the blood stream. T_{\max} is the time it takes to reach V_{\max} , with animals that can mount a response early in infection expected to have a shorter T_{\max} .

Curve characteristics that relate to the host's response to the post-peak, clearance-dominant phase of PRRSV infection can also be derived from the Wood's model. The maximal decay rate (ΔV) is reached when the rate of viral clearance from serum is highest compared to the rate of viral replication. Time to maximal decay (ΔT) was derived by setting the second derivative of the Wood's equation to zero and solving for t :

$$\Delta T = \frac{\hat{b} + \sqrt{\hat{b}}}{\hat{c}}$$

Substituting this value in for t in the first derivative and taking the absolute value gave ΔV :

$$\Delta V = \left| -\hat{a}\sqrt{\hat{b}} \left(\frac{\hat{b} + \sqrt{\hat{b}}}{\hat{c}} \right)^{\hat{b}-1} e^{-(\hat{b}+\sqrt{\hat{b}})} \right|$$

ΔV is thus defined as the absolute value of the first derivative for ease of interpretation, whereby an animal with a larger ΔV cleared viraemia from the serum more quickly.

In this thesis the estimation of the Woods model parameters was carried out using 2 alternative approaches: linear mixed models and Bayesian inference. The derived parameters from the Woods model will be used for genetic analysis in Appendix 4.

1.7.5 Bayesian inference: Mathematical functions can be fit to longitudinal data in a classical frequentist framework (incorporated e.g. with PROC MIXED in SAS in Chapters 2 and 4) or via Bayesian inference (Chapter 3). Due to limitations encountered in the model fitting in Chapter 2 we adopt a Bayesian model fitting approach in Chapter 3. In depth reviews of the benefits and limitations of the Bayesian approach can be found in [184-188]. Bayesian inference allows a way of combining prior information with data within a solid decision theoretical framework. Bayesian model fitting has a typically higher computational cost, especially in models with a large number of parameters, than the frequentist approach. In Chapter 3 model fitting was conducted using Bayesian inference with a likelihood framework. This approach allows for the fitting of a wider range of functions to the data than the linear mixed models approach, i.e. the fitting of bimodal functions. Model parameter

inferences follow from Bayes' theorem, and posterior distributions are obtained for the model parameters:

$$P(\theta|data) = \frac{P(data|\theta)P(\theta)}{P(D)}$$

Where $P(\theta|data)$ is the posterior distribution of the parameter given the data, $P(data|\theta)$ is the likelihood, $P(\theta)$ is the prior distribution for the parameters, and $P(D) = \int_{-\infty}^{\infty} P(D|\theta)P(\theta)d\theta$ is a normalizing constant.

1.8 Thesis outline

The overarching aim of this thesis is to gain insights into the within-host dynamics of an *in-vivo* PRRSV infection using a statistical modelling approach. We aimed to quantify the inter-host variation, explore the time trends of the longitudinal viraemia and cytokine measures, and determine the influencing factors on these as well as the relationship between the viraemia and immune response characteristics over time. Data analysis was conducted on longitudinal viraemia, cytokine measures and nAbs cross-protection data generated by the recent PRRS Host Genetic Consortium (PHGC) infection trials; in which pigs were challenged with one of two PRRS virus isolates (NVSL or KS06).

Various mathematical functions will be applied to the data generated from the PRRSV challenge study in this thesis. The candidate functions will be chosen according to visual properties of the data with the ideal candidate capturing the biological phenomenon, removing experimental noise and being a suitable description of the data for obtaining derived phenotypes with biological relevance. Spline functions will be applied in cases where a clear pattern is not observed. Alternative highly relevant functions that could have been applied to the data include, but not limited to: Legendre polynomials [189], the Ali-Schaeffer curve [190], the Wilink curve [191], the Lidauer-Mäntysaari function [192], and regression splines [193].

In Chapter 2 we apply the linear mixed model framework to analyse viraemia time trends and the corresponding influencing factors. In particular, two alternative approaches (repeated measures models and linearized mathematical power functions) are used to address the following questions:

- What are the typical time trends in the PHGC viraemia data?
 - How are these time trends influenced by the virus isolate, genetic background, trial and WUR genotype?
- Can the variation in viraemia time trends of pigs be adequately captured by linear mixed models?

- What impact do bimodal profiles have on the model fits and the significant fixed effects?
- How suitable is the linear mixed modelling approach for modelling the full range of observed viraemia trends and what are the limitations?

The longitudinal viraemia measures from the PHGC PRRSV challenge experiment reveal substantial differences in the viraemia profiles between hosts infected with the same PRRSV challenge dose, pointing to considerable variation in the host response to PRRSV infections. The limitations in the ability to fit bimodal functions and the poor fit of the linearized approach in Chapter 2 led to a Bayesian model fitting approach being adopted in Chapter 3. Given the apparent diversity in viraemia patterns, several important questions will be explored in Chapter 3:

- Is the viraemia rebound (or bimodal viraemia profile) phenomenon genuine and evenly distributed across all trials?
- Can the information derived from the early stage of infection be used to predict the serum viraemia characteristics at the later stage of infection?
- Can we quantify inter-host variation from all types of viraemia profiles with a mathematical function?
- Can we define an objective method of classifying viraemia profiles?
- Can we adequately represent the full range of viraemia profiles obtained from a large scale PRRSV infection experiment, and use these to determine quantitative characteristics of infection dynamics?
- Is there a relationship between the breadth of the nAb response and the WUR genotype or viraemia profile classes?

In Chapter 4 we combine the viraemia profiles with measures of the immune response in the form of longitudinal cytokine profiles. Linear and non-linear mixed models are used in Chapter 4 to explore and answer the following questions:

- What are the typical time trends in the PHGC cytokine data?
 - How are these time trends influenced by the virus isolate, genetic background, trial and WUR genotype?
 - Are host differences in viraemia patterns also reflected by differences in the cytokine expression profiles?
- How are the cytokine responses related to each other?
 - Is the strength of cytokine response related between the cytokines and how does this relationship change over the time course of the experiment?

- Which cytokines are related to each other and what are the key timings of the strongest associations?
- Is there a relationship between the cytokine responsiveness and the WUR genotype, host genetic background or viraemia profile classes defined in Chapter 3?
- What is the relationship between cytokine and viraemia response over time?
 - Does a stronger cytokine response imply a faster rate of viraemia decline?
 - Is the strength of the cytokine response related to the strength of the viraemia load?
 - Which were the key serum cytokines, and timings for serum viral dynamics?
- Do cytokines drive viraemia characteristics or vice versa?

In the General Discussion we summarise the novel findings of this thesis outlining the limitations and implications of the findings for future PRRSV research. Furthermore the host genetic impact on the new phenotypes derived in Chapter 3 are used in the quantitative genetic study presented in Appendix 3.

References for Chapter 1

1. Brockmeier SL, Halbur PG, Thacker EL (2002) Porcine respiratory disease complex.
2. Lunney JK, Fang Y, Ladinig A, Chen N, Li Y, et al. (2015) Porcine Reproductive and Respiratory Syndrome Virus (PRRSV): Pathogenesis and Interaction with the Immune System. *Annual review of animal biosciences* 4 (2016): : 129-154.
3. Neumann EJ, Kliebenstein JB, Johnson CD, Mabry JW, Bush EJ, et al. (2005) Assessment of the economic impact of porcine reproductive and respiratory syndrome on swine production in the United States. *Journal of the American Veterinary Medical Association* 227: 385-392.
4. OIE (2015) Porcine reproductive and respiratory syndrome. *OIE Terrestrial Manual* 2015.
5. Goyal SM (1993) Porcine reproductive and respiratory syndrome. *Journal of Veterinary Diagnostic Investigation* 5: 656-664.
6. Dietze K, Pinto J, Wainwright S, Hamilton C, Khomenko S (2011) Porcine reproductive and respiratory syndrome (PRRS). *Focus on 5*.
7. Tian K, Yu X, Zhao T, Feng Y, Cao Z, et al. (2007) Emergence of fatal PRRSV variants: unparalleled outbreaks of atypical PRRS in China and molecular dissection of the unique hallmark. *PloS one* 2: e526.
8. Wu J, Li J, Tian F, Ren S, Yu M, et al. (2009) Genetic variation and pathogenicity of highly virulent porcine reproductive and respiratory syndrome virus emerging in China. *Archives of virology* 154: 1589-1597.
9. Li B, Fang L, Liu S, Zhao F, Jiang Y, et al. (2010) The genomic diversity of Chinese porcine reproductive and respiratory syndrome virus isolates from 1996 to 2009. *Veterinary microbiology* 146: 226-237.
10. Duan X, Nauwynck H, Pensaert M (1997) Effects of origin and state of differentiation and activation of monocytes/macrophages on their susceptibility to porcine reproductive and respiratory syndrome virus (PRRSV). *Archives of virology* 142: 2483-2497.
11. Lawson SR, Rossow KD, Collins JE, Benfield DA, Rowland RRR (1997) Porcine reproductive and respiratory syndrome virus infection of gnotobiotic pigs: sites of virus replication and co-localization with MAC-387 staining at 21 days post-infection. *Virus Research* 51: 105-113.
12. Thanawongnuwech R, Halbur PG, Thacker EL (2000) The role of pulmonary intravascular macrophages in porcine reproductive and respiratory syndrome virus infection. *Animal Health Research Reviews* 1: 95-102.
13. Sirinarumitr T, Zhang Y, Kluge JP, Halbur PG, Paul PS (1998) A pneumo-virulent United States isolate of porcine reproductive and respiratory syndrome virus induces apoptosis in bystander cells both in vitro and in vivo. *Journal of general virology* 79: 2989.
14. Kimman TG, Cornelissen LA, Moormann RJ, Rebel JMJ, Stockhofe-Zurwieden N (2009) Challenges for porcine reproductive and respiratory syndrome virus (PRRSV) vaccinology. *Vaccine* 27: 3704-3718.
15. Lewis CRG, Ait-Ali T, Clapperton M, Archibald AL, Bishop S (2007) Genetic perspectives on host responses to porcine reproductive and respiratory syndrome (PRRS). *Viral immunology* 20: 343-358.
16. Lunney JK, Chen H (2010) Genetic control of host resistance to porcine reproductive and respiratory syndrome virus (PRRSV) infection. *Virus Research* 154: 161-169.
17. Mateu E, Diaz I (2008) The challenge of PRRS immunology. *The Veterinary Journal* 177: 345-351.
18. Albina E, Piriou L, Hutet E, Cariolet R, L'Hospitalier R (1998) Immune responses in pigs infected with porcine reproductive and respiratory syndrome virus (PRRSV). *Veterinary immunology and immunopathology* 61: 49-66.
19. Zimmerman J, Yoon KJ, Wills R, Swenson S (1997) General overview of PRRSV: a perspective from the United States. *Veterinary microbiology* 55: 187-196.
20. Molitor T, Bautista E, Choi C (1997) Immunity to PRRSV: double-edged sword. *Veterinary microbiology* 55: 265-276.

21. Lunney JK, Steibel JP, Reecy JM, Fritz E, Rothschild MF, et al. Probing genetic control of swine responses to PRRSV infection: current progress of the PRRS host genetics consortium; 2011. BioMed Central Ltd. pp. 30.
22. Ladinig A, Lunney JK, Souza CJ, Ashley C, Plastow G, et al. (2014) Cytokine profiles in pregnant gilts experimentally infected with porcine reproductive and respiratory syndrome virus and relationships with viral load and fetal outcome. *Veterinary research* 45: 113.
23. Ladinig A, Detmer SE, Clarke K, Ashley C, Rowland RRR, et al. (2015) Pathogenicity of three type 2 porcine reproductive and respiratory syndrome virus strains in experimentally inoculated pregnant gilts. *Virus Research* 203: 24-35.
24. Ouyang K, Hiremath J, Binjawadagi B, Shyu D-L, Dhakal S, et al. (2016) Comparative analysis of routes of immunization of a live porcine reproductive and respiratory syndrome virus (PRRSV) vaccine in a heterologous virus challenge study. *Veterinary research* 47: 1.
25. Yoon K-J, Zimmerman JJ, Chang CC, Cancel-Tirado S, Harmon KM, et al. (1999) Effect of challenge dose and route on porcine reproductive and respiratory syndrome virus (PRRSV) infection in young swine. *Veterinary research* 30: 629-638.
26. Hermann J, Munoz-Zanzi C, Roof M, Burkhart K, Zimmerman J (2005) Probability of porcine reproductive and respiratory syndrome (PRRS) virus infection as a function of exposure route and dose. *Veterinary microbiology* 110: 7-16.
27. Boddicker N, Waide E, Rowland R, Lunney J, Garrick D, et al. (2012) Evidence for a major QTL associated with host response to Porcine Reproductive and Respiratory Syndrome virus challenge. *Journal of Animal Science* 90: 1733-1746.
28. Lawson S, Lunney J, Zuckermann F, Osorio F, Nelson E, et al. (2010) Development of an 8-plex Luminex assay to detect swine cytokines for vaccine development: assessment of immunity after porcine reproductive and respiratory syndrome virus (PRRSV) vaccination. *Vaccine* 28: 5356-5364.
29. Rowland RR, Steffen M, Ackerman T, Benfield DA (1999) The evolution of porcine reproductive and respiratory syndrome virus: quasispecies and emergence of a virus subpopulation during infection of pigs with VR-2332. *Virology* 259: 262-266.
30. Reiner G, Willems H, Pesch S, Ohlinger V (2009) Variation in resistance to the porcine reproductive and respiratory syndrome virus (PRRSV) in Pietrain and Miniature pigs. *Journal of Animal Breeding and Genetics* 127: 100-106.
31. Vincent A, Thacker B, Halbur P, Rothschild M, Thacker E (2005) In vitro susceptibility of macrophages to porcine reproductive and respiratory syndrome virus varies between genetically diverse lines of pigs. *Viral immunology* 18: 506-512.
32. Vincent A, Thacker B, Halbur P, Rothschild M, Thacker E (2006) An investigation of susceptibility to porcine reproductive and respiratory syndrome virus between two genetically diverse commercial lines of pigs. *Journal of Animal Science* 84: 49-57.
33. Boddicker NJ, Bjorkquist A, Rowland RRR, Lunney JK, Reecy JM, et al. (2014) Genome-wide association and genomic prediction for host response to porcine reproductive and respiratory syndrome virus infection. *Genetics Selection Evolution* 46.
34. Boddicker NJ, Garrick DJ, Rowland RRR, Lunney JK, Reecy JM, et al. (2013) Validation and further characterization of a major quantitative trait locus associated with host response to experimental infection with porcine reproductive and respiratory syndrome virus. *Animal Genetics*: n/a-n/a.
35. Hess AS, Boddicker N, Rowland B, Lunney J, Plastow G, et al. (2014) Validation of the Effects of a SNP on SSC4 Associated with Viral Load and Weight Gain in Piglets Experimentally Infected with a 2006 PRRS Virus Isolate. *Animal Industry Report* 660: 89.
36. Halbur P, Rothschild M, Thacker B, Meng XJ, Paul P, et al. (1998) Differences in susceptibility of Duroc, Hampshire, and Meishan pigs to infection with a high virulence strain (VR2385) of porcine reproductive and respiratory syndrome virus (PRRSV). *Journal of Animal Breeding and Genetics* 115: 181-189.

37. Lowe JF, Husmann R, Firkins LD, Zuckermann FA, Goldberg TL (2005) Correlation of cell-mediated immunity against porcine reproductive and respiratory syndrome virus with protection against reproductive failure in sows during outbreaks of porcine reproductive and respiratory syndrome in commercial herds. *Journal of the American Veterinary Medical Association* 226: 1707-1711.
 38. Ait-Ali T, Wilson AD, Westcott DG, Clapperton M, Waterfall M, et al. (2007) Innate immune responses to replication of porcine reproductive and respiratory syndrome virus in isolated Swine alveolar macrophages. *Viral immunology* 20: 105-118.
 39. Rowland RR, Joan Lunney, and Jack Dekkers. (2012) Control of porcine reproductive and respiratory syndrome (PRRS) through genetic improvement in disease resistance and tolerance. *Frontiers of Livestock Genomics*: 3:260.
 40. Petry D, Holl J, Weber J, Doster AR, Osorio FA, et al. (2005) Biological responses to porcine respiratory and reproductive syndrome virus in pigs of two genetic populations. *Journal of Animal Science* 83: 1494-1502.
 41. Reiner G, Willems H, Pesch S, Ohlinger V (2010) Variation in resistance to the porcine reproductive and respiratory syndrome virus (PRRSV) in Pietrain and Miniature pigs. *Journal of Animal Breeding and Genetics* 127: 100-106.
 42. Lewis C, Torremorell M, Galina-Pantoja L, Bishop S (2009) Genetic parameters for performance traits in commercial sows estimated before and after an outbreak of porcine reproductive and respiratory syndrome. *Journal of Animal Science* 87: 876-884.
 43. Lewis C, Torremorell M, Bishop S (2009) Effects of porcine reproductive and respiratory syndrome virus infection on the performance of commercial sows and gilts of different parities and genetic lines. *J Swine Health Prod* 17: 140-147.
 44. Boddicker NJG, Dorian J.; Reecy, James M.; Rowland, Bob; Lunney, Joan K.; and Dekkers, Jack C. M. (2013) Quantitative Trait Locus on *Sus scrofa* Chromosome 4 Associated with Host Response to Experimental Infection with Porcine
- Reproductive and Respiratory Syndrome Virus Animal Industry Report AS 659, ASL R2823.
45. Boddicker NJ, Garrick DJ, Rowland RRR, Lunney JK, Reecy JM, et al. (2014) Validation and further characterization of a major quantitative trait locus associated with host response to experimental infection with porcine reproductive and respiratory syndrome virus. *Animal Genetics* 45: 48-58.
 46. Boddicker N, Waide EH, Rowland RRR, Lunney JK, Garrick DJ, et al. (2012) Evidence for a major QTL associated with host response to Porcine Reproductive and Respiratory Syndrome Virus challenge. *Journal of Animal Science* 90: 1733-1746.
 47. Kim J, Ahn H, Woo H-M, Lee E, Lee G-S (2014) Characterization of porcine NLRP3 inflammasome activation and its upstream mechanism. *Veterinary research communications* 38: 193-200.
 48. Shenoy AR, Wellington DA, Kumar P, Kassa H, Booth CJ, et al. (2012) GBP5 Promotes NLRP3 Inflammasome Assembly and Immunity in Mammals. *Science* 336: 481-485.
 49. Koltes JE, Fritz-Waters E, Easley CJ, Choi IS, Bao H, et al. (2015) Identification of a putative quantitative trait nucleotide in guanylate binding protein 5 for host response to PRRS virus infection. *BMC Genomics* 16: (28 May 2015)-(2028 May 2015).
 50. Snijder EJ, Kikkert M, Fang Y (2013) Arterivirus molecular biology and pathogenesis. *Journal of general virology* 94: 2141-2163.
 51. Chand RJ, Tribble BR, Rowland RRR (2012) Pathogenesis of porcine reproductive and respiratory syndrome virus. *Current Opinion in Virology*: 2:256-263.
 52. Wensvoort G, Terpstra C, Pol J, Ter Laak E, Bloemraad M, et al. (1991) Mystery swine disease in The Netherlands: the isolation of Lelystad virus. *Veterinary Quarterly* 13: 121-130.
 53. Dea S, Gagnon C, Mardassi H, Pirzadeh B, Rogan D (2000) Current knowledge on the structural proteins of porcine reproductive and respiratory syndrome (PRRS) virus: comparison of the North American and European isolates. *Archives of virology* 145: 659-688.
 54. Dokland T (2010) The structural biology of PRRSV. *Virus Research* 154: 86-97.

55. Chang CC, Yoon KJ, Zimmerman J, Harmon K, Dixon P, et al. (2002) Evolution of porcine reproductive and respiratory syndrome virus during sequential passages in pigs. *Journal of virology* 76: 4750-4763.
56. Wills RW, Zimmerman JJ, Yoon KJ, McGinley MJ, Hill HT, et al. (1997) Porcine reproductive and respiratory syndrome virus: A persistent infection. *Veterinary Microbiology* 55: 231-240.
57. Wills RW, Doster AR, Galeota JA, Sur JH, Osorio FA (2003) Duration of infection and proportion of pigs persistently infected with porcine reproductive and respiratory syndrome virus. *Journal of Clinical Microbiology* 41: 58-62.
58. Mulupuri P, Zimmerman JJ, Hermann J, Johnson CR, Cano JP, et al. (2008) Antigen-specific B-cell responses to porcine reproductive and respiratory-syndrome-virus infection. *Journal of Virology* 82: 358-370.
59. Doeschl-Wilson A, Kyriazakis I, Vincent A, Rothschild M, Thacker E, et al. (2009) Clinical and pathological responses of pigs from two genetically diverse commercial lines to porcine reproductive and respiratory syndrome virus infection. *Journal of Animal Science* 87: 1638-1647.
60. Islam ZU, Bishop SC, Savill NJ, Rowland RR, Lunney JK, et al. (2013) Quantitative Analysis of Porcine Reproductive and Respiratory Syndrome (PRRS) Viremia Profiles from Experimental Infection: A Statistical Modelling Approach. *PloS one* 8: e83567.
61. Klinge KL, Vaughn EM, Roof MB, Bautista EM, Murtaugh MP (2009) Age-dependent resistance to Porcine reproductive and respiratory syndrome virus replication in swine. *Virology journal* 6: 1.
62. Loving CL, Brockmeier SL, Sacco RE (2007) Differential type I interferon activation and susceptibility of dendritic cell populations to porcine arterivirus. *Immunology* 120: 217-229.
63. Wills RW, Doster AR, Galeota JA, Sur J-H, Osorio FA (2003) Duration of infection and proportion of pigs persistently infected with porcine reproductive and respiratory syndrome virus. *Journal of clinical microbiology* 41: 58-62.
64. Petry D, Lunney J, Boyd P, Kuhar D, Blankenship E, et al. (2007) Differential immunity in pigs with high and low responses to porcine reproductive and respiratory syndrome virus infection. *Journal of Animal Science* 85: 2075-2092.
65. Yoo D, Song C, Sun Y, Du Y, Kim O, et al. (2010) Modulation of host cell responses and evasion strategies for porcine reproductive and respiratory syndrome virus. *Virus Research* 154: 48-60.
66. Lunney JK, Fritz ER, Reecy JM, Kuhar D, Prucnal E, et al. (2010) Interleukin-8, interleukin-1 β , and interferon- γ levels are linked to PRRS virus clearance. *Viral immunology* 23: 127-134.
67. Goldberg TL, Lowe JF, Milburn SM, Firkins LD (2003) Quasispecies variation of porcine reproductive and respiratory syndrome virus during natural infection. *Virology* 317: 197-207.
68. Prieto C, Vázquez A, Núñez JI, Álvarez E, Simarro I, et al. (2009) Influence of time on the genetic heterogeneity of Spanish porcine reproductive and respiratory syndrome virus isolates. *The Veterinary Journal* 180: 363-370.
69. Goldberg TL, Lowe JF, Milburn SM, Firkins LD (2003) Quasispecies variation of porcine reproductive and respiratory syndrome virus during natural infection☆. *Virology* 317: 197-207.
70. Murtaugh MP, Stadejek T, Abrahante JE, Lam TTY, Leung FCC (2010) The ever-expanding diversity of porcine reproductive and respiratory syndrome virus. *Virus Research* 154: 18-30.
71. Darwich L, Díaz I, Mateu E (2010) Certainties, doubts and hypotheses in porcine reproductive and respiratory syndrome virus immunobiology. *Virus Research* 154: 123-132.
72. Li B, Xiao S, Wang Y, Xu S, Jiang Y, et al. (2009) Immunogenicity of the highly pathogenic porcine reproductive and respiratory syndrome virus GP5 protein encoded by a synthetic ORF5 gene. *Vaccine* 27: 1957-1963.

73. Johnson CR, Griggs TF, Gnanandarajah J, Murtaugh MP (2011) Novel structural protein in porcine reproductive and respiratory syndrome virus encoded by an alternative ORF5 present in all arteriviruses. *Journal of general virology* 92: 1107-1116.
74. <http://www.porcilis-prrs.com/microbiology-prrsv-structure.asp> (2016) PRRS virus structure
75. Vanhee M, Van Breedam W, Costers S, Geldhof M, Noppe Y, et al. (2011) Characterization of antigenic regions in the porcine reproductive and respiratory syndrome virus by the use of peptide-specific serum antibodies. *Vaccine* 29: 4794-4804.
76. Weesendorp E, Morgan S, Stockhofe-Zurwieden N, Popma-De Graaf DJ, Graham SP, et al. (2013) Comparative analysis of immune responses following experimental infection of pigs with European porcine reproductive and respiratory syndrome virus strains of differing virulence. *Veterinary microbiology* 163: 1-12.
77. Murtaugh M, Elam M, Kakach L (1995) Comparison of the structural protein coding sequences of the VR-2332 and Lelystad virus strains of the PRRS virus. *Archives of virology* 140: 1451-1460.
78. Darwich L, Gimeno M, Sibila M, Diaz I, De La Torre E, et al. (2011) Genetic and immunobiological diversities of porcine reproductive and respiratory syndrome genotype I strains. *Veterinary microbiology* 150: 49-62.
79. Mengeling W, Vorwald A, Lager K, Brockmeier S (1996) Comparison among strains of porcine reproductive and respiratory syndrome virus for their ability to cause reproductive failure. *American journal of veterinary research* 57: 834-839.
80. Diaz I, Darwich L, Pappaterra G, Pujols J, Mateu E (2005) Immune responses of pigs after experimental infection with a European strain of porcine reproductive and respiratory syndrome virus. *Journal of general virology* 86: 1943-1951.
81. grosse Beilage E, Nathues H, Meemken D, Harder TC, Doherr MG, et al. (2009) Frequency of PRRS live vaccine virus (European and North American genotype) in vaccinated and non-vaccinated pigs submitted for respiratory tract diagnostics in North-Western Germany. *Preventive veterinary medicine* 92: 31-37.
82. Truong HM, Lu Z, Kutish GF, Galeota J, Osorio FA, et al. (2004) A highly pathogenic porcine reproductive and respiratory syndrome virus generated from an infectious cDNA clone retains the in vivo virulence and transmissibility properties of the parental virus. *Virology* 325: 308-319.
83. Ostrowski M, Galeota JA, Jar AM, Platt KB, Osorio FA, et al. (2002) Identification of neutralizing and nonneutralizing epitopes in the porcine reproductive and respiratory syndrome virus GP5 ectodomain. *Journal of Virology* 76: 4241-4250.
84. Ansari IH, Kwon B, Osorio FA, Pattnaik AK (2006) Influence of N-linked glycosylation of porcine reproductive and respiratory syndrome virus GP5 on virus infectivity, antigenicity, and ability to induce neutralizing antibodies. *Journal of virology* 80: 3994-4004.
85. Pirzadeh B, Gagnon CA, Dea S (1998) Genomic and antigenic variations of porcine reproductive and respiratory syndrome virus major envelope GP(5) glycoprotein. *Canadian Journal of Veterinary Research-Revues Canadienne De Recherche Veterinaire* 62: 170-177.
86. Renukaradhya GJ, Alekseev K, Jung K, Fang Y, Saif LJ (2010) Porcine Reproductive and Respiratory Syndrome Virus–Induced Immunosuppression Exacerbates the Inflammatory Response to Porcine Respiratory Coronavirus in Pigs. *Viral immunology* 23: 457-466.
87. Johnsen C, Bøtner A, Kamstrup S, Lind P, Nielsen J (2002) Cytokine mRNA profiles in bronchoalveolar cells of piglets experimentally infected in utero with porcine reproductive and respiratory syndrome virus: association of sustained expression of IFN- γ and IL-10 after viral clearance. *Viral immunology* 15: 549-556.
88. Suradhat S, Thanawongnuwech R, Poovorawan Y (2003) Upregulation of IL-10 gene expression in porcine peripheral blood mononuclear cells by porcine reproductive and respiratory syndrome virus. *Journal of general virology* 84: 453-459.

89. Abbas AK, Lichtman AH, Pillai S (2014) Cellular and Molecular Immunology: with STUDENT CONSULT Online Access: Elsevier Health Sciences.
90. Gómez-Laguna J, Salguero FJ, De Marco MF, Pallarés FJ, Bernabé A, et al. (2009) Changes in lymphocyte subsets and cytokines during European porcine reproductive and respiratory syndrome: increased expression of IL-12 and IL-10 and proliferation of CD4⁺ CD8^{high}. *Viral immunology* 22: 261-271.
91. Gomez-Laguna J, Salguero F, Barranco I, Pallares F, Rodriguez-Gomez I, et al. (2010) Cytokine expression by macrophages in the lung of pigs infected with the porcine reproductive and respiratory syndrome virus. *Journal of comparative pathology* 142: 51-60.
92. Van Reeth K, Labarque G, Nauwynck H, Pensaert M (1999) Differential production of proinflammatory cytokines in the pig lung during different respiratory virus infections: correlations with pathogenicity. *Research in veterinary science* 67: 47-52.
93. Thanawongnuwech R, Thacker B, Halbur P, Thacker EL (2004) Increased production of proinflammatory cytokines following infection with porcine reproductive and respiratory syndrome virus and *Mycoplasma hyopneumoniae*. *Clinical and diagnostic laboratory immunology* 11: 901-908.
94. Albina E, Carrat C, Charley B (1998) Short Communication: Interferon- α Response to Swine Arterivirus (PoAV), the Porcine Reproductive and Respiratory Syndrome Virus. *Journal of interferon & cytokine research* 18: 485-490.
95. Murtaugh MP, Xiao Z, Zuckermann F (2002) Immunological responses of swine to porcine reproductive and respiratory syndrome virus infection. *Viral immunology* 15: 533-547.
96. Lopez-Fuertes L, Campos E, Domenech N, Ezquerro A, Castro J, et al. (2000) Porcine reproductive and respiratory syndrome (PRRS) virus down-modulates TNF- α production in infected macrophages. *Virus Research* 69: 41-46.
97. Murtaugh MP, Genzow M (2011) Immunological solutions for treatment and prevention of porcine reproductive and respiratory syndrome (PRRS). *Vaccine* 29: 8192-8204.
98. Gómez-Laguna J, Salguero FJ, Pallarés FJ, Carrasco L (2013) Immunopathogenesis of porcine reproductive and respiratory syndrome in the respiratory tract of pigs. *The Veterinary Journal* 195: 148-155.
99. Calzada-Nova G, Schnitzlein WM, Husmann RJ, Zuckermann FA (2011) North American porcine reproductive and respiratory syndrome viruses inhibit type I interferon production by plasmacytoid dendritic cells. *Journal of virology* 85: 2703-2713.
100. Lee S-M, Schommer SK, Kleiboeker SB (2004) Porcine reproductive and respiratory syndrome virus field isolates differ in in vitro interferon phenotypes. *Veterinary immunology and immunopathology* 102: 217-231.
101. Dwivedi V, Manickam C, Binjawadagi B, Linhares D, Murtaugh MP, et al. (2012) Evaluation of immune responses to porcine reproductive and respiratory syndrome virus in pigs during early stage of infection under farm conditions. *Virology journal* 9: 1.
102. Souza C, Choi I, Araujo K, Abrams S, Kerrigan M, et al. Comparative serum immune responses of pigs after a challenge with porcine reproductive and respiratory syndrome virus (PRRSV); 2013.
103. Yoon KJ, Zimmerman JJ, Swenson SL, McGinley MJ, Eernisse KA, et al. (1995) Characterization of the humoral immune response to porcine reproductive and respiratory syndrome (PRRS) virus infection. *Journal of Veterinary Diagnostic Investigation* 7: 305.
104. Nguyen KB, Salazar-Mather TP, Dalod MY, Van Deusen JB, Wei X-q, et al. (2002) Coordinated and distinct roles for IFN- $\alpha\beta$, IL-12, and IL-15 regulation of NK cell responses to viral infection. *The Journal of Immunology* 169: 4279-4287.
105. Dwivedi V, Manickam C, Patterson R, Dodson K, Weeman M, et al. (2011) Intranasal delivery of whole cell lysate of *Mycobacterium tuberculosis* induces protective immune responses to a modified live porcine reproductive and respiratory syndrome virus vaccine in pigs. *Vaccine* 29: 4067-4076.

106. Janeway C, Murphy KP, Travers P, Walport M (2008) Janeway's immunobiology: Garland Science.
107. Takeda K, Kaisho T, Akira S (2003) Toll-like receptors. *Annual review of immunology* 21: 335-376.
108. Song S, Bi J, Wang D, Fang L, Zhang L, et al. (2013) Porcine reproductive and respiratory syndrome virus infection activates IL-10 production through NF- κ B and p38 MAPK pathways in porcine alveolar macrophages. *Developmental & Comparative Immunology* 39: 265-272.
109. Flores-Mendoza L, Silva-Campa E, Reséndiz M, Osorio FA, Hernández J (2008) Porcine reproductive and respiratory syndrome virus infects mature porcine dendritic cells and up-regulates interleukin-10 production. *Clinical and Vaccine Immunology* 15: 720-725.
110. Wang X, Eaton M, Mayer M, Li H, He D, et al. (2007) Porcine reproductive and respiratory syndrome virus productively infects monocyte-derived dendritic cells and compromises their antigen-presenting ability. *Archives of virology* 152: 289-303.
111. Thanawongnuwech R, Young TF, Thacker BJ, Thacker EL (2001) Differential production of proinflammatory cytokines: in vitro PRRSV and Mycoplasma hyopneumoniae co-infection model. *Veterinary immunology and immunopathology* 79: 115-127.
112. Carter QL, Curiel RE (2005) Interleukin-12 (IL-12) ameliorates the effects of porcine respiratory and reproductive syndrome virus (PRRSV) infection. *Veterinary immunology and immunopathology* 107: 105-118.
113. Chung H-K, Chae C (2003) Expression of interleukin-10 and interleukin-12 in piglets experimentally infected with porcine reproductive and respiratory syndrome virus (PRRSV). *Journal of comparative pathology* 129: 205-212.
114. Murtaugh MP, Johnson CR, Xiao Z, Scamurra RW, Zhou Y (2009) Species specialization in cytokine biology: Is interleukin-4 central to the T_H 1–T_H 2 paradigm in swine? *Developmental & Comparative Immunology* 33: 344-352.
115. Peng J, Wang J, Wu J, Du Y, Li J, et al. (2013) Positive inductive effect of swine Interleukin-4 on immune responses elicited by modified live porcine reproductive and respiratory syndrome virus (PRRSV) vaccine. *Viral immunology* 26: 404-414.
116. Xiao Z, Batista L, Dee S, Halbur P, Murtaugh MP (2004) The level of virus-specific T-cell and macrophage recruitment in porcine reproductive and respiratory syndrome virus infection in pigs is independent of virus load. *Journal of virology* 78: 5923-5933.
117. Butler J, Lager K, Golde W, Faaberg KS, Sinkora M, et al. (2014) Porcine reproductive and respiratory syndrome (PRRS): an immune dysregulatory pandemic. *Immunologic research* 59: 81-108.
118. Wongyanin P, Buranapraditkul S, Yoo D, Thanawongnuwech R, Roth JA, et al. (2012) Role of porcine reproductive and respiratory syndrome virus nucleocapsid protein in induction of interleukin-10 and regulatory T-lymphocytes (Treg). *Journal of general virology* 93: 1236-1246.
119. Silva-Campa E, Flores-Mendoza L, Reséndiz M, Pinelli-Saavedra A, Mata-Haro V, et al. (2009) Induction of T helper 3 regulatory cells by dendritic cells infected with porcine reproductive and respiratory syndrome virus. *Virology* 387: 373-379.
120. Silva-Campa E, Mata-Haro V, Mateu E, Hernández J (2012) Porcine reproductive and respiratory syndrome virus induces CD4⁺ CD8⁺ CD25⁺ Foxp3⁺ regulatory T cells (Tregs). *Virology* 430: 73-80.
121. Silva-Campa E, Cordoba L, Fraile L, Flores-Mendoza L, Montoya M, et al. (2010) European genotype of porcine reproductive and respiratory syndrome (PRRSV) infects monocyte-derived dendritic cells but does not induce Treg cells. *Virology* 396: 264-271.
122. Cecere TE, Todd SM, LeRoith T (2012) Regulatory T cells in arterivirus and coronavirus infections: do they protect against disease or enhance it? *Viruses* 4: 833-846.
123. Lopez OJ, Osorio FA (2004) Role of neutralizing antibodies in PRRSV protective immunity. *Veterinary Immunology and Immunopathology* 102: 155-163.

124. Burton DR (2002) Antibodies, viruses and vaccines. *Nature Reviews Immunology* 2: 706-713.
125. Chand RJ, Tribble BR, Rowland RRR (2012) Pathogenesis of porcine reproductive and respiratory syndrome virus. *Current Opinion in Virology* 2: 256-263.
126. Lewis CRG, Ait-Ali T, Clapperton M, Archibald AL, Bishop SC (2007) Genetic perspectives on host responses to porcine reproductive and respiratory syndrome (PRRS). *Viral Immunology* 20: 343-357.
127. Hess A, Islam Z, Hess MK, Rowland RRR, Lunney JK, et al. (2016) Comparison of Host Genetic Factors Influencing Piglet Response to Infection with Two Isolates of Porcine Reproductive and Respiratory Syndrome Virus. Submitted to *Genet Sel Evol*.
128. Lopez O, Osorio F (2004) Role of neutralizing antibodies in PRRSV protective immunity. *Veterinary immunology and immunopathology* 102: 155-163.
129. Ostrowski M, Galeota J, Jar A, Platt K, Osorio FA, et al. (2002) Identification of neutralizing and nonneutralizing epitopes in the porcine reproductive and respiratory syndrome virus GP5 ectodomain. *Journal of virology* 76: 4241-4250.
130. Cancel-Tirado SM, Evans RB, Yoon K-J (2004) Monoclonal antibody analysis of porcine reproductive and respiratory syndrome virus epitopes associated with antibody-dependent enhancement and neutralization of virus infection. *Veterinary immunology and immunopathology* 102: 249-262.
131. Sang Y, Rowland RRR, Blecha F (2011) Interaction between innate immunity and porcine reproductive and respiratory syndrome virus. *Animal Health Research Reviews* 12: 149.
132. Johnson W, Roof M, Vaughn E, Christopher-Hennings J, Johnson CR, et al. (2004) Pathogenic and humoral immune responses to porcine reproductive and respiratory syndrome virus (PRRSV) are related to viral load in acute infection. *Veterinary immunology and immunopathology* 102: 233-247.
133. Lopez O, Oliveira M, Garcia EA, Kwon BJ, Doster A, et al. (2007) Protection against porcine reproductive and respiratory syndrome virus (PRRSV) infection through passive transfer of PRRSV-neutralizing antibodies is dose dependent. *Clinical and Vaccine Immunology* 14: 269-275.
134. de Lima M, Pattnaik AK, Flores EF, Osorio FA (2006) Serologic marker candidates identified among B-cell linear epitopes of Nsp2 and structural proteins of a North American strain of porcine reproductive and respiratory syndrome virus. *Virology* 353: 410-421.
135. Oleksiewicz M, Bøtner A, Toft P, Normann P, Storgaard T (2001) Epitope mapping porcine reproductive and respiratory syndrome virus by phage display: the nsp2 fragment of the replicase polyprotein contains a cluster of B-cell epitopes. *Journal of virology* 75: 3277-3290.
136. Geldhof MF, Van Breedam W, De Jong E, Rodriguez AL, Karniychuk UU, et al. (2013) Antibody response and maternal immunity upon boosting PRRSV-immune sows with experimental farm-specific and commercial PRRSV vaccines. *Veterinary microbiology* 167: 260-271.
137. Nelson EA, Christopher-Hennings J, Benfield DA (1994) Serum immune responses to the proteins of porcine reproductive and respiratory syndrome (PRRS) virus. *Journal of Veterinary Diagnostic Investigation* 6: 410-415.
138. Guzman MG, Alvarez M, Halstead SB (2013) Secondary infection as a risk factor for dengue hemorrhagic fever/dengue shock syndrome: an historical perspective and role of antibody-dependent enhancement of infection. *Archives of virology* 158: 1445-1459.
139. Mulupuri P, Zimmerman JJ, Hermann J, Johnson CR, Cano JP, et al. (2008) Antigen-specific B-cell responses to porcine reproductive and respiratory syndrome virus infection. *Journal of virology* 82: 358-370.
140. Meier WA, Galeota J, Osorio FA, Husmann RJ, Schnitzlein WM, et al. (2003) Gradual development of the interferon-[gamma] response of swine to porcine reproductive and respiratory syndrome virus infection or vaccination. *Virology* 309: 18-31.

141. Renukaradhya GJ, Meng X-J, Calvert JG, Roof M, Lager KM (2015) Live porcine reproductive and respiratory syndrome virus vaccines: current status and future direction. *Vaccine* 33: 4069-4080.
142. Schroyen M, Steibel JP, Koltes JE, Choi I, Raney NE, et al. (2015) Whole blood microarray analysis of pigs showing extreme phenotypes after a porcine reproductive and respiratory syndrome virus infection. *BMC genomics* 16: 516.
143. Schroyen M, Easley C, Koltes JE, Fritz-Waters E, Choi I, et al. (2016) Bioinformatic analyses in early host response to Porcine Reproductive and Respiratory Syndrome virus (PRRSV) reveals pathway differences between pigs with alternate genotypes for a major host response QTL. *BMC genomics* 17: 1.
144. Perelson AS, Kirschner DE, De Boer R (1993) Dynamics of HIV infection of CD4+ T cells. *Mathematical biosciences* 114: 81-125.
145. Dominik Wodarz ALL, Vincent A. A. Jansen And Martin A. Nowak (1999) Dynamics of Macrophage and T cell infection by HIV. *Journal of Theoretical Biology* 196: 101-113.
146. Perelson AS, Neumann AU, Markowitz M, Leonard JM, Ho DD (1996) HIV-1 dynamics in vivo: virion clearance rate, infected cell life-span, and viral generation time. *Science* 271: 1582-1586.
147. Leslie A, Pfafferott K, Chetty P, Draenert R, Addo M, et al. (2004) HIV evolution: CTL escape mutation and reversion after transmission. *Nature medicine* 10: 282-289.
148. Wodarz D, Nowak MA (2002) Mathematical models of HIV pathogenesis and treatment. *BioEssays* 24: 1178-1187.
149. Wei XP, Ghosh SK, Taylor ME, Johnson VA, Emini EA, et al. (1995) Viral Dynamics In Human-Immunodeficiency-Virus Type-1 Infection. *Nature* 373: 117-122.
150. Saenz RA, Quinlivan M, Elton D, MacRae S, Blunden AS, et al. (2010) Dynamics of influenza virus infection and pathology. *Journal of virology* 84: 3974-3983.
151. Pawelek KA, Huynh GT, Quinlivan M, Cullinane A, Rong L, et al. (2012) Modeling within-host dynamics of influenza virus infection including immune responses. *PLoS computational biology* 8: e1002588.
152. Beauchemin C, Samuel J, Tuszynski J (2005) A simple cellular automaton model for influenza A viral infections. *Journal of Theoretical Biology* 232: 223-234.
153. Go N (2014) Modelling the immune response to the Porcine Reproductive and Respiratory Syndrome virus: AgroParisTech.
154. Doeschl-Wilson A, Galina-Pantoja L (2010) Using Mathematical Models to Gain Insight into Host-Pathogen Interaction in Mammals: Porcine Reproductive and Respiratory Syndrome. *Host-Pathogen Interactions: Genetics, Immunology, Physiology* Nova Science Publishers Inc, New York

109-131

155. Brown H, Prescott R (2006) *Applied mixed models in medicine*: John Wiley West SussexUK.
156. Wolfinger RD (1997) An example of using mixed models and PROC MIXED for longitudinal data. *Journal of Biopharmaceutical statistics* 7: 481-500.
157. Verbeke G, Molenberghs G (1997) *Linear mixed models in practice: a SAS oriented approach*. New York: Springer-Verlag
158. Meetings A-A-CN (2002) *Mixed Model Workshop*. Canada.
159. Littell R, Henry P, Ammerman C (1998) Statistical analysis of repeated measures data using SAS procedures. *Journal of Animal Science* 76: 1216-1231.

160. Trefan L, Bünger L, Bloom-Hansen J, Rooke J, Salmi B, et al. (2011) Meta-analysis of the effects of dietary vitamin E supplementation on α -tocopherol concentration and lipid oxidation in pork. *Meat Science* 87: 305-314.
161. Institute S (1985) SAS user's guide: statistics: Sas Inst.
162. Snijders TAB (2005) Fixed and Random Effects. *Encyclopedia of Statistics in Behavioral Science* Volume 2, 664-665. .
163. Seltman HJ (2005) Experimental Design and Analysis. Carnegie Mellon University.
164. Lindstrom MJ, Bates DM (1990) Nonlinear mixed effects models for repeated measures data. *Biometrics*: 673-687.
165. Wold S (1974) Spline functions in data analysis. *Technometrics* 16: 1-11.
166. Desquilbet L, Mariotti F (2010) Dose-response analyses using restricted cubic spline functions in public health research. *Statistics in medicine* 29: 1037-1057.
167. Brandl N, Jørgensen E (1996) Determination of live weight of pigs from dimensions measured using image analysis. *Computers and electronics in agriculture* 15: 57-72.
168. Druet T, Jaffrézic F, Boichard D, Ducrocq V (2003) Modeling lactation curves and estimation of genetic parameters for first lactation test-day records of French Holstein cows. *Journal of dairy science* 86: 2480-2490.
169. Bohmanova J, Misztal I, Bertrand J (2005) Studies on multiple trait and random regression models for genetic evaluation of beef cattle for growth. *Journal of Animal Science* 83: 62-67.
170. Girolami M (2008) Bayesian inference for differential equations. *Theoretical Computer Science* 408: 4-16.
171. Steri R, Dimauro C, Canavesi F, Nicolazzi EL, Macciotta NPP (2012) Analysis of lactation shapes in extended lactations. *animal* 6: 1572-1582.
172. Wood PDP (1967) ALGEBRAIC MODEL OF LACTATION CURVE IN CATTLE. *Nature* 216: 164-&.
173. Maiwashe A, Nengovhela NB, Nephawe KA, Sebei J, Netshilema T, et al. (2013) Estimates of lactation curve parameters for Bonsmara and Nguni cattle using the weigh-suckle-weigh technique. *South African Journal of Animal Science* 43: S12-S16.
174. Boujenane I, Hilal B (2012) Genetic and non genetic effects for lactation curve traits in Holstein-Friesian cows. *Archiv Fur Tierzucht-Archives of Animal Breeding* 55: 450-457.
175. Grossman M, Koops W (2003) Modeling extended lactation curves of dairy cattle: a biological basis for the multiphasic approach. *Journal of dairy science* 86: 988-998.
176. Perochon L, Coulon J, Lescourret F (1996) Modelling lactation curves of dairy cows with emphasis on individual variability. *Animal Science* 63: 189-200.
177. Beever D, Rook A, France J, Dhanoa M, Gill M (1991) A review of empirical and mechanistic models of lactational performance by the dairy cow. *Livestock Production Science* 29: 115-130.
178. Papajcsik I, Boderó J (1988) Modelling lactation curves of Friesian cows in a subtropical climate. *Animal Production* 47: 201-207.
179. Winsor CP (1932) The Gompertz curve as a growth curve. *Proceedings of the National Academy of Sciences of the United States of America* 18: 1.
180. Grimm KJ, Ram N (2009) Nonlinear growth models in M plus and SAS. *Structural Equation Modeling* 16: 676-701.
181. Khamis A, Ismail Z, Haron K, Mohammed AT (2005) Nonlinear growth models for modeling oil palm yield growth. *Journal of Mathematics and Statistics* 1: 225-233.
182. Zwietering M, Jongenburger I, Rombouts F, Van't Riet K (1990) Modeling of the bacterial growth curve. *Applied and environmental microbiology* 56: 1875-1881.
183. Beyer J, Fichtner D, Schirrmeier H, Polster U, Weiland E, et al. (2000) Porcine reproductive and respiratory syndrome virus (PRRSV): Kinetics of infection in lymphatic organs and lung. *Journal of Veterinary Medicine Series B-Infectious Diseases and Veterinary Public Health* 47: 9-25.

184. Robert CP (2001) The Bayesian choice: From decisiontheoretic foundations to computational implementation (springer texts in statistics) by.
185. Bernardo JM, Smith AF (2001) Bayesian theory. IOP Publishing.
186. Berger J (1985) Statistical decision theory and Bayesian analysis.
187. Berger JO, Wolpert RL, Bayarri M, DeGroot M, Hill BM, et al. (1988) The likelihood principle. Lecture notes-Monograph series 6: iii-199.
188. Carlin BP, Louis TA (2000) Bayes and empirical Bayes methods for data analysis.
189. Pool M, Janss L, Meuwissen T (2000) Genetic parameters of Legendre polynomials for first parity lactation curves. Journal of dairy science 83: 2640-2649.
190. Buttchereit N, Stamer E, Junge W, Thaller G (2010) Evaluation of five lactation curve models fitted for fat: protein ratio of milk and daily energy balance. Journal of dairy science 93: 1702-1712.
191. Torshizi ME, Aslamenejad A, Nassiri M, Farhangfar H (2011) Comparison and evaluation of mathematical lactation curve functions of Iranian primiparous Holsteins. South African Journal of Animal Science 41: 104-115.
192. Kheirabadi K, Rashidi A, Alijani S, Imumorin I (2014) Modeling lactation curves and estimation of genetic parameters in Holstein cows using multiple-trait random regression models. Animal Science Journal 85: 925-934.
193. Meyer K (2005) Random regression analyses using B-splines to model growth of Australian Angus cattle. Genetics Selection Evolution 37: 473-500.

Chapter 2

Examining PRRS viraemia profiles of pigs from an experimental challenge: a repeated measures and mixed modelling approach

2.0 Introduction

Viraemia profiles of pigs experimentally challenged with PRRSV are valuable indicators of the severity and progression of the infection in the host, and thus provide crucial information for the required subsequent disease control measures [1,2]. The course of a typical PRRSV infection is characterised by an acute stage lasting approximately 4 weeks followed by a stage characterised by low levels and eventual resolution of viraemia [3]. Previous studies suggest that in the majority of animals viraemia reaches undetectable levels typically by 4-6 weeks, although the virus may still be isolated months later in the lymphoid tissues [4]. In the PRRS Host Genetic Consortium (PHGC) trials, pigs were challenged with one of two PRRSV isolates (here denoted as NVSL and KS06, respectively) [2]. Visual observation of the viraemia profiles (Figure 2.1) indicates that the majority of viraemia profiles exhibit uni-modal or bi-modal trends.

The longitudinal viraemia profiles from the PHGC PRRSV challenge experiment used in this study reveal substantial differences in the temporal viraemia patterns between hosts infected with the same PRRSV challenge strain and dose, pointing to considerable variation in the host response to PRRSV infections (Figure 2.1 A and B). Following infection at 0dpi with the same isolate and infection dose, a rise to peak viraemia level by approximately 10dpi for NVSL and 7dpi for KS06 was observed. This is followed by a decline in viral load and eventual resolution of viraemia by 42dpi. Inter-host variation increases with time for both isolates and there is substantial variation in the rate of viraemia decline. Visual inspection of viraemia profiles indicates that the general trend in profiles could be described by the Wood's model. The latter model is based on a gamma-type function often used to empirically describe lactation curves in dairy cattle [5-7], and appears to be a suitable candidate model as it matches the above described data characteristics of a sharp rise followed by a peak and gradual decline of the uni-modal profiles and the primary phase of the bimodal viraemia profiles. Furthermore, it is determined by only three parameters with straightforward interpretation and can easily be linearized, thus facilitating statistical analysis and providing a biological interpretation of the results.

Previous studies using the PHGC challenge data identified heritable genetic components to the cumulative viraemia (viraemia AUC 0-21dpi), and weight gain, and found an association between the single nucleotide polymorphism (SNP) WUR10000125 (henceforth referred to as WUR) on chromosome 4 and these two host response traits [8-12]. It is not known to what extent the WUR SNP affects the time course of infection such as the rate of increase nor the rate of post-peak viraemia

decline. The effect of the WUR genotype on pigs' response to infection has been validated on NVSL infected piglets only. It is currently not known whether the host genetic influence to PRRSV infection is consistent across all PRRSV isolates. The WUR genotype is associated with infection data from the primary phase of infection (0-21dpi). It would thus be interesting to assess the impact, if any, it has on the full viraemia profiles (0-42dpi). Furthermore, variation in host response has only been quantified in terms of cumulative (AUC 0-21dpi) viraemia; it has not been fully specified how the PHGC viraemia profiles differ over time.

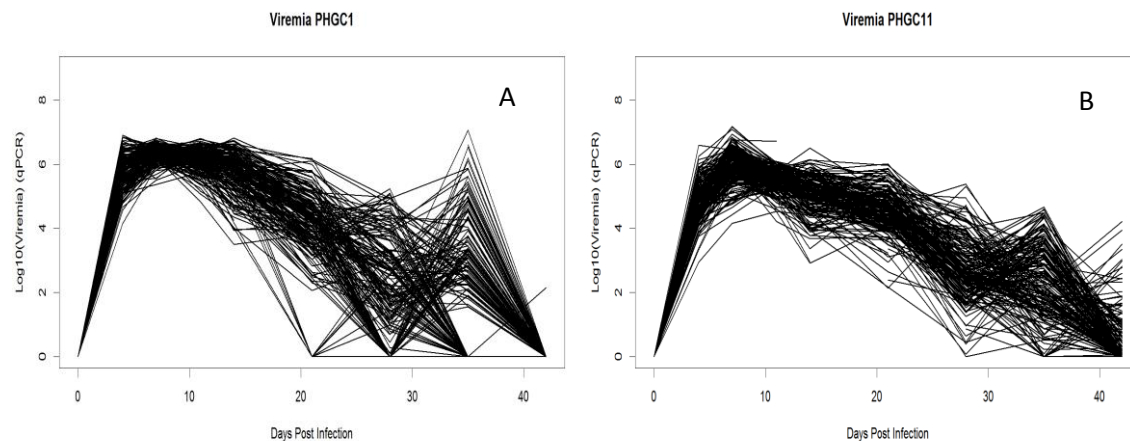


Figure 2.1 Viraemia profiles from a PRRSV challenge at 0dpi with either PRRSV isolate NVSL or KS06. **Figure 2.1 A** Viraemia profiles from PHGC trial 1 in which pigs were challenged with the PRRSV isolate NVSL. **Figure 2.1 B** Viraemia profiles from PHGC trial 11 in which pigs were challenged with the PRRSV isolate KS06.

The primary objective of this chapter is to gain an insight into the factors of significant influence on the observed viraemia time trends such as the different viral strains, the pig's genetic background (breed cross & breeding company), the WUR resistance genotype and other random effects that may possibly influence viraemia trends. In this chapter we apply the well-established methodology of linear mixed models for the statistical analysis of the longitudinal viraemia data due to the ability of these models to include both fixed and random effects [13-17]. Our analysis is conducted via two alternative approaches: a repeated measures model and a linearized version of the non-linear uni-modal Wood's function. The repeated measures model provides least square mean (LSM) estimates for log-transformed viraemia at the observation times, but does not capture the non-linear time trend of the individual viraemia profiles. In contrast, the linearized Wood's model implemented in the mixed model framework provides LSM estimates of the Wood's model parameters, and impact of the various factors on these. The Wood's model allows construction of viraemia curves based on these parameter estimates, thus making it a powerful approach to analyse changes of infection severity over time since it is not restricted to the observation times only.

2.1 Materials and Methods

2.1.1 The Experimental Data

The data analysed in this study was obtained from the PRRS Host Genetic Consortium (PHGC) trials, the largest PRRSV in-vivo challenge study to date. Pigs from the same breeding company and the same breed cross were considered to be from the same genetic background. The full dataset in this chapter consisted of: 13 PHGC trials, 8 genetic backgrounds and 2 PRRSV isolates as outlined in Table 2.1. Nine trials used infection with NVSL and five trials used KS06. A detailed description of the experimental protocol and the two PRRSV isolates is outlined in [2,18] and in the Chapter 1 of the thesis.

PRRS Virus Isolate	Trial Number	Number of Animals	Breed Cross ¹	Genetic Background ²
NVSL-97-7895 (NVSL)	1	188	LW x LR	1
	2	190	LW x LR	1
	3	184	LW x LR	1
	4	191	Duroc x LW/LR	2
	5	182	Duroc x LR/LW	3
	6	109	LR x LR	4
	7	186	Pietran x LW/LR	5
	8	158	Duroc x LW/LR	6
	15	166	Pietran x LW	7
	Total	1554	-	1-7
KS-2006-72109 (KS06)	10	184	Pietran x LW	7
	11	177	LW x LR	1
	12	146	LR x LW	8
	14	165	Duroc x LR/LW	3
	Total	672	-	1,3,7,8

Table 2.1 Animal composition across the PHGC trials. ¹LW = Large White; LR = Landrace. ²Genetic background is defined as pigs from the same breeding company and the same breed cross.

Briefly, viraemia data was obtained from pigs which were experimentally infected with a PRRSV isolate in thirteen separate infection trials (ca. 200 pigs/ trial) with an infection dose of 10^5 tissue culture dose₅₀ (TCID₅₀). In trials 1-8 and 15 the virulent PRRSV isolate NVSL 97-7985 (NVSL) was used [19,20], and in trials 10-14 the more contemporary PRRSV isolate KS-2006-72109 (KS06) was used. Trial 9 had only one WUR genotype and thus was excluded from the analysis in this study, since the exploration of genotype effects on the viraemia is one of the main objectives of this chapter. Trial 13 was also excluded from the analysis due to a likely co-infection resulting in unusual viraemia profiles not observed in any other infection trial. Some trial 13 animals showed delayed presence of

serum viraemia, and all individuals had low and noisy viraemia levels compared to individuals in other trials, suggesting the virus was attenuated or the piglets were not naïve.

Pigs were from the same high health farm, except for trials 5, 8 and 12, which each included pigs from one supplier but two farms. Prior to challenge pigs were tested to be free of PRRSV, *Mycoplasma hypopneumoniae* and swine influenza virus. Animals were transported at weaning (average age of 21 days) to Kansas State University, randomly placed into pens of 10 to 15 pigs, and were infected with PRRSV after a 7 day acclimation period, i.e. at 0dpi. Blood samples were collected immediately before infection (0dpi) and at 4, 7, 11, 14, 21, 28, 35, 42dpi. The level of PRRS viraemia was measured using a semi-quantitative TaqMan PCR assay for PRRSV RNA. The viraemia quantity data from RT-PCR was transformed on the logarithmic scale to the base 10 before the model fitting. Due to the sensitivity of RT-PCR the threshold of detection was set at 1 unit on the \log_{10} scale [8]. Pigs were euthanized at 42 dpi. Trials 7 and 8 were stopped at 35 dpi due to facility unavailability.

WUR genotype: The WUR genotype accounted for in this study refers to the presence or absence of the favourable B-allele at the single nucleotide polymorphism (SNP) WUR 1000125 on *Sus Scrofa* (SSC) chromosome 4 previously identified to be strongly associated with lower cumulative viral load (viraemia AUC 0-21dpi) [8,10,12]. This SNP was identified using 60K SNP chip panels for trials 1-3 of the dataset analysed in this chapter, and has further been verified for most PHGC trials and both PRRS isolate types (see Appendix 3) [8]. The WUR SNP was found to act in a dominant manner without imprinting, with the B allele estimated to decrease AUC of the viraemia and increase the weight gain irrespective of whether the favorable B allele is inherited from the sire or dam [10].

Isolate differences: The two PRRSV isolates used in this study, NVSL 97-7985 and KS-2006-72109, here denoted as NVSL and KS06 respectively, were isolated from different geographic regions nearly ten years apart, and are 89% similar at the GP5 nucleotide sequence level. PRRSV glycoprotein 5 (GP5) is a major envelope protein that plays a vital role in the virion's formation and infectivity, and harbours a major neutralizing epitope [21]. This gene is often used to assess genetic differences between PRRSV isolates and is suggestive of differences in virulence between isolates [22]. Variation in GP5 impacts the pig's ability to produce neutralizing antibodies, which may not be protective against different isolates [22,23].

2.1.2 Classifying bimodal profiles and subdividing the viraemia dataset

Visual inspection showed that viraemia profiles were either uni-modal or bimodal. Uni-modal profiles were typically in a decline phase from the peak viraemia levels during 21-42dpi. Bimodal profiles experienced a second peak during 21-42dpi. In line with a previous study on the first three trials in this dataset [1], profiles were classed as bimodal if the viraemia observations from 21dpi onwards

rebounced by a value of greater than or equal to 1.5 on the log base 10 scale. This was calculated using observation differences on the \log_{10} scale when:

- 1) $\log_{10} \text{RT-PCR at 42dpi} - \log_{10} \text{RT-PCR at 35dpi} \geq 1.5$ therefore bimodal
- 2) $\log_{10} \text{RT-PCR at 35dpi} - \log_{10} \text{RT-PCR at 28dpi} \geq 1.5$ therefore bimodal
- 3) $\log_{10} \text{RT-PCR at 28dpi} - \log_{10} \text{RT-PCR at 21dpi} \geq 1.5$ therefore bimodal

To quantify the effect of virus isolate and other factors on the viraemia profiles, a repeated measures model and the linearized Wood's model was fit to transformed viraemia data as outlined below.

However, the Wood's function only describes uni-modal profiles and cannot capture the secondary phase of bimodal profiles as shown in Table 2.2.

To explore whether bimodal profiles affect the influence of other factors on viraemia trends the model fitting was carried out on the full dataset (dataset 1) and then on a dataset with the bimodal profiles removed (dataset 2). The first dataset includes all profiles, i.e. bimodal profiles are not treated as outliers that need to be removed from the dataset and hence conduct the analysis including bimodal profiles. Furthermore, in contrast to most previous studies on these viraemia data, the dataset is not truncated to only contain the primary phase of infection (0-21dpi) as that would result in the loss of valuable information corresponding to the infection dynamics at the later stage of infection.

Beginning with all profiles for the full time course of infection (dataset 1), the best model is identified and used to test the effect on model parameter estimates and viraemia predictions. The impact of the bimodal profiles on the model fit, significant effects and the parameter estimates is then tested using the second dataset (bimodal profiles removed) as shown in Table 2.2.

Dataset	Including bimodal profiles	Time Period (dpi)	Number of samples (pigs)
1	Yes	0-42	2640
2	No	0-42	2072

Table 2.2 Two longitudinal PRRS viraemia datasets used in this statistical analysis. The full viraemia dataset was subdivided through the removal of bimodal profiles.

2.1.3 Statistical analysis

Repeated measures model

The following repeated measures model was fit in SAS for both the viraemia datasets (datasets 1 and 2) with the random effects of pig and pen within trial. The fixed effects of WUR genotype, virus isolate type, parity, sex, age, genetic background, trial, time and all their interactions were also fit, as defined by:

$$Y_{ijklmnop} = \mu + W_l + S_j + P_k + A_l + G_m + T_n + V_o + I + RI_i + RP_p + \epsilon_{in}$$

Where Y is the viraemia quantity from RT-PCR on the the log₁₀ scale of individual i of: WUR genotype W_i, sex S_j, parity P_k, age A_i, genetic background G_m, of time T_n, virus isolate V_o, ε_{in} is the residual , and I represents all possible interactions between all the fixed effects. RI_i and RP_p are the random effects of individual and pen within trial respectively. Note that trial was not fitted in these models due to confounding with genetic background and PRRSV isolate. The PROC MIXED procedure of SAS was used where autocorrelation between repeated measurements could be taken into account using the repeated statement. Autocorrelations between repeated measures were examined using the repeat statement of PROC MIXED, and various residual covariance matrix structures were explored (e.g vc -standard variance components; ar(1) -first order autoregressive; cs- compound symmetry; un -unstructured; toep –toeplitz). A stepwise approach was adopted for identifying the model of best fit, starting from a model that included all the fixed effects and covariates described above and their interactions, followed by stepwise removal of statistically non-significant factors at the 95% significance level (P<0.05) using the likelihood ratio test (LRT).

The impact of the following fixed effects on the repeated measure LSM (least square mean) estimates was explored:

1. Virus isolate,
2. WUR genotype
3. Genetic background

The contrast statement (F –test statistic) was used to assess the differences between various levels of the fixed effects in the LSM viraemia measures.

Since most trials consisted of pigs from different genetic backgrounds or the same genetic background but different virus isolate, the estimated effects associated with different genetic backgrounds and virus isolate are potentially confounded with trial effects. For this reason additional models were fitted in which the genetic background was substituted by the PHGC trial.

The linearized Wood's model

The Wood's function is given by the following equation and can be linearized by taking the natural log transformation:

$$y = at^b e^{-ct}$$

where y represents the level of viraemia in the blood (log₁₀ RT-PCR) at t days post infection (dpi). The parameter a is a scalar quantity and impacts upon the magnitude of all the points on the curve. The parameter b is an indicator of the initial rate of increase to the peak viraemia level and the parameter c is an indicator of the rate of decline after the peak and dominates the function as

$t \rightarrow +\infty$. Thus the Wood's model parameters have a biological relevance and the function can be linearized by taking the natural log transformation for fitting in SAS using the procedure PROC MIXED. The linearised version of the Woods function is a function with variables $T1 = \ln(t)$ and $T2 = t$ and parameters $A = \ln(a)$, b and c as specified above, i.e. $\ln(y) = A + b T1 - c T2$. Individual-specific random effects were added to the initial fixed effects model as perturbations of one of the model parameters at a time or a combination of model parameters. Furthermore when the pen within trial was included in the model it failed to converge and hence it was not included in the final model. The covariance structure adopted for the random effects was unstructured, which is the most liberal covariance structure. As for the repeated measurement model, used above, the: virus isolate type, genetic background, trial, WUR genotype, sex, and parity as well as all significant interactions were included as potential fixed effects, in all the model parameters. Significance of the fixed effects was determined by the F-test at the 95% significance level ($P < 0.05$). The contrast statement in SAS was used to determine statistically significant differences in the LSM parameter estimates associated with different levels of the fixed effects [15]. The model fitting was conducted on both datasets (datasets 1 and 2) to determine the impact of the bimodal profiles on the significance of the fixed effects on the model parameters.

Assessment of goodness of fit and comparisons of the different Wood's mixed models with different fixed and random effects were based on the: likelihood ratio test, Akaike's Information Criteria (AIC), Pearson's correlation (R), Residual Standard Deviation ($RSD = \sqrt{\frac{\sum residual^2}{(n-p)}}$, where p is the number of model parameters) and inspection of the Wood's model residuals. The statistical significance for inclusion of one or more random effects in the model parameters was determined by the likelihood ratio test between the model with (n) random effects and the null model fewer (i.e. $n-1$) random effects, based on the chi-square test statistics with the corresponding degrees of freedom.

2.2 Results

2.2.1 Qualitative assessment and univariate statistics of the longitudinal PRRS viraemia data

Visual inspection of the individual viraemia profiles from both PRRSV isolates indicated a general trend of rise to a peak followed by a decline. Boxplots allow us to obtain a preliminary description of the PRRS viraemia dataset before model fitting in SAS. The maximum viraemia values occur at 7dpi for both NVSL and KS06 with more variation in NVSL than KS06 at 4, 28, and 35dpi as shown in Figures 1.2 A&B. Viraemia values were generally higher for the more virulent isolate NVSL than KS06. Larger variation in both isolates from 28dpi onwards could be due to an increased inter-host variation in profiles from 21dpi onwards and the presence of bimodal profiles in the datasets. Removal of the bimodal profiles (Figures 1.2 C &D) reduced the inter-host variation in the dataset at 28-42 dpi for both NVSL and KS06.

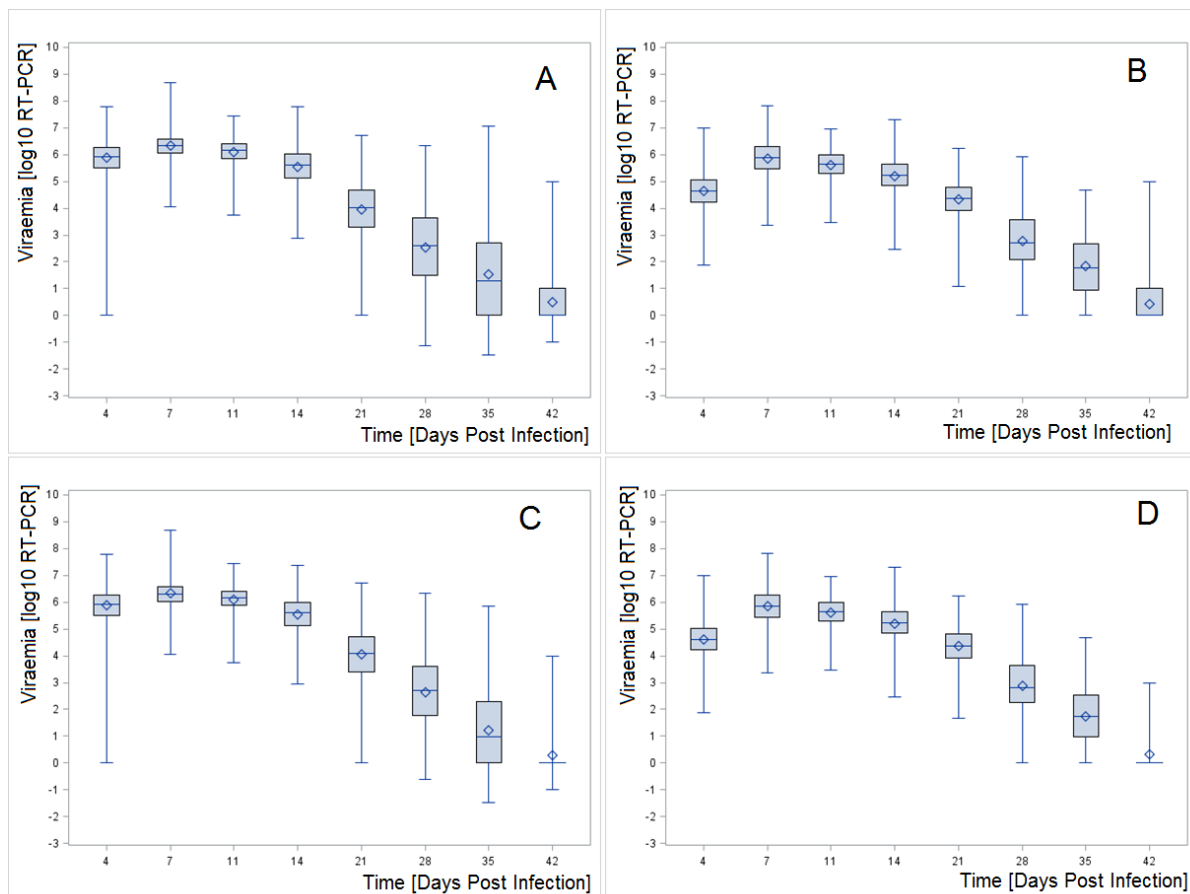


Figure 2.2 Boxplots of the viraemia data from the PHGC trials. **Figure 2.2A** NVSL virus isolate, **Figure 2.2B** KS06 virus isolate, **Figure 2.2C** NVSL with the bimodal profiles removed, **Figure 2.2D** KS06 with the bimodal profiles removed. The length of the box represents the interquartile range, the diamond in the box interior represents the group mean, the horizontal line in the box interior represents the group median and the vertical lines (whiskers) issuing from the box extend to the minimum and maximum values at each time point of the experiment.

Frequency of the WUR genotype in the viraemia dataset across PHGC trials

The WUR 0 [AA] genotype was the most frequent (45-92%), whilst WUR 2 [BB] was the least frequent (0-12%) genotype across all trials (Table 2.3). There was variation in the distribution of the WUR genotypes between the trials. Trial 6 had the fewest percentage of WUR 0. Trials 6, 8 10 and 12 had no WUR 2 pigs. Trial 7 and 10 had the largest percentages of WUR 0 genotypes. The distribution of WUR genotypes was similar for both PRRSV isolates.

PRRS Virus Isolate	Trial Number	WUR 0 [AA] (%)	WUR 1 [AB or BA] (%)	WUR 2 [BB] (%)	Genetic Background
NVSL-97-7895 (NVSL)	1	134 (75.7%)	39 (22%)	4 (2.3%)	1
	2	143 (75%)	43 (23%)	4 (2%)	1
	3	112 (61%)	63 (34%)	8 (4%)	1
	4	163 (84%)	28 (14%)	4 (2%)	2
	5	134 (68%)	60 (30%)	4 (2%)	3
	6	114 (91.2%)	11 (8.8%)	0	4
	7	88 (45%)	86 (44%)	23 (12%)	5
	8	169 (85%)	29 (15%)	0	6
	15	156 (78%)	42 (21%)	2 (1%)	7
	Total	1213 (73%)	401 (24%)	49 (3%)	-
KS-2006-72109 (KS06)	10	170 (53.5%)	30 (46.5%)	0	7
	11	157 (80.5%)	37 (19%)	1 (0.5%)	1
	12	158 (85%)	27 (15%)	0	8
	14	144 (77%)	36 (19%)	7 (4%)	3
	Total	629 (82%)	130 (17%)	9 (1%)	-

Table 2.3 The distribution of the WUR genotype across the PHGC trials. The percentages were calculated within each trial.

Frequency of bimodal profiles in the viraemia dataset across PHGC trials

The frequency of bimodal profiles was consistent between trials within each PRRSV isolate (Table 2.4). Overall KS06 had fewer bimodal profiles than NVSL (total of 16% for KS06 compared to 27% for NVSL).

PRRS Virus Isolate	Trial Number	Number of Animals	Uni-model (%)	Bimodal (%)	Genetic Background
NVSL-97-7895 (NVSL)	1	188	125 (66%)	63 (34%)	1
	2	190	133 (70%)	57 (30%)	1
	3	184	124 (67%)	60 (33%)	1
	4	191	124 (65%)	67 (35%)	2
	5	182	129 (71%)	53 (29%)	3
	6	109	87 (80%)	22 (20%)	4
	7	186	161 (87%)	25 (13%)	5
	8	158	129 (82%)	29 (18%)	6
	15	166	120 (72%)	46 (28%)	7
	Total	1554	1132 (73%)	422 (27%)	
KS-2006-72109 (KS06)	10	184	162 (88%)	22 (12%)	7
	11	177	142 (80%)	35 (20%)	1
	12	146	108 (74%)	38 (26%)	8
	14	165	153 (93%)	12 (7%)	3
	Total	672	565 (84%)	107 (16%)	

Table 2.4 The frequency of bimodal profiles across the PHGC trials.

The distribution of the WUR genotypes across uni- and bimodal viral profiles

The WUR genotypes were distributed similarly across uni- and bimodal profiles for both isolates as shown in Table 2.5. For the KS06 infection there was a marginally higher percentage of WUR 0 [AA] genotypes than there were for NVSL. Overall, the similar distributions of the WUR genotype across trials, PRRSV isolates and viraemia profile classes minimises the risk of confounding in the statistical results.

PRRS Virus Isolate	Bimodal/ Uni-modal	WUR 0 [AA] (%)	WUR 1 [AB or BA] (%)	WUR 2 [BB] (%)
NVSL-97-7895 (NVSL)	Uni-modal	896 (72%)	305 (25%)	39 (3%)
	Bimodal	317 (75%)	96 (23%)	10 (2%)
KS-2006-72109 (KS06)	Uni-modal	635 (78%)	164 (20%)	10 (1%)
	Bimodal	118 (82%)	21 (15%)	4 (3%)

Table 2.5 The frequency of the WUR genotypes across uni and bimodal viral profiles. The percentages are calculated for each bimodal/uni-modal class within the PRRSV isolate.

2.2.2 Repeated measures models of PRRS viraemia

The full repeated measures model contains all the fixed and random effects was reduced after removing non-significant effects at the 95% significance level ($P > 0.05$). The final repeated measures model for the viraemia data with a first order autoregressive covariance structure and the random effect of pig and pen within trial was:

$$Y_{ijlmnop} = \mu + W_l + S_j + A_l + G_m + T_n + V_o + G_m * T_n + W_k * T_n + V_o * T_n + RI_i + RP_p + \epsilon_{in}$$

Where t is the time (dpi), W is the WUR genotype, G is the genetic background, S is the sex, V is the virus isolate, RI and RP are the random individual and pen within trial effects respectively, ϵ is the error, and $*$ indicate interactions between the fixed effects.

The results of the significant effects in the repeated measures model imply that the viraemia trends were statistically different between genetic background, the WUR genotype and the virus isolate. These differences are explored by examining the differences between the least square means (LSMs) of these groups over time. Sex and age of the pigs also contributed to the variation in viraemia measures, but did not correspond to different time trends. Although trial was not included in the original statistical model due to confounding with genetic background and virus isolate type, models including trial instead of genetic backgrounds showed that Trial and the Trial*Time effects were both statistically significant. The final model was the same for both dataset 1 and dataset 2; the inclusion of

bimodal profiles did not change the significance of the effects in the model. Therefore, the significant effects were robust with the inclusion of bimodal profiles.

The model residuals

The repeated measures model was applied to both dataset 1 (all profiles) and dataset 2 (only uni-modal profiles) and their model residuals are shown in Figure 2.3A and 1.3B respectively. In Figure 2.3A the value range of the residuals at 21dpi were within 3 \log_{10} units and within 5 \log_{10} units at 35dpi; these large residuals thus indicate that the repeated measurements model provides a poor fit to dataset 1 from 21dpi onwards. The model residuals are normally distributed around 0 for 4-28dpi but there is a bias of under-prediction at 35-42dpi. The model residuals increase with time, which is expected due to the increased inter-host variation in the rate of viraemia decline from the peak and the presence of bimodal profiles.

Removal of the bimodal profiles improves the model fit as indicated by model residuals up to 3 to 4 \log_{10} units (for 5 pigs) at all observed time points (Figure 2.3b). Residual variation still increases over time indicating that the repeated measures model is not good at capturing the increase in inter-host variation at the later stage of infection. However, removal of the bimodal profiles reduces the bias of under-prediction at 35dpi (Figure 2.3B).

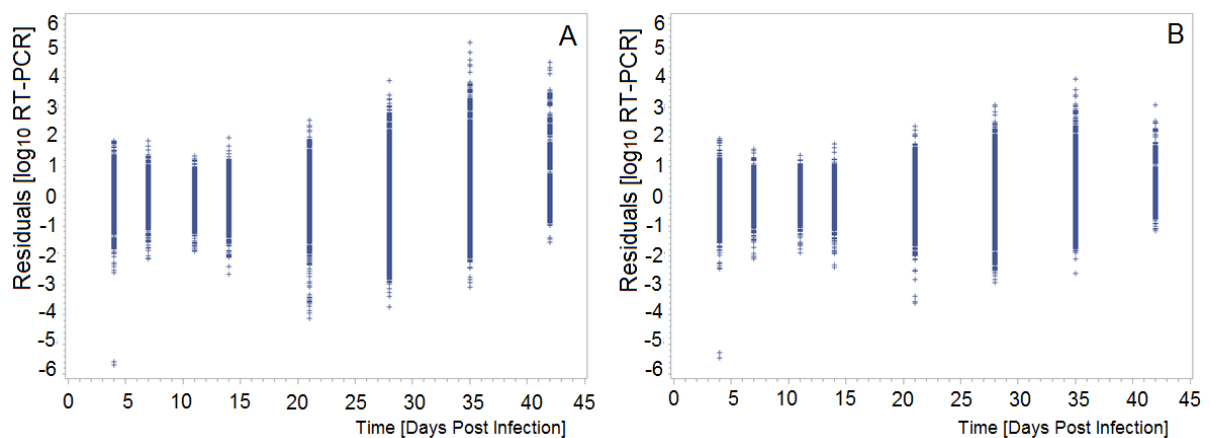


Figure 2.3 The model residuals from fitting the final repeated measures model to the full dataset 1 (Figure 2.3A) and the reduced dataset 2 (Figure 2.3B).

Examining the impact of fixed effects on the repeated measure model LSM viraemia estimates

Below the impact of the virus isolate, genetic background, WUR genotype and trial on the LSM viraemia estimates is examined. The interaction between time and the fixed effect of interest is included in the final repeated measures model.

1. The virus isolate

The LSMs for each virus isolate obtained from fitting the repeated measures model to dataset 1 (all profiles) are shown in Table 2.6 and depicted in Figure 2.4. Except for day 4, the LSMs for both virus isolates differed by less than one log-unit with statistically significant differences at all days of the experiment except for 42dpi (Table 2.6). The average profiles for both PRRS virus infections consist of a period of rise to peak viraemia at 7dpi followed by decline to clearance (Figure 2.4). However, NVSL has a significantly higher peak viraemia at around 7dpi and a faster rate of decline than KS06, as indicated by significantly higher LSM estimates for KS06 between 21 and 35dpi. Differences between the virus isolates are smaller from 21 dpi onwards compared to the earlier stages of the infection. Note that due to the large sample size the SEMs are small at all observation times of the experiment, even at the later time points when measurements are more scattered (Table 2.6 and Figure 2.4).

Time (dpi)	NVSL LSM (SEM)	KS06 LSM (SEM)	Statistical difference between NVSL and KS06 (p value)
4	5.9046 (0.03)	4.6056 (0.04)	<.0001
7	6.3372 (0.03)	5.8381 (0.04)	<.0001
11	6.1106 (0.03)	5.574 (0.04)	<.0001
14	5.5687 (0.04)	5.1608 (0.04)	<.0001
21	3.9594 (0.04)	4.2929 (0.05)	<.0001
28	2.5559 (0.04)	2.7525 (0.06)	<.0001
35	1.554 (0.04)	1.8099 (0.07)	<.0001
42	0.5017 (0.04)	0.4152 (0.05)	0.07

Table 2.6 The least square mean estimates (standard error of the mean) for each PRRSV isolate from fitting the repeated measures model to dataset 1.

Removing bimodal profiles

Similar significant differences between the LSMs, and time trends for the two PRRSV isolates were found when the bimodal profiles were removed from the data i.e. when the repeated measures model was fit to dataset 2 (Table 2.7). Removal of bimodal profiles leads to small differences in the LSMs estimated (Figure 2.4). Figure 2.4 further shows that the LSMs from dataset 2 are slightly smaller than for dataset 1 at 35dpi with stronger differences for NVSL for which viraemia rebound was more pronounced. Overall, the statistical results with regards to the impact of the virus isolate are robust to

the inclusion of bi-modal profiles. Bimodal profiles only affect the goodness of fit, but not the size or direction of estimated effects for the virus isolate.

Time (dpi)	NVSL LSM (SEM)	KS06 LSM (SEM)	Statistical difference between NVSL and KS06 (p value)
4	5.8522 (0.03)	4.5527 (0.04)	<.0001
7	6.2914 (0.03)	5.7859 (0.04)	<.0001
11	6.0655 (0.03)	5.5461 (0.04)	<.0001
14	5.5141 (0.03)	5.1336 (0.04)	<.0001
21	4.0076 (0.03)	4.3067 (0.04)	<.0001
28	2.6254 (0.03)	2.8193 (0.04)	<.0001
35	1.1875 (0.03)	1.6983 (0.04)	<.0001
42	0.1803 (0.04)	0.2698 (0.04)	0.06

Table 2.7 The least square mean estimates, LSM (standard errors of the mean, SEM) for each PRRSV isolate from fitting the repeated measures model to dataset 2.

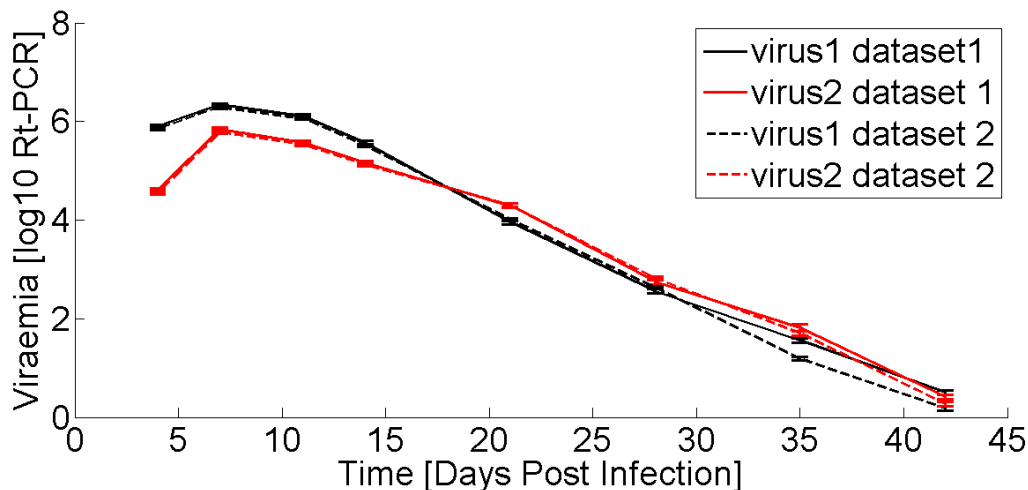


Figure 2.4 Comparison of the least square mean estimates obtained from fitting the repeated measures model to both datasets. NVSL (virus 1) is in black and KS06 (virus 2) is in red. The LSMs from dataset 2 (bimodal profiles removed) are denoted by the dashed lines.

2. The WUR genotype

The LSMs for each WUR genotype obtained from fitting the repeated measures model to dataset 1 (all profiles) are shown in Table 2.8. The LSMs for all three WUR genotypes had a similar range on the logarithmic scale with statistically significant differences between WUR 0 and WUR 1 at 11-35dpi, WUR 0 and WUR 2 at 35dpi and WUR 1 and WUR 2 at 28dpi. The average profiles for all three WUR genotypes consist of the same time trends of a period of rise to peak viraemia at 7dpi followed by decline to clearance (Figure 2.5). The WUR 0 genotype had significantly higher viraemia LSM at most observations than the other genotypes, which would explain the observed differences in the area under the viraemia curve associated with this SNP. However despite the statistical

significance of the differences between the LSMs of the WUR genotypes the actual LSM differences are less than 0.55 log units at all time points (Table 2.8).

Time (Days Post Infection)	WUR 0 (AA)	WUR 1 (AB or BA)	WUR 2 (BB)	Significantly different between WUR 0 & 1 (p-value)	Significantly different between WUR 0 & 2 (p-value)	Significantly different between WUR 1 & 2 (p-value)
4	5.5184 (0.02)	5.4459 (0.04)	5.3418 (0.13)	0.1409	0.1851	0.4514
7	6.2146 (0.02)	6.0791 (0.04)	6.0286 (0.13)	0.0056	0.1591	0.7124
11	5.99 (0.02)	5.7806 (0.04)	5.8742 (0.13)	<.0001	0.3931	0.5053
14	5.5114 (0.02)	5.205 (0.04)	5.2477 (0.13)	<.0001	0.05	0.7596
21	4.148 (0.02)	3.7964 (0.04)	3.8737 (0.14)	<.0001	0.0516	0.5958
28	2.6879 (0.02)	2.3173 (0.04)	2.8629 (0.14)	<.0001	0.21	0.0002
35	1.6744 (0.02)	1.4776 (0.04)	1.358 (0.14)	<.0001	0.0248	0.4118
42	0.4932 (0.02)	0.3979 (0.05)	0.7143 (0.19)	0.0944	0.2382	0.1

Table 2.8 The LSMs for each WUR genotype from fitting the repeated measures model to dataset 1. Significant differences at the 95% significance level are in bold.

Removing bimodal profiles

Comparison of the repeated measures model LSMs between dataset 1 and 2 indicate that the results are almost identical when the bimodal profiles are removed (Figure 2.5). With the exception of the LSM differences between WUR 0 and WUR 2 at 35dpi, which are no longer statistically significant when bimodal profiles are reduced ($p < 0.37$), the majority of the statistical results with regards to the impact of the WUR genotype are robust to the inclusion of bi-modal profiles (Tables 1.8 and 1.9).

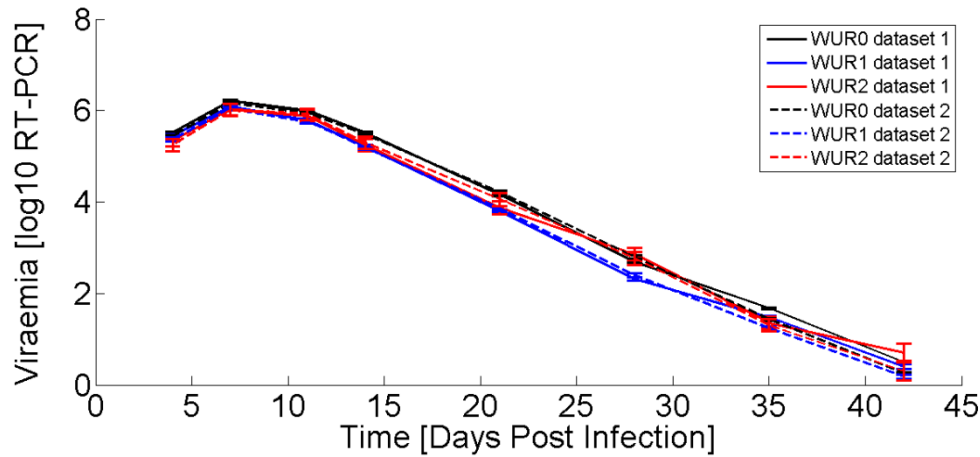


Figure 2.5 Comparison of the LSMs from dataset 1 (lines) and dataset 2 (dashed lines) for each WUR genotype (WUR 0 is in black, WUR 1 is in blue, WUR 2 is in red).

Time (Days Post Infection)	WUR 0 (AA)	WUR 1 (AB or BA)	WUR 2 (BB)	Significantly different between WUR 0 & 1 (p-value)	Significantly different between WUR 0 & 2 (p-value)	Significantly different between WUR 1 & 2 (p-value)
4	5.4444 (0.02)	5.3695 (0.04)	5.2472 (0.13)	0.1317	0.1357	0.3706
7	6.1646 (0.02)	6.0392 (0.04)	6.0127 (0.13)	0.011	0.2458	0.8447
11	5.9472 (0.02)	5.7541 (0.04)	5.9177 (0.13)	0.0001	0.8264	0.2386
14	5.4686 (0.02)	5.1858 (0.04)	5.2944 (0.13)	<.0001	0.1924	0.4314
21	4.2145 (0.03)	3.853 (0.05)	4.0539 (0.14)	<.0001	0.2524	0.1652
28	2.8034 (0.03)	2.3964 (0.05)	2.766 (0.14)	<.0001	0.7866	0.0095
35	1.4294 (0.03)	1.231 (0.05)	1.304 (0.14)	0.0001	0.3746	0.6156
42	0.2533 (0.03)	0.1814 (0.05)	0.2965 (0.19)	0.2114	0.823	0.5602

Table 2.9. The least square mean estimates for each WUR genotype, from fitting the repeated measures model to dataset 2. Significant differences ($p < 0.05$) are in bold. Differences that were found to be significant for dataset 1 that are no longer significant for dataset 2 are in blue.

3. The genetic background

Genetic background had a significant effect on the LSMs for viraemia. The least square mean estimates for each genetic background obtained from fitting the repeated measures model to dataset 1 (all profiles) are shown in Figure 2.6. The least square means for all 8 genetic backgrounds had a similar range on the logarithmic scale and followed similar time trends; however there were differences in the magnitude of the peak and rate of decline from the peak viraemia between genetic

backgrounds. For ease of interpreting the results, the LSMs that were **not** significantly different with each other at the 95% significance level are presented in Table 2.10.

Genetic backgrounds 7 and 8 were infected with KS06 only, whilst pigs from genetic backgrounds 1 and 3 were infected with virus isolate NVSL or KS06 in separate infection trials. Below the trial differences, in order to disentangle the effect of virus isolate type from the genetic background, are examined.

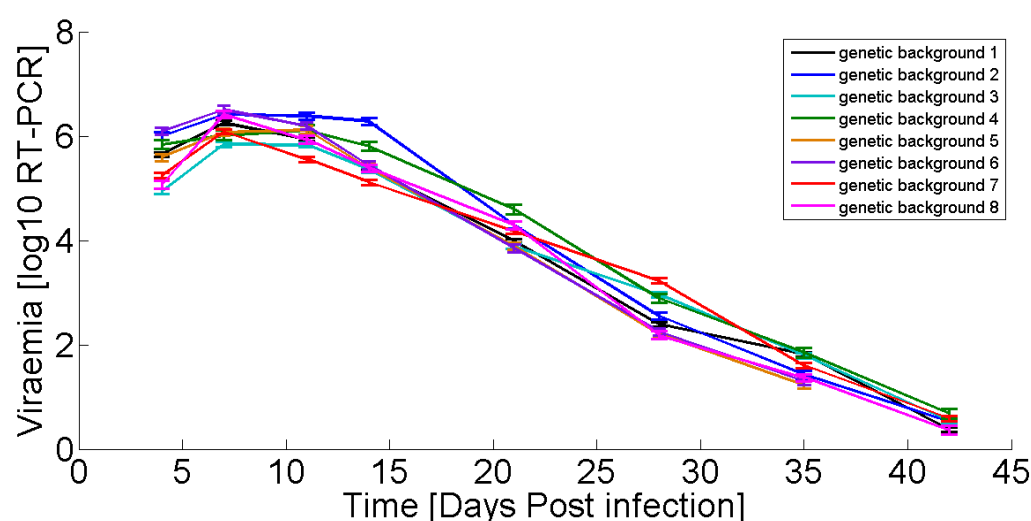


Figure 2.6 The least square mean estimates for each genetic background at each observation of the PRRSV challenge experiment.

Genetic background \ Time (dpi)	1	2	3	4	5	6	7	8
4		6	8			2	8	3,7
7		6,8		7	7	2,8		2,6
11	3,8			5,8	4,6	5		1,4
14	3,5,6,8		1,5,6		1,3,8	1,8		1,5
21	3,5	7,8	1,5		1,3,6		2,8	2,7
28	6		4	3	6,8	1,8		5,6
35	3,4	6,8	1	1	6,8			2,5
42		3,4,7,8	2	2			2	2

Table 2.10 The non-significant differences between the LSMs of the genetic backgrounds at each experimental observation at the 95% significance level.

Removing bimodal profiles

The same significant differences between the LSMs, and time trends for the 8 genetic backgrounds were found when the bimodal profiles were removed from the data i.e. when the repeated measures model was fit to dataset 2. Comparison of the LSM trends associated with both datasets in Figure 2.7

further indicates that the removal of bimodal profiles leads to only very small differences in the LSMs estimated. Thus the statistical results with regards to the impact of the genetic background are robust to the inclusion of bi-modal profiles. Bimodal profiles only affect the goodness of fit, but not the size or direction of estimated effects for the genetic background.

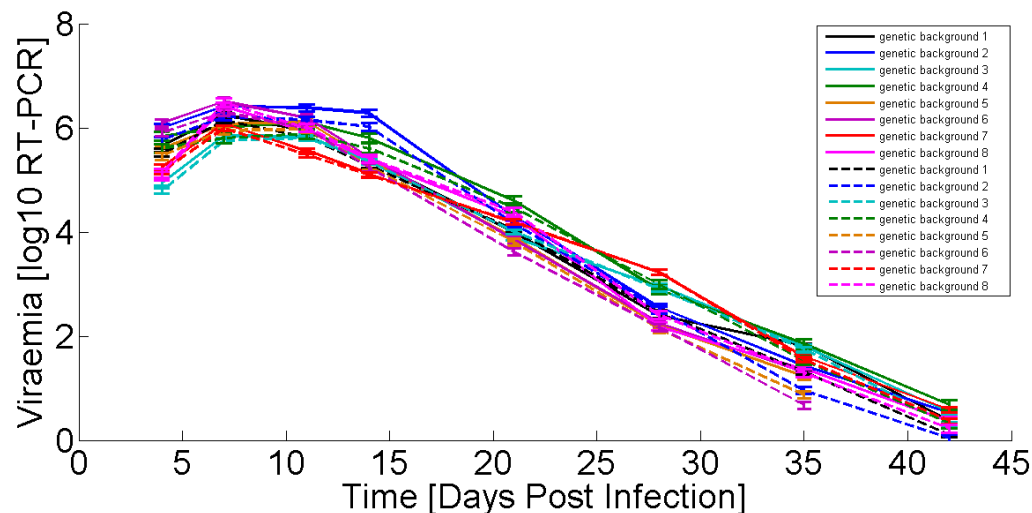


Figure 2.7 Comparison of LSM estimates for different genetic background from dataset 1 (solid lines) and 2 (dashed lines).

4. The PHGC trial

Trial differences allow us to examine the genetic background differences whilst separating out the virus isolate differences. Substituting the PHGC trial for the genetic background in the final repeated measure model yielded the LSMs estimates for each trial shown in Figure 2.8A for NVSL and 1.8B for KS06 infections.

Except for trials 1-3, trials within each virus isolate used pigs from different genetic backgrounds, thus causing confounding between trial and genetic background. However, trials 1-3 using the same genetic background and same virus isolate resulted in significantly different LSM viraemia estimates from 21dpi onwards ($p < 0.05$) (Table 2.11), which suggests in addition to genetic background, the trial may have a significant effect on viraemia profiles, particularly in the later stage of infection.

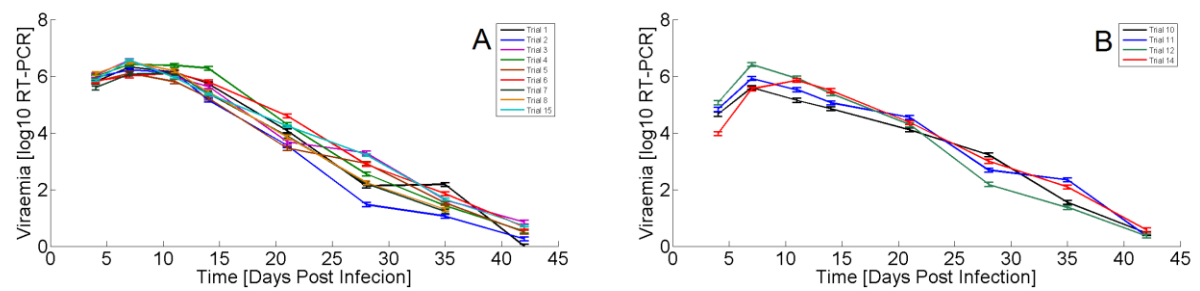


Figure 2.8 The LSMs for each trial fitting the repeated measures model with trial substituted for genetic background to dataset 1. Figure 2.8A shows trials infected with NVSL and Figure 2.8B shows trials infected with KS06.

To disentangle virus isolate and genetic background the LSMs for the trials from genetic backgrounds 1, 3 and 7 are shown in Table 2.11. There were significant differences between trials infected with NVSL and KS06 within the same genetic background at the majority of the observation times. However virus isolate differences could be confounded between trials.

Genetic Background	7 (SEM)		1 (SEM)				3 (SEM)	
Virus	1	2	1	1	1	2	1	2
Trial	15	10	1	2	3	11	5	14
Time (dpi)								
4	5.82* (0.07)	4.61 (0.07)	5.75* (0.07)	5.91* (0.07)	6.03 (0.07)	4.81** (0.07)	5.82* (0.07)	3.96 (0.07)
7	6.53* (0.07)	5.55 (0.07)	6.28* (0.07)	6.18** (0.07)	6.56* (0.07)	5.90** (0.07)	6.12* (0.07)	5.54 (0.07)
11	5.92* (0.07)	5.11 (0.07)	6.09* (0.07)	6.08* (0.07)	5.98* (0.07)	5.50*** (0.07)	5.82 (0.07)	5.83 (0.07)
14	5.33* (0.07)	4.80 (0.07)	5.69*** (0.07)	5.11** (0.07)	5.64** (0.07)	5.04** (0.07)	5.24* (0.07)	5.48 (0.08)
21	4.20 (0.07)	4.06 (0.07)	4.03** (0.07)	3.50** (0.08)	3.68** (0.07)	4.53*** (0.07)	3.47* (0.07)	4.35 (0.08)
28	3.18 (0.07)	3.18 (0.07)	2.08*** (0.07)	1.43*** (0.08)	3.30** (0.08)	2.66*** (0.07)	2.93 (0.07)	2.98 (0.07)
35	1.63 (0.07)	1.50 (0.07)	2.13 (0.07)	1.02** (0.08)	1.65** (0.08)	2.32** (0.07)	1.53* (0.07)	2.07 (0.08)
42	0.69* (0.07)	0.41 (0.07)	-0.04*** (0.07)	0.21* (0.08)	0.86** (0.08)	0.35** (0.08)	0.51 (0.07)	0.55 (0.08)

Table 2.11 LSM differences for trials from the same genetic backgrounds. * indicates significant differences between the LSMs at that time associated with NVSL and KS06 at the 95% significance level, for genetic background 1 the colour of the asterisk indicates the trial LSMs being compared.

Removing bimodal profiles

Removal of bimodal profiles led to only very small differences in the estimated viraemia LSMs associated with different trials (Figure 2.9) and led to almost identical results to those reported for dataset 1.

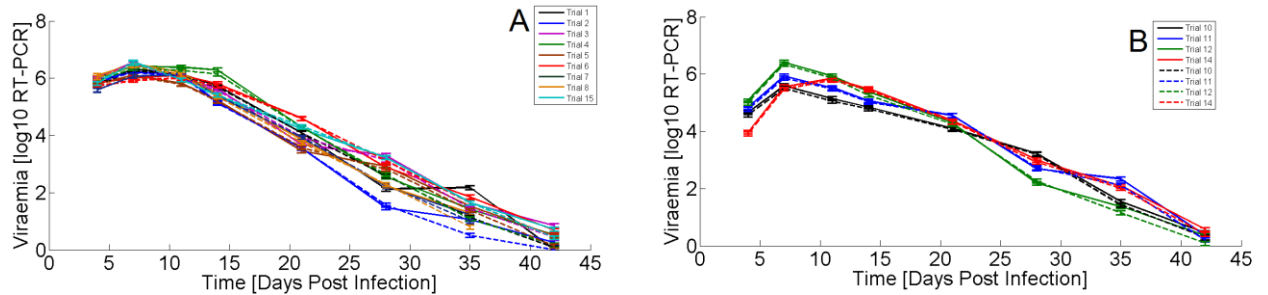


Figure 2.9 Comparison of the LSMs for each trial from fitting the repeated measures model with trial substituted for genetic background to dataset 1 (lines) and dataset 2 (dashed lines). Figure 2.9A shows trials infected with NVSL and Figure 2.9B shows trials infected with KS06.

2.2.3 Fitting the linearized Wood's function for modelling viraemia profiles

Identifying the fixed and random effects in the linearized Wood's model

Firstly, the significant random effects in the mixed model incorporating the linearized Wood's function was identified, since they will impact upon the predictions of the fixed effects [24]. The resulting fit statistics from fitting the linearized Wood's function to all the viraemia data with an unstructured covariance structure between the random effects are shown in Table 2.12. Comparisons of the Wood's models with different random effects (Table 2.12) indicate that significantly better fits were achieved with models allowing for individual variation in parameter c . This result is expected due to the fact that the variation in parameter c reflects variation in the rate of decline from the peak viraemia which captures the increased inter-host variation from 7dpi onwards. The AIC was smallest when there was individual variation in all three model parameters. The Pearson's correlation was highest between the data and predictions when there was a random effect in parameters b and c , thus allowing for individual variation in the time of the peak viraemia which is defined by $= \frac{b}{c}$. The residual standard deviation was lowest for the model with a random effect in parameters a and c .

Overall, according to the likelihood ratio test and the AIC, the best model is one in which there was a random effect in two model parameters: b and c . The likelihood ratio test in Table 2.12 is the result from testing the model in consideration with the models with 1 less random effects thus allowing us to determine how many and which random effects are needed in the final model.

Model name	AIC	R squared	RSD	-2 log likelihood (null)	-2 log likelihood (model)	Null model name
Wood's model with no random effects	10415.2	0.75346	0.3632	-	10413.2*	-
Wood's model with random effect in parameter A	10379.3	0.79158	0.3379	10413.2	10375.3*	Wood's model with no random effects
Wood's model with random effect in parameter b	9967.2	0.81559	0.3203	10413.2	9963.2*	Wood's model with no random effects
Wood's model with random effect in parameter c	8901.3	0.84417	0.2969	10413.2	8897.3*	Wood's model with no random effects
Wood's model with random effect in parameters A ,b	8311.5	0.79869	0.3324	9963.2	8305.5*	Wood's model with random effect in parameter b
Wood's model with random effect in parameters A, c	7745.4	0.83743	0.2919	8897.3	7739.4*	Wood's model with random effect in parameter c
Wood's model with random effect in parameters b, c	7576.5	0.84949	0.3021	8897.3	7568.5*	Wood's model with random effect in parameter c
Wood's model with random effect in parameters A, b ,c	6932.2	0.83261	0.3059	7568.5	8897.3	Wood's model with random effect in parameters b, c

Table 2.12 Comparison of goodness of fit indicators for each model in which there were different random effects in the Wood's model parameters. Model fit statistics were Akaike's information criteria (AIC), Pearson's correlation between predicted and observed values (R squared), residual standard deviation (RSD) and the -2log likelihood for the model with the additional random effect and the null model specific to that model where * indicates LRT significant at the 95% significance level. The model parameters are the Woods parameters A, b and c from the equation $\ln(y) = A + b T1 - c T2$ (see materials and methods for a further description of this function).

As shown in Table 2.12 the final linearized Wood's model had a random effect in parameter b and c only. In the final linearized Wood's model the significant fixed effects (95% significance level) were: the genetic background in all the model parameters, the virus in all the model parameters, and sex only in model parameter c.

$$\text{Ln}(y)_{\text{moij}} = [\mu + G_m + V_o] + [G_m * T1 + V_o * T1 + R_i * T1] + [G_m * T2 + V_o * T2 + S_j * T2 + R_i * T2] + \epsilon_i$$

Where $\text{Ln}(y)$ is the natural log transformed \log_{10} RT-PCR viraemia data, G is the genetic background, V is the virus isolate, S is sex and R is an individual random effect in the linearized Wood's parameter.

Assessing individual model fits to the data

Individual Wood's model fits are shown in Figure 2.10, which illustrate that the general shape of the Wood's function follows the same typical time trends of the viraemia profiles. From visual inspection of all individual model fits, the Wood's model appears to be overall an adequate candidate model to represent individual uni-modal viraemia profiles. However, as shown below, the model residuals are generally large and visual inspection of the individual profiles and residuals indicates a bias of over-prediction at the later stages of infection (Figure 2.10).

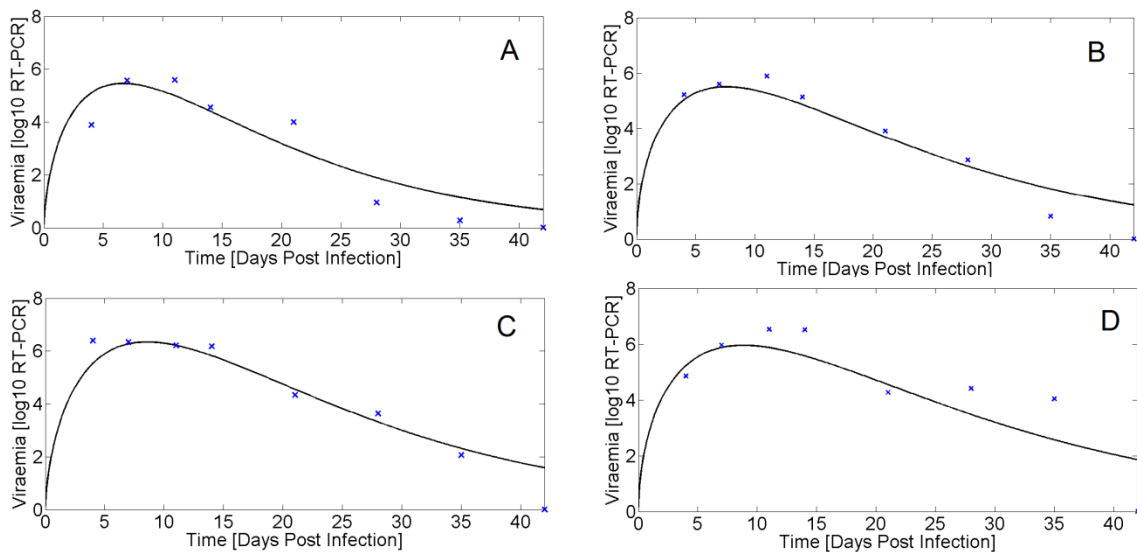


Figure 2.10 Individual Wood's model fits (black solid line) to the \log_{10} viraemia data (blue crosses).

The residuals from fitting the final linearized Wood's function to dataset 1 and 2 are shown in Figure 2.10A and B. These residuals increase with time being largest between 28-35dpi. The residuals are generally normally distributed except for a bias of over-prediction at 28 and 35dpi. The residuals in Figure 2.10A and B indicate that differences between the transformed data and the model predictions are within 1-2 units on the transformed $\text{Ln}(\log_{10}$ RT-PCR) scale. When the predictions and data are back transformed to be on the \log_{10} scale the residuals are generally within 4 \log_{10} units (Figures

2.10C and D). Removal of the bimodal profiles significantly improves the Woods model fit to the data particularly from 21-42dpi (Figures 2.10B and D).

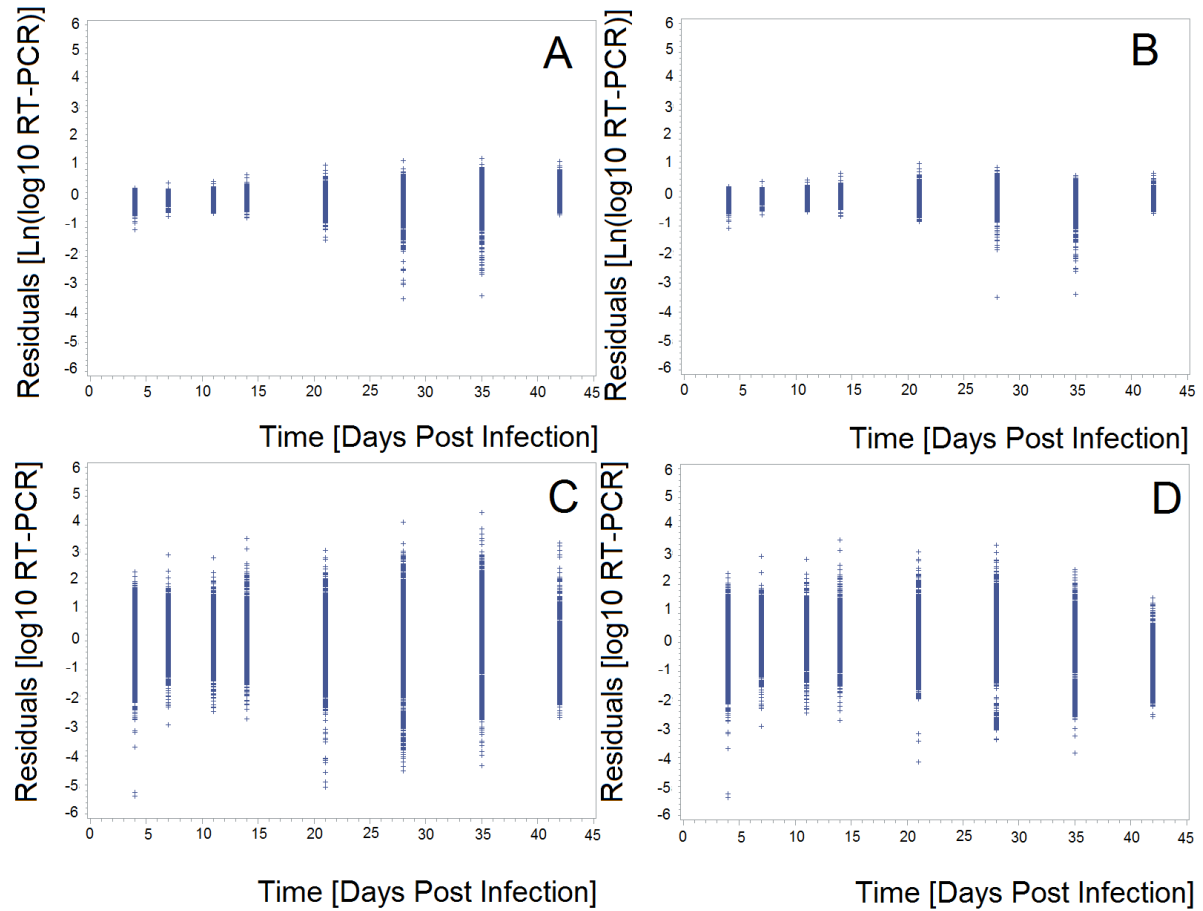


Figure 2.11. Plot of the residuals from fitting the final linearized Wood's model. The residuals are denoted by blue crosses. Figure 2.11A and B are the residuals directly from the linearized model fitting and are on the $\text{Ln}(\log_{10} \text{RT-PCR})$ scale. **Figure 2.11A** are the residuals from fitting the linearized model to dataset 1. **Figure 2.11B** are the residuals from fitting the linearized Woods model to dataset 2. **Figure 2.11C** and **1.11D** are the residuals from the back transformed data and model predictions i.e. on the $\log_{10} \text{RT-PCR}$ scale. **Figure 2.11C** are the residuals from dataset 1 and **Figure 2.11D** are the residuals from dataset 2.

As shown in Table 2.5, removal of bimodal profiles changes the LSM estimates for all parameters. However, differences in the model fit and LSM values of the Wood's parameter estimates did not translate into drastic differences in the resulting viraemia predictions (Figure 2.11). The removal of bimodal profiles results in the predicted profile having a slightly higher peak and faster rate of decline (Figure 2.11).

Dataset	LSM Parameter Estimates						AIC*
	A (SE)	b (SE)	c (SE)	V _{1,1} (SE)	V _{2,1} (SE)	V _{2,2} (SE)	
1 (all)	1.25 (0.02)	0.54 (0.01)	0.07 (0.0009)	0.0003 (0.00002)	-0.001 (0.0001)	0.0008 (0.0006)	7576.5
2 (no bimodal)	1.07 (0.016)	0.69 (0.01)	0.08 (0.0009)	0.0005 (0.00003)	-0.002 (0.0001)	0.008 (0.0008)	7385.5

Table 2.5. LSM estimates for the parameters of the linearized Woods model fit to the full dataset (dataset 1) and when bimodal profiles were removed (dataset 2). Note that AIC depends partly on the sample size. Hence quantitative comparison of goodness of fit associated with both datasets, based on AIC, or any of the other fit statistics, is not feasible. The parameters $V_{1,1}$, $V_{2,1}$, and $V_{2,2}$ are the components of the variance-covariance matrix for the Woods parameters b and c .

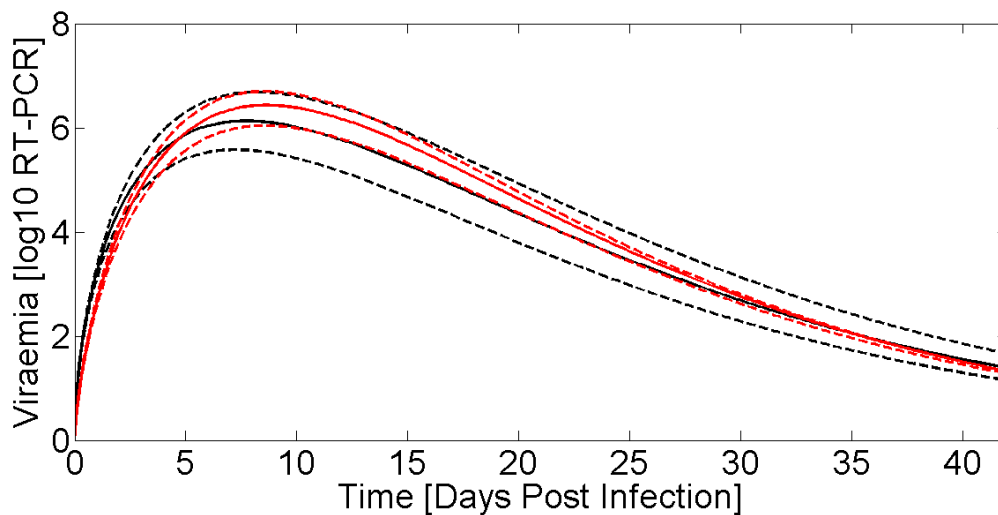


Figure 2.12 Estimated viraemia curves obtained from LSM parameter estimates obtained when fitting the final linearized Wood's model. The profiles for dataset 1 are in black and dataset 2 are in red. The dashed lines depict the respective confidence intervals constructed by the model predictions from the upper and lower parameter estimates determined by: $\text{LSM}(\text{model parameter}) \pm 1.96 \text{ SE}(\text{model parameter})$.

Examining the impact of fixed effects on the linearized Woods model parameters and resulting viraemia profiles

Below the impact of the virus isolate, genetic background, WUR genotype and trial on the linearized Wood's parameters and their resulting viraemia profiles is examined. The fixed effect of interest was fit in all the model parameters in addition to significant fixed and random effects of the final linearized model. Significance was taken at the 95% significance level.

1. The virus isolate

There were significant differences between NVSL and KS06 in all three Wood's parameters as shown in Table 2.13. NVSL had a much higher value of Wood's parameter A ($=\ln(a)$), and lower values for the Wood's parameters b and c than KS06. The differences in parameters translated to differences in the Wood's model predictions particularly in the early phase of infection i.e. 0-14dpi (Figure 2.13). The model predicts that NVSL has an earlier and higher peak viraemia than KS06. The magnitude of all points on the Wood's curve for NVSL are larger than that of KS06, furthermore the differences between the two PRRSV isolates decreases with time.

Parameter	NVSL	KS06	Significantly different between NVSL & KS06 (p-value)
A (SE)	1.65 (0.044)	0.90 (0.060)	p<0.001
b (SE)	0.43 (0.028)	0.83 (0.038)	p<0.001
c (SE)	0.08 (0.002)	0.10 (0.003)	p<0.001

Table 2.14. The estimated Wood's parameters for the two virus isolates, all three Wood's parameters are significantly different between the two viruses at the 95% significance level.

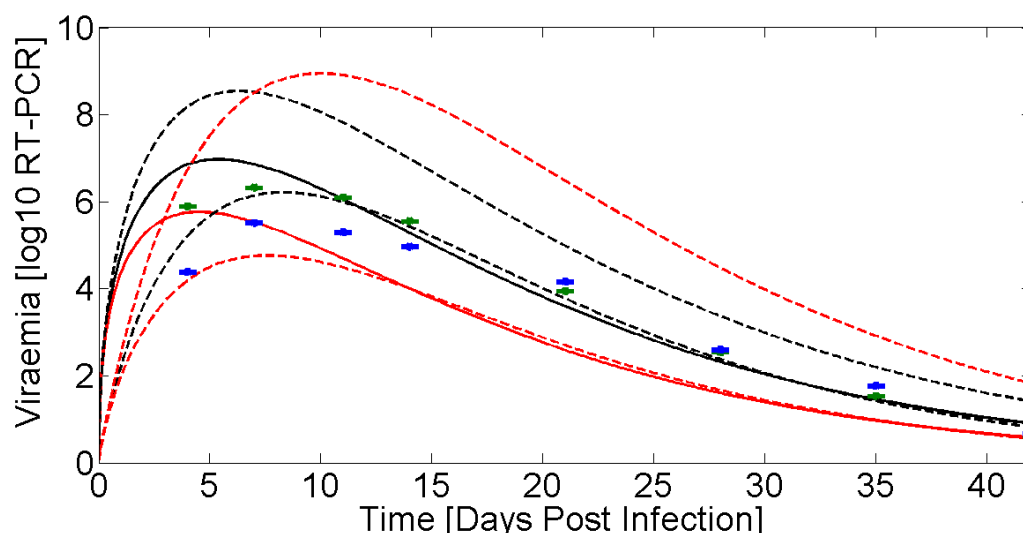


Figure 2.13. Predicted viraemia profiles estimated by the linearised Wood's model (lines), together with the estimates produced by the repeated measures models (green and blue points with confidence limits). Viraemia profiles for NVSL are shown in black and those for KS06 in red. The dashed lines delimit the respective confidence intervals constructed by the model predictions from the upper and lower parameter estimates determined by: $LSM(\text{model parameter}) \pm 1.96 SE(\text{model parameter})$. For the repeated measures model LSM estimates with confidence intervals for NVSL are shown in green and for KS06 in blue

2. The WUR genotype

There were no statistically significant differences between the linearized Wood's parameters for the WUR genotypes as shown in Table 2.15. The WUR 0 and 1 profiles were very similar throughout the infection. Despite the parameters not being significantly different between the WUR genotypes, Figure 2.14 shows that the WUR 2 genotype has viral profile with a lower magnitude throughout the experiment compared to WUR 0 and 1. The statistical results with regards to impact of fixed effects on Wood's parameters and resulting profiles are robust to the inclusion of bi-modal profile (see Appendix 1).

Parameter	WUR 0 (AA)	WUR 1 (AB or BA)	WUR 2 (BB)	Significantly different between WUR 0 & 1 (p-value)	Significantly different between WUR 0 & 2 (p-value)	Significantly different between WUR 1 & 2 (p-value)
A (SE)	0.910 (0.113)	0.924 (0.116)	0.90 (0.127)	0.74	0.91	0.81
b (SE)	0.82 (0.075)	0.80 (0.074)	0.79 (0.083)	0.43	0.64	0.87
c (SE)	0.09 (0.006)	0.09 (0.006)	0.10 (0.006)	0.68	0.48	0.40

Table 2.15 Estimated parameters of the Wood's model for WUR 0, 1, 2. No significant differences were found at the 95% significant level, the standard errors are in brackets.

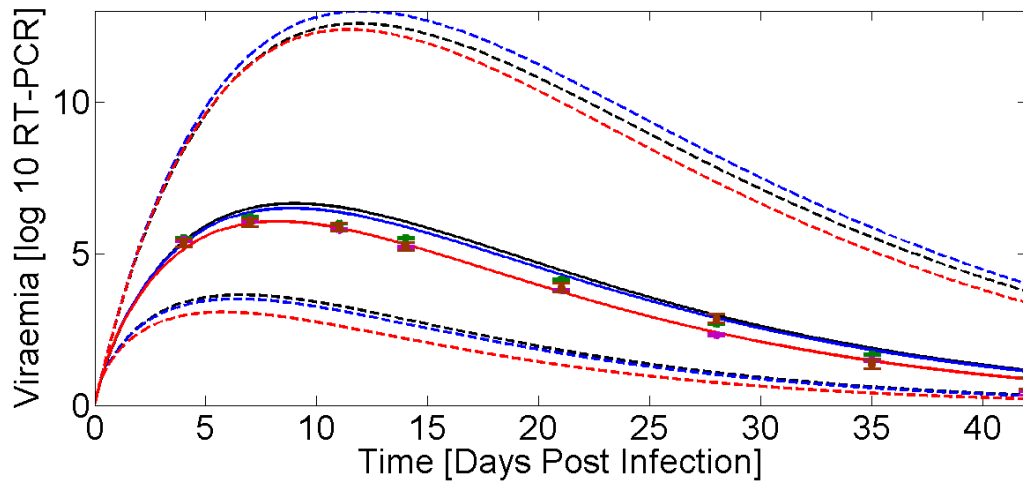


Figure 2.14 Wood's model predictions for WUR genotypes. The WUR genotype 0, 1 and 2 are in black, blue and red respectively. The WUR genotype 0 (AA) has the highest level of peak viraemia compared to WUR 1 and 2, implying that the B allele confers lower levels of peak viraemia. The dashed lines delimit the respective confidence intervals determined by: $LSM(\text{model parameter}) \pm 1.96 SE(\text{model parameter})$. The corresponding LSM estimates with confidence interval from the repeated measures model are shown for comparison, where the different colours refer to the different WUR genotypes 0(green), 1(purple), 2(brown).

3. Genetic background

Genetic background had a significant effect on all three Wood's model parameter with LSM parameter estimates for each genetic group shown Figure 2.15 and Table 2.16. Pairwise contrasts were conducted in SAS to determine differences in the Wood's parameters between genetic groups, as shown in Table 2.17. Our focus is the impact of genetic background within the same virus isolate. In section 4 (below) the trial differences in order to disentangle virus isolate type from the genetic background is examined.

The differences within the virus isolate were smaller than between virus isolates. It is not surprising that genetic backgrounds 1,3 and 8 were significantly different from the other backgrounds since they included trials infected with KS06. Examining for NVSL only (genetic backgrounds: 2, 4, 5 and 6) only a few significant differences between the linearized Wood's parameters were observed: genetic background 2 was significantly different in parameter A only with backgrounds 4 and 5, and genetic background 6 was significantly different in parameter A and b with backgrounds 4 and 5. Genetic background within NVSL affected the magnitude of the profiles (A) and rate of increase to the peak (b).

Genetic background	A (SE)	b (SE)	c (SE)	Virus	Trials
1	0.90 (0.07)	0.69 (0.05)	0.08 (0.004)	NVSL & KS06	1-3 & 11
2	0.52 (0.09)	1.03 (0.06)	0.11 (0.005)	NVSL	4
3	0.67 (0.08)	0.80 (0.05)	0.08 (0.004)	NVSL & KS06	5 & 14
4	0.49 (0.10)	1.00 (0.66)	0.09 (0.005)	NVSL	6
5	0.53 (0.10)	0.96 (0.06)	0.10 (0.005)	NVSL	7
6	0.79 (0.10)	0.94 (0.06)	0.09 (0.005)	NVSL	8
7	0.70 (0.08)	0.84 (0.05)	0.09 (0.004)	NVSL & KS06	15 & 10
8	0.91 (0.06)	0.82 (0.04)	0.10 (0.003)	KS06	12

Table 2.16 Estimated parameters of the Wood's model for each genetic background with a breakdown of the virus and trials involved. The standard errors are in brackets.

Genetic background	1	2	3	4	5	6	7	8	Virus	Trials
1	-								NVSL & KS06	1-3 & 11
2	X*O	-							NVSL	4
3	X*O	X*O	-						NVSL & KS06	5 & 14
4	X*O	O	X*O	-					NVSL	6
5	X*O	O	*O		-				NVSL	7
6	X*O			X*	X*	-			NVSL	8
7	X*O	X*O	O	X*	X		-		NVSL & KS06	15 & 10
8	X*O	*O	XO	X*	X	O	XO	-	KS06	12

Table 2.17 Significant differences (95% significance level) in the LSM estimates of the Woods parameters ($p < 0.05$) denoted by: X for parameter A, * for parameter b, and O for parameter c.

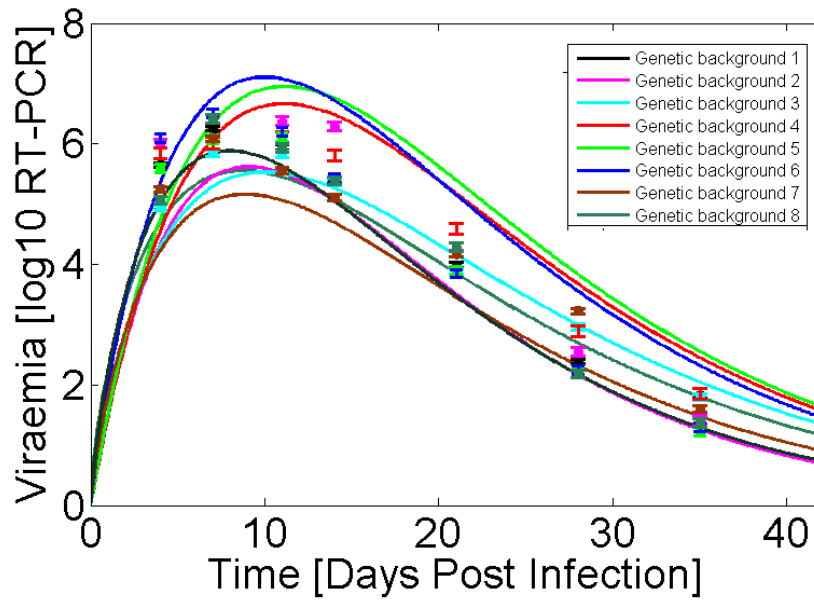


Figure 2.15. Wood's model predictions for each genetic background (lines) together with the corresponding estimated LSM viraemia at the observation times obtained from repeated measures model (asterisks).

4. The PHGC Trial

Trial differences allow us to examine the genetic background differences whilst separating out the virus isolate differences. The predicted Wood's profiles for all the trials separated by virus isolate are shown in Figure 2.16A and B; the repeated measures model and Woods model approaches lead to similar results. There were significant differences between the Wood's parameters between trials within virus isolate. Differences between trials could be due to the virus or the genetic background. The Wood's parameters from the trials, which were from the same genetic background are shown in Table 2.18. The Wood's parameters for trials 1-3 were not significantly different from each other; which indicate that the differences between the other trials would mainly be due to genetic background and virus type as opposed to a function of trial (which is simply an artefact of the experimental protocol).

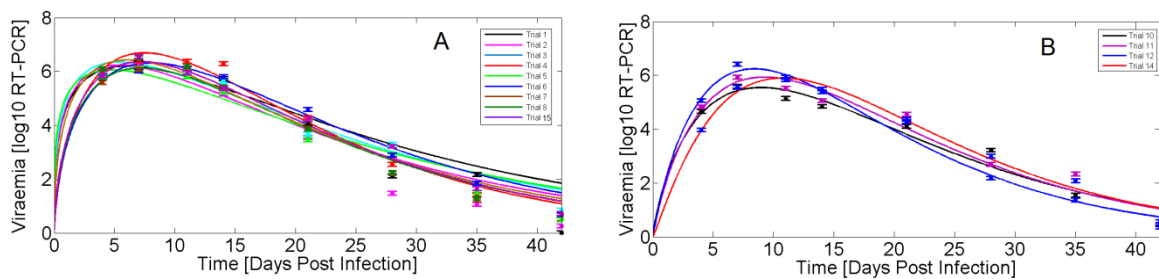


Figure 2.16. Wood's model predictions for each trial (lines) and corresponding LSM viraemia estimates obtained from the repeated measures models (asterisks). Figure 2.6A refers to the trials with infection with NVSL, and Figure 2.6B refers to trials with infection with KS06.

Genetic Background	7 (SEM)		1 (SEM)				3 (SEM)	
Virus	NVSL	KS06	NVSL	NVSL	NVSL	KS06	NVSL	KS06
Trial Parameter	15	10	1	2	3	11	5	14
A (SE)	1.58* (0.06)	1.60 (0.08)	1.58* (0.08)	1.60* (0.08)	1.65* (0.08)	1.00*** (0.08)	1.67* (0.08)	0.42 (0.08)
b (SE)	0.55* (0.04)	0.73 (0.05)	0.30* (0.06)	0.32* (0.05)	0.29* (0.05)	0.47*** (0.05)	0.23* (0.05)	0.97 (0.05)
c (SE)	0.08 (0.003)	0.08 (0.004)	0.05* (0.004)	0.06* (0.004)	0.05* (0.004)	0.07*** (0.004)	0.05* (0.003)	0.09 (0.004)

Table 2.18 Estimated parameters of the Wood's model for trials from the same genetic background. *indicates significant differences at the (95% significance level) within each genetic background. For genetic background 1 the colour of the asterisk indicates the trial's parameter being compared. Significance at the 95% significance level between trial x and trial 1 (red), 2 (purple), 3 (green), and 11 would be represented by ***.

The effect of removing the bimodal profiles on the linearized Woods model

The removal of bimodal profiles results in the same significant fixed and random effects in the final linearized Wood's model for the fixed effects: virus isolate, WUR genotype, genetic background and trial. There were slight differences in the LSM Wood's parameter estimates but these translated to small differences in the final Wood's curves as shown in the Appendix 1. Generally the removal of the bimodal profiles lowers the predicted Wood's profiles, making them closer to the LSMs of the repeated measures model. The removal of the bimodal profiles from the dataset leads to the same significant differences between parameter estimates.

2.3 Discussion

Empirical mathematical models have proven useful for describing the temporal evolution of a response variable and filtering stochastic noise from dynamic biological systems whilst retaining the most fundamental features [6,13,25,26]. Linear mixed models are a well-established methodology used to model longitudinal data with the inclusion of both fixed and random effects [13-17]. The comprehensive PHGC dataset comprising of repeated PRRS viraemia measurements from 2640 commercial pigs in this chapter provided a unique opportunity to assess the influential factors on PRRS viraemia profiles. The main aims of this chapter were to gain insights into temporal changes in viraemia and the factors which may potentially contribute to the observed viraemia time trends such as the different viral strains, the host's own genetic background, and the WUR genotype. For this purpose, two alternative approaches were implemented into the linear mixed model framework.

The advantage of the repeated measures modelling approach is that no prior information about the shape of the viraemia profiles is needed and is thus a logical place from which to begin analysing the impact of diverse influencing factors on longitudinal viraemia data [15,17]. Through the repeated measures model LSMs for viraemia were obtained at each observation time, and the effects of the influencing factors on these were examined. But the repeated measures modelling approach did not capture the full non-linear time trends of the individual viraemia profiles, thus the Wood's model fitting approach was adopted which allowed us to construct full viraemia curves for the entire time course of the experiment, and also examine the effect of the various factors on the model parameter estimates.

The fixed effects of virus isolate, genetic background or trial were consistently significant in both statistical modelling approaches. In the repeated measures model, however, the WUR genotype, age and sex were also a significant fixed effects but not in the Woods model. The age range was only 17-36 days. The lack of significance of age in the linearized Wood's model could be due to the age range of the pigs not being large enough to capture the variation it could contribute to the viraemia profile. Furthermore one can hypothesize that at a later age, that would be captured in a future experiment which contains a larger age range of pigs, the sex could have a more significant impact upon the viraemia in the linearized Woods model.

The significance of the genetic background on the viraemia profiles supports the increasing evidence in support of the host genetic contribution to a PRRS virus infection. Previous PRRSV challenge experiments have already revealed breed differences in viraemia levels and duration [1,27-29]. Reiner et al.[30] observed that Pietrain pigs infected with an attenuated PRRSV strain had longer viraemia lasting until 72 days post infection (dpi), whilst for Miniature pigs the viraemia only lasted up to 35dpi. Viraemia profiles in Pietrain pigs revealed both uni- and bimodal curves similar to the bimodal

profiles observed in this chapter [31]. Significant differences between genetic background, within each virus isolate, found in both linear mixed modelling approaches in this chapter is in line with the previously observed concept of inter-breed variation in viraemia. The WUR SNP was found in several previous quantitative genetic studies that already been performed on a subset of the viraemia data used in this chapter [8,10,12,32]. Using the repeated measures models the WUR genotype 0 had higher viraemia values at all stages of infection than the WUR 1 and 2 genotypes and the WUR 2 genotype had lower Wood's profile, despite non-significant Wood's parameter differences, than the other genotypes, in this chapter. These results for the WUR genotype are in line with the previous studies on this dataset which have shown that the WUR SNP resulted in reduced AUC of viraemia [8,10,32]. In a previous study as part of the PHGC consortium the WUR genotype has been tested for the Hardy-Weinberg equilibrium and the BB homozygotes were less frequent than expected[8].

Significant differences between the viraemia profiles (for 0-21dpi) of the two virus isolates NVSL and KS06 were found using both statistical approaches. The viraemia profiles between the two isolates differed in the rate of increase to peak viraemia, magnitude of the peak, the time of the peak and the rate of clearance. The viraemia LSMs for both virus isolates obtained from the repeated measures model were not significantly different at 42dpi, which would suggest that the host's immune response to NVSL infections was similarly effective at the later stages of infection as the response to KS06. According to the Wood's model, NVSL infection generates on average a faster increase to a higher and earlier peak than infection with KS06, followed by a faster rate of decline. However the virus isolate differences reduce over time. NVSL had lower parameter values for b and c , higher parameter A than KS06 and a shorter time to the peak (b/c dpi). Different virus strains can differ in virulence levels and their ability to cause reproductive failure [33]. The isolate differences were expected since NVSL is known as a highly virulent isolate [19,20]. A previous study found strain differences manifesting in differences between the viraemia profiles [34]. Furthermore these differences could be related to differences in the immune response to the particular PRRS viral strains, such as differences in expression of the anti-viral cytokine interferon alpha [34]. In Chapter 4 the relationship between viraemia and cytokine profiles from a subset of the NVSL profiles will be analysed.

The majority of profiles were uni-modal, however bimodal viraemia profiles were also observed: 16% for KS06 compared to 27% for NVSL. Bimodal profiles were observed across all trials, genetic backgrounds and WUR genotypes. There were a similar percentage of bimodal profiles between trials within each virus isolate. The WUR genotypes were distributed similarly between the uni- and bimodal profiles within each virus isolate. Overall NVSL had a higher percentage of bimodal profiles than KS06. This could be due to the faster viraemia dynamics allowing for a second peak to be captured in the current time course of the experiment. The slower dynamics of a typical KS06 viraemia profile could result in a second peak hypothetically arising after 42dpi and would thus not be captured in the experiment. The statistical results with regards to the impact of fixed effects on the

repeated measures LSMs, Wood's parameters and resulting profiles were robust to the inclusion of bimodal profiles, with only one discrepancy in the significance of the repeated measures LSMs between the WUR genotype 0 and 2 at 35dpi. Inspection of the model residuals for the repeated measures model revealed that the model was adequate for the early phase of infection (up to 14dpi) with residuals within 2 units on the \log_{10} scale. Inspection of the raw data indicated that inter-host variation increased over time. In line with this increase of variation, residual variation also increased at the later infection stages. However, residuals reached magnitudes of up to 5 units on the \log_{10} scale, indicating a poor model fit. The fit of the repeated measures model improved substantially after removal of bimodal profiles. Nevertheless, there were still residuals greater than 3 units on the \log_{10} scale at 35dpi suggesting that the repeated measures model did not adequately capture the late stage viral dynamics for all profiles.

The Wood's model appeared a suitable candidate model for the data associated with uni-modal profiles since its shape matches the shape of a typical uni-modal viraemia profile. Furthermore the Wood's model captures the time trends concisely in only three model parameters which also have a biological relevance. Overall the best fitting Wood's model was when there was a random effect in Wood's parameters b and c according to the LRT. In particular, models with individual variation in the parameter c provided better fits than those without variation in this parameter. This result is expected due to the fact that the variation in parameter c results in variation in the rate of decline from the peak viraemia which captures the increased inter-host variation from 7dpi onwards. There is a general tendency for the Woods model to over-predict viraemia at 42dpi, which can easily be explained by the fact that the Wood's curve converges to but never reaches, zero. This latter property of the Wood's function may in fact be a clearer representation of reality; we are never able to confirm that viraemia levels truly reach zero, but only that they have reached levels below the detection threshold determined by the accuracy of experimental observations.

The residuals from fitting the final linearized Wood's function revealed that, as with the repeated measures approach, the bimodal profiles reduced the model fit to the data. The magnitude of the residuals on the scale on which they are calculated were a misleading indication of the model fit; back-transformation of the data and predictions to the \log_{10} scale revealed that the residuals were actually relatively high values reaching 3 units of the \log_{10} scale. Similar to the repeated measures model, the Woods model fit was adequate from 0- 14dpi. However, from 14dpi the range of residuals was high and indicative of poor fits particularly at 35dpi. Comparison of the residuals revealed that the repeated measures approach led to a slightly better fit to the data, particularly at 0-14dpi. A better fit is needed in order to determine the host genetic influence on viraemia profiles and to explore the relationship between viraemia profiles and the immune response. The poor Wood's model fits are likely a manifestation of the linearization process as opposed to a reflection of the suitability of the Wood's function as a candidate model for viraemia profiles. Ideally a nonlinear function would be fit

directly to the data since the process of linearizing the function provides LSM estimates and standard errors for the parameters of the linearized model on the natural log-scale. Directly fitting the nonlinear Wood's function to the log-transformed viraemia data would overcome this problem. However when this approach was adopted and PROC NLMIXED was used, it failed to converge when random effects were included into the model. Thus in Chapter 3 the method of directly fitting the Woods model to the data using a Bayesian model fitting approach will be adopted.

The Wood's model is a uni-modal function and cannot capture the second phase of the bimodal profiles. In order to capture the full range of viraemia profiles the Wood's model needs to be extended. Fitting a bimodal Wood's function is not possible in the linear mixed modelling framework used in this chapter. Furthermore the current method of bimodal classification was derived from visual observation and results from calculating the differences between two observations separately. A better approach may be to evaluate the whole infection period and use the statistical significance of the fit of a bimodal model to derive viraemia classification, which will be explored in the next chapter. Deriving a better model fit in the next chapter will allow for a deeper analysis of the time trends of viraemia profiles from a PRRSV challenge. However the correlations between the AUC of the viraemia and the profile type would not be a useful analysis since by definition the viraemia bimodality or "viraemia rebound" results in a larger AUC. Conversely a more useful scientific question to explore is whether the information derived from the early phase of infection can be used to inform predictions about the outcomes in the later phase of infection.

References for Chapter 2

1. Doeschl-Wilson A, Kyriazakis I, Vincent A, Rothschild M, Thacker E, et al. (2009) Clinical and pathological responses of pigs from two genetically diverse commercial lines to porcine reproductive and respiratory syndrome virus infection. *Journal of Animal Science* 87: 1638-1647.
2. Lunney JK, Steibel JP, Reecy JM, Fritz E, Rothschild MF, et al. Probing genetic control of swine responses to PRRSV infection: current progress of the PRRS host genetics consortium; 2011. BioMed Central Ltd. pp. 30.
3. Chand RJ, Tribble BR, Rowland RRR (2012) Pathogenesis of porcine reproductive and respiratory syndrome virus. *Current Opinion in Virology*: 2:256-263.
4. Loving CL, Brockmeier SL, Sacco RE (2007) Differential type I interferon activation and susceptibility of dendritic cell populations to porcine arterivirus. *Immunology* 120: 217-229.
5. Beever D, Rook A, France J, Dhanoa M, Gill M (1991) A review of empirical and mechanistic models of lactational performance by the dairy cow. *Livestock Production Science* 29: 115-130.
6. Grossman M, Koops W (2003) Modeling extended lactation curves of dairy cattle: a biological basis for the multiphasic approach. *Journal of dairy science* 86: 988-998.
7. Wood PDP (1967) Algebraic Model of the Lactation Curve in Cattle. *Nature* 216: 164-165.
8. Boddicker N, Waide E, Rowland R, Lunney J, Garrick D, et al. (2012) Evidence for a major QTL associated with host response to Porcine Reproductive and Respiratory Syndrome virus challenge. *Journal of Animal Science* 90: 1733-1746.
9. Boddicker NJ, Bjorkquist A, Rowland RRR, Lunney JK, Reecy JM, et al. (2014) Genome-wide association and genomic prediction for host response to porcine reproductive and respiratory syndrome virus infection. *Genetics Selection Evolution* 46.
10. Boddicker NJG, Dorian J.; Reecy, James M.; Rowland, Bob; Lunney, Joan K.; and Dekkers, Jack C. M. (2013) Quantitative Trait Locus on *Sus scrofa* Chromosome 4 Associated with Host Response to Experimental Infection with Porcine Reproductive and Respiratory Syndrome Virus Animal Industry Report AS 659, ASL R2823.
11. Boddicker NJ, Garrick DJ, Rowland RRR, Lunney JK, Reecy JM, et al. (2014) Validation and further characterization of a major quantitative trait locus associated with host response to experimental infection with porcine reproductive and respiratory syndrome virus. *Animal Genetics* 45: 48-58.
12. Hess AS, Boddicker N, Rowland B, Lunney J, Plastow G, et al. (2014) Validation of the Effects of a SNP on SSC4 Associated with Viral Load and Weight Gain in Piglets Experimentally Infected with a 2006 PRRS Virus Isolate. *Animal Industry Report* 660: 89.
13. Brown H, Prescott R (2006) *Applied mixed models in medicine*: John Wiley West SussexUK.
14. Wolfinger RD (1997) An example of using mixed models and PROC MIXED for longitudinal data. *Journal of Biopharmaceutical statistics* 7: 481-500.
15. Verbeke G, Molenberghs G (1997) *Linear mixed models in practice: a SAS oriented approach*. New York: Springer-Verlag
16. Meetings A-A-CN (2002) *Mixed Model Workshop*. Canada.
17. Littell R, Henry P, Ammerman C (1998) Statistical analysis of repeated measures data using SAS procedures. *Journal of Animal Science* 76: 1216-1231.
18. Rowland RR, Joan Lunney, and Jack Dekkers. (2012) Control of porcine reproductive and respiratory syndrome (PRRS) through genetic improvement in disease resistance and tolerance. *Frontiers of Livestock Genomics*: 3:260.

19. Fang Y, Schneider P, Zhang W, Faaberg K, Nelson E, et al. (2007) Diversity and evolution of a newly emerged North American Type 1 porcine arterivirus: analysis of isolates collected between 1999 and 2004. *Archives of virology* 152: 1009-1017.
20. Truong HM, Lu Z, Kutish GF, Galeota J, Osorio FA, et al. (2004) A highly pathogenic porcine reproductive and respiratory syndrome virus generated from an infectious cDNA clone retains the in vivo virulence and transmissibility properties of the parental virus. *Virology* 325: 308-319.
21. Ostrowski M, Galeota JA, Jar AM, Platt KB, Osorio FA, et al. (2002) Identification of neutralizing and nonneutralizing epitopes in the porcine reproductive and respiratory syndrome virus GP5 ectodomain. *Journal of Virology* 76: 4241-4250.
22. Ansari IH, Kwon B, Osorio FA, Pattnaik AK (2006) Influence of N-linked glycosylation of porcine reproductive and respiratory syndrome virus GP5 on virus infectivity, antigenicity, and ability to induce neutralizing antibodies. *Journal of Virology* 80: 3994-4004.
23. Pirzadeh B, Gagnon CA, Dea S (1998) Genomic and antigenic variations of porcine reproductive and respiratory syndrome virus major envelope GP(5) glycoprotein. *Canadian Journal of Veterinary Research-Revue Canadienne De Recherche Veterinaire* 62: 170-177.
24. Barr DJ, Levy R, Scheepers C, Tily HJ (2013) Random effects structure for confirmatory hypothesis testing: Keep it maximal. *Journal of memory and language* 68: 255-278.
25. Trefan L, Bünger L, Bloom-Hansen J, Rooke J, Salmi B, et al. (2011) Meta-analysis of the effects of dietary vitamin E supplementation on α -tocopherol concentration and lipid oxidation in pork. *Meat Science* 87: 305-314.
26. English S, Bateman AW, Clutton-Brock TH (2012) Lifetime growth in wild meerkats: incorporating life history and environmental factors into a standard growth model. *Oecologia* 169: 143-153.
27. Reiner G, Willems H, Pesch S, Ohlinger V (2009) Variation in resistance to the porcine reproductive and respiratory syndrome virus (PRRSV) in Pietrain and Miniature pigs. *Journal of Animal Breeding and Genetics* 127: 100-106.
28. Petry D, Lunney J, Boyd P, Kuhar D, Blankenship E, et al. (2007) Differential immunity in pigs with high and low responses to porcine reproductive and respiratory syndrome virus infection. *Journal of Animal Science* 85: 2075-2092.
29. Petry D, Holl J, Weber J, Doster AR, Osorio FA, et al. (2005) Biological responses to porcine respiratory and reproductive syndrome virus in pigs of two genetic populations. *Journal of Animal Science* 83: 1494-1502.
30. Reiner G, Willems H, Pesch S, Ohlinger V (2010) Variation in resistance to the porcine reproductive and respiratory syndrome virus (PRRSV) in Pietrain and Miniature pigs. *Journal of Animal Breeding and Genetics* 127: 100-106.
31. Yoo D, Song C, Sun Y, Du Y, Kim O, et al. (2010) Modulation of host cell responses and evasion strategies for porcine reproductive and respiratory syndrome virus. *Virus Research* 154: 48-60.
32. Boddicker NJ, Garrick DJ, Rowland RRR, Lunney JK, Reecy JM, et al. (2013) Validation and further characterization of a major quantitative trait locus associated with host response to experimental infection with porcine reproductive and respiratory syndrome virus. *Animal Genetics*: n/a-n/a.
33. Mengeling W, Vorwald A, Lager K, Brockmeier S (1996) Comparison among strains of porcine reproductive and respiratory syndrome virus for their ability to cause reproductive failure. *American journal of veterinary research* 57: 834-839.
34. Wesley RD, Lager KM, Kehrli Jr ME (2006) Infection with Porcine reproductive and respiratory syndrome virus stimulates an early gamma interferon response in the serum of pigs. *Canadian journal of veterinary research* 70: 176-182.

Chapter 3

Quantitative analysis of Porcine Reproductive and Respiratory Syndrome (PRRS) viraemia profiles from experimental infection: a Bayesian statistical modelling approach

3.0 Introduction

Empirical mathematical models have proven useful for describing the temporal evolution of a response variable and filtering stochastic noise from dynamic biological systems whilst retaining the most fundamental features [6,13,25,26]. In the previous chapter linear mixed models were used to capture the viraemia profiles from a PRRSV challenge however better model fit is needed in order to determine the host genetic influence on viraemia profiles and to explore the relationship between viraemia profiles and the immune response. The poor Wood's model fits are likely a manifestation of the linearization process as opposed to a reflection of the suitability of the Wood's function as a candidate model for viraemia profiles. Ideally a nonlinear function would be fit directly to the data since the process of linearizing the function provides LSM estimates and standard errors for the parameters of the linearized model on the natural log-scale. Directly fitting the nonlinear Wood's function to the log-transformed viraemia data would overcome this problem. Thus in this chapter the method of directly fitting the Woods model to the data using a Bayesian model fitting approach is adopted.

In Chapter 2 the Wood's model appeared a suitable candidate model for the data associated with uni-modal profiles since its shape matches the shape of a typical uni-modal viraemia profile. Furthermore the Wood's model captures the time trends concisely in only three model parameters which also have a biological relevance. However the Wood's model is a uni-modal function and cannot capture the second phase of the bimodal profiles. In order to capture the full range of viraemia profiles the Wood's model needs to be extended. Fitting a bimodal Wood's function is not possible in the linear mixed modelling framework hence a Bayesian approach is adopted in this chapter. Furthermore the method of bimodal classification in Chapter 2 was derived from visual observation and results from calculating the differences between two observations separately. A better approach in Chapter 3 may be to evaluate the whole infection period and use the statistical significance of the fit of a bimodal model to derive viraemia classification. Deriving a better model fit in this chapter will allow for a deeper analysis of the time trends of viraemia profiles from a PRRSV challenge. The primary objective of this chapter was to find mathematical functions that adequately represent the full range of viraemia profiles obtained from a large scale PRRSV infection experiment, and use these to determine quantitative characteristics of infection dynamics. The functions will be used to derive an objective

method of classification of viraemia profiles based on statistical inference and to assess the relationship between the breadth of nAb response and viraemia profile.

Chapter 3 has been published in Plos One and below is an outline of the contribution of the authors:

Zeenath U. Islam: carried out the analysis, developed hypotheses

Stephen C. Bishop, Andrea B. Doeschl- Wilson: directed the analysis and informed the development of hypotheses

Raymond R.R. Rowland, Joan K. Lunney, Benjamin Tribble: provided the viraemia and nAb data.

Nicholas J. Savill: provided the computer program for fitting the functions to the viraemia data.

Quantitative Analysis of Porcine Reproductive and Respiratory Syndrome (PRRS) Viremia Profiles from Experimental Infection: A Statistical Modelling Approach

Zeenath U. Islam^{1*}, Stephen C. Bishop¹, Nicholas J. Savill², Raymond R. R. Rowland³, Joan K. Lunney⁴, Benjamin Triple³, Andrea B. Doeschl-Wilson¹

1 The Roslin Institute & R(D)SVS, University of Edinburgh, Edinburgh, Midlothian, United Kingdom, **2** Institute of Immunology and Infection Research, University of Edinburgh, Edinburgh, United Kingdom, **3** Department of Diagnostic Medicine and Pathobiology, College of Veterinary Medicine, Kansas State University, Manhattan, Kansas, United States of America, **4** United State Department of Agriculture, Beltsville Agricultural Research Center, Beltsville, Maryland, United States of America

Abstract

Porcine reproductive and respiratory syndrome (PRRS) is one of the most economically significant viral diseases facing the global swine industry. Viremia profiles of PRRS virus challenged pigs reflect the severity and progression of infection within the host and provide crucial information for subsequent control measures. In this study we analyse the largest longitudinal PRRS viremia dataset from an in-vivo experiment. The primary objective was to provide a suitable mathematical description of all viremia profiles with biologically meaningful parameters for quantitative analysis of profile characteristics. The Wood's function, a gamma-type function, and a biphasic extended Wood's function were fit to the individual profiles using Bayesian inference with a likelihood framework. Using maximum likelihood inference and numerous fit criteria, we established that the broad spectrum of viremia trends could be adequately represented by either uni- or biphasic Wood's functions. Three viremic categories emerged: cleared (uni-modal and below detection within 42 days post infection(dpi)), persistent (transient experimental persistence over 42 dpi) and rebound (biphasic within 42 dpi). The convenient biological interpretation of the model parameters estimates, allowed us not only to quantify inter-host variation, but also to establish common viremia curve characteristics and their predictability. Statistical analysis of the profile characteristics revealed that persistent profiles were distinguishable already within the first 21 dpi, whereas it is not possible to predict the onset of viremia rebound. Analysis of the neutralizing antibody(nAb) data indicated that there was a ubiquitous strong response to the homologous PRRSV challenge, but high variability in the range of cross-protection of the nAbs. Persistent pigs were found to have a significantly higher nAb cross-protectivity than pigs that either cleared viremia or experienced rebound within 42 dpi. Our study provides novel insights into the nature and degree of variation of hosts' responses to infection as well as new informative traits for subsequent genomic and modelling studies.

Citation: Islam ZU, Bishop SC, Savill NJ, Rowland RRR, Lunney JK, et al. (2013) Quantitative Analysis of Porcine Reproductive and Respiratory Syndrome (PRRS) Viremia Profiles from Experimental Infection: A Statistical Modelling Approach. PLoS ONE 8(12): e83567. doi:10.1371/journal.pone.0083567

Editor: Xiang-Jin Meng, Virginia Polytechnic Institute and State University, United States of America

Received: September 17, 2013; **Accepted:** November 13, 2013; **Published:** December 17, 2013

Copyright: © 2013 Islam et al. This is an open-access article distributed under the terms of the Creative Commons Attribution License, which permits unrestricted use, distribution, and reproduction in any medium, provided the original author and source are credited.

Funding: The development of the model fitting code was supported by a Wellcome Trust Project grant to NJS (Grant No. 091078/Z/09/Z, <http://www.wellcome.ac.uk/>). The characterization of neutralizing antibody responses to PRRSV and association with host factors was supported by the NPB (Grant No. 12–120, <http://www.pork.org/filelibrary/ResearchGrants/Funded2012.pdf>). Funding for the project also came from "Genome Canada: Application of Genomics to Improve Swine Health and Welfare" (<http://www.swineimprovement.com/>) and "CSHB: Development of genetic selection tools to enhance sow health using a novel acclimation challenge model in Canadian commercial herds" (<http://www.swinehealth.ca/program-research-proj-11.php>). This work was supported by the Roslin Institute Strategic Grant funding from the BBSRC (ISPG 1). The funders had no role in study design, data collection and analysis, decision to publish, or preparation of the manuscript.

Competing Interests: The authors received funding from a commercial source, Genome Canada, and are not related to the organisation in the form of: employment, consultancy, patents, products in development, or marketed products. This source of funding does not alter the authors' adherence to all the PLOS ONE policies on sharing data and materials.

* E-mail: zeenath.islam@roslin.ed.ac.uk

Introduction

Porcine reproductive and respiratory syndrome (PRRS) is one of the most important infectious diseases threatening pig production worldwide [1]. PRRS reduces reproductive performance in breeding animals and increases respiratory problems in animals of all ages, leading to impaired growth in young piglets and, in some cases, mortality [2–4]. Infection with the PRRS virus (PRRSV) results in viremia and virus replication in multiple organs within the host; the targets for replication are macrophages in various tissues, primarily the lung but also in lymph nodes, spleen, placenta and umbilical cord [5–7]. One of the most

significant challenges facing the eradication of the disease is the persistent nature of the etiological agent, PRRSV, which may persist within the host for several weeks or months, in some cases maintaining a sub-clinical lifetime persistence [8,9]. If the persistently PRRSV infected individuals also remain infectious, they can drive the epidemiological dynamics of the disease within the population through perpetuating the cycle of transmission to susceptible animals [10].

Viremia profiles of *in-vivo* experimentally PRRSV challenged pigs are valuable indicators of the severity and progression of the infection in the host, and thus provide crucial information for the required subsequent disease control measures [11]. The course of

a typical PRRSV infection is characterised by an acute viremic stage lasting approximately 4 weeks followed by a stage characterised by low levels and eventual resolution of viremia. Previous studies suggest that in the majority of animals viremia reaches undetectable levels typically by 4–6 weeks, although the virus may still be isolated months later in the lymphoid tissues [12,13].

PRRSV challenge experiments with longitudinal viremia measures reveal substantial differences in the viremia profiles between hosts infected with the same PRRSV challenge dose, pointing to considerable variation in the host response to PRRSV infections. For example, numerous studies have shown breed differences in viremia levels and duration and also in antibody production [11,14–16]. Reiner et al. [17] observed that Pietrain pigs infected with an attenuated PRRSV strain had longer viremia lasting until 72 days post infection (dpi), and a less efficient antibody production than Miniature pigs whose viremia only lasted up to 35 dpi. Viremia was classified as persistent in Pietrain pigs, however the profiles revealed both uni- and biphasic curves which could be a manifestation of viremia reactivation from the original infection within the host or reinfection between the pigs [18]. Using longitudinal viremia records collected over a 42 day period from 531 pigs challenged with a virulent PRRSV strain, Boddicker et al. [19] reported substantial differences between individual viremia profiles and also in total viremia, summarised as “area under the curve” (AUC) or viral load (VL). Furthermore, based on visual inspection, they classified pigs into two categories, i.e. non-rebounders and rebounders, characterised by mono- and bi-phasic serum viral profiles, respectively.

Given the apparent diversity in viremia patterns, several important questions arise. For example, for vaccine development or consideration of genetic disease control strategies it is important to determine whether and to what extent the observed differences in the profiles are influenced by the host and the virus genotype. In the longitudinal study of Boddicker et al. [20], the VL measure was found moderately heritable ($h^2 = 0.3$), pointing to significant host genetic influence underlying disease severity and progression. Rebound was however not found to be heritable and thus thought to be controlled more by the virus than the host genotype [20]. However, the low heritability estimate of this trait (0.03) may have arisen due to the limited dataset, insufficient observations to capture the rebound phase, or the potential misclassification of individuals based on visual inspection of the profiles. Furthermore, there may be other profile characteristics representing host genetic variation in specific immune functions.

One hallmark of PRRSV is its high genetic diversity due to its fast mutation rate, resulting in continuous emergence of new quasi-species that may evade the host's immune system [21,22]. Antibodies with PRRSV-neutralising activity usually appear from 14–28 days post infection (dpi) and are correlated with the reduction of PRRSV in the lung and the peripheral blood [23]. Despite conflicting reports on the significance of neutralizing antibodies (nAb) in anti-PRRSV protection [24], one would expect that diversity in the nAb response is important for cross-protective immunity against different PRRSV isolates, mutants or quasi-species. Thus, it would be useful to know whether host differences in viremia patterns are also reflected by differences in the breadth of nAb, and whether these measures are directly related. For example, one may hypothesize that a host that is able to clear the virus faster may have a less diverse nAb response than hosts with persistent or bi-phasic viremia profiles experiencing more cycles of virus replication and mutation.

From an epidemiological perspective, viremia rebound may constitute a problem as pigs diagnosed as cleared may have high

levels of infectious virus a few days later. It would be useful to know whether viremia rebound reflects genuinely viremia reactivation rather than fluctuations in circulating virus load or measurement errors, and whether all or only a subset of pigs experience rebound. In particular, it would be useful to know whether virus rebound, or persistence, can be predicted based on early serum profile characteristics.

Addressing the questions raised above would require frequent repeated measurements of viremia, as well as of nAb diversity, on a large number of pigs subjected to the same experimental PRRSV challenge conditions. Such data are now available from the PRRS Host Genetic Consortium [1]. However, raw viremia data are inherently noisy and incomplete. Empirical mathematical functions have proven a useful tool for smoothing noisy data profiles and for exploring characteristics of dynamic patterns [25,26]. Thus, an appropriate mathematical function may be able to concisely represent the full range of viremia profiles using only a few parameters. In particular, functions in which individual parameters represent specific curve characteristics provide an opportunity to apply rigorous statistical analysis to quantify differences in viremia patterns.

The primary objective of this study was to find mathematical functions that adequately represent the full range of viremia profiles obtained from a large scale PRRSV infection experiment, and use these to determine quantitative characteristics of infection dynamics. The functions will be used to derive an objective method of classification of viremia profiles based on statistical inference and to assess the relationship between the breadth of nAb response and viremia profile.

Materials and Methods

Experimental Data

The data analysed in this study was obtained from the PRRS Host Genetic Consortium (PHGC) trials, the largest PRRSV in-vivo challenge study to date; a detailed description of the experimental protocol is outlined in [1,27]. Briefly, viremia data was obtained from pigs which were experimentally infected with NVSL 97–7985, a virulent isolate of PRRSV, [28], in eight separate infection trials (ca. 200 pigs/trial) with an infection dose of 10^5 tissue culture dose₅₀ (TCID₅₀). The challenged pigs came from high health farms that were free of PRRSV, *Mycoplasma hyopneumoniae* and swine influenza virus. Pigs were placed randomly in pens of 10–15 pigs and were infected with PRRSV after a 7 day acclimation period, i.e. at 0 days post infection (0 dpi). Blood samples were collected immediately before infection (0 dpi) and at 4, 7, 11, 14, 19/21, 28, 35, 40/42 dpi and the level of PRRS viremia was measured using a semi-quantitative TaqMan PCR assay for PRRSV RNA. The viremia quantity data from RT-PCR was transformed on the logarithmic scale to the base 10 before the model fitting. Due to the sensitivity of RT-PCR the threshold of detection was set at 1 units on the log₁₀ scale [20].

For the purpose of this study, only individuals with a minimum of 6 serum viremia observations were retained. This resulted in a viremia dataset comprising 1371 pigs in total, with over 170 pigs per trial, with the exception of trial 6 for which data from 89 pigs with less than 6 viremia observations had to be discarded. The majority of missing observations in Trial 6 were from 14 dpi onwards due to the outbreak of a bacterial infection, thus reducing the potential to capture viremia rebound. All individuals from Trials 7 and 8 were missing the last observation at 40/42 dpi due to management issues in the experimental facility.

To explore hypotheses surrounding the association between viremia profiles and the variability of the nAb response to PRRSV, nAb data from serum collected at 42 dpi was obtained for 490 individuals from the first three trials using a virus neutralization assay as outlined in [29]. Briefly, serum neutralising assays were conducted to examine the presence of cytopathic effects on the homologous PRRSV strain as used in the *in-vivo* challenge experiment (NVSL-7985 denoted henceforth as NVSL) and three additional PRRSV isolates: KS06-72109 (KS06), P-129 and VR-2332 (VR). These type 2 PRRSV isolates were chosen for genetic differences based on viral ORF5 sequence. KS06 had been isolated in 2006 and as a more contemporary isolate is still found in the field. Excluding the relatedness between P129 and NVSL (95%), nucleotide comparisons within ORF5 show that the PRRSV isolates differed from each other by 10% or greater. Each serum sample was reacted with the panel of four type 2 viral isolates, where the NVSL isolate served as the homologous virus in the serum neutralisation assays. Serum samples were considered positive for PRRSV nAb at a titre of eight or higher. Individuals in PHGC Trials 1–3 were assigned to one of the following five nAb categories: 1) failed to produce a nAb response, 2) only produced antibodies against the challenge virus (homologous nAb response), 3) produced nAb against the original and a different isolate (mild heterologous response), 4) produced nAb against the original and two different isolates (moderate heterologous response), 5) produced nAb against all four isolates (broad response). Analysis was conducted on the combined nAb categories of no cross protection (categories 1–2) and cross-protection (categories 3–5) as this was the most biologically relevant grouping of the nAb classes.

Viremia Profile Characteristics and Mathematical Models

Visual inspection of the individual viremia profiles from the raw data indicated that the profiles can be empirically grouped into three categories, illustrated in Figure (1): undetectable viremia levels at 42 dpi, persistence up to 42 dpi, and apparent clearance within the first 35 dpi followed by viremia rebound. Thus, observed profiles were either uni- or biphasic. Apparent viremia rebound occurred from 28 dpi onwards. A suitable mathematical model should thus be able to represent both uni-modal clearance and persistence as well as biphasic viremia rebound. Despite large inter-host variation in the individual profiles, visual inspection further indicated that all non-rebound viremia profiles and the primary phase of rebound profiles are characterised by a relatively rapid viremia increase towards the peak followed by a gradual exponential decline. Furthermore inter-host variation in the profiles is initially small, but increases over time.

Wood's Model

The Wood's function, a gamma-type function often used to empirically describe lactation curves in dairy cattle [25,30,31], was chosen as candidate model as it appears to satisfy the above described data characteristics of the uni-modal profiles and the primary phase of the biphasic profiles. The function is given in equation (0.1):

$$y(t) = a_1 t^{b_1} e^{-c_1 t} \quad (0.1)$$

where $y(t)$ represents the level of viremia in the blood (\log_{10} RT-PCR) at t days post infection (dpi). The constant a_1 is a scalar quantity and impacts upon the magnitude of all the points on the curve. The parameter b_1 is an indicator of the initial rate of increase to the peak viremia level and the parameter c_1 is an indicator of the rate of decline after the peak and dominates the

function as $t \rightarrow +\infty$. The maximum viremia load is achieved at time $t_1 = \frac{b_1}{c_1}$ dpi, and the value of the maximum viremia is $isv_1 = a_1 \left(\frac{b_1}{c_1}\right)^{b_1} e^{-b_1}$. Other curve characteristics, such as the rate of viremia decline at any point in time or the cumulative viremia load up to a given time t post infection can be readily obtained by differentiation or integration of the above function.

Extended Wood's Model

In order to represent the bi-phasic profiles, the Wood's function was extended to a biphasic function described by equation (0.2):

$$y(t) = a_1 t^{b_1} e^{-c_1 t} + \max(0, a_2(t - t_0)^{b_2} e^{-c_2(t - t_0)}) \quad (0.2)$$

where the model parameters a_1, b_1 and c_1 define the primary phase of the rebound profile as described for the Wood's model above. Time t_0 denotes the onset of the second phase of the profile, which is assumed to follow the same (Wood's) shape as the primary phase and is thus defined by the second set of Wood's model parameters: a_2, b_2, c_2 . For $t < t_0$ the Extended Wood's model is equivalent to the Wood's model. The Extended Wood's model has the derived parameters denoting the time and value of the first and second peaks respectively: $t_1, v_1, t_2 = t_0 + \frac{b_2}{c_2}, v_2 = a_2 \left(\frac{b_2}{c_2}\right) e^{-b_2}$. Similarly, rates of viremia decline or cumulative viremia load at any time post infection can be calculated through differentiation and numerical integration of the Extended Wood's function.

Model Fitting and Parameter Estimation

Both the Wood's and Extended Wood's function were fitted to the individual data profiles using Bayesian inference with a likelihood framework. This was implemented by using an adaptive, population based Markov chain Monte Carlo method with power posteriors as described in [32–35]. The prior distributions for the function parameters were assumed to be uniformly distributed within a biologically realistic range. Parameters were estimated separately for each pig. The resulting inferences are based on 3000 samples, thinned from 2×10^5 iterations of a non-adaptive Markov chain, with the first half of the chain discarded as burn in. For observations greater than the RT-PCR measurement threshold of 1 units on the \log_{10} scale the errors were assumed normally distributed around 0 with a standard deviation of 0.5 log units, and for observations less than or equal to the RT-PCR observation threshold the errors were assumed cumulative normal.

Both the Wood's and Extended Wood's functions were fitted to all pigs. Thus the fitting procedure provided for each individual pig posterior distributions for every parameter of the Wood's and Extended Wood's function, respectively, from which parameter means, modes and credibility intervals were derived.

Assessment of Model Fit

The accuracy of the model fit and choice of best model was assessed based on the Akaike's Information Criterion (AIC), together with inspection of the predicted model profiles with 95% posterior credibility intervals for every individual, to gain insight into both the accuracy and potential bias of the model predictions over the time course of the experiment. This included plotting histograms of the parameter estimates, inspection of the residuals, as well as calculating the (product moment) correlation between observations and predictions at each sampling time point.

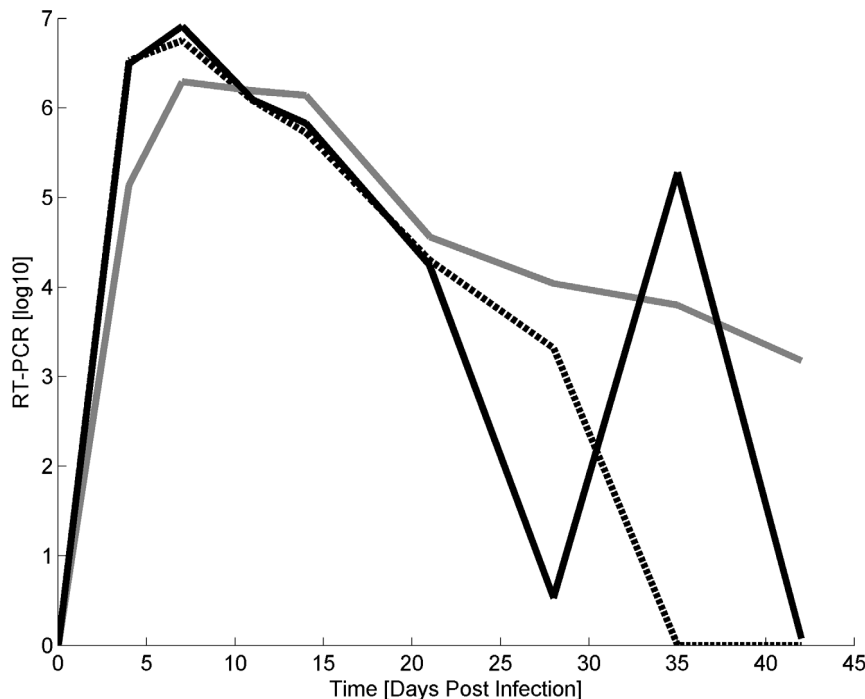


Figure 1. Raw phenotypic data profiles of three representative pigs experimentally infected with PRRSV. The viremia profile categories are: undetectable within 42 dpi (black dotted line), mono-phasic experimental persistence up to 42 dpi (grey line), and bi-phasic rebound (black line).

doi:10.1371/journal.pone.0083567.g001

Objective Classification of Profiles

Due to the high degree of fluctuation in the viremia measurements, classification of the raw data profiles into the three categories shown in Figure 1 is somewhat arbitrary and not always straight-forward. However, the two alternative mathematical viremia models, i.e. the Wood's and the Extended Wood's model, together with statistical measures of goodness-of-fit provided an objective method for assigning the profiles into uni-modal and biphasic categories.

An individual was classified as experiencing viremia rebound if the biphasic Extended Wood's model had a statistically superior fit to the data than the uni-modal Wood's model at the 95% significance level. For this purpose, both models were separately fitted to the individual's \log_{10} RT-PCR data and the Akaike's Information Criterion (AIC) was obtained. The AIC difference between the competing models for each individual pig is analogous to the likelihood ratio test statistic (D) when adjusted for twice the difference in the number of model parameters of the two models. The Wood's model has 3 parameters and the Extended Wood's model has 7 parameters, thus the AIC difference adjusted for the number of parameters becomes: $AIC_{WOODS} - AIC_{EXTENDEDWOODS} = D - 2(7 - 3) = D - 8$. Thus at the 95% significance level the required likelihood ratio test, obtained from the chi-squared distribution, with 4 degrees of freedom, was $D = 9.488$ [36], corresponding to a critical difference in the AIC of $AIC_{WOODS} - AIC_{EXTENDEDWOODS} = 9.488 - 8 = 1.488$. Thus, if the AIC difference was greater than or equal to this value (1.488) then the profile was classed into the biphasic rebound category, otherwise it was classed as uni-modal.

Transient experimental persistence henceforth referred to as persistence was defined as a subset within the non-rebound profiles according to the Wood's model prediction at the end of the

experiment, i.e. at 42 dpi. If the model prediction at that time point remained above the detection threshold of one RT-PCR unit on the \log_{10} scale then the profile was classified as 'persistent' within the 42 day observation period, otherwise it was referred to as 'cleared'.

Assessment of Individual Viremia Profile Properties

Description of the individual viremia profiles by analytical functions provides the opportunity to explore whether viremia features associated with different phases of the infection are related, and to construct and test hypotheses. Pearson product-moment correlations were calculated between individual Wood's and Extended Wood's function parameter estimates and the derived parameters $-(t_1, v_1, t_2, v_2)$ to determine whether general patterns were apparent in the fitted profiles (e.g. is there an association between viremia increase before the local peak and post-peak decrease, etc.). In particular, within the category of rebounders, associations between the shapes of the viremia curves describing the primary and the rebound phase of infection (i.e. $t < t_0$ and $t > t_0$, respectively) were tested.

Furthermore, to determine whether the phenomenon of transient persistence or viral rebound could be predicted by the shape of the profile during the earlier phase of infection, the Wood's model was fitted to the truncated dataset comprising observations from all pigs (rebounders and non-rebounders) from 0 to 21 dpi only. A linear mixed model analysis (using PROC MIXED of SAS 9.3) was then carried out to assess statistical differences in the individual Wood's curve parameter estimates associated with the different profile types (cleared, persistent and rebound), respectively. The dependent variables were the individual mean values of the estimated posterior distributions of the Wood's model and derived parameters obtained from the primary phase: a_1, b_1, c_1, t_1, v_1 . Fitted random effects were pen within trial

and dam within trial. In the full model the fixed effects were the rebound class, trial, sex, parity and the interaction between trial and parity. Fixed and random effects were hierarchically removed according to statistical significance. Pairwise differences between the profile classes were assessed using the contrast statement of SAS PROC MIXED, which uses the F-test statistic.

Association Between Viremia Profiles and Neutralising Antibody Response

To test the hypothesis whether viremia rebound, clearance or persistence was associated with greater within host viral diversity and thus more diverse neutralizing antibodies, logistic regression was carried out for the 439 pigs with nAB assays, using PROC GLIMMIX in SAS 9.3, assuming an exponential distribution of the data, conditional on random effects. In the full mixed model the dependent variable was the neutralising antibody class (i.e. binary as the nAB categories were pooled), the independent variables were the class of the viremia profiles (i.e. cleared, persistent or rebound). In addition, trial, profile class, parity, sex and corresponding interactions were fitted as fixed effects and dam within trial and pen within trial were fitted as random effects. Similar to the mixed model analysis above, the number of random and fixed effects in the full model was hierarchically reduced by examining their impact on the AIC model fit statistics, and according to statistical significance of individual fixed effects, respectively.

Results

Classification of Profiles

Visual inspection of the predicted individual profiles (example shown in Figure 2) confirmed the appropriateness of the statistical classification method based on goodness of model fit. Only 12 and 4 of 1371 individuals had to be removed as outliers from the Wood's and Extended Wood's analysis, respectively, as several of their predicted viremia values differed from the corresponding observed values by more than 2 log differences. Overall 17% of the individuals were classified to experience viremia rebound while 83% were classified as non-rebounders (Table 1). Within the class of pigs with a uni-modal viremia profile, 46% of pigs were classified as pigs with persistent viremia whilst the remaining 54% of the non-rebounders appeared to have cleared the viremia. The percentages differed slightly between trials (Table 1). The lower percentage of rebounding profiles in trials 6–8 (7%, 6%, and 9% respectively), was possibly due to the higher number of missing values particularly in the later stage of the infection in these trials. Trials 7 and 8 were terminated at 35 dpi.

Goodness of Model Fits

Inspection of the individual model fits (e.g. Figure 2), residual plots (Figure 3), and the Pearson product-moment correlations (Figure 4), revealed that the vast majority of profiles are adequately described by either the Wood's or the Extended Wood's model. The mean of the Wood's model residuals was close to zero at all sampling times and the majority of the residuals were within 2 standard deviations from the mean residual, with an increased residual variance and a slight tendency towards over-prediction from 28 dpi onwards (Figure 3). The Wood's model Pearson product-moment correlations (Figure 4) indicated that the model predictions and the data were highly correlated throughout the experiment. The average predicted time for the peak viremia was 7 dpi (Figure 4A), which coincided with the time of the second observation in the experiment, however a small subset of individuals with flat observations between 4 and 14 dpi contrib-

uted to a bias towards over-prediction at 7 dpi, leading to the lowest correlation between the predictions and the data being observed at this time point. The Wood's model also had a tendency to over-predict viremia at the late stages between 35–42 dpi, resulting from the fact that by model definition viremia levels are always positive (i.e. converge to zero but never reach zero), whereas data were truncated to zero when viremia was below the detection level. In fact, only 4 individuals had observations of viremia level below detection at 19 dpi and 21 dpi, however by 28 dpi 15% of the observations were below detection. By the end of the experiment 77% of the 492 individuals with viremia observations at 42 dpi were below detection.

The extended Wood's model gave a tighter plot of residuals (Figure 3B) with a reduced overall bias, and stronger correlations between observed data and fitted values (Figure 4B), than the Wood's curve. However, for individual pigs there were wide posterior predictive intervals (PPIs) around the second viremia peak for the biphasic profiles (see example in Figure 2D), with this uncertainty resulting from the fact that the viremic rebound was generally represented by only one or two data points. As with the Wood's model, the Extended Wood's model had a tendency to over-predict the initial peak and also to over-predict viremia around the second peak, a tendency most likely compounded by the sparse data around these points.

Properties of Individual Viremia Profiles

Shape characteristics. The Pearson product-moment correlations between the individual model parameters (Table 2) reveal a strong relationship between the individual model parameter estimates describing the first mode of the viremia profiles (a_1, b_1, c_1, t_1, v_1), but not between the parameter estimates related to the second mode (a_2, b_2, c_2, t_2, v_2), indicating a higher variation in the predicted individual profile shapes related to the rebound phase. In particular the estimates of the Wood's parameters b_1 and c_1 were highly correlated with a correlation of 0.92 and 0.87 for uni- and biphasic profiles respectively, indicating that a rapid increase to the peak viremia also corresponds to a rapid post peak viremia decline during this phase. This was confirmed by highly negative correlations ($r = -0.84$ and -0.88) between the derivatives of the viremia functions at 4 and 19/21 dpi for the Wood's and Extended Wood's model, respectively. This association did not occur for the rebound phase (the correlation between b_2 and c_2 was 0.15). As expected, the time of the second peak (t_2) and the value for the time of onset of the rebound phase t_0 were highly correlated; later onset of the secondary phase corresponded to a later time of peak viremia in the secondary phase. Correlations between the times and levels of peak viremia (i.e. between t_1 and v_1 , and between t_2 and v_2 , respectively) were generally weak. Furthermore, the correlations between the corresponding Extended Wood's model parameters defining the first and second mode of the viremia curve, i.e. (a_1, b_1, c_1, t_1, v_1) and ($a_2, b_2, c_2, t_0, t_2, v_2$), respectively, were generally weak, with the exception for a moderately strong negative correlation of -0.52 between the parameters c_1 and c_2 . Thus a fast viremia decline in the primary phase tended to correspond to a slower decline in the secondary phase and vice versa. Interestingly, the analysis revealed an apparently strong negative association between the predicted peak viremia and subsequent decline associated with the rebound phase only (i.e. $r(v_2, c_2) = -0.89$, but $r(v_1, c_1) = 0.23$).

Is viremia clearance, persistence or rebound predictable. The final mixed models for original and derived Wood's model parameters obtained from the truncated data from the primary phase only (0–21 dpi), included fixed effects of profile class (cleared, persistent or rebound) determined on the complete

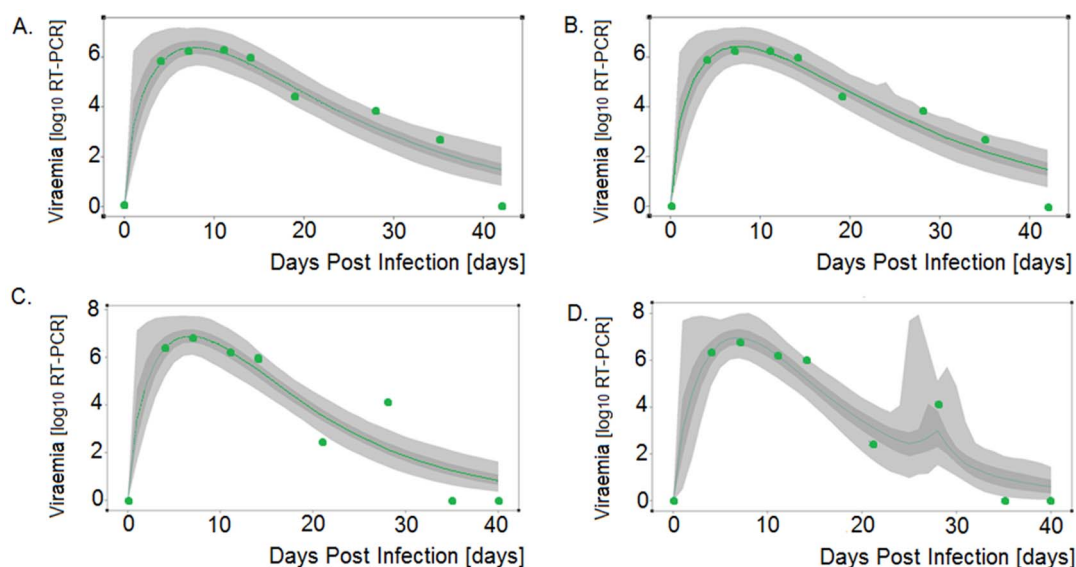


Figure 2. Wood's and Extended Wood's model fits to viremia data of two representative pigs classified as non-rebounder (top graphs) and rebounder (bottom graphs). Light-grey regions correspond to 95% posterior predictive intervals (PPI); dark-grey regions correspond to 50% PPIs. The actual data are shown as green dots and the green solid lines give the best-fit solutions for the Wood's model (A,C) and Extended Wood's model (B, D), respectively.
doi:10.1371/journal.pone.0083567.g002

dataset, as well as the trial and the trial by parity interaction, with pen within trial and dam within trial as random effects. Statistically significant differences for all the individual Wood's curve parameter estimates (i.e. a_1, b_1, c_1, t_1 and v_1) were found between animals classified into the cleared and persistent viremia classes, and between those classified as persistent and rebounders, but not between animals classed as cleared and rebound (Table 3). Inspection of the pairwise scatter plots of Wood's model parameter estimates (Figures 5A-C) shows clustering associated with the different profile categories, in concordance with the statistical test statistics (Table 3). Furthermore, identified differences between parameters corresponding to persistent and non-persistent profiles are also transparent in plots of the mean viremia predictions together with their 95% confidence intervals (Figure 5D). Thus,

the results suggest that whereas persistence is predictable based on the profile of the first 21 dpi, viremia rebound is not.

Association Between Viremia Profiles and Neutralising Antibody (nAb) Response

The percentages of individuals in each nAb category for each viremia profile class are presented in Table 4 and odds ratios of nAb cross-productivity associated with different viremia profiles classes are presented in Table 5. The final model used to test the association between the profile-class and the nAb response contained only the nAb class as dependent variable and the viremia profile class as independent variable, with no other fixed or random effects. There was a statistically significant association

Table 1. Summary of the statistical classifications of the viremia profiles from the PRRSV challenge experiment

Trial	Number (percentage) of individuals within a specific viremia profile category		
	Class 1: Uni-modal		Class 2: Biphasic
	Clearance within 42 dpi	Persistence until 42 dpi	Rebound
1	79 (61)	50 (39)	55 (30)
2	119 (83)	24 (17)	28 (16)
3	51 (37)	86 (63)	36 (21)
4	71 (47)	81 (53)	39 (20)
5	70 (48)	77 (52)	36 (20)
6	35 (35)	66 (65)	8 (7)
7	96 (55)	78 (45)	12 (6)
8	85 (59)	58 (41)	15 (9)
All (% of total)	606 (45)	520 (38)	229 (17)

Classifications of the viremia profiles are based on the likelihood ratio test comparing the Wood's and the Extended Wood's models. Trial 6 had 48% death prior to 21 dpi. Due to facility availability issues trials 7 and 8 had to be terminated at 35 dpi. Overall 17% were rebound, 38% were persistent and the remaining 45% were clearance profiles.

doi:10.1371/journal.pone.0083567.t001

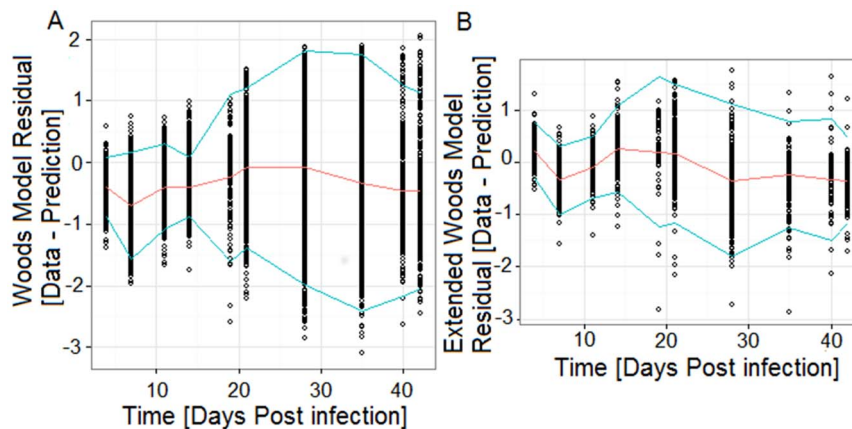


Figure 3. The Wood's model residuals (3A) and the Extended Wood's model residuals (3B). The red line shows the residual mean and the blue lines delimit two standard deviations from the mean.
doi:10.1371/journal.pone.0083567.g003

(at the 95% significance level) between the profile class and the diversity of the nAb response when the nAb categories were pooled into two groups (i.e. no nAb cross-protection and cross-protection). Clearance corresponded to a less diverse nAb response than persistence and pigs with persistent viremia had a more diverse nAb response than those with rebound profiles (Table 5). However, there was no statistical significant difference in nAb cross-protectivity between pigs that cleared viremia within 42 dpi and rebounders (Table 5).

The results thus suggest that the slower clearance rate of viremia in the persistent profiles, but not viremia rebound, is associated with a more diverse nAb response.

Discussion

Empirical mathematical models have proven useful for describing the temporal evolution of a response variable and filtering stochastic noise from dynamic biological systems whilst retaining the most fundamental features [31,37–39]. Previous studies have used such models for the quantitative analysis of growth, weight gain and lactation [37,40]; however to our knowledge this is the first study in which they have been applied to infection profiles. The comprehensive PHGC dataset comprising repeated PRRS viremia measurements from 1371 commercial pigs provided a unique opportunity to assess the nature and degree of variation in the host response to PRRSV infection. The main aims of this study were to obtain a mathematical function to aid the characterisation and to further our current understanding surrounding the wide spectrum of observed PRRS viremia profiles.

Using maximum likelihood inference and numerous model fit criteria, we established that the broad spectrum of observed viremia trends from 0–42 dpi could be adequately represented by either the uni- or biphasic Wood's functions. Representative parameter estimates of the data resulting in good model fits and residuals were obtained for the vast majority of individuals, and pigs could be objectively classified into one of three viremic categories. This together with the convenient biological interpretation of the model parameters and derived parameter estimates, such as the time and level of viremia peak, allowed us not only to quantify inter-host variation, but also to establish common viremia curve characteristics and determine their predictability.

Assessment of the fitted models revealed a generally close fit of the Wood's and Extended Wood's model to the log transformed viremia data over the whole 42 day duration of the experiment,

with few exceptions. The lowest data-prediction correlation was observed at 7 dpi, which corresponds to the average time for the peak viremia level. The residuals showed that for certain individuals the model over-predicts the value at this observation. There are two main factors which may contribute to this lack of fit: firstly for individuals whose peak viremia may lie between 4–7 dpi, the lack of data representing the dynamics of the infection during this period of rapid change may contribute to the over-prediction. Secondly for individuals with a fairly flat plateau of observations between 4–14 dpi the issue lies with the Wood's model itself; in this case the model systematically predicts a higher and sharper peak than the data would suggest as it is unable to produce a flat plateau near the peak. The Wood's (and Extended Wood's) model itself is constrained by the model parameters; the time of the peak viremia level is dependent on both parameters b_1 and c_1 which in turn contribute to the rates of pre-peak viremia increase and post-peak viremia decline. In contrast, the general tendency to over-predict viremia from 28 dpi onwards for non-rebounders can easily be explained by the fact that the Wood's curve converges to, but never reaches, zero. This latter property of the Wood's function may in fact be a clearer representation of reality; we are never able to confirm that viremia levels truly reach zero, but only that they have reached levels below the detection threshold determined by the accuracy of experimental observations. Note that theoretically the log-transformed viremia data could reach negative values which the Wood's model would be unable to capture. However such viremia observations never arise in practice due to the experimental threshold of detection and hence a function such as the Wood's model that approaches zero is appropriate for the current PRRS viremia dataset.

By parsimony, in the absence of more frequent measurements, the Extended Wood's model was chosen as it is a simple model representing the main features of the biphasic profiles. It encapsulates the assumption that the second phase of the profile has the same essential shape characteristics as the primary phase. Furthermore the Extended Wood's model parameters were also able to encapsulate the possible anamnestic nature of the immune response; the parameters allowed for variation in the size, timing, rate of increase and rate of decline in the secondary phase. The consistency of the model residuals and correlations indicate that the Extended Wood's model provides indeed a good fit during both phases of the profile; in fact the correlations between the data and model predictions were highest during the second phase. The second phase was generally shorter (28–42 dpi) and less severe

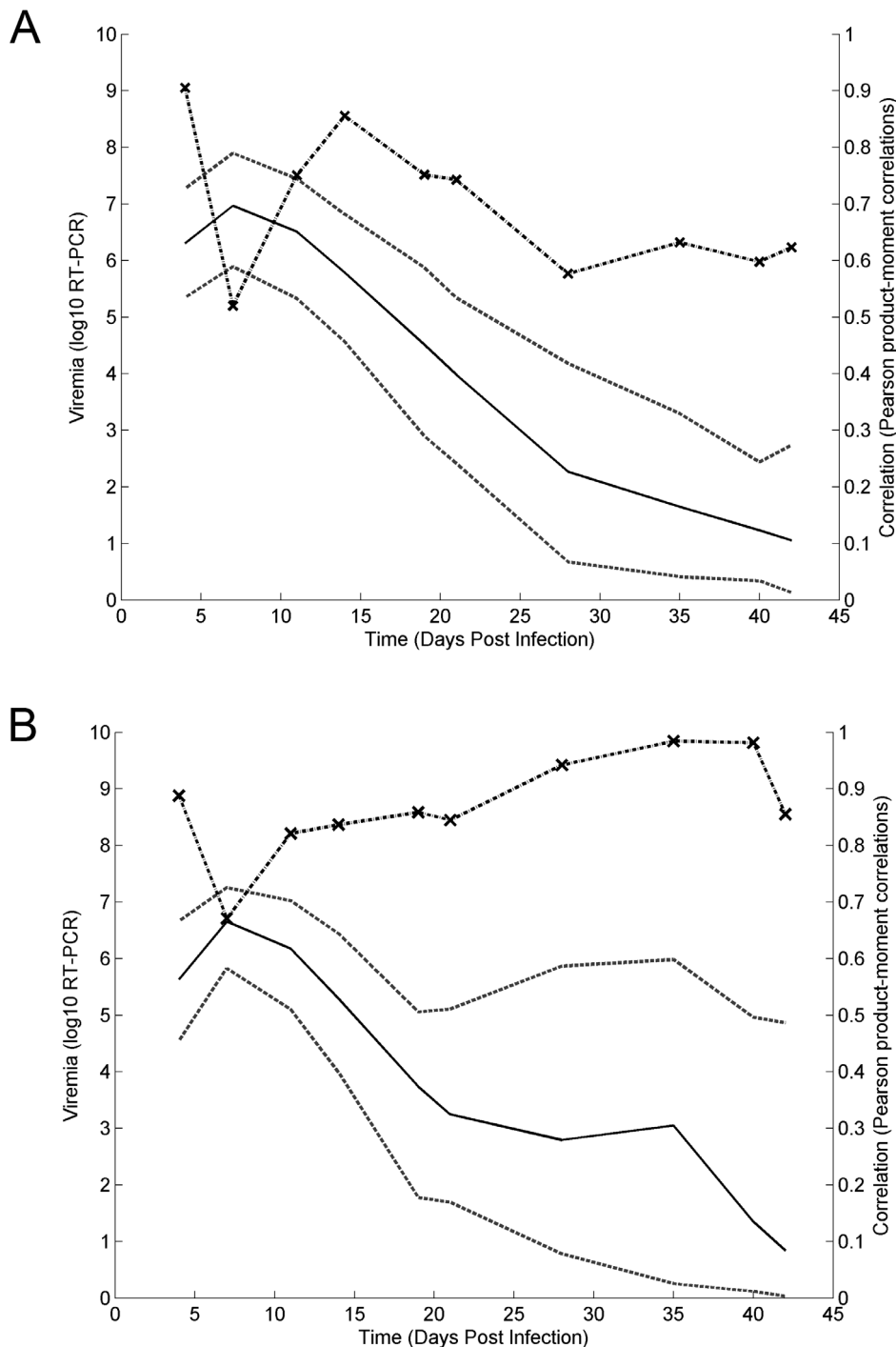


Figure 4. The Wood's(4A) and Extended Wood's(4B) model mean predictions and data-prediction correlations. The black lines outline the mean model predictions, and the dashed grey lines delimit the 95% prediction confidence intervals. The dotted black lines joined with crosses show the Pearson product-moment correlations between observed data and predicted values.
doi:10.1371/journal.pone.0083567.g004

than the first phase (0–28 dpi), as indicated by greater predicted rates of viremia increase and decline in the second phase of the profile (parameter means for the primary and secondary phase were: $\text{mean}(b_1, c_1) = (0.66, 0.10)$ and $\text{mean}(b_2, c_2) = (4.67, 3.78)$), and lower levels of peak viremia associated with the second phase. This contrast in timing and size of the primary and secondary

phases supports evidence of the anamnestic nature of an individual's immune response in a rebound profile.

Despite the generally good fit of the Wood's and Extended Wood's models, it is likely that a candidate model of greater mathematical complexity could provide a better empirical fit to the data; indeed much effort has been dedicated to the identification of appropriate functions to describe e.g. lactation

Table 2. The Wood's and Extended Wood's model parameter's Pearson product-moment correlations.

Extended Wood's Parameters	a_1	b_1	c_1	t_1	v_1	a_2	b_2	c_2	t_0	t_2
a_1	-	-0.91	-0.71	-0.81	0.04					
b_1	-0.85	-	0.92	0.59	0.21					
c_1	-0.52	0.87	-	0.26	0.26					
t_1	-0.84	0.52	0.39	-	0.004					
v_1	0.19	0.12	0.23	-0.16	-					
a_2	-0.05	0.07	0.10	-0.02	-0.01	-				
b_2	0.02	0.01	0.04	-0.03	0.02	-0.10	-			
c_2	0.03	-0.30	-0.52	0.33	-0.27	-0.08	0.15	-		
t_0	0.15	-0.14	0.07	-0.13	0.05	-0.04	-0.09	-0.09	-	
t_2	0.17	-0.10	0.57	-0.20	0.10	-0.06	-0.05	-0.24	0.98	-
v_2	0.07	0.25	0.47	-0.33	0.30	0.14	0.08	-0.89	0.13	0.29

Upper triangle in bold: Wood's model parameter correlations. Lower triangle: correlations between the Extended Wood's model parameters.

doi:10.1371/journal.pone.0083567.t002

or growth profiles in livestock [31,40]. Amongst these candidates are spline functions, which indeed were able to provide a closer fit to the present viremia data (results not shown). However their increased complexity requires biological interpretation and does not lend itself to a quantitative assessment of profile characteristics. The Wood's and Extended Wood's models in contrast constitute worthy candidates for this analysis, particularly as biologically meaningful interpretations can be given to their parameters.

The 42 day study period gave rise to uni- or biphasic viremia profiles only. It is possible that the observed biphasic profiles represent damped oscillations which are truncated after 6 weeks

post infection. Oscillations often represent negative feedbacks with delay in biological systems [41]. Such behaviour could arise from the virus-host immune response interactions. An oscillatory mathematical function such as a sine function may constitute a plausible alternative to the Wood's functions presented here and would be attractive from the mathematical perspective due to the few parameters needed to determine the period of the cycles and damping factor of the oscillations. However the current dataset doesn't span a sufficient duration to inform parameter estimates for such models; data from longer PRRS virus challenge experiments would be required to test these hypotheses.

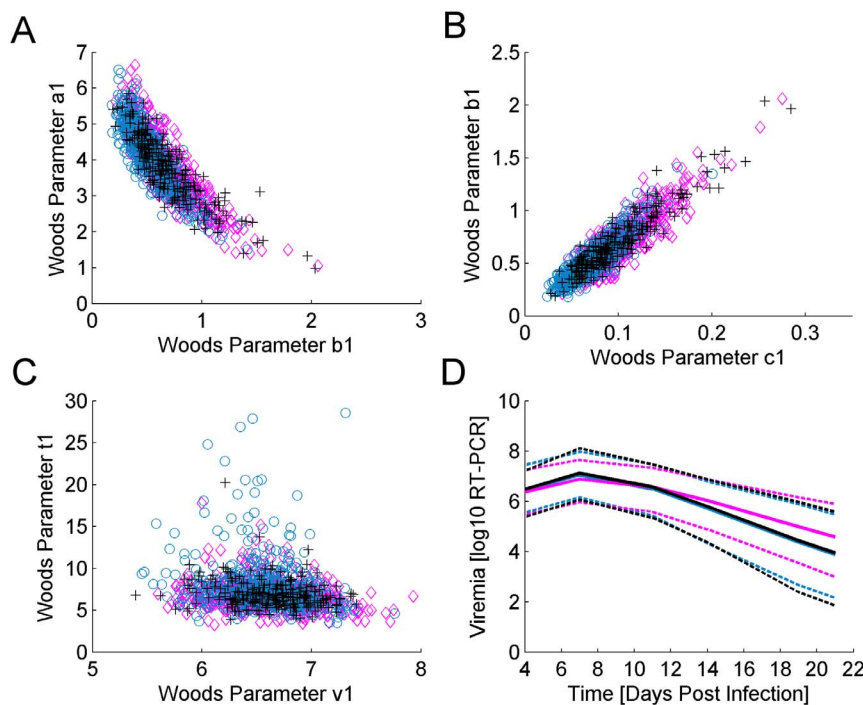


Figure 5. Woods parameters and mean model predictions for the 3 profile classes. Figure 5A-C. Pair-wise scatter plots and clustering of primary phase Wood's model parameters for the 3 profile classes: cleared (blue circles), persistent (pink diamonds) and rebound (black crosses). Figure 5D. Mean Woods model predictions with the 95% Confidence Intervals (dashed lines) based on the truncated data from 0–21 dpi for individuals previously classified as rebound (black), persistent (pink) and cleared (blue), respectively.

doi:10.1371/journal.pone.0083567.g005

Table 3. Viremia profile class and their Least Square Means (LSM) from the truncated data.

Wood's parameter	LSM (SE): Cleared	LSM (SE): Persistent	LSM (SE): Rebound	P _{CP}	P _{CR}	P _{PR}
a ₁	3.83 (0.049)	4.16 (0.051)	3.84 (0.066)	<.01	0.98	<.01
b ₁	0.68 (0.011)	0.53 (0.012)	0.68 (0.017)	<.01	0.91	<.01
c ₁	0.097 (0.0014)	0.072 (0.0015)	0.096 (0.0022)	<.01	0.92	<.01
t ₁	6.90 (0.11)	7.82 (0.12)	6.99 (0.16)	<.01	0.58	<.01
v ₁	6.60(0.018)	6.56 (0.019)	6.61 (0.024)	0.02	0.78	0.04

The LSM parameters estimates and standard errors (SE) derived from fitting the Wood's model to the truncated dataset from 0–21 dpi for pigs whose viremia profiles were classified as cleared, persistent and rebound, respectively. P-values corresponding to the associated test between the profile groups denoted by the subscript C, P, R for cleared, persistent and rebound respectively.

doi:10.1371/journal.pone.0083567.t003

One of the advantages of fitting alternative mathematical functions to viremia data is that it provided an objective method for distinguishing uni-modal from biphasic viremia profiles based on statistical inference. This helped to confirm previous observations from smaller scale studies (e.g. [17] and [20]) that viremia rebound is a genuine and common phenomenon in PRRSV infections. This may have important epidemiological consequences, as individuals diagnosed as non-viremic at time of sampling may harbour and shed infectious virus some days later. Similarly, individuals with persistent viremia profiles are likely to be infectious for longer. The question thus arises whether serum viremia persistence or rebound can be predicted, e.g. based early profile characteristics. Our statistical analyses, using data from the primary phase (0–21 dpi) of the experimental infection, revealed that profiles classed as persistent had, on average, a faster increase to the peak and slower decline from the peak viral load than both the rebound and clearance profiles. However, the results also

suggest that rebound and clearance profiles cannot be distinguished based on information from the primary phase. This result has however important implications with regards to the following hypothesis: considering that serum viremia data were only collected for 42 dpi, one may hypothesise that every pig may eventually experience rebound, provided that the virus has not been completely cleared, and that rebound could only be observed for a subset of pigs in this study due to censoring. However, if this hypothesis was correct, there would be a higher probability of observing rebound in individuals with faster viremia decline within 21 dpi. But, since no statistical difference was observed between rebound and clearance on the truncated dataset, the existing evidence would suggest that only a subset of pigs experiences viremia rebound. Furthermore, we also observed that none of the pigs with non-detectable viremia levels for 2 or more weeks experienced viremia rebound within 42 dpi (results not shown),

Table 4. Neutralising antibody (nAb) data and viremia class.

nAb category (1–5)	Class	Number Of Individuals	Percentage [% of Class]
1	Rebound	6	5.9
2	Rebound	55	53.9
3	Rebound	11	10.8
4	Rebound	21	20.6
5	Rebound	9	8.8
Total (1–5)	Rebound	102	-
1	Cleared	21	9.4
2	Cleared	104	46.6
3	Cleared	51	22.9
4	Cleared	33	14.8
5	Cleared	14	6.3
Total (1–5)	Cleared	223	-
1	Persistent	16	14
2	Persistent	61	54
3	Persistent	21	18
4	Persistent	11	10
5	Persistent	5	4
Total (1–5)	Persistent	114	-

Frequency and percentages of individuals classified as cleared, persistent and rebound, within each neutralizing antibody (nAb) category. nAb category 2 refers to individuals whose serum contains nAb that can only neutralize the homologous PRRSV strain (NVSL) as used in the in-vivo infections; nAb categories 3–5 correspond to nAb response to the homologous strain and k-2 other PRRSV strains.

doi:10.1371/journal.pone.0083567.t004

Table 5. Odds ratios of the cross protectivity of neutralising antibodies (nAbs) from individuals from profile Class 1 relative to that of nAbs from individuals from viremia profile Class 2.

Class 1	Class 2	Odds ratio (95% Confidence interval)	P- value
Clearance	Persistence	0.61 (0.38, 0.98)	0.04
Clearance	Rebound	0.86 (0.53, 1.38)	0.53
Persistence	Rebound	1.40 (0.80, 2.45)	0.24

The columns class 1 and class 2 indicate which two viremia categories are being compared. The nAb class was a pooled into a binary trait: cross-protective (nAb class 1–2) or not cross-protective (nAb class 3–5). The 95% significance level was used ($p < 0.05$). For further explanation see text.

doi:10.1371/journal.pone.0083567.t005

thus indicating that rebound is unlikely to occur if the serum virus has been cleared for a period of several weeks.

Analysis of the nAbs of infected pigs collected at 42 dpi indicated that there was a strong homologous response to the PRRSV challenge, in agreement with observations from previous studies [42,43]. Our study not only revealed a high degree of inter-pig variation in viremia profiles but also high variability in the range of cross-protection of neutralizing antibodies collected at 42 dpi. Furthermore, a statistical association between the two quantities was identified, which may point to the host-pathogen interactions underlying the observed viremia and antibody patterns. Both virus persistence within the host and cross-protection of host antibodies have been previously linked to virus mutation and emergence of quasi-species [9,38]. PRRSV evolves rapidly in infected pigs with a high mutation rate of $1 - 3 \times 10^{-2}$ substitutions per nucleotide and year [21,44]. Furthermore, multiple variants of PRRSV were found to exist simultaneously within individual animals [22]. Thus, in order to efficiently clear the range of PRRSV quasi-species, a versatile neutralizing antibody response would be required.

Our study revealed that pigs that manage to clear the virus from the blood within 42 dpi have on average a less diverse nAb response than pigs with persistent viremia profiles. In light of the pathogen co-evolution, these results could be interpreted as rapid clearance of the virus limiting the duration in which the virus may evolve, resulting in an efficient, but relatively narrow antibody response. Persistent profiles, in contrast, may be the result of a host immune response that is inefficient in clearing the virus but in which the diversification of the neutralizing antibody response is driven by rapid virus mutation. Rebound is characterised by two phases; the viremia decline in the first phase may be caused by an effective, but narrow nAb response. However, before the immune response has managed to fully clear the virus within the primary phase, the emergence of a new quasi-species capable of escaping the existing antibodies may cause the viremia to increase in a second phase driving the continual diversification of nAbs that eventually reduce viremia again. Thus, given that the majority of rebound profiles are at the declining phase by 42 dpi, viremia rebound would be expected to be associated with a more versatile nAb response at 42 dpi than clearance, but a more narrow response than persistence, which is in agreement with the results, although the differences were not always found to be statistically significant.

It should be noted, however, that the observed associations between the nAb response and viremia patterns may equally arise from confounding immune quantities affecting both nAb and viremia, which were not measured in these studies. Indeed, several

alternative hypotheses, not necessarily involving virus mutation, emerge as potential causes for viremia rebound. For example viremia rebound may correspond to the second cycle of an oscillating viremia profile which may arise naturally (and in the absence of virus mutation) from predator-prey type interactions between the virus and the immune response [45,46]. Alternatively, rebound could arise from the heterogeneity of the virus distribution in various tissues within the host. Previous studies have observed that although viremia may be below detection in the serum, persistent infection in the tonsils and lymphoid tissues can last for longer than 6 months [18]. Thus, the site of replication may be hidden from the serum and the infection may remain localised in certain tissues. Rebound may be a manifestation of the virus from these localised tissue infections being poured back into the system; thus becoming detectable in the serum. The influx of virus into the serum may occur in occasional bursts or as a final out-pouring into the serum determined by some environmental stimulus, immune response mechanism, or stochastic process. This second hypothesis would imply that viremia rebound follows more a distinct bi- or multi-modal pattern rather than a damped oscillatory behaviour. Virus rebound manifesting itself in biphasic viremia profiles is a common phenomenon in equine influenza infections, the causative processes of which remain a mystery [47]. Additional information about virus heterogeneity and/or nAb characteristics at different stages post infection would be needed to assess these hypotheses.

Similar arguments may be used to interpret the observed high inter-host variation in viremia decline post the initial viremia peak. Variation in the rate of viremia reduction may be a function of the host's own immune response, virus mutation mechanisms or the interaction between both processes. The moderate negative correlation between parameters c_1 and c_2 (-0.52) indicates that a slow decline in the first cycle corresponds to faster decline in the second cycle and vice versa. This association may be indicative of the temporal evolution of the immune response. A slow immune response in the primary phase may prolong the conditions required to produce neutralising antibodies and thus manifest in a stronger or more diverse nAb at the end of the second phase. Conversely, a fast initial immune response may indicate an effective, but narrow nAb response during the primary phase so that fewer or less diverse nAb are available for the second phase. The identified association between nAb and viremia categories would support this hypothesis, since persistent profiles have the broadest response of all the profile categories.

From the current study we cannot affirm that there would be infectious and epidemiological consequences in the secondary phase of rebound profiles. Inferences made on infectiousness and epidemiological consequences using the data obtained via quantitative RT-PCR may be limited due to the potential discrepancy between the measured viral genome load and the non-measured true viral load. Thus, the observed secondary phase of rebound may be the result of detecting circulating junk genomes rather than genomes of infectious particles and may thus have no significant epidemiological consequence. However, previous studies have explored the relationship between diverse viremia measurements an infectiousness of pigs infected with PRRSV [29,48,49]. For example, Charpin et al. [48] detected viral genome in the blood of inoculated pigs from 7–77 dpi using RT-PCR, whereas viral genome shedding was detectable from nasal swabs from 2–48 dpi. Furthermore their study concluded that infectiousness was indeed correlated with the time course of viral-genome in the blood measured by RT-PCR and that the decrease in infectiousness was related to the increase in antibodies [48]. In a study by Rowland et al. [49] it was observed that even when there

were low levels of the virus replication the virus was easily transmitted and it was only by 260 dpi that pigs were no longer able to transmit the virus to sentinel pigs [49]. Thus it has been established that some PRRSV-infected pigs can support virus replication and transmit infection for an extended period far beyond the duration of the secondary phase of the profiles in our study. By this logic one may argue that the observed rebound in viral genome load may indeed have biological consequences in terms of viral shedding and transmission to susceptible animals.

Previous PRRS studies alluded to the phenomenon of viremia rebound [14,20,50] based on qualitative inspection of viremia profiles, but have not analysed the duration, defining characteristics or relationship with the antibody response of this phenomenon. Using data from the first 3 out of the 8 trials analysed in this study, Boddicker et al. [20] defined biphasic profiles subjectively by a rebound of 2 units on the logarithmic (base 10) scale of viremia observations from 21 dpi onwards. Using this definition rebound was not found to be heritable, indicating that rebound is more likely to be determined by either the virus or the environment as opposed to host genetics [20]. However, the low heritability estimate of this phenotypic trait (0.03) may be due to poor trait definition arising from too few successive observations to accurately capture the rebound phase (i.e. between 21–42 dpi), and hence errors in classifying animals. The statistical classification used in this study resulted in 22% of the pigs from trials 1–3

classified as rebounders as opposed to the 33% of pigs classed into the rebound category in the previous study [20].

Lastly, there is accumulating evidence for substantial host genetic variation in response to PRRSV [1,4], increasing the potential for the control of PRRS through genetic selection. In particular, a quantitative trait locus (QTL) was identified for the area under the viremia curve spanning the first 21 days post infection [20]. Our study provides opportunity to assess whether clearance, persistence or rebound, and other derived features, such as level of or time to peak viremia and the rates of increase and decline in the profiles are genetically determined, and to potentially identify QTL associated with these new phenotypes. The new derived phenotypes may provide deeper insights into the underlying molecular mechanisms. Furthermore, the hypotheses for host-pathogen interactions emerging from the current study will be used to inform and validate process-based dynamic mathematical models of *in-vivo* PRRSV infections in future studies.

Author Contributions

Conceived and designed the experiments: ZUI SCB NJS RRRR JKL BT ABD. Performed the experiments: ZUI SCB NJS RRRR JKL BT ABD. Analyzed the data: ZUI SCB NJS JKL ABD. Contributed reagents/materials/analysis tools: ZUI SCB NJS RRRR JKL BT ABD. Wrote the paper: ZUI SCB ABD.

References

- Lunney JK, Steibel JP, Reecy JM, Fritz E, Rothschild MF, et al. (2011) Probing genetic control of swine responses to PRRSV infection: current progress of the PRRS host genetics consortium. *BioMed Central Ltd.* pp. S30.
- Lewis CRG, Ait-Ali T, Clapperton M, Archibald AL, Bishop S (2007) Genetic perspectives on host responses to porcine reproductive and respiratory syndrome (PRRS). *Viral immunology* 20: 343–358.
- Neumann EJ, Kliebenstein JB, Johnson CD, Mabry JW, Bush EJ, et al. (2005) Assessment of the economic impact of porcine reproductive and respiratory syndrome on swine production in the United States. *Journal of the American Veterinary Medical Association* 227: 385–392.
- Lunney JK, Chen H (2010) Genetic control of host resistance to porcine reproductive and respiratory syndrome virus (PRRSV) infection. *Virus Research* 154: 161–169.
- Duan X, Nauwynck H, Pensaert M (1997) Effects of origin and state of differentiation and activation of monocytes/macrophages on their susceptibility to porcine reproductive and respiratory syndrome virus (PRRSV). *Archives of virology* 142: 2483–2497.
- Lawson SR, Rossow KD, Collins JE, Benfield DA, Rowland RRR (1997) Porcine reproductive and respiratory syndrome virus infection of gnotobiotic pigs: sites of virus replication and co-localization with MAC-387 staining at 21 days post-infection. *Virus Research* 51: 105–113.
- Thanawongnuwech R, Halbur PG, Thacker EL (2000) The role of pulmonary intravascular macrophages in porcine reproductive and respiratory syndrome virus infection. *Animal Health Research Reviews* 1: 95–102.
- Wensvoort G, Terpstra C, Pol J, Ter Laak E, Bloemraad M, et al. (1991) Mystery swine disease in The Netherlands: the isolation of Lelystad virus. *Veterinary Quarterly* 13: 121–130.
- Chand RJ, Tribble BR, Rowland RRR (2012) Pathogenesis of porcine reproductive and respiratory syndrome virus. *Current Opinion in Virology* 2:256–263.
- Chang CC, Yoon KJ, Zimmerman J, Harmon K, Dixon P, et al. (2002) Evolution of porcine reproductive and respiratory syndrome virus during sequential passages in pigs. *Journal of virology* 76: 4750–4763.
- Doeschl-Wilson A, Kyriazakis I, Vincent A, Rothschild M, Thacker E, et al. (2009) Clinical and pathological responses of pigs from two genetically diverse commercial lines to porcine reproductive and respiratory syndrome virus infection. *Journal of Animal Science* 87: 1638–1647.
- Loving CL, Brockmeier SL, Sacco RE (2007) Differential type I interferon activation and susceptibility of dendritic cell populations to porcine arterivirus. *Immunology* 120: 217–229.
- Wills RW, Doster AR, Galcota JA, Sur J-H, Osorio FA (2003) Duration of infection and proportion of pigs persistently infected with porcine reproductive and respiratory syndrome virus. *Journal of clinical microbiology* 41: 58–62.
- Reiner G, Willems H, Pesch S, Ohlinger V (2009) Variation in resistance to the porcine reproductive and respiratory syndrome virus (PRRSV) in Pietrain and Miniature pigs. *Journal of Animal Breeding and Genetics* 127: 100–106.
- Petry D, Lunney J, Boyd P, Kuhar D, Blankenship E, et al. (2007) Differential immunity in pigs with high and low responses to porcine reproductive and respiratory syndrome virus infection. *Journal of Animal Science* 85: 2075–2092.
- Petry D, Holl J, Weber J, Doster AR, Osorio FA, et al. (2005) Biological responses to porcine reproductive and respiratory syndrome virus in pigs of two genetic populations. *Journal of Animal Science* 83: 1494–1502.
- Reiner G, Willems H, Pesch S, Ohlinger V (2010) Variation in resistance to the porcine reproductive and respiratory syndrome virus (PRRSV) in Pietrain and Miniature pigs. *Journal of Animal Breeding and Genetics* 127: 100–106.
- Yoo D, Song C, Sun Y, Du Y, Kim O, et al. (2010) Modulation of host cell responses and evasion strategies for porcine reproductive and respiratory syndrome virus. *Virus Research* 154: 48–60.
- Boddicker N, Waide E, Rowland R, Lunney J, Garrick D, et al. (2012) Evidence for a major QTL associated with host response to porcine reproductive and respiratory syndrome virus challenge. *Journal of Animal Science* 90: 1733–1746.
- Boddicker N, Waide E, Rowland R, Lunney J, Garrick D, et al. (2012) Evidence for a major QTL associated with host response to Porcine Reproductive and Respiratory Syndrome virus challenge. *Journal of Animal Science*.
- Prieto C, Vázquez A, Núñez JI, Álvarez E, Simarro I, et al. (2009) Influence of time on the genetic heterogeneity of Spanish porcine reproductive and respiratory syndrome virus isolates. *The Veterinary Journal* 180: 363–370.
- Goldberg TL, Lowe JF, Milburn SM, Firkins LD (2003) Quasispecies variation of porcine reproductive and respiratory syndrome virus during natural infection. *Virology* 317: 197–207.
- Murtaugh MP, Xiao Z, Zuckermann F (2002) Immunological responses of swine to porcine reproductive and respiratory syndrome virus infection. *Viral immunology* 15: 533–547.
- Lopez O, Osorio F (2004) Role of neutralizing antibodies in PRRSV protective immunity. *Veterinary immunology and immunopathology* 102: 155–163.
- Wood PDP (1967) Algebraic Model of the Lactation Curve in Cattle. *Nature* 216: 164–165.
- Winsor CP (1932) The Gompertz curve as a growth curve. *Proceedings of the National Academy of Sciences of the United States of America* 18: 1.
- Rowland RR, Lunney J, Dekkers J (2012) Control of porcine reproductive and respiratory syndrome (PRRS) through genetic improvement in disease resistance and tolerance. *Frontiers of Livestock Genomics* 3:260.
- Fang Y, Schneider P, Zhang W, Faaborg K, Nelson E, et al. (2007) Diversity and evolution of a newly emerged North American Type 1 porcine arterivirus: analysis of isolates collected between 1999 and 2004. *Archives of virology* 152: 1009–1017.
- Rowland RR, Steffen M, Ackerman T, Benfield DA (1999) The evolution of porcine reproductive and respiratory syndrome virus: quasispecies and emergence of a virus subpopulation during infection of pigs with VR-2332. *Virology* 259: 262–266.
- Beever D, Rook A, France J, Dhanoa M, Gill M (1991) A review of empirical and mechanistic models of lactational performance by the dairy cow. *Livestock Production Science* 29: 115–130.

31. Grossman M, Koops W (2003) Modeling extended lactation curves of dairy cattle: a biological basis for the multiphasic approach. *Journal of dairy science* 86: 988–998.
32. Savill NJ, Chadwick W, Reece SE (2009) Quantitative analysis of mechanisms that govern red blood cell age structure and dynamics during anaemia. *PLoS computational biology* 5: e1000416.
33. Haario H, Saksman E, Tamminen J (2001) An adaptive Metropolis algorithm. *Bernoulli*: 223–242.
34. Girolami M (2008) Bayesian inference for differential equations. *Theoretical Computer Science* 408: 4–16.
35. Friel N, Pettitt AN (2008) Marginal likelihood estimation via power posteriors. *Journal of the Royal Statistical Society: Series B (Statistical Methodology)* 70: 589–607.
36. Lindley DV, Scott WF (1995) *New Cambridge statistical tables*: Cambridge University Press.
37. Trefan L, Bünger L, Bloom-Hansen J, Rooke J, Salmi B, et al. (2011) Meta-analysis of the effects of dietary vitamin E supplementation on α -tocopherol concentration and lipid oxidation in pork. *Meat Science* 87: 305–314.
38. English S, Bateman AW, Clutton-Brock TH (2012) Lifetime growth in wild meerkats: incorporating life history and environmental factors into a standard growth model. *Oecologia* 169: 143–153.
39. Brown H, Prescott R (2006) *Applied mixed models in medicine*: John Wiley West SussexUK.
40. Steri R, Dimauro C, Canavesi F, Nicolazzi EL, Macciotta NPP (2012) Analysis of lactation shapes in extended lactations. *animal* 6: 1572–1582.
41. Friesen WO, Block GD, Hocker CG (1993) Formal approaches to understanding biological oscillators. *Annual review of physiology* 55: 661–681.
42. Lager K, Mengeling W, Brockmeier SL (1997) Duration of homologous porcine reproductive and respiratory syndrome virus immunity in pregnant swine. *Veterinary microbiology* 58: 127–133.
43. Mengeling WL, Lager KM, Vorwald AC, Clouser DF (2003) Comparative safety and efficacy of attenuated single-strain and multi-strain vaccines for porcine reproductive and respiratory syndrome. *Veterinary microbiology* 93: 25–38.
44. Kimman TG, Cornelissen LA, Moormann RJ, Rebel JMJ, Stockhofe-Zurwieden N (2009) Challenges for porcine reproductive and respiratory syndrome virus (PRRSV) vaccinology. *Vaccine* 27: 3704–3718.
45. Nowak M, May RM (2000) *Virus dynamics: mathematical principles of immunology and virology*: Oxford university press.
46. Kumar R, Clermont G, Vodovotz Y, Chow CC (2004) The dynamics of acute inflammation. *Journal of Theoretical Biology* 230: 145–155.
47. Pawelek KA, Huynh GT, Quinlivan M, Cullinane A, Rong L, et al. (2012) Modeling within-host dynamics of influenza virus infection including immune responses. *PLoS computational biology* 8: e1002588.
48. Charpin C, Mahe S, Keranflech A, Madec F, Belloc C, et al. (2012) Estimation of time-dependent infectiousness of pigs infected by the Porcine Reproductive and Respiratory Syndrome virus (PRRSV): correlation with the viral genome load in blood, nasal swabs and the serological response. *Institut du Porc*. pp. 67–72.
49. Rowland R, S Lawson, K Rossow, DA Benfield (2003) Lymphotropism of porcine reproductive and respiratory syndrome virus replication during persistent infection of pigs originally exposed to virus in utero. *Vet Micro* 96: 219–235.
50. Mulupuri P, Zimmerman JJ, Hermann J, Johnson CR, Cano JP, et al. (2008) Antigen-specific B-cell responses to porcine reproductive and respiratory syndrome virus infection. *Journal of virology* 82: 358–370.

3.1 Conclusion

The Bayesian approach in Chapter 3 allowed for:

1. Directly fitting of nonlinear functions to the viraemia data
2. Fitting the uni modal Woods model and the bimodal extended Woods model to the data
3. A better fit to the data than via the linearized mixed models approach in Chapter 2

Using maximum likelihood inference and numerous model fit criteria, we established that the broad spectrum of observed viraemia trends from 0-42dpi could be adequately represented by either the uni- or biphasic Wood's functions. Representative parameter estimates of the data resulting in good model fits and residuals were obtained for the vast majority of individuals, and pigs could be objectively classified into one of three viraemic categories. This together with the convenient biological interpretation of the model parameters and derived parameter estimates, such as the time and level of viraemia peak, allowed us not only to quantify inter-host variation, but also to establish common viraemia curve characteristics and determine their predictability.

The Woods model was an adequate description of the viraemia profiles across the PRRSV isolates (NVSL and KS06). The residual plots for the KS06 challenged pigs are presented in Appendix 2.

Figure 3.1 outlines the derived parameters obtained for each pig from the model fitting in this chapter. The derived parameters will be used in the next chapter of this thesis for analysis of the associations between viraemia and cytokine measures and also in subsequent genetic analysis such as Appendix 3.

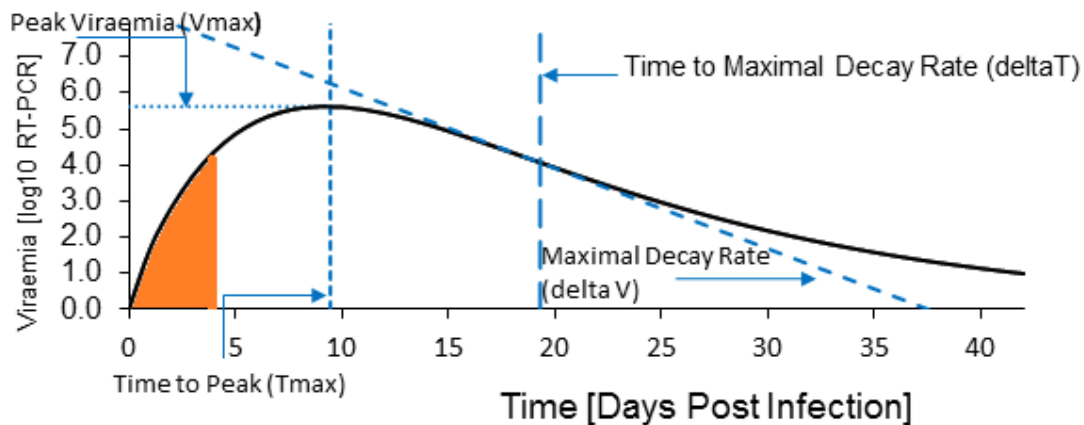


Figure 3.1 A typical viraemia profile with the derived variables from the Woods model annotated. The AUC up to 4dpi i.e. I4 is denoted by the orange region and the variables V_{max} , T_{max} , ΔT and ΔV are annotated. (Figure taken from the manuscript in Appendix 3)

Chapter 4

Exploring the relationship of PRRS viraemia profiles with longitudinal cytokine expression

4.0 Introduction

In Chapter 3 we established three types of viraemia profiles from the same PRRS virus infection: (i) cleared (resolution of viraemia to levels below detection at 42 days post infection (dpi)), (ii) transient experiment persistence hitherto referred to as persistence (viraemia remains above the level of detection at 42dpi), and (iii) rebound (bimodal) profiles [1]. Exact knowledge about the underlying immune mechanisms responsible for the observed discrepancy between viraemia profiles is still sparse. Previous studies of the same dataset as used here identified a single nucleotide polymorphism (SNP) WUR10000125 (WUR) on chromosome 4 associated with reduced cumulative viral load [2-4] and the GBP5 candidate gene. GBP5 plays a role in the innate immune response during infection and interacts with the inflammasome NLRP3 multi-protein complex that acts as a sensor for pathogen associated damage and is associated with the cleavage of some pro-inflammatory cytokines [5,6]. The WUR SNP accounts for 15.7% of the total variation in cumulative viraemia [7]. Gaining a more comprehensive understanding of the underlying immune mechanisms would be useful to aid the control of infection which is a major issue for swine production. For this purpose, measurements of cytokines and neutralising antibodies (nAbs) have been collected for a subset of the pigs in the PHGC infection trials.

Cytokines play a fundamental role in both the innate and adaptive immune response and are thus likely to have a significant influence on the observed viraemia patterns. Numerous cytokines have been reported to influence responses of pigs to PRRSV infection [8-16]. The quantity of innate cytokines secreted in PRRSV-infected pigs has been found to be strain-dependent (i.e. between north American strains VR-2323 and KS06)[17], significantly lower than for other viral infections (i.e. swine influenza virus (SIV) and porcine respiratory coronavirus (PRCV)) [13], and could be partly responsible for the delayed activation and dampened adaptive immunity [13,18,19]. Secretion of several serum cytokines such as IL-8, IL-1b and IFN-gamma have been found to be correlated to virus level accounting for ~84% of the observed variation in viraemia up to 42dpi [16].

Previous studies have linked the pro-inflammatory cytokines IL-1b and IL8 to viral persistence in PRRSV infections. For the innate cytokines IL-8 and IL-1b it was found that levels were up-regulated by 7dpi and that persistent pigs had a higher concentration of IL-1b and a lower concentration of IL-8 [16]. Substantial inter-host variation in the ability to synthesise IL-8 has been previously reported,

where strong IL-8 synthesis is associated with high host resistance to PRRSV defined by the susceptibility of target cells *in vitro* [20].

PRRSV infection typically results in low levels of innate antiviral cytokines [8]; however previous studies have established that the anti-viral cytokines IFNA (interferon alpha), IFN-gamma, and TNF-A (tumour necrosis factor alpha) play a key role in the clearance of PRRS viraemia [16,21-23]. There are conflicting reports on IFNA expression following PRRSV infection: the North American PRRS virus has been shown to inhibit type-1 interferon production [24], resulting in no significant increases in expression of type-1 interferon following PRRSV infection [9,25]. Conversely, isolate dependent increases in IFNA expression have also been observed [12,26-28]. Similarly, TNF-A response to PRRSV infection is variable, often weak, and also strain-dependent [23,29]. Other known cytokines with immune-regulatory roles in PRRSV infection include IL-12, IFN-gamma, IL-6, IL-4, TGF-b (transforming growth factor beta), and IL-10 [8,21,30-32]. NK cell function regulation during PRRSV infections is coordinated by multiple cytokines, such as IFN-A/B, IL-12, and IL-15 [33]. Pigs with low levels of IFNA secretion have been shown to elicit reduced NK (natural killer) cell activity [15,34,35]. Reduced NK (natural killer) cell cytotoxicity have also been associated with increased plasma concentrations of IL-4, IL-10 and IL-12 [27].

Cytokines do not act in isolation and are thus most likely highly correlated. Furthermore cytokine responses are transient [36]. In order to better understand the role of cytokines in shaping virus load profiles, it would be beneficial to consider the temporal profiles of various cytokines simultaneously. Most previous studies of cytokine response to PRRSV infection either explored the expression of a very limited number of cytokines or only contained cross-sectional or limited numbers of repeated measures [12,16]. The recent development of Fluorescent Microsphere Immunoassays (FMIA) allows reliable, effective simultaneous quantification of multiple cytokines in porcine sera but is not limited to swine data only [25]. FMIA is a new method of cytokine detection for PRRSV and has only been used in one previous study for PRRSV infection [12]. In this chapter, FMIA provided 8 longitudinal measures from 6 cytokines taken weekly 0-42dpi (days post infection) for 228 pigs from trials 1, 3 and 5 of the PHGC challenge experiments. The cytokines measured in this chapter were chosen due of the availability of the relevant assays.

The overarching aim of this chapter is to explore the association between the observed PRRS viraemia profile characteristics and the corresponding measures of the immune response in the form of longitudinal cytokine profiles. We determine the characteristic features and time trends of each cytokine profile, and examine the associations amongst cytokines. We assess the responsiveness of pigs to all cytokines and examine the impact of the viral profile class, WUR genotype and genetic background on the breadth of cytokine response. We then determine the association between viraemia and the ensuing cytokine measures and also the cytokines and the ensuing viraemia measures, and

answer the question whether the strength of the serum cytokine response is associated with the rate of the serum viraemia decline. Through a multiple regression approach we explore whether cytokines drive viraemia profile characteristics and vice versa.

4.1 Materials and Methods

4.1.1 Experimental Data

The data analysed in this chapter was obtained from a subset of the PRRS PHGC infection trials; a detailed description of the experimental protocol is outlined in the introduction and [37,38]. Briefly, the pigs were experimentally infected with NVSL 97-7985, a virulent isolate of PRRSV, [39], with an infection dose of 10^5 tissue culture dose₅₀ (TCID₅₀). The cross-bred pigs used in these trials were supplied by different commercial breeding companies, so that animals in different trials were unrelated and from different genetic backgrounds [40] as outlined in Table 4.1. Hence for the cytokine data analysed in this Chapter, trial and genetic background are confounded, as shown in Table 4.1. Pigs had been weaned in high health farms that were free of PRRSV, mycoplasma hypopneumoniae and swine influenza virus. Upon arrival at the challenge facilities, the commercial cross-bred pigs aged between 25 and 35 days were placed randomly in pens of 10-15 pigs and were infected with PRRSV after a 7 day acclimation period, i.e. at 0 days post infection (0 dpi).

Data	Trial Number	Number of Animals	Breed Cross ¹	Genetic Background ²
Cytokine repeated measures 0-42dpi	3	35	LW x LR	1
	5	77	Duroc x LR/LW	3
	7	117	Pietran x LW/LR	5
	Total	229	-	-

Table 4.1 Animal composition across a subset of the PHGC trials used for studying the cytokine profiles. ¹LW = Large White; LR = Landrace. ²Genetic background is defined as pigs from the same breeding company and the same breed cross.

Virus load: Blood samples were collected immediately before infection (0 dpi) and at 4, 7, 11, 14, 19/21, 28, 35, 40/42 dpi and the level of PRRS viraemia was measured using a semi-quantitative TaqMan PCR assay for PRRSV RNA. The viraemia quantity data from RT-PCR was transformed on the logarithmic scale to the base 10.

Cytokines: Cytokine data from serum collected at 0, 4, 7, 10, 14, 21, 28, 35, 42dpi was obtained for 228 randomly chosen individuals from the three PHGC trials 3, 5, and 7 (with cytokine data from 35, 77, and 117 pigs in each trial respectively) using Fluorescent Microsphere Immunoassay (FMIA) outlined in [25] and [12]. The FMIA Luminex multiplex swine cytokine assay provided simultaneous quantitative measures of the concentration of four innate (IL-1 β , IL-8, IFN α , IL-12), two regulatory (IL-10) and Th2 (IL-4) cytokines and a chemokine (CCL2) at each time point of the infection. There

was no successful assay for IFN γ as the monoclonal antibody that made the assay is no longer available. Trial 7 had missing values at 42dpi and Trial 3 had no observations for IL-1b. The log₁₀ of the cytokine observations was used to normalise the data. The cytokine data and the nAb data were obtained from separate projects within the PHGC consortium and hence the cytokine data does not overlap with the nAb data thus we cannot explore hypotheses between these two measures. The units of the cytokine measurements are log 10 pg/mL.

Genotyping: Ear tissue was collected from all pigs for DNA isolation. Tissues or DNA samples from the PHGC trials in this chapter were genotyped with Illumina's Porcine SNP60 Beadchip v1 (San Diego, California) at GeneSeek Inc. (Lincoln, Nebraska). In line with previous studies that identified the SNP WUR10000125 (WUR) to be associated with lower cumulative viral load [7,41,42], the genotype of the pig is defined by the frequency of the beneficial allele (WUR 0, 1 or 2) at this locus.

4.1.2 Smoothing and classification of viraemia and cytokine profiles

Smoothing Viraemia: As outlined in Chapter 3, the \log_{10} of PRRSV RNA copies per ml of serum were fitted to the Wood's and extended Wood's functions to provide continuous estimates for log-transformed viraemia over the 42-day observation period [1]. The Wood's model was fit to uni-modal profiles (~67% pigs) and the extended Wood's model was fit to bi-modal profiles (~33% pigs). The Wood's curve, an incomplete gamma function often used to model lactation yield in dairy cattle [37-39], and the extended Wood's curve was shown to appropriately model viraemia profiles in all the PHGC trials in Chapter 3.

Briefly, the uni-modal Wood's function is defined as $y(t) = a_1 t^{b_1} e^{-c_1 t}$, where $y(t)$ represents the level of viraemia in the blood (\log_{10} RT-PCR) at t days post infection (dpi). The constant a_1 is a scalar quantity and impacts upon the magnitude of all the points on the curve. The parameter b_1 is an indicator of the initial rate of increase to the peak viraemia level and the parameter c_1 is an indicator of the rate of decline after the peak and dominates the function as $t \rightarrow +\infty$.

The bimodal extended Wood's model fit to bimodal viraemia profiles is described by the equation:

$$y(t) = a_1 t^{b_1} e^{-c_1 t} + \max(0, a_2 (t - t_0)^{b_2} e^{-c_2 (t - t_0)})$$

where the model parameters a_1, b_1 and c_1 define the primary phase of the rebound profile as described for the Wood's model above. Time t_0 denotes the onset of the second phase of the profile, which is assumed to follow the same (Wood's) shape as the primary phase and is thus defined by the second set of Wood's model parameters: a_2, b_2, c_2 . For further details on the model fitting and the derived model parameters see Chapter 3.

The full time course of the experiment was considered in this analysis. However the dataset contained only a limited number (28) of pigs with bimodal profiles. Therefore extended Wood's parameter estimates associated with the rebound phase only were omitted from the analysis. The viraemia measures used in the analyses of this chapter are listed in Table 4.2. Figure 4.1 illustrates the fitted Wood's curve with its characteristic measures.

Viraemia measures	Explanation
V4, V7, V10, V14, V21, V28, V35, V42	Wood's model prediction at 4, 7, 10 ...42dpi
A1, B1, C1	Wood's model parameters associated with the primary phase of the infection
Tmax	Time of peak viraemia
Vmax	Peak viraemia value
deltaT	Time of maximal viraemia decline
deltaV	Value of maximal viraemia decline
cleared, persistent, rebound	The viral profile classification
I4, I21, I28, I35, I42	AUC of the viral profile up to 4, 21, 28, 35, and 42dpi

Table 4.2 The viraemia measures generated from the Wood's model fitting to viraemia profiles

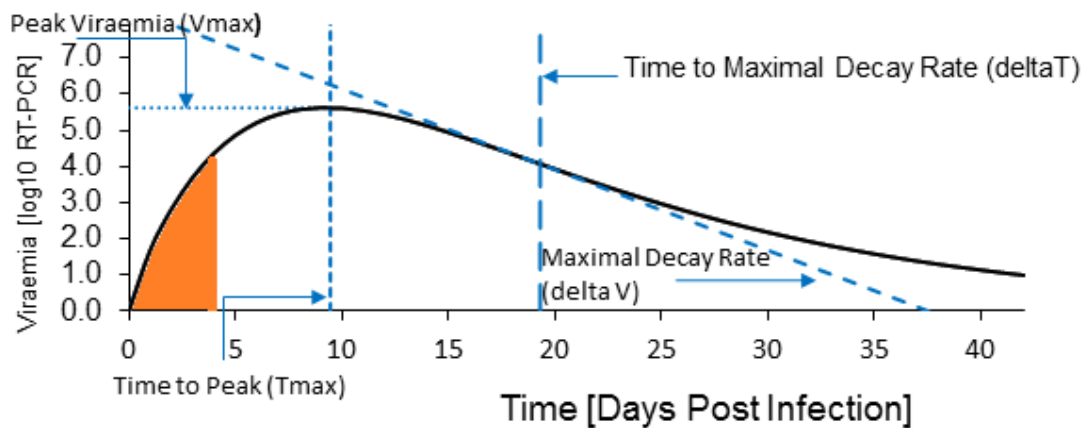


Figure 4.1 A typical viraemia profile with the derived variables from the Woods model annotated. The AUC up to 4dpi i.e. I4 is denoted by the orange region and the variables Vmax, Tmax, deltaT and deltaV are annotated. (Figure taken from the manuscript in Appendix 3)

Smoothing cytokines profiles: Visual inspection of individual cytokine profiles indicated that these could not be readily represented by known uni- or bimodal functions comprising few parameters. Therefore, in order to remove noise from the log-transformed cytokine measures, a cubic spline was fit to each individual cytokine profiles, using the data points as knots, in MATLAB[43]. The cytokine measures created from the cubic spline fitting are outlined in Table 4.3 and annotated on a CCL2 profile in Figure 4.2.

Cytokine measures	Explanation
IL8_0, IL8_4, IL8_10, IL8_14, IL8_21, IL8_28, IL8_35, IL8_42	Spline predictions of the \log_{10} of the cytokine observation at 0-42dpi (in this example IL8)
d_IL8_0_4, d_IL8_4_7, d_IL8_7_10, d_IL8_10_14, d_IL8_14_21, d_IL8_21_28, d_IL8_2835, d_IL8_3542	Difference between the cytokine spline observations associated with different time points. d_IL8_0_4 corresponds to the difference between the observations at 4 and 0dpi
A_IL8_4, A_IL8_7, A_IL8_10, A_IL8_14, A_IL8_21, A_IL8_28, A_IL8_35, A_IL8_42	AUC from 0dpi to 4-42dpi as a measure for the overall strength of the cytokine response over the indicated time period.
AA_IL8_4, AA_IL8_7, AA_IL8_10, AA_IL8_14, AA_IL8_21, AA_IL8_28, AA_IL8_35, AA_IL8_42	AUC above the baseline response (AAUC)
R_IL8	Binary trait as to whether an individual is a responder or non-responder for each cytokine respectively.

Table 4.3 Cytokine measures associated with IL-8 generated from cubic spline fitting. The same measures were obtained for the other cytokines considered in this study (IL-4, IL-10, IL-12, IL-1b, IFNA, and CCL2). The baseline response is the level of the cytokine expression at 0dpi.

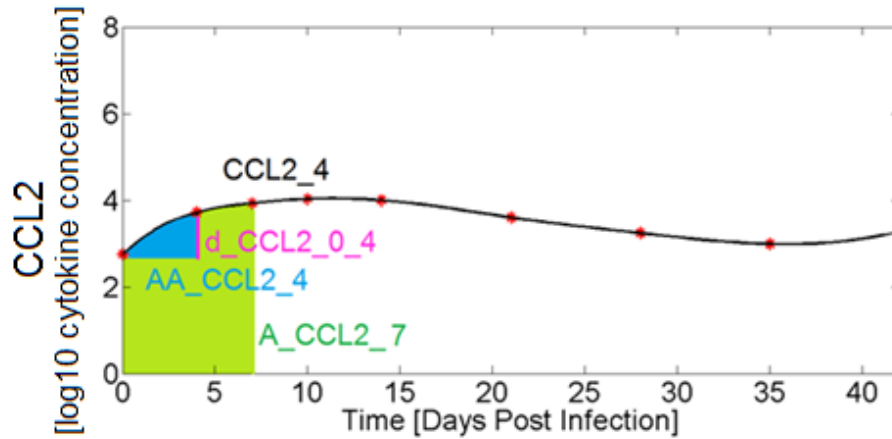


Figure 4.2 Typical CCL2 cytokine profile obtained from cubic spline fitting with the derived variables annotated. The black line delimits the spline model profile; the data is denoted by red asterisk; the spline observation at 4dpi i.e. CCL2_4 is denoted by a black dot; the difference between spline observations at 0 and 4 dpi i.e. d_CCL2 is shown in pink; the AUC up to 7dpi i.e. A_CCL2 is denoted in green; the AUC up to 4dpi with the baseline removed i.e. AA_CCL2_4 is denoted in blue.

The resulting smoothed cytokine profiles were then used to classify an individual as either responder or non-responder to that cytokine. A profile that was a non-responder for a particular cytokine meant that all its' subsequent observations did not significantly differ from the baseline spline observation in subsequent measures. To capture potential variation due to experimental measurement accuracy, a profile whose subsequent observations did not differ from the baseline within a threshold of 0.5 units on the \log_{10} scale was classed as a non-responder in that particular cytokine. A threshold value of 0.5 units was set based on visual inspection of profiles and taking into account potential variation caused by the measurement accuracy of the FMIA.

We further defined pigs according to their breadth of cytokine response. Individuals in PHGC Trials 3, 5, and 7 were assigned to one of the following 7 cytokine categories: 0) failed to produce a cytokine response in any cytokines 1) only produced a response in one cytokine, 2) produced a cytokine response in two cytokines, 3) produced a cytokine response in three cytokines 4) produced a cytokine response in four cytokines, 5) produced a cytokine response in five cytokines, 6) produced a cytokine response in six cytokines, 7) produced a cytokine response in all the measured cytokines. Analysis was conducted on the combined cytokine response class for a broad cytokine response (class 6-7) and a narrow cytokine response (class 0-5).

4.1.3 Statistical Analysis

The baseline model

Data and smoothed cytokine and viraemia profiles were analysed using repeated measures, logistic regression and multiple regression models, all implemented in a mixed model framework. The following baseline model was adapted to explore different objectives outlined below. Broadly we began with a null model containing the fixed and random effects representing the different sources of variation within the experimental protocol. Non-significant ($P > 0.05$) fixed and random effects were removed from the null model according to significance of the F-test (for fixed effects) and the likelihood ratio test (LRT for random effects). The full list of potential fixed effects in the null model included: WUR genotype (W), sex (S), age (A), parity (P), trial (T), genetic background (G), viral profile class (V), and all corresponding interactions. For testing the association between the viraemia and cytokine measures additional covariates (c) were added to the null model and significance was determined by the F-test and the LRT compared with the null model (i.e. without X_c).

Null model for continuous data:

$$Y = X_b b + Zu + \varepsilon \quad (1)$$

Final model for continuous data:

$$Y = X_b b + X_c c + Zu + \varepsilon \quad (2)$$

Where Y is the vector of the response variables (viraemia or cytokine), b is the vector of fixed effects included in the null model, c is the vector of fixed effects for the additional covariates, u is the vector of random effects, and ε is the vector of the residual effects. The matrices X_b , X_c , and Z are incidence matrices assigning individuals to their corresponding effects. The additional covariates are the potential predictors added to the null model (equation 1) and were either cytokine or viraemia variables from Table 4.2 or 3.3 for testing the associations between viraemia and cytokine and vice versa.

For analysis of categorical data a generalized linear mixed model (GLMM) was applied with a logit link function:

$$E[Y|u] = g^{-1}(Xb + Zu) \quad (3)$$

Where Y is the vector of the response variable (i.e. either nAb cross-protection, or breadth of cytokine responsiveness), b is the vector of fixed effects, u is the vector of random effects and g^{-1} is the inverse logit link function. The matrices X and Z are incidence matrices assigning individuals to their corresponding effects.

The logit link function is a standard link function and is defined as follows:

$$g(p) = \ln\left(\frac{p}{1-p}\right) \quad (4)$$

Unless stated otherwise, residual errors were assumed to be independently normally distributed. However, models that included repeated measurements serial correlations between consecutive measures were implemented in the residual error structure.

Determining cytokine response over time and examining the associations between cytokines

The null model defined by equation 1 adapted into a repeated measures model to determine how cytokine response changes over time. The null model was extended with the inclusion of the observation time T_k ($T_k = 0, 4, 7, \dots, 42\text{dpi}$) as a class effect in the model together with all possible interactions with the other fixed effects, and an autocorrelation structure between the repeated measures. A repeated measures model was used for the identification of significant fixed effects on the cytokine response over time, implemented with PROC MIXED in SAS 9.3. Autocorrelations between repeated measures were examined using the repeat statement of PROC MIXED, and various residual covariance matrix structures were explored (e.g. vc -standard variance components; ar(1) - first order autoregressive; cs- compound symmetry; un -unstructured; toep -toeplitz). The model produced least square mean (LSM) estimates for cytokine response at each observation time point. The F-test statistics was used to assess whether cytokine profiles differed between pigs from different genetic backgrounds, WUR genotypes (0, 1 or 2), or viraemia profile classes (rebound, clearance or persistence).

4.1.4 Associations between cytokine responsiveness with viral profile class, WUR genotype and genetic background

A GLMM, defined by equation 3, was used to obtain odds ratios in order to determine the association of nAb cross protection and cytokine responsiveness with viral profile class, WUR and genetic background (nAb data was from the same genetic background and hence was not explored). Logistic regression was carried out using PROC GLIMMIX in SAS 9.3, assuming an exponential distribution of the data, conditional on random effects. The categorical response variable was the cytokine responsiveness (low or high).

4.1.5 The association between viraemia and cytokine responses

Multiple regression analysis was carried out to determine the associations between viraemia measures and their preceding cytokine measures, i.e. using viraemia measures as the response variables and the cytokine measures as the potential predictors. Potential predictors were always chosen to be measures taken before or at the same time point as the response variable. Additional potential predictors were added to the null model by adding them as fixed covariates into the null model, which were the measures taken from Table 4.3, i.e. the cytokine spline predictions, cytokine spline prediction differences, area under the cytokine spline profiles, and interactions with the binary cytokine response class.

The classification as a responder or non-responder for each cytokine was included as a potential predictor. Furthermore the interaction between responder/non-responder binary trait interaction with spline observations was also included as a potential predictor (e.g. $R_IL8 * L_IL8_0$) to account for the fact that a significant association between cytokine and viraemia response can only be observed in individuals eliciting a cytokine response.

Using the cytokine spline estimates as predictors allows us to determine which are the key cytokines and key time points of association with viraemia measures. Inclusion of temporal changes in cytokine spline estimates as potential predictors allows us to determine if specific changes in cytokine expression is associated with the viraemia characteristics in question. Finally, including the AUC or AAUC of the cytokine spline estimates allows us to determine if it is the cumulative strength of cytokine response, or the response due to infection that plays a significant role in the viraemia profiles.

Stepwise removal of non-significant additional potential predictors was performed in the full models using the F –test at the 95% significance level ($P < 0.05$). A likelihood ratio test was conducted between the null model and the final model including the significant potential predictors only to assess whether these predictors significantly improve the model fit. To estimate the impact of the additional predictors the AIC and Pearson's correlation coefficients (R^2) values of the final models were compared with the null model.

Mixed models do not automatically account for co-linearity between predictors, which needs to be dealt with due to the risk of over-fitting. Therefore only significant predictors with pairwise R^2 less than 0.5 were included in the final models. In the case that significant predictors were correlated with R^2 values greater than 0.5, the model was refit and the predictor by removing one of the pairs in turn and the predictor resulting in the best model according to the AIC was chosen.

Furthermore, in order to explore the association between cytokines and the preceding viraemia measures the same method applied as outlined above; however the dependent variables were cytokine measures (from Table 4.3) and additional potential predictors were the viraemia measures up to and including the time point of the response variable (from Table 4.2) i.e. the Wood's model predictions, the areas under the viraemia curves, and the Wood's model parameters. To explore the association between the cytokines both the response variable and the potential predictors added to the null model were cytokine measures taken from Table 4.3.

4.2 Results

4.2.1 Qualitative assessment of cytokine profiles and classification into cytokine response categories

As shown in Table 4.4, the available cytokine data are not evenly distributed amongst genetic backgrounds and viraemia profile classes. Genetic background 5 provided over half of the cytokine data, and the majority of cytokine measures came from individuals with cleared and persistent viraemia profiles (at approximately equal proportions within and between genetic backgrounds). There were only 28 rebound individuals in the cytokine dataset, with 17 of them originating from genetic background 3. The relatively small proportion of rebounders in the cytokine dataset limited the ability to determine the cytokine characteristics associated with this phenomenon.

Genetic background (Trial)	Cleared (%)	Persistent (%)	Rebound (%)	Total
1 (3)	17 (49%)	14 (40%)	4 (11%)	35
3 (5)	28 (37%)	31 (41%)	17 (22%)	76
5 (7)	64 (55%)	46 (39%)	7 (6%)	117
Total	109 (48%)	91 (40%)	28 (12%)	228
Genetic background (Trial)	WUR 0 (%)	WUR 1 (%)	WUR 2 (%)	Total
1 (3)	17 (49%)	12 (34%)	6 (17%)	35
3 (5)	51 (67%)	22 (29%)	3 (4%)	76
5 (7)	51 (44%)	52 (44%)	14 (12%)	117
Total	119 (52%)	86 (38%)	23 (10%)	228

Table 4.4 The number of cleared, persistent and rebound individuals in the cytokine dataset. The percentage within genetic background (trial) is shown in brackets.

The WUR genotypes were approximately evenly distributed between the genetic backgrounds as shown in Table 4.5. Genetic background 3 had a lower proportion of WUR 2 and a higher proportion of WUR 0 than the other genetic backgrounds; WUR 0, 1 and 2 refers to the number of copies of the beneficial B allele found in previous studies [2-4].

Visual inspection of the \log_{10} cytokine profiles revealed substantial inter-host variation in the measured serum cytokine concentrations for all studied cytokines at all the time points, with differences of 2-3 log units between the extremes (Figure 4.3). The cubic splines provided a good fit

to the \log_{10} of the cytokine data for all cytokines with the maximum difference between the data and the spline values of only 0.05 \log_{10} units. As shown in Figure 4.3, the cubic splines successfully removed noise from the data whilst retaining the fundamental features of the profiles.

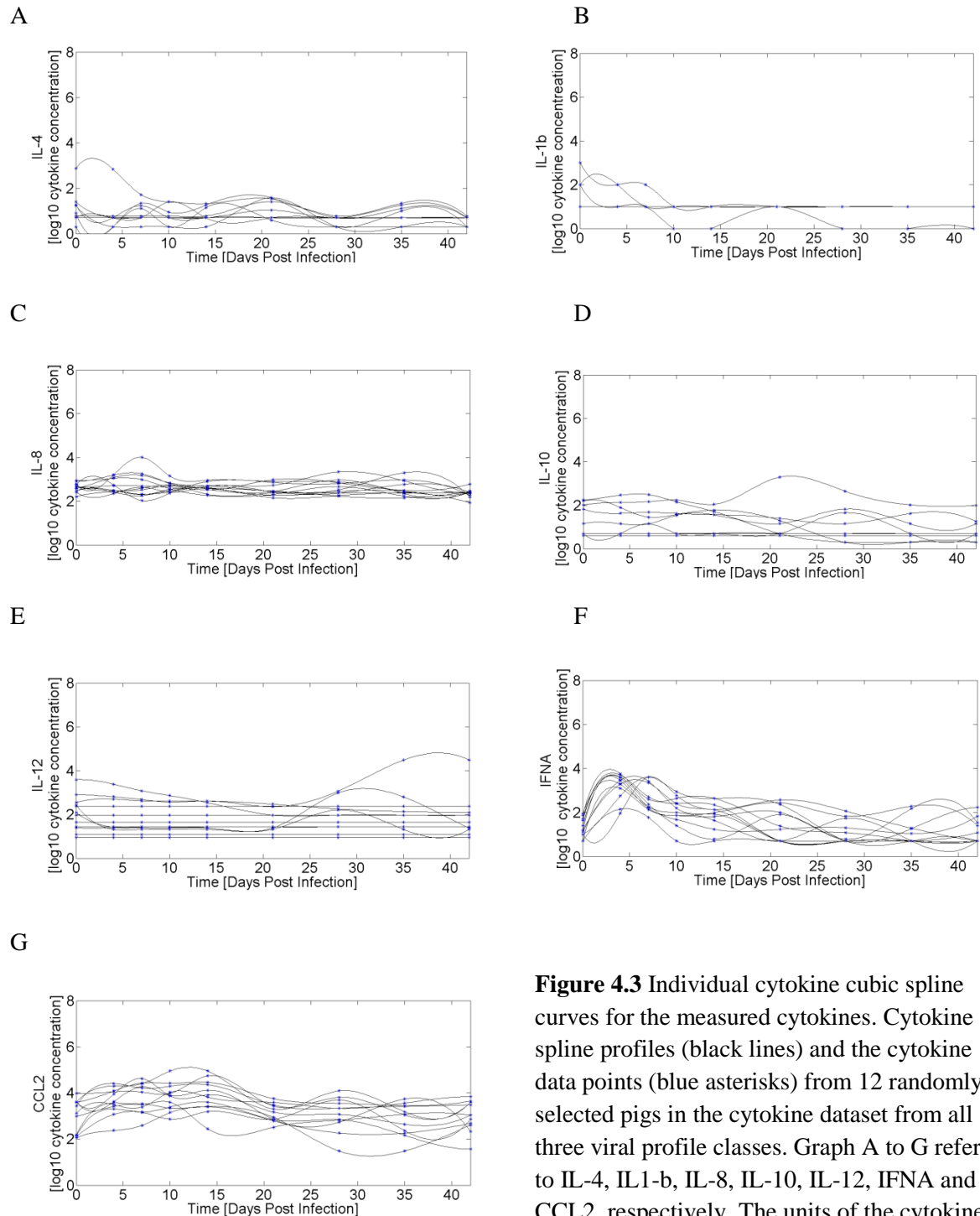


Figure 4.3 Individual cytokine cubic spline curves for the measured cytokines. Cytokine spline profiles (black lines) and the cytokine data points (blue asterisks) from 12 randomly selected pigs in the cytokine dataset from all three viral profile classes. Graph A to G refer to IL-4, IL1-b, IL-8, IL-10, IL-12, IFNA and CCL2, respectively. The units of the cytokine measurements are \log_{10} pg/mL.

Visual inspection of the smoothed cytokine profiles further indicated that a proportion of cytokine profiles only showed minor fluctuations with limited elevation above the baseline levels. In particular,

for IL4, IL1-b, IL-8, IL-12 the majority of profiles showed only minor fluctuations of less than 1 log units between cytokine concentrations associated with different time points. In contrast, many of the IFNA and CCL2 profiles tend to exhibit systematic uni- or bi-modals trends (Figure 4.3 F and G). In particular, peak levels of IFNA were often reached within the first seven days of infection, whereas CCL2 levels tended to peak slightly later between 7-14 dpi. A smaller second peak in IFNA was typically observed as early as 21dpi although for some pigs it occurred between 21-28dpi and for CCL2 at 28-35dpi.

4.2.2 Associations between cytokines and factors affecting cytokine response over time

The overall strength of cytokine response due to PRRSV infection was captured by the area under the curve (AUC) of the smoothed spline cytokine profiles with the baseline response removed (the adjusted AUC, henceforth denoted by AAUC). The AAUC up to 35dpi was used due to missing observations at 42dpi for genetic background 5. The immune regulatory cytokines were highly correlated with each other, as shown in Table 4.5. The anti-viral cytokine IFNA was moderately positively correlated with both the immune regulatory and pro-inflammatory cytokines. The cytokines could be grouped into two correlation groups. The first group consisted of: IL-4, IL-10, IL-12 and IL1b, and the second group contained: IL-8, IFNA and CCL2 (Table 4.5). The strongest correlation among immune regulatory cytokines was found at 35dpi, whilst the strongest correlation between the immune regulatory cytokines and the antiviral, or pro-inflammatory, cytokines was at 14dpi. With the exception of pro-inflammatory cytokines (IL-1b, IL-8 and CCL2), the cytokine correlations were the lowest at 4dpi. The strength of CCL2 and IFNA expression were highly correlated at 14 and 35dpi, with the strongest correlation at 14dpi.

AAUC (0-35dpi)	IL-4 ¹	IL-10 ¹	IL-12 ¹	IL-1b ²	IL-8 ²	IFN A ³
IL-4 ¹	-					
IL-10 ¹	0.41*	-				
IL-12 ¹	0.45*	0.65*	-			
IL-1b ²	0.45*	0.59*	0.75*	-		
IL-8 ²	0.12	0.14*	0.27*	0.12*	-	
IFN A ³	0.25*	0.30*	0.33*	0.38*	0.23*	-
CCL2 ²	0.12	0.17*	0.32*	0.14*	0.56*	0.38*
AAUC (0-14dpi)	IL-4 ¹	IL-10 ¹	IL-12 ¹	IL-1b ²	IL-8 ²	IFN A ³
IL-4 ¹	-					
IL-10 ¹	0.35*	-				
IL-12 ¹	0.40*	0.61*	-			
IL-1b ²	0.36*	0.45*	0.67*	-		
IL-8 ²	0.22*	0.08	0.31*	0.16*	-	
IFN A ³	0.21*	0.04	0.21*	0.20*	0.38*	-
CCL2 ²	0.21*	0.11	0.39*	0.13*	0.59*	0.48*
AAUC (0-4dpi)	IL-4 ¹	IL-10 ¹	IL-12 ¹	IL-1b ²	IL-8 ²	IFN A ³
IL-4 ¹	-					
IL-10 ¹	0.17*	-				
IL-12 ¹	0.27*	0.46*	-			
IL-1b ²	0.28*	0.25*	0.48*	-		
IL-8 ²	0.15*	0.02	0.43*	0.21*	-	
IFN A ³	0.06	-0.08	0.16*	0.12	0.12	-
CCL2 ²	0.13	-0.00026	0.47*	0.20*	0.20*	0.12

Table 4.5 Pearson correlations of pairwise log₁₀ cytokine concentration area under the curves above the baseline response (AAUC). The strongest significant cytokine associations between the AAUCs at 4, 14 or 35dpi are in bold. ¹The immune regulatory cytokines, ²the pro-inflammatory cytokines and ³the antiviral cytokines. *indicates statistical significance at the 95% significance level.

The association of cytokine characteristics between cytokines

In the null models, pen within trial was not significant. The significant fixed effects were dependent on the response variable; however genetic background and parity were consistently significant across the models for the majority of the cytokines. A selection of the mixed models of best fit to the data for the viraemia predictions are presented in Table 4.6. As opposed to the correlations the strongest associations in the multiple regression models were found in the early stage of infection from 0-10dpi. The cytokines were poor predictors of each other at the later stage of infection. IFNA and CCL2 were consistently significant predictors for each other in their respective final models, with IFNA being a better predictor for CCL2 as opposed to the other way around. IFNA was also significantly associated with baseline IL-4 and IL-1b, while CCL2 was also significantly associated with IL-8, IL-10, IL-1b and IL-12. The cytokines were poor predictors for IL-8. IL-4 was significantly associated with baseline IL-8, IFNA and IL-1b. IL-10 was significantly associated with baseline IL-4, IL-8 and IL-12. IL-12 was significantly associated with IL-1b, IL-10 and IL-4. IL-1b was significantly associated with baseline IL-4, IFNA and IL-12. Overall, the inclusion of cytokine measures as predictors for cytokines at a specific time point or over a given time period improved the model fit, as confirmed by a reduction of the AIC value, improved log-likelihoods and increase in the R² values.

Response	Significant predictors (F-test)	AIC difference (AIC_{null}-AIC_{final})	R squared	R squared difference (R²_{final}-R²_{null})	-2 Log likelihood final model	-2 Log likelihood null model
IFNA_4	L_CCL2_0 L_CCL2_4 Genetic background	64.5	0.24	0.13	294.2*	358.7
IFNA_10	IL4_0 CCL2_0 Genetic background Parity Viral class	21.2	0.33	0.08	318.6	339.8
AA_IFNA_35	AA_CCL2_28 AA_IL1b_28 Sex	59	0.28	0.24	2028.1*	2087.1
CCL2_4	IL10_0 IFNA_0 IFNA_4 Genetic background	51.5	0.37	0.20	279.8	331.3
CCL2_7	IL8_0 IFNA_0 IFNA_7	39.4	0.50	0.13	234.8*	274.2

	Genetic background					
AA_CCL2_35	AA_IL12_28 AA_IL1b_28 AA_IFNA_28 Genetic background Parity Age	49.9	0.39	0.19	1826.9*	1874.8
AA_IL4_35	IL1b_0 Parity Sex Genetic background	332.5	0.34	0.23	1466.3*	1798.8
AA_IL1b_35	AA_IL12_28 AA_IFNA_28 AA_CCL2_28 Genetic background Parity Sex	124	0.65	0.33	1790.7*	1914.7
AA_IL10_35	IL12_0 AA_IL12_28 AA_IL4_28 Genetic background Parity	140.5	0.54	0.31	1779.0*	1919.5
AA_IL12_35	AA_IL10_28 AA_IL1b_28 Genetic background Parity Sex	158.8	0.80	0.54	1801*	1959

Table 4.6 A selection of the final multiple regression models for testing the associations between cytokines. The AUC up to Xdpi with the baseline removed for a particular cytokine is represented by AA_cytokine_X.

The full repeated measures model with all the fixed and random effects was reduced according to significance of the potential effects and interactions at the 95% significance level. None of the three-way interactions (i.e. the interactions between three fixed effects) were significant. A summary of the significant fixed and random effects in the final repeated measures model for each cytokine is presented in Table 4.7. According to the likelihood ratio test at the 95% significance level ($P < 0.05$) the random effect of pen within trial was significant for all the cytokines. The model residuals were normally distributed for each cytokine.

Cytokine	Significant fixed effects (95% significance F-test)	Significant random effects (95% significance LRT)
IL-4	G, T	Pen
IL-8	P, G*T	Pen
IL-10	G, P, T, G*T	Pen
IL-12	W, G, P, A, T, G*T	Pen
IL-1b	P, T, G*T	Pen
IFNA	G, P, A, T, G*T, V*T	Pen
CCL2	G, P, T, G*T, V*T	Pen

Table 4.7 Summary of the significant effects in the repeated measures models for longitudinal cytokine profiles. Where W is the WUR genotype, P is the parity, A is the age, V is the viral profile class, G is the genetic background, T is the time, and * represents fixed effect interactions.

Effects of viraemia classes, genetic background and WUR resistance genotypes on cytokine profiles

The LSMs for the cytokine at different time points for each genetic background, viraemia class, and WUR genotype are presented below for each cytokine in Figures 4.4, 4.5 and 4.6, respectively. Out of these fixed effects considered, the genetic background had the biggest influence on LSM cytokine response.

Although time was a significant factor in the repeated measures models for all cytokines, the LSM profiles indicate that the profiles of the majority of the cytokines do not deviate substantially from the baseline observations at most observation times. However LSM IFNA and CCL2 profiles showed systematic time trends, with the general trend for IFNA represented by an increase to a peak around 4dpi followed by decline to baseline levels by 14dpi (Figure 4.4F). The dynamics of CCL2 appear slower than IFNA, with a gradual increase to peak expression by 10dpi followed by gradual decline, as shown in Figure 4.4 G.

Different genetic backgrounds had different baseline cytokine values or overall magnitudes of expression (IFNA, CCL2). Response patterns for the time-trends of the LSM estimates were overall

similar (Figure 4.4), although interaction between genetic background and time was significant in the repeated measures models of all cytokines. Indeed, genetic background 3 had a tendency to decrease from baseline expression in IL-1b, IL-12 and IL-10, whereas IL-1b for genetic background 1 saw a general trend of increase from the baseline (Figures 4.4 C, D & E). Furthermore cytokine response from genetic backgrounds 1 and 5 remained closer to baseline levels in IL-10 and IL-12 profiles compared to genetic background 3. In IFNA the rebound at 28dpi was the strongest for pigs from genetic background 5. The CCL2 profiles had similar time trends but genetic background 1 had significantly lower levels of expression for the majority of the infection (4-35dpi).

There were statistically significant differences between the viral profile classes. Rebounders elicited a stronger response in most of the cytokines at the later stages of infection (from 28dpi onwards) than non-rebounders (Figure 4.5), although the differences were not always statistically significant. There were statistically significant differences ($P < 0.05$) between rebound CCL2 at 28dpi and both cleared and persistent profiles. Rebound profiles also had statistically significant higher levels of IFNA expression at 28-35dpi than cleared profiles and higher IL-8 expression at 35dpi. Differences between pigs with cleared and persistent profiles were small and not statistically significant. Rebound viraemia profiles begin with a significantly higher baseline level of IFNA than cleared viraemia profiles. The CCL2 profiles for the cleared and persistent viraemia pigs decline to baseline levels after peak CCL2 expression, viraemia rebound pigs, however, initially follow the same decline from the CCL2 peak but then experience a “rebound” in CCL2 values.

The time trends and LSM estimates for the profiles of IL-4, IL-8, CCL2 and IFNA were similar for the three WUR genotypes as shown in Figure 4.6. The WUR genotype had only a significant effect in the final model for IL-12, with significant differences observed in the magnitudes of expression between the WUR genotypes in this cytokine. Interestingly the WUR 2 genotype was associated with the lowest LSM predictions whilst WUR 1 with the highest. Non-significant differences in the expression of cytokines between the WUR genotypes was also observed; WUR 2 had generally higher expressions of CCL2 between 4-21dpi, IFNA at 4dpi, IL-10 at 0-7dpi and 20-35dpi, and slower dynamics in IL-1b between 0-7dpi than WUR 0 or 1.

The only statistically significant difference between the WUR genotypes in any of the measured cytokines was found at 4dpi between WUR 1 and 2: WUR 2 had a higher estimated level of IFNA expression at this observation. Based on the AUC of viraemia WUR 2 represents the more resistant individuals which could be related to eliciting a stronger early antiviral response. WUR 2 individuals also had slightly higher LSMs for CCL2, IL-8 and IL-10 at the early phase of infection (0-21dpi); however these elevations were not statistically significant.

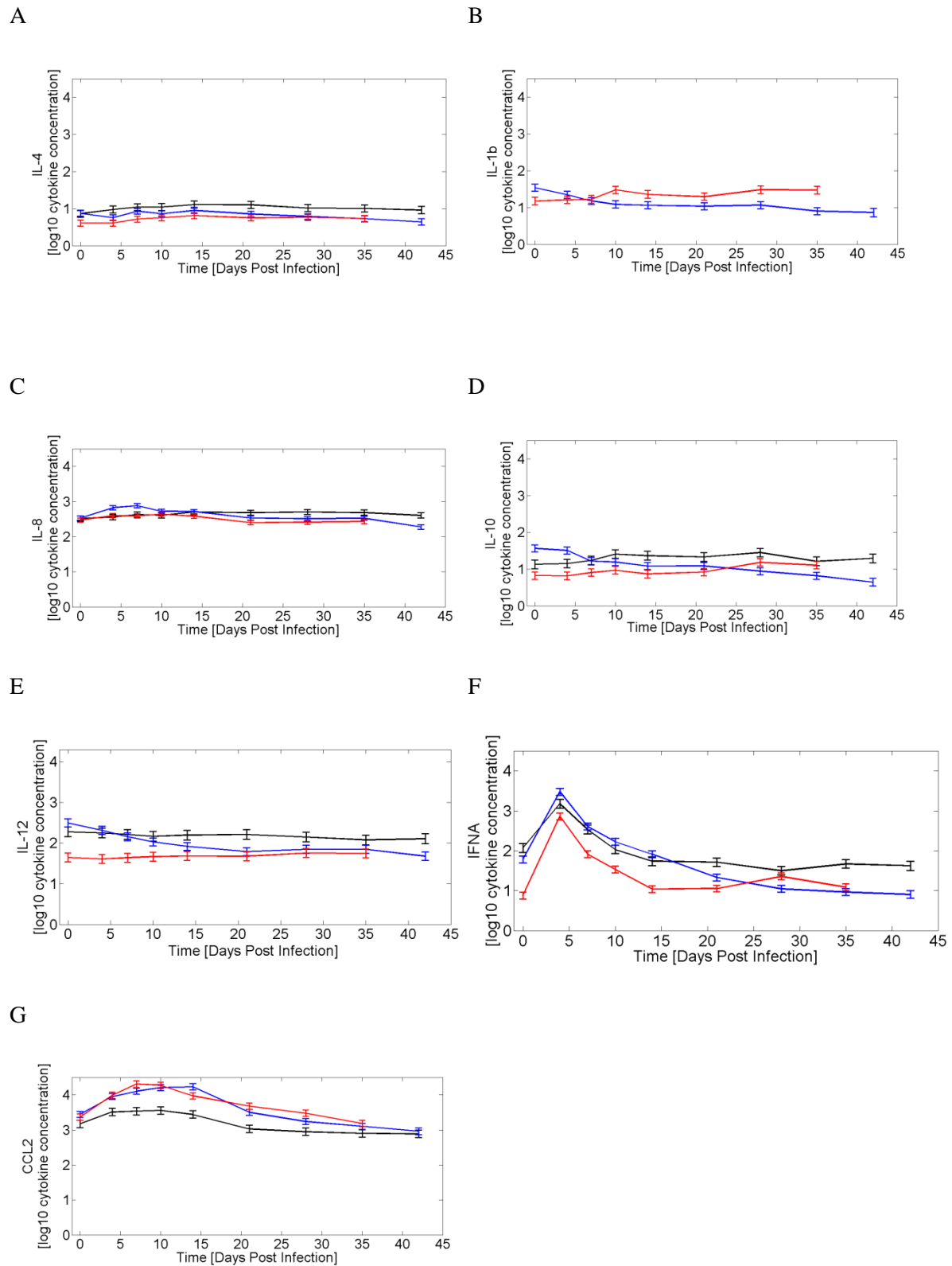


Figure 4.4 The effect of genetic background on cytokine profiles. The LSMs with standard errors for each genetic background: genetic background 1 is in black, genetic background 3 is in blue, and genetic background 5 is in red. There were no IL-1b observations for genetic background 1. The units of the cytokine measurements are log 10 pg/mL.

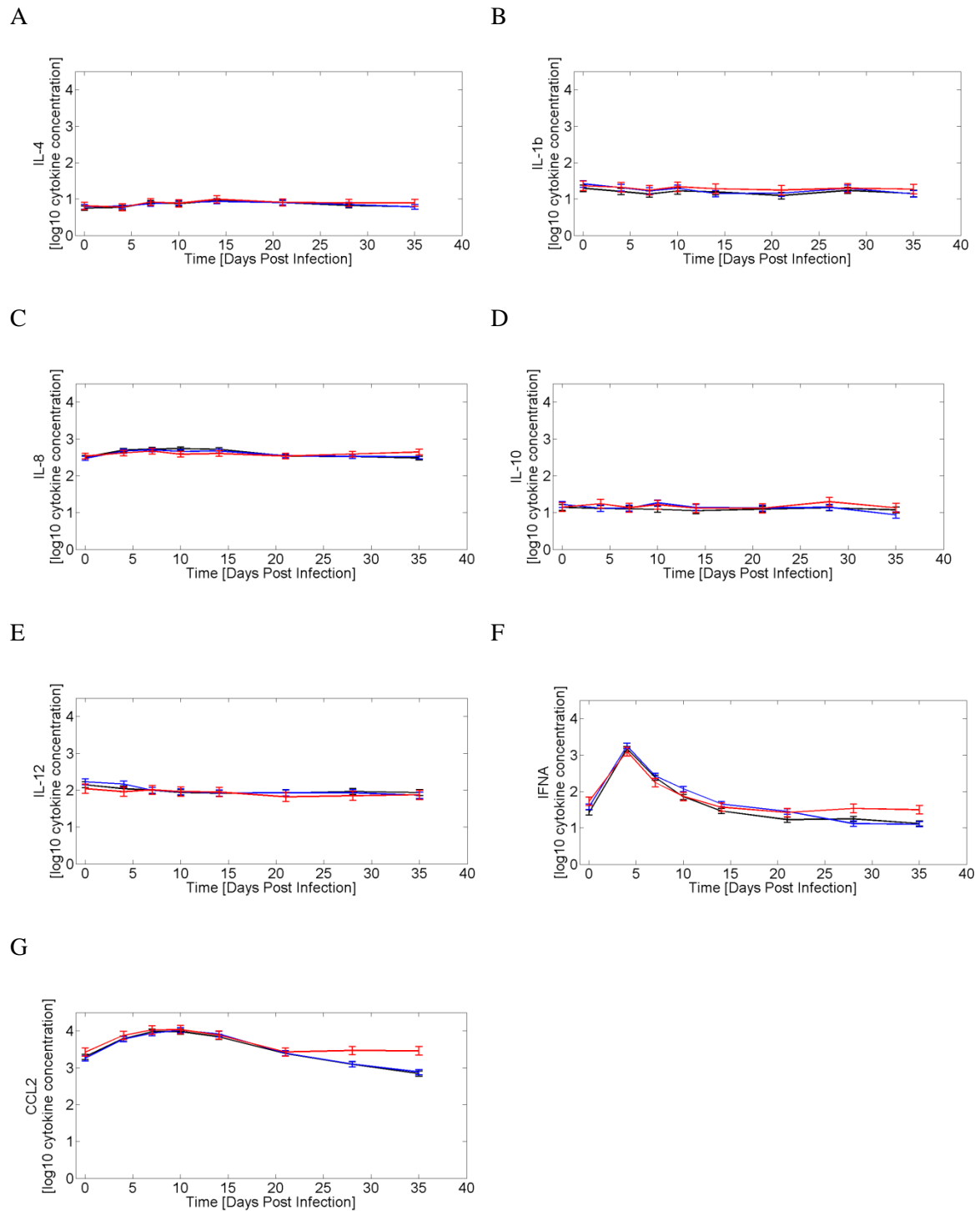


Figure 4.5 The effect of viral class on the cytokine profile. The LSMs with standard errors for each viral class: cleared is in black, persistent is in blue, and rebound is in red. The units of the cytokine measurements are log 10 pg/mL.

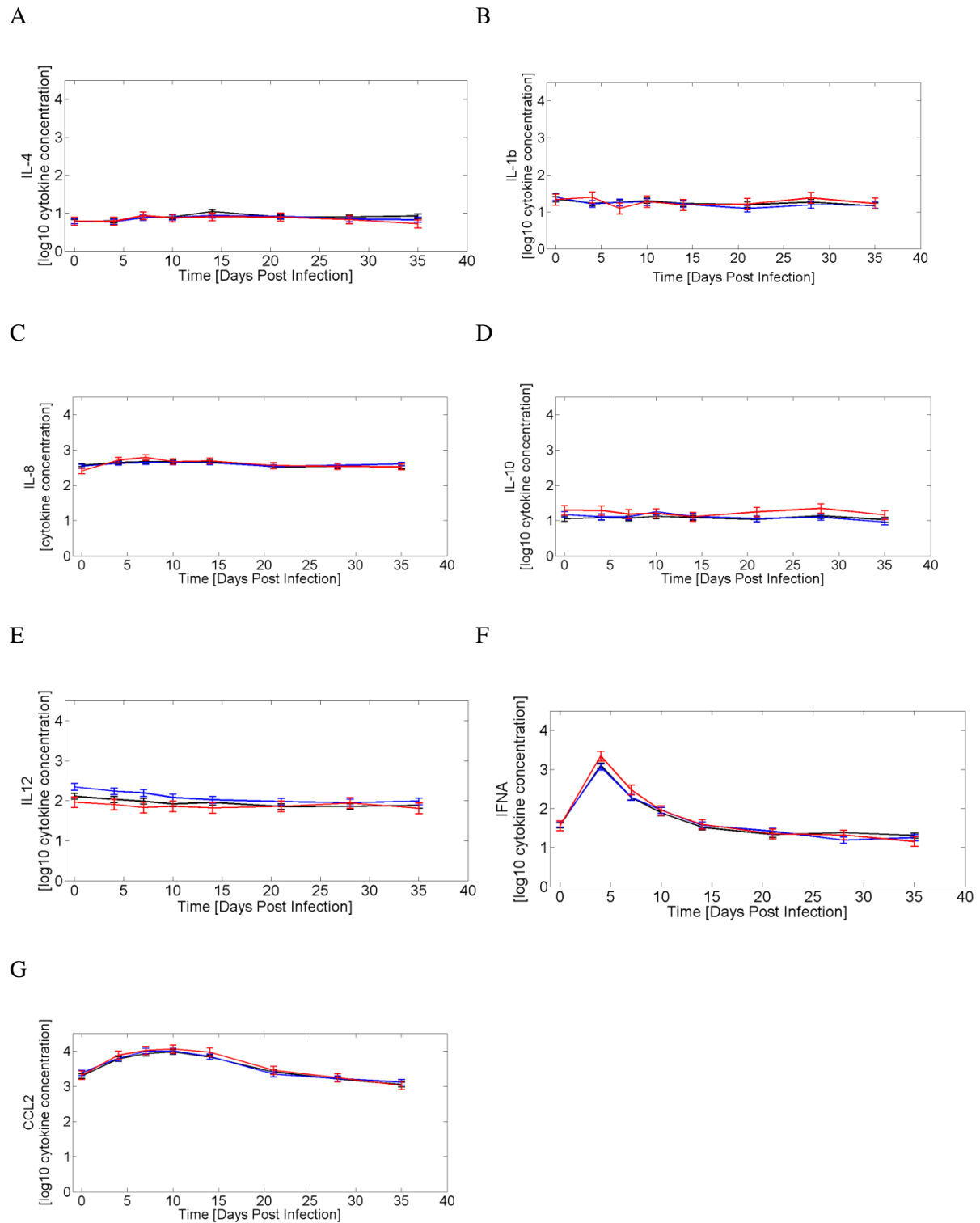


Figure 4.6 The effect of WUR on the cytokine profile. The LSMs for each WUR genotype: WUR 0 is in black, WUR 1 is in blue, and WUR 2 is in red. The units of the cytokine measurements are log 10 pg/mL.

4.2.4 Cytokine responsiveness and the association with viral profile class, WUR genotype and genetic background

Individual cytokine profiles could be classed as responders or non-responders to PRRSV infection. A profile was defined as a non-responder if all cytokine spline estimates after 0 dpi differed from the baseline level at 0 dpi by less than 0.5 units on the \log_{10} scale. The threshold of 0.5 units was chosen to account for variation in observations caused by measurement or smoothing error, and was based on visual inspection of the spline profiles.

A breakdown of the distribution of responder and non-responders within each cytokine is shown in Table 4.8. The majority of the pigs responded in the pro-inflammatory and anti-viral cytokines (IL-1b, IL-8, CCL2 and IFNA) and also the immune regulatory cytokine IL-10. In particular, the highest percentage of responders was found for INFA and CCL2, for which over 95% of pigs elicited a noticeable response. The immune regulatory cytokines IL-4 and IL-12 had the highest percentage of non-responders (71% and 54%, respectively) compared to the other cytokines. A breakdown of the distribution of responders according to viraemia profile class, genetic background and WUR genotype within each cytokine is shown in Table 4.9 and Figures 4.7-4.9.

Cytokine	Responder (%)	Non-responder (%)
IL-4 ¹	66 (29)	162 (71)
IL-10 ¹	209 (92)	19 (8)
IL-12 ¹	96 (46)	114 (54)
IL-1b ²	160 (70)	68 (30)
IL-8 ²	182 (80)	46 (20)
CCL2 ²	221 (97)	7 (3)
IFNA ³	227 (99.6)	1 (0.4)

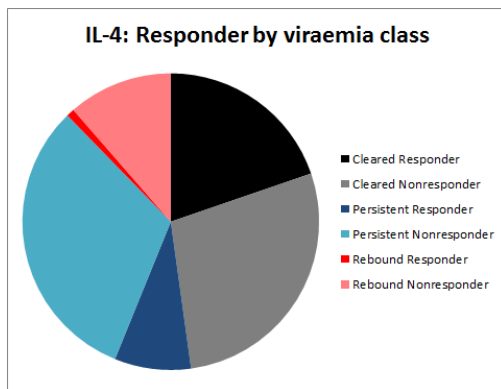
Table 4.8 The distribution of responders and non-responders for each cytokine. Superscripts refer to ¹ immune regulatory cytokines, ² pro-inflammatory cytokines and ³ antiviral cytokines.

Cytokine	Cleared (%)	Persistent (%)	Rebound (%)
IL-4	45 (41)	19 (21)	2 (7)
IL-8	88 (81)	74 (81)	20 (72)
IL-10	101 (93)	86 (95)	22 (79)
IL-12	55 (50)	47 (52)	13 (45)
IL-1b	59 (64)	52 (68)	14 (58)
IFNA	109 (100)	91 (100)	27 (96)
CCL2	105 (96)	90 (99)	26 (93)
Cytokine	Genetic Background 1 (%)	Genetic Background 3 (%)	Genetic Background 5 (%)
IL-4	0 (0)	0 (0)	66 (56)
IL-8	16 (46)	49 (64)	117 (100)
IL-10	28 (80)	64 (84)	117 (100)
IL-12	30 (86)	46 (61)	38 (32)
IL-1b	-	47 (62)	78 (66.7)
IFNA	35 (100)	76 (100)	116 (99)
CCL2	33 (94)	73 (96)	115 (98)
Cytokine	WUR 0 (%)	WUR 1 (%)	WUR 2 (%)
IL-4	33 (28)	27 (31)	6 (26)
IL-8	91 (76)	72 (83)	19 (83)
IL-10	110 (92)	80 (93)	19 (83)
IL-12	64 (54)	38 (44)	12 (52)
IL-1b	28 (27)	18 (24)	3 (18)
IFNA	118 (99)	86 (100)	23 (100)
CCL2	117 (98)	81 (94)	23 (100)

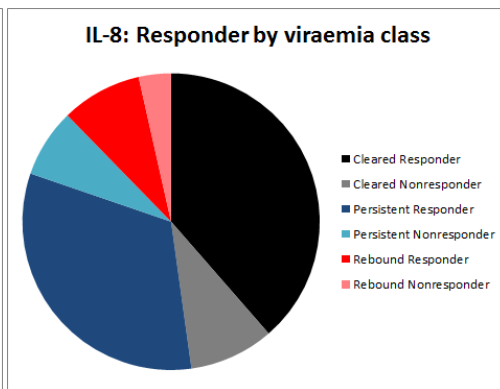
Table 4.9 The number and percentage of responders for each cytokine according to viraemia class, genetic background and WUR genotype.

Figures 4.7-4.9 illustrate the distribution of the responders across viraemia class, genetic background and WUR genotype respectively. The distribution between responders and non-responders is roughly similar between the viraemia classes for IFNA, CCL2, IL-1b, IL-10 and IL-8 (Figure 4.7). For IL-4 the cleared profiles have a larger percentage of non-responders than the rebound or persistent classes (Figure 4.7A). Genetic background 5 had a bigger proportion of responders in IL-4 than genetic backgrounds 1 and 3 (Figure 4.8A). However the distribution of responders and non-responders for the other cytokines were similar across the genetic backgrounds for IL-1b, IFNA and CCL2 only (Figure 4.8). Genetic background 5 had the highest proportion of responders in IL-8 and IL-10 but the highest proportion of non-responders in IL-4 and IL-12 than the other genetic backgrounds. Figure 4.9 shows that the distribution between responders and non-responders is roughly similar between the WUR genotypes, except for IL-4 which had a smaller proportion of responders in WUR 2 than the other genotypes.

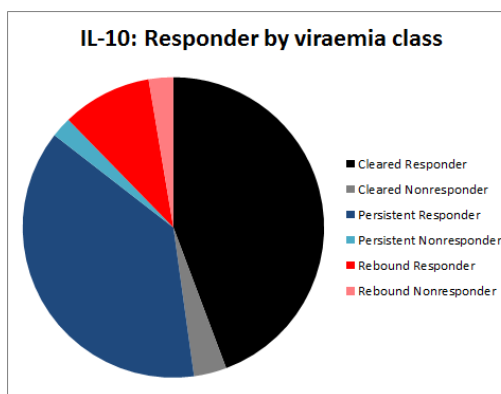
A



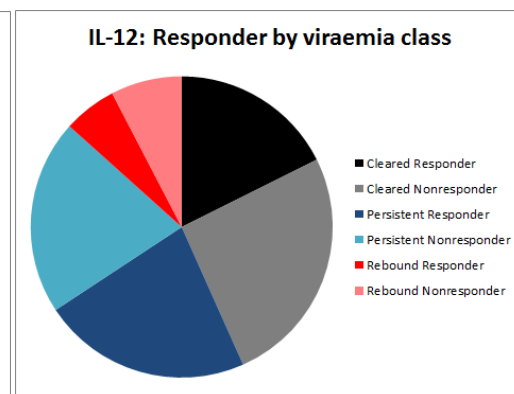
B



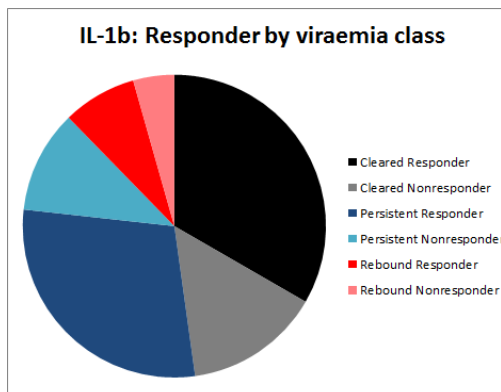
C



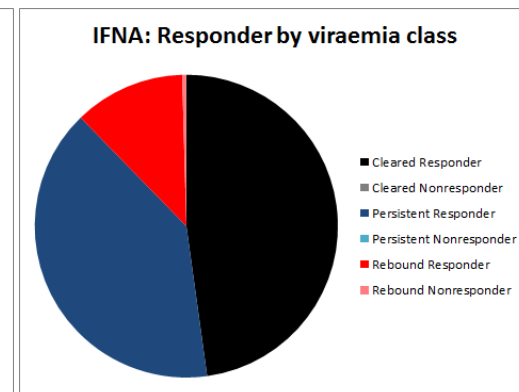
D



E



F



G

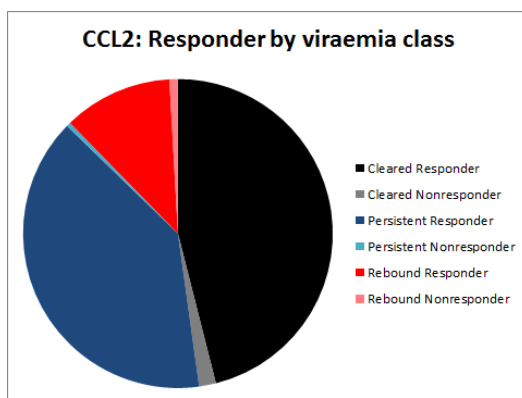
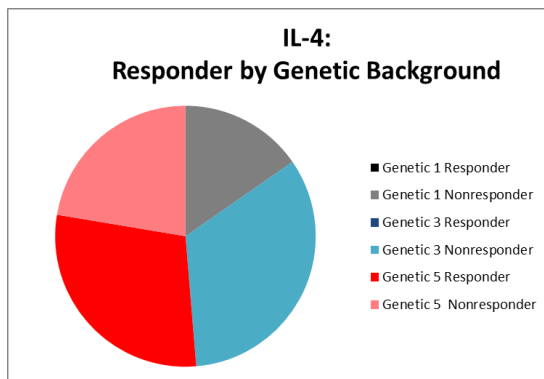
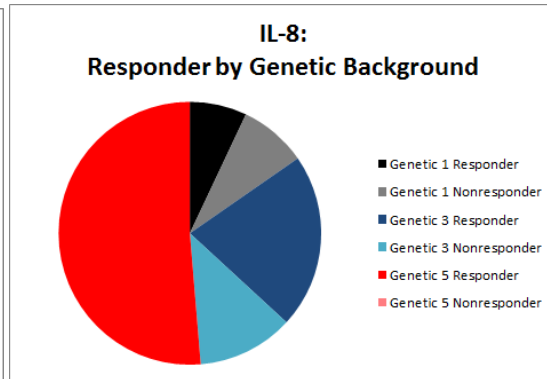


Figure 4.7 The distribution of responder and non-responders for each cytokine by viraemia class.

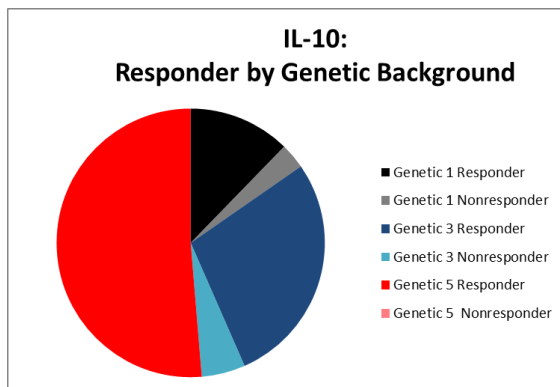
A



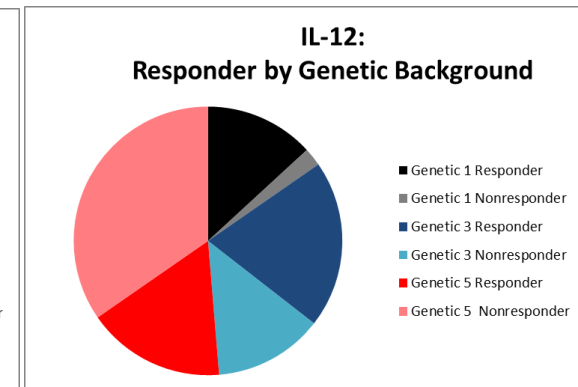
B



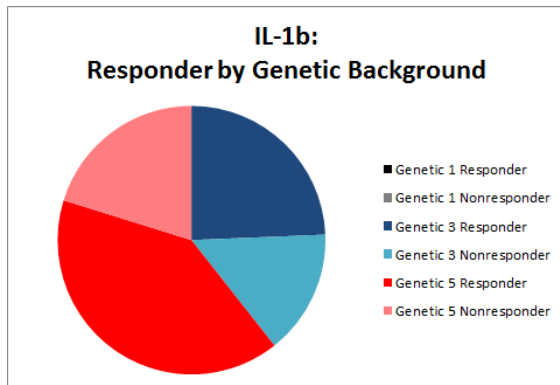
C



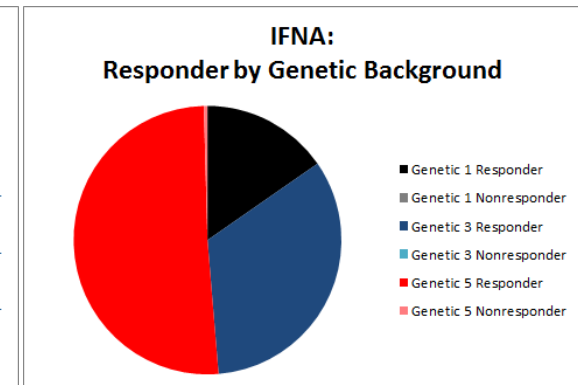
D



E



F



G

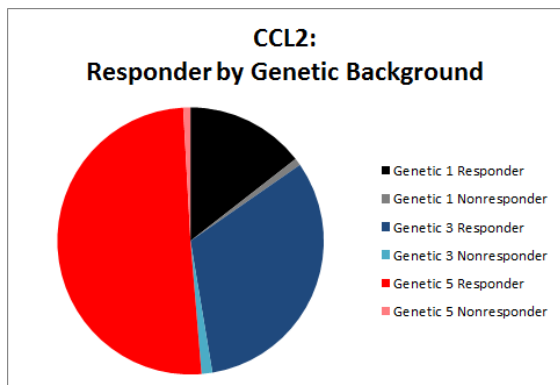
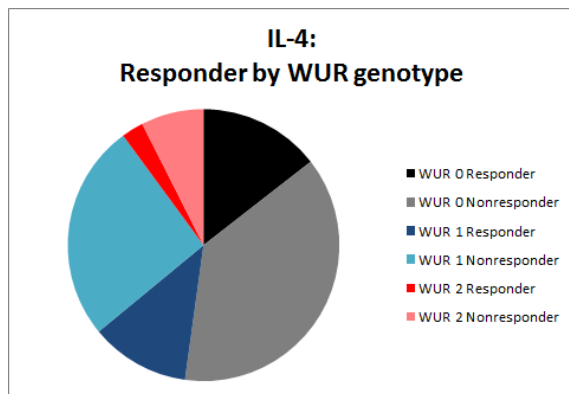
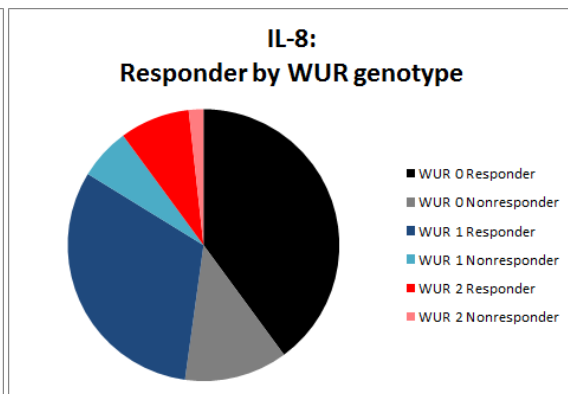


Figure 4.8 The distribution of responder and non-responders for each cytokine by genetic background. NB. There were missing values for IL-1b for genetic background 1.

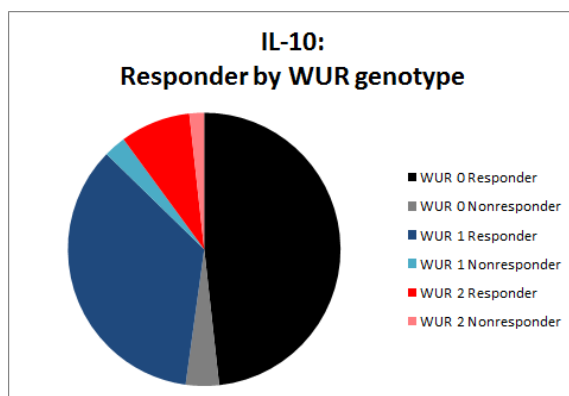
A



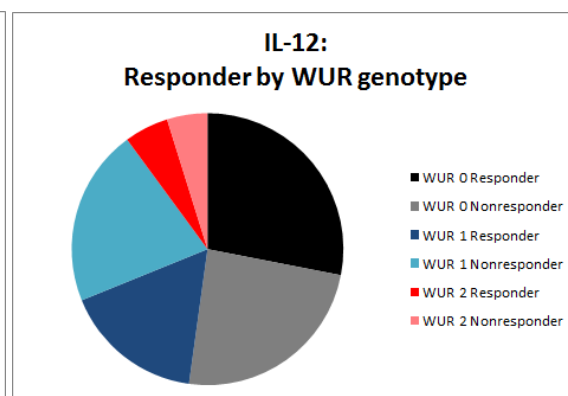
B



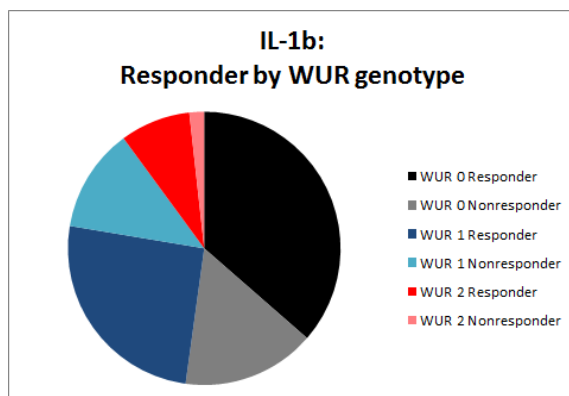
C



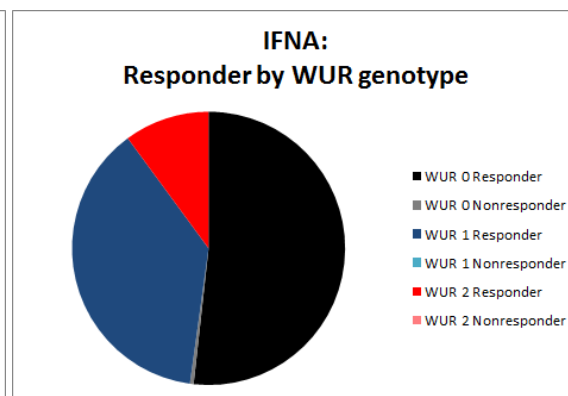
D



E



F



G

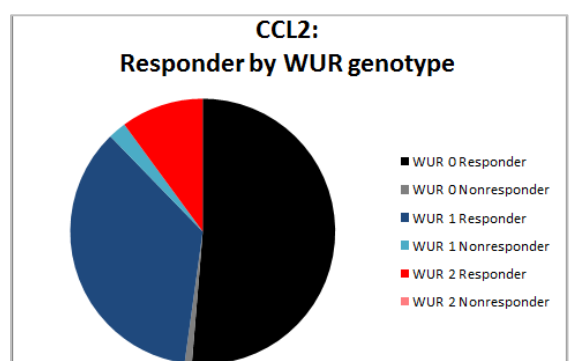


Figure 4.9 The distribution of responder and non-responders for each cytokine according to WUR genotype.

A measure of the total cytokine responsiveness for each individual was calculated by summation of the cytokine responsiveness across all of the observed the cytokines as outlined in Table 4.10. The cytokine response classes ranged from 3 to 7. The modal cytokine response class was 6. The cytokine response classes were then divided into being a broad or narrow cytokine response, where a broad response was defined by elevated expressions in 6-7 cytokines and a narrow cytokine response was defined by elevated expression in only 0-5 cytokines. The distribution of broad and narrow responses by each viral profile class, genetic background and WUR genotype are shown in Table 4.11. The odds ratios of the breadth of cytokine response associated with different viraemia profiles classes, genetic backgrounds, and WUR genotypes are presented in Table 4.12.

The final model used to test the association between the profile-class, genetic background or WUR genotype against the cytokine breadth of response contained parity as the only significant fixed effect at the 95% significance level ($P < 0.05$), with no other fixed or random effects.

Cytokine response class (#cytokines the pig responds)	Broad/Narrow class	Number of individuals (%)
0	Narrow	0
1	Narrow	0
2	Narrow	0
3	Narrow	6 (3)
4	Narrow	43 (19)
5	Narrow	62 (27)
6	Broad	94 (41)
7	Broad	23 (10)
	Total Broad	117 (51)
	Total Narrow	111 (49)
	Total	228 (100)

Table 4.10 The pooled cytokine response classes. The cytokine response class refers to the number of cytokines the individual responds in. The classes were then pooled into a broad or narrow cytokine response according to the cytokine response class. (Broad: cytokine response class 6-7, narrow cytokine response class 0-5).

Given that the allele acts in a dominant manner the WUR classes 1 and 2 were pooled (WUR Y) and further odds ratios were obtained to compare differences between the WUR 0 and pigs with the favourable B allele.

Viral class	Broad (% within class)	Narrow (% within class)
Cleared	60 (55)	49 (45)
Persistent	50 (55)	41(45)
Rebound	7 (25)	21 (75)
Genetic background		
1	24 (69)	11 (31)
3	31 (41)	45 (59)
5	62 (53)	55 (47)
WUR genotype		
0	66 (55)	53 (45)
1	42 (49)	44 (51)
2	9 (39)	14 (61)
Y (Pooled WUR 1 & 2)	51 (47)	58 (53)

Table 4.11 Summary of the distribution of the breadth of cytokine response for viral profile class, genetic background and WUR genotype.

There was a statistically significant association ($p<0.05$) between the viraemia profile class and the breadth of the cytokine response when the cytokine response was pooled into two groups (i.e. broad or narrow). The direction of the odds ratios indicated that rebounders had a significantly narrower cytokine response than non-rebounders ($p<0.05$) (Table 4.12).

There was a statistically significant association (at the 95% significance level) between the genetic background and the breadth of the cytokine response when the cytokine response was pooled into two groups (i.e. broad or narrow). The direction of the odds ratios indicated that genetic background 1 had a broader response than genetic background 3 ($p<0.05$) (Table 4.12).

There were not any statistically significant associations (at the 95% significance level) between the WUR genotype and the breadth of the cytokine response when the cytokine response was pooled into two groups (i.e. broad or narrow) as shown in Table 4.12.

Class 1	Class 2	Odds ratio (95% Confidence interval)	P- value
Clearance	Persistence	1.086 (0.607, 1.944)	0.78
Clearance	Rebound	4.414 (1.556, 12.526)	<0.05*
Persistence	Rebound	4.063 (1.418, 11.643)	<0.05*
Class 1	Class 2	Odds ratio (95% Confidence interval)	P- value
Genetic background 1	Genetic background 3	4.332 (1.674, 11.212)	<0.05*
Genetic background 1	Genetic background 5	3.617 (0.974, 13.435)	0.05
Genetic background 3	Genetic background 5	0.835 (0.293, 2.377)	0.73
Class 1	Class 2	Odds ratio (95% Confidence interval)	P- value
WUR 0	WUR 1	1.330 (0.733, 2.413)	0.35
WUR 0	WUR 2	1.837 (0.711, 4.747)	0.21
WUR 1	WUR 2	1.382 (0.526, 3.631)	0.51
WUR 0	WUR Y	1.424 (0.813, 2.494)	0.22

Table 4.12 Odds ratios for the breadth of cytokine response. Odds ratios indicated the effect of the breadth of cytokine response from individuals from Class 1 relative to that from individuals from the Class 2. Breadth of cytokine response was classified as narrow response (cytokine class 6-7) or broad response (cytokine class 3-5). *statistical significance at the 95% significance level ($p<0.05$). WUR Y refers to the pooled WUR 1 and 2 genotypes.

4.2.4 Associations between viraemia and cytokine responses

Correlations between the strength of the cytokine response (AAUC) and infection severity (AUC of viraemia curve) were generally weak, indicating that pigs with overall higher viral load did not elicit a stronger cytokine response (Table 4.13). The strongest statistically significant correlations (at the 95% significance level) were between AUC of viraemia and INFA between 0-21dpi ($r = 0.23$), and between the AUC of viraemia with IFNA and CCL2 between 0-4dpi ($r = 0.16$ and 0.19), respectively. The results indicate that the association between cytokine and viraemia response is stronger at the early stage of infection.

	I4	I21	I35
IL-4 ¹	-0.01	0.03	-0.01
IL-8 ¹	0.04	0.09	0.06
IL-10 ¹	-0.03	0.05	-0.02
IL-12 ¹	0.03	0.04	0.001
IL-1b ²	-0.04	0.04	-0.03
IL-8 ²	0.04	0.09	0.06
IFNA ³	0.16*	0.23*	0.09
CCL2 ²	0.19*	0.05	0.03

Table 4.13 Pearson correlations of pairwise cytokine AAUC and viraemia AUC at 4, 21 and 35dpi (denoted as I4, I21 and I35, respectively). Superscripts refer to ¹immune regulatory cytokines, ²pro-inflammatory cytokines and ³ antiviral cytokine is in red.*indicates statistical significance at the 95% significance level ($p < 0.05$).

Associations between cytokine response and resolution of infection

Rebounders were removed from the analysis to determine if a stronger cytokine response was associated with the faster resolution of infection. The results of fitting a mixed model with the Wood's parameter C1 as the response variable and the AAUCs for different cytokines as potential predictors are shown in Table 4.14. In the null model the random effect of pen within genetic background was significant and the viral profile class was the only significant fixed effect. The strongest associations were found using the cytokine AAUCs at 28dpi.

Response	Significant predictors (f-test p<0.05)	AIC difference (AIC_{null}-AIC_{final})	R squared	R squared difference (R²_{final}-R²_{null})	-2 Log likelihood final model	-2 Log likelihood null model
C1	AA_IL10_28 AA_IL12_28 AA_IL1b_28 Viral class	32.7	0.55	0.04	-920.1	-949.8

Table 4.14 Goodness of fit statistics for the final mixed model exploring the association between cytokine measures and the rate of post viraemia peak decline captured by the Woods parameter C1. The strength of the cytokine responses i.e. the AAUCs of IL-10, IL-12 and IL-1b were potential predictors in the final model. * indicates significance of the LRT between the final model and the null model at the 95% significance level.

However, the final model for the Wood's parameter C1 that included cytokine measures as predictors was not a statistically significant improvement at the 95% significance level to the null model without cytokine measures as shown in Table 4.14.

Cytokine characteristics as predictors of the viraemia curve characteristics

In the null models pen within trial was only a significant random effect for V4 and Vmax. The fixed effects of parity, viral class, WUR, genetic background and age were significant dependent on the response variable as outlined in Table 4.15. As expected, IFNA and CCL2 were the two key cytokines associated with the viraemia traits. Interactions between the cytokine measures and the responder classification in that class were not significant. Genetic background had a significant effect on the models. Interactions between WUR and the cytokine predictors were not significant. The genetic background interaction was only significant for IFNA at 4dpi in the model for viraemia at 4dpi (V4), as shown in Table 4.16. The viraemia class interaction was only significant on the IFNA for viraemia at 42dpi.

The mixed models of best fit to the data for the viraemia predictions are presented in Table 4.15. Overall the inclusion of cytokine measures as predictors for viraemia at a specific time point or over a given time period improved the model fit, as confirmed by reduction of the AIC value, improved log-likelihoods and increase in the R² values. Including cytokine predictors significantly improved the models according to the LRT for all the viraemia traits listed in Table 4.15, except for V42 which had a p value of 0.054.

Response	Significant predictors (f-test)	AIC difference (AIC_{null}- AIC_{final})	R squared	R squared difference (R^2_{final}- R^2_{null})	-2 Log likelihood final model	-2 Log likelihood null model
V4	IFNA_4 IFNA_4*Genetic background d_IL10_0_4 d_CCL2_0_4 Parity Viral Class Age	36	0.47	0.13	271.9*	303.0
V21	IFNA_10 CCL2_10 WUR Parity Viral class	44.4	0.60	0.10	370.0*	414.4
V42	d_IFNA_7_10 d_IFNA_7_10*Viral class Viral class	6.6	0.39	0.02	371.0	383.3
I4	L_IFNA_4 Parity Viral class	30.8	0.45	0.08	1073.5	1104.3
I21	L_IFNA_10 WUR Genetic background Viral class Age	45.4	0.62	0.08	1398.2*	1443.6
I42	L_IFNA_10 L_IFNA_21 L_CCL2_21 WUR Genetic background, Parity, Viral class, Age	54.6	0.71	0.07	1710.8*	1765.6
Tmax	L_IL8_0 L_IFNA_4 L_IFNA_10 L_CCL2_4 L_CCL2_7 Genetic background Parity	63.9	0.35	0.21	731*	794.9

Vmax	L_IFNA_0 L_IFNA_4 L_IFNA_10 WUR Genetic background Age	12.9	0.40	0.07	139.6	150.3
DeltaT	L_IFNA_4 L_IFNA_10 Parity Viral Class	35	0.39	0.11	952.2*	989.7

Table 4.15 The final mixed models when the viraemia traits were the response variables and the cytokines were the potential predictors. There were no significant cytokine predictors for the viraemia trait DeltaV (the value of viraemia at the maximal rate of decline defined in Table 4.15).* indicates significance of the LRT between the final model and the null model at the 95% significance level.

IFNA was consistently a key cytokine associated with the viraemia characteristics. CCL2 was also a significant predictor, and the baseline expression of IL-8 was associated with the time of the peak viraemia. The predictive power of cytokine measures for viraemia levels declined over time, suggesting that the variation we observe in viraemia resolution is not captured through the observed serum cytokines. The value of the peak viraemia was associated with early IFNA observations. Although the effects are significant the improvement to the R^2 values are relatively small. Interactions between the viraemia predictors and the WUR or genetic background were not significant.

When cytokines were assumed as response variables and viraemia traits the potential predictors in the mixed models there was no significant association with the viraemia traits for the majority of cytokines, i.e. IL-8, IL-10, IL-1b or CCL2. For IL-4 one significant association with viraemia was found, but the relationship was very weak with only 6% of total variance explained by all predictors together (Table 4.16). In contrast, for IFNA estimates within the first 2 weeks of infection, several significant viral predictors were found, all of which are shown in Table 4.16. Genetic background and parity are consistently significant effects in the final models.

Response	Significant predictors (F-test)	AIC difference ($AIC_{null} - AIC_{final}$)	R squared	R squared difference ($R^2_{final} - R^2_{null}$)	-2 Log likelihood final model	-2 Log likelihood null model
IL4_35	V28 Genetic background	0.1	0.06	0.02	330.6	330.7
IFNA_4	V4 Genetic	30.1	0.24	0.12	328.2*	358.7
IFNA_10	V4, I4, V7, I7 Genetic background, Parity Viral class	28.4	0.37	0.12	311.4*	313.4
IFNA_14	I4, V7, I7, Genetic background, Parity	20.3	0.41	0.09	336.7*	338.7

Table 4.16 The final mixed models when cytokines were the response variables and the viraemia traits were the potential predictors. * indicates significance of the LRT between the final model and the null model at the 95% significance level. Where Vx and Ix refer to the Woods viraemia predictions and AUC at x dpi as defined in Table 4.2.

4.3 Discussion

Typically PRRSV elicits weak innate and adaptive immune responses, is associated with immune modulation, but induces a strong immunosuppressive response, resulting in delayed onset of a Th1 immune response [11,31,34,44]. Out of the seven measured serum cytokines in this study, strongest responses following PRRSV infection were observed in the pro-inflammatory cytokine CCL2 and the antiviral cytokine IFNA. Inter-host variation was observed in the cytokine responsiveness across the measured cytokines in this study and the nAb cross-protectivity. Viraemia profile class differences were captured in the breadth of the cytokine responsiveness across the measured cytokines.

Rebounders had a significantly narrower cytokine response than non-rebounders. Genetic background differences had a significant impact upon cytokine responsiveness with genetic background 1 having a broader response than genetic background 3. Furthermore it was found that pigs varied in the breadth of their nAb cross-protection from exhibiting no neutralising response to exhibiting a nAb response against four different PRRSV isolates. Viraemia profile class was also captured in the breadth of the nAb cross-protectivity. Viraemia clearance profiles corresponded to a less diverse nAb response than persistence and pigs with persistent viraemia had a more diverse nAb response than those with rebound profiles. These results suggest that a slower clearance rate of viraemia in the persistent profiles is associated with a more diverse nAb response; this does not hold true for viraemia rebound. The WUR genotype did not have any significant association with the nAb cross-protectivity or cytokine responsiveness. It is thus likely that host genes other than WUR are likely to capture the host genetic contribution to nAb cross-protectivity and cytokine responsiveness. Furthermore it has been proposed that many immune competence parameters including in-vitro innate cytokines, adaptive cytokines and the host's IgG response, could be under genetic control and that there may be scope for them to be included in future the selection protocols [45-48]. Thus the statistical categorization of the nAb cross-protectivity and cytokine responsiveness defined in this chapter could be of potential use in future studies in the development of an immune competent pig which is discussed further in the General Discussion chapter of this thesis.

Associations between cytokine response and viraemia characteristics were significant but only moderately strong, thus highlighting the complexity of the immune response. IFNA and CCL2 profiles showed systematic time trends, with the general trend for IFNA represented by an increase to a peak around 4dpi followed by decline to baseline levels by 14dpi, whilst the dynamics of CCL2 was typically slower i.e. with a gradual increase to peak expression by 10dpi followed by gradual decline in expression. Previous studies have already established the antiviral role of IFNA and its association with viraemia clearance [49-51], however the role of CCL2 during a PRRSV infection has not yet been fully determined. However in this chapter it was found that, CCL2 and IFNA were strongly associated with each other in two regards, firstly there were high correlations in the strength of the

responses at 14 and 35dpi (AAUC) and secondly their measures were consistently statistically significant predictors of each other throughout the entire duration of the experiment. IFNA was a marginally better predictor for CCL2 than the reverse relationship. This is a novel finding and indicates that CCL2 may play a key role during a PRRSV infection. However the relationships among the other cytokines were neither as strong nor as consistent across the full profiles. It is important to note however that the lack of observing elevated expressions the majority of the cytokines in this study, may be a result of the time intervals between observations (4-7 days) being too large to capture the rapid immune dynamics following infection.

Of the list of potential fixed effects, the genetic background had the largest impact on cytokine expression profiles, with differences being observed at various phases of the infection profile depending on the cytokine; typically, the strongest impact was between 4-14dpi. Genetic backgrounds differed in the baseline levels of cytokine expression and also the overall magnitudes of expression, in particular for IFNA and CCL2. Response patterns for the time-trends of the LSM estimates were overall similar across the different genetic backgrounds, although some slight differences in the overall trends were observed for some cytokines. For example, pigs from genetic background 3 had a tendency to decrease from baseline expression in IL-1b (by $\sim 0.7 \log_{10}$ units) whilst pigs from genetic background 1 saw a general trend of increase from the baseline IL-1b levels (by $\sim 0.7 \log_{10}$ units). Furthermore expression in IL-10 and IL-12 in genetic backgrounds 1 and 5 remained overall closer to baseline levels compared to the corresponding decreasing levels observed in genetic background 3 (by $\sim 0.7 \log_{10}$ units and $\sim 1 \log_{10}$ units respectively).

The WUR “resistance” genotype (WUR 1 and 2) previously found to correspond to lower cumulative viraemia (viraemia AUC 0-21dpi) [3,4,7,42] had minimal impact on the cytokine expression profiles throughout the infection duration (0-42dpi) for the majority of cytokines in this study. However the WUR genotype differences were captured in IL-12 during the primary phase of infection, i.e. from 0-21dpi, with low expression in WUR 2 and high expression in WUR 1 genotypes, and in the antiviral cytokine IFNA resulting in a higher peak expression at 4dpi for WUR 2. Given the impact the genotype has on the viraemia it is surprising that these differences between WUR 0 and WUR 1 and 2 were not reflected in the longitudinal cytokine expression profiles.

Viral profile class differences were captured in the pro-inflammatory cytokines IL-8, CCL2, and the antiviral cytokine IFNA. Rebounder pigs elicited overall a stronger response in most of the cytokines at the later stages of infection (from 28dpi onwards) than non-rebounders, although the differences were not always statistically significant. “Rebounding” i.e. increased expression of CCL2 at 28dpi, IFNA at 28-35dpi and IL-8 at 35dpi was observed for the viraemia rebound pigs (with rebound in viraemia typically occurring between 21-42dpi see Chapter 3 for further details). However differences in cytokine expression between pigs with cleared and persistent viraemia profiles were small and not

statistically significant at all stages of the infection.

Consistent with the longitudinal expression profiles, IFNA and CCL2 were the two key cytokines significantly associated with the viraemia traits in the multiple regression models. Inclusion of cytokine measures as predictors for viraemia significantly improved the null models capturing differences in pig genetic make-up and the experimental setup across the full time course of the infection (0-42dpi). The predictive power of cytokine measures for viraemia levels increased over time, suggesting that the variation we observe in viraemia resolution could be partly captured through the observed serum cytokines. The value of the peak viraemia was associated with early IFNA observations accounting for approximately 40% of the variation. The rate of viraemia decline was best captured in the strength of the expression of the immune regulatory cytokines IL-10 and IL-12 and the pro-inflammatory cytokine IL-1b, however the final model was not a significant improvement on the null model. Conversely, the viraemia measures emerged generally as poor predictors for the majority of the cytokines in the study across the full time course of the experiment (0-42dpi). One significant association between IL-4 and viraemia was found, but the relationship was very weak with only 6% of total variance explained by all predictors in the final model. With the exception of a weak relationship between IL-4 and viral predictors, viral predictors with significant influence on cytokine expression were only found for IFNA estimates within the first 2 weeks of infection. The results reflect that pro-inflammatory and immune-regulatory cytokines are only indirectly related.

Cytokine response can be very transient [36], thus a 4-7 day window may not capture sharp responses. Cytokines and virus in serum are a 'spill-over' from those in the infection target site. This, together with the fact that some cytokines are locally produced may weaken the strength of the true associations between cytokine and viraemia that would be found directly at the site of infection. In addition to viraemia and other known factors of influence, parity surprisingly emerged as a significant predictor in the multiple regression models for cytokine response in this chapter, however this was not the case for the viraemia profiles in Chapter 2. One potential explanation for this could be due to the immune response of sows changing between parities which would influence our results in the resulting infected piglets from different parities due to the presence of maternal antibodies in the piglets. Cytokine responses to PRRSV have been explored extensively in previous studies both *in vitro* and *in vivo* for numerous PRRSV strains[10-14,16,52]; however there are often fewer numbers of repeated measures from 0-42dpi than in the present study and hence the associations between serum cytokine expression and serum viraemia trends such as viraemia rebound have not been previously studied.

It is known that the pro-inflammatory innate cytokine IL-8 is released by the macrophages that first encounter pathogens and recruits neutrophils, which enter the infected tissue in large numbers in the

early stage of the induced response. Their influx usually peaks within the first six hours of an inflammatory response [53]. For PRRSV infection, large inter-host variation in the ability to synthesise IL-8 has been reported, where strong IL-8 synthesis has been associated with high host resistance to PRRSV [20]. In an *in vivo* PRRSV study involving two different breed crosses (NE Index line and a Hampshire-Duroc crossbreed pigs) than those used in the current PHGC trials, pigs were categorized into high or low disease burden [54]. High viraemia levels were associated with high IL-8 expression in the lung particularly prior to the peak viraemia [54]. In our study breed differences were also observed in IL-8 expression, however IL-8 was more strongly associated with the later dynamics of the viraemia profile in our study. An elevated response at 35dpi in serum IL-8 was observed for the viraemia rebound pigs in our study when compared to the cleared pigs at this time (35dpi). Furthermore in an *in vivo* study investigating the cytokines associated with viral persistence of a different North American strain (VR-2332) found that persistent pigs had a lower concentration of IL-8 than non-persistent pigs at 14dpi and that IL-8 levels were generally up-regulated early after infection with the earliest serum measurement taken at 7dpi [16]. However, a study using the same North American strain as in this thesis (NVSL) found that IL-8 levels remained high and largely unaffected by the presence of the virus [12]. In the present study we found that the IL-8 cytokine profiles of PRRSV infected piglets were generally flat with differences in expression levels of less than 1 log unit. However, the lack of capturing elevated expressions in this cytokine, may be a result of the time intervals between observations (4-7 days) being too large to capture the rapid immune dynamics, with the possible peak within 6 hours of infection [53].

IFNA was consistently a significant predictor for viraemia characteristics, which is unsurprising due to its already established antiviral role and association with viraemia clearance [49-51]. Previous studies differ in the nature and magnitude of the IFNA response following a PRRSV infection, with the more widely reported lack of significant and low IFNA response compared to other infections [9,19,25,51], contrasted with reported increases in serum IFNA levels following PRRSV infection [12,27,55], which is in line with our results. In a previous *in vitro* study it was demonstrated that North American PRRS viruses can inhibit the production of type 1 interferon in plasmacytoid dendritic cells, which are sources of IFNA [24,56]. This *in vitro* result could potentially reflect an absence of triggering one or more pathways leading to cytokine production and cell maturation *in vivo*. Conversely it has been demonstrated that some PRRSV strains (including north American strains: VR-2332, SS144, MN184, JA-1262 and the highly pathogenic field isolate from China SY060) induced IFNA secretion by plasmacytoid dendritic cells with little or no down-regulation of IFNA production [57]. There is evidence for strain differences in the *in-vitro* IFNA levels of suppression following infection. The highly pathogenic Chinese type 2 isolate SY0608 had a 52% inhibitory effect, the type 2 isolate VR-2332 inhibited by 34% and the highly virulent type 2 isolates SS144, MN184 and JA-1262, showed lower levels or no inhibitory activity in the *in vitro* study after

20 hours pi [57]. Furthermore a recent *in vivo* study of the cytokine expression profiles from NVSL infected pregnant gilts, with observations taken at 2, 6 and 19dpi only, found a strong expression of serum IFNA following infection at 2dpi which could corroborate our finding of increased expression of serum IFNA at 4dpi in our study [12]. Given the evidence for strain dependent IFNA suppression we could thus hypothesise that NVSL is in line with the other the highly virulent type 2 isolates SS144, MN184 and JA-1262 in the low level of IFNA suppression. Furthermore the genetic background had a significant effect on IFNA profiles. Indeed IFNA expression was breed dependent resulting in either increased or no change in expression from uninfected pigs in the *in vivo* study by Petry et al [54]. The dynamics of serum CCL2 reflected slower dynamics than the IFNA profiles. However unlike IFNA, the dynamics or role of the cytokine CCL2 in PRRSV infections has not been determined in previous studies.

It is difficult to compare the full time trends observed in the present study to other PRRS studies due to the novelty of the several repeated measures taken across the 42day observation period, however the changes in serum cytokine expression measured at 6 and 19dpi in a companion study on NVSL infected pregnant gilts are similar to the 7dpi and 21dpi measures in our study across all seven serum cytokines [12]. However the latter study showed trends of lower levels of expression than baseline levels at 2dpi for IL-8, IL-10, IL-1b and IL-12, which was not captured in our study at 4dpi.

In this chapter, the strength of IL-10, IL-12 and IL-1b expression (i.e. area under the cytokines profiles from 0-28dpi with the baseline removed) was positively associated with a faster resolution of infection. High serum levels of the pro-inflammatory innate cytokine IL-1b at 14dpi have been previously linked to pigs classed as persistently infected following PRRSV infection with a different type 2 PRRSV strain [16]. In previous studies IL-12 positive cells have been detected in the lung as early as 1 day post infection (dpi) [58]. Furthermore treatment with IL-12 during an infection with type 2 PRRSV isolate NADC-8 led to reduced viraemia *in vivo* [59]. In this Chapter the IL-10 expression due to infection was relatively weak, without significant up-regulation from the baseline levels of expression (i.e. expression at 0dpi). In the PRRSV literature however there are conflicting reports in the literature on whether PRRSV infection elicits an up-regulation of IL-10 expression or not. Up-regulation of IL-10 has been found in the lung for a type 1 PRRSV infection [10], following *in vitro* infection with various type 2 PRRSV strains [10,44,60,61]. Increased IL-10 expression following PRRSV infection can reduce the expression of cytokines involved in viral clearance i.e. IFNA, TNFA, IL-12, and IFN-gamma [10]. Conversely no significant IL-10 response was observed for different type 2 PRRSV strains SD-23983 and VR-2385 [62,63].

In many species IL-4 is a cytokine of the adaptive immune response with the principle cellular sources from CD4⁺ T cells and mast cells, targeting B cells (causing isotype switching), T cells (causing differentiation and proliferation), and Mast cells (causing proliferation)[64]. However the role of IL-4 is species dependent and in swine IL-4 is not a stimulatory factor for porcine B cells, instead it blocks antibody and IL-6 secretion and suppresses the antigen-stimulated proliferation of B cells [52]. Following a PRRSV infection IL-4 is up-regulated and appears to have some immunomodulatory consequences [27]. One study reports that swine IL-4 markedly enhanced the protective immune response of pigs and improved the efficacy of a modified live vaccine in preventing PRRS disease and resulted in a higher antibody titre, higher sera neutralizing efficacy, higher ratio of CD3⁺CD4⁺/CD3⁺CD8⁺ T lymphocytes, and lower virus loads in peripheral blood [65]. The expression profiles of IL-4 were the least affected by PRRSV infection in our study. Following *in vivo* PRRSV infection serum IL-4 was up-regulated at 2dpi (increased by ~90%) in a previous study under farm conditions [27], which was not captured at 4dpi in our study. In future studies it would be informative to include a smaller sampling interval in order to capture the rapid dynamics of IL-4 expression.

There are other cytokines known to play a role in PRRSV infection that were not measured in the current study. For example, IFN-gamma has been found to be up-regulated following infection with NVSL, and other type 2 PRRSV strains and is associated with viral clearance [16,66-68]. Serum IL-6 expression was also not measured in this study however previous studies have found that pigs with high viraemia pigs from 0-14dpi (PRRSV strain 97-7985 infection) had on average higher IL-6 expression [54].

It is difficult to fully disentangle the cause and effect in the associations between the various viraemia and immune components, as biologically both types of measures are likely to effect each other with possible “predator-prey” type dynamics between the virus and the cytokines or the immune processes in which they are involved. For example before the PRRSV challenge one could potentially assume that the serum cytokines levels remain at the baseline in the absence of PRRSV infection. Thus we could view the early serum cytokine response following infection as being driven by the virus and an indication of the host mounting an immune response against the virus. However these elevated cytokines may then in turn drive the viraemia i.e. the viraemia clearance dynamics through the signalling and triggering of immune processes that reduce the infectivity of target cells or reduce the virus replication rate etc., and thus resulting in reduced viral loads. These reduced viraemia levels could in turn drive reduced expression of serum cytokines. Fast return of cytokine levels towards baseline levels could potentially provide low defence against the remaining or a mutated virus strain, thus allowing viral rebound to occur. The viraemia rebound then drives the cytokine dynamics as before thus explaining the elevated IL-8, IFNA and CCL2 observed during the rebound stage of infection. However in the multiple regression approach a stronger association was found when

preceding cytokines were predictors for viraemia characteristics at subsequent time points as opposed to *vice versa* which suggests that the cytokines are driving the viraemia dynamics rather than the other way round.

In Chapter 3 the analysis of the nAbs of NVSL infected pigs in collected at 42dpi indicated that there was a strong homologous response to the PRRSV challenge, in agreement with observations from previous studies [69,70]. We were unable to test the impact of the genetic background on the nAb cross-protection since the data on nAb were from pigs of the same genetic background. The WUR genotype had no significant impact upon the nAb cross-protection (Appendix 2b), different host genes are likely to capture the differences in nAb cross-protectivity. A statistical association between viraemia characteristics and nAb cross-protectivity was identified in Chapter 3, which may point to the host-pathogen interactions underlying the observed viraemia and antibody patterns. Both virus persistence within the host and cross-protection of host antibodies have been previously linked to virus mutation and emergence of quasi-species [9, 38]. It should be noted, however, that the observed associations between the nAb response and viraemia patterns may equally arise from confounding immune quantities affecting both nAb and viraemia, such as immune-regulatory or anti-viral cytokines which have been measured in this chapter. Indeed, several alternative hypotheses, not necessarily involving virus mutation, emerge as potential causes for viraemia rebound based on our findings. For example viraemia rebound may correspond to the second cycle of an oscillating viraemia profile which may arise naturally (and in the absence of virus mutation) from predator-prey type interactions between the virus and the immune response [71,72]. The majority of the serum cytokine expression profiles in this chapter do not support this hypothesis, however the statistically significant elevated expression of IL-8, IFNA and CCL2 coinciding with viraemia rebound, which could potentially reflect the hypothesised oscillating behaviour arising from dynamic interactions between the virus and immune response. Alternatively, rebound could arise from the heterogeneity of the virus distribution in various tissues within the host. Previous studies have observed that although viraemia may be below detection in the serum, persistent infection in the tonsils and lymphoid tissues can last for longer than 6 months [73]. Thus, the site of replication may be hidden from the serum and the infection may remain localised in certain tissues. Rebound may be a manifestation of the virus from these localised tissue infections being poured back into the system; thus becoming detectable in the serum. The influx of virus into the serum may occur in occasional bursts or as a final out-pouring into the serum determined by some environmental stimulus, immune response mechanism, or stochastic process. If this were the case we could expect this to be reflected in cytokine profiles related to viral clearance or load potentially in the form of bimodal cytokine profiles. The result that IFNA and CCL2 were statistically significantly higher for the rebound class at the later phase of infection could potentially support this hypothesis. Furthermore the viraemia rebound peak is often smaller than the first viraemia peak, due to the initial PRRSV challenge, which may explain why the

increased rebound expression of IL-8, CCL2 and IFNA is relatively small. Virus rebound manifesting itself in biphasic viraemia profiles is a common phenomenon in equine influenza infections, the causative processes of which remain a mystery [74]. Additional information about virus heterogeneity and/or nAb characteristics at different stages post infection would be needed to assess these hypotheses.

Similar arguments may be used to interpret the observed high inter-host variation in viraemia decline post the initial viraemia peak. Variation in the rate of viraemia reduction may be a function of the host's own immune response, virus mutation mechanisms or the interaction between both processes.

In Chapter 3 the moderate negative correlation between the NVSL Wood's parameters c_1 and c_2 (-0.52) indicates that a slow decline in the first cycle corresponds to faster decline in the second cycle and vice versa. This association may be indicative of the temporal evolution of the immune response. Furthermore viraemia rebound profiles are associated with high levels of CCL2 during the secondary phase of infection, which is interesting from a biological perspective since the role of CCL2 is thought to be that of causing an influx of macrophages to the site of infection [53]. A potential hypothesis that emerges from the present study is that the increase in CCL2 could result in an influx of new PRRSV target cells thus driving the rebound in viraemia that we observe [75,76]. Furthermore, rebound pigs had a statistically significantly higher expression of IL-8 at 35dpi than cleared profiles, with an increase of 0.16 units on the \log_{10} scale. This statistically significant rebound in IL-8 may support the hypothesis that rebound could be caused by a reinfection or could be an indication that higher viraemia levels at this stage of the infection result in higher IL-8 expression, ultimately it is difficult to disentangle the cause and effect. However the associations between IL-8 and viraemia levels were weak during the early phase of infection when the initial viraemia peak is observed; furthermore persistent pigs did not have significantly higher IL-8 expression than cleared pigs at 35 or 42dpi.

If viral rebound was due to immune escape by the virus, which is recognized as re-exposure to the virus by the host then we could hypothesize that rebound pigs would have a greater memory B cell activity of memory B cells resulting in a higher level of antibody than non-rebound [77]. Alternatively, high antibody levels could place selective pressure on the virus which could manifest in an increased likelihood of viral rebound occurring [78-82]. Longitudinal antibody response measures would thus be needed to test these hypotheses and further determine the relationships between viraemia profiles and the antibody response.

Virulent field PRRSV isolates exhibit longer and more elevated viraemia profiles and can induce a faster and more intense humoral response [83]. In the study by Johnson et al [83] highly virulent PRRSV field isolates replicated to a substantially higher *in vivo* titres than attenuated or lower virulent isolates. N-protein antibody responses were higher in pigs infected with more virulent isolates, as were their viraemia measures. The antibody trends were similar between the isolates but differed in

magnitude; thus providing evidence for a strong association between the humoral response and the serum viraemia load. The magnitude of the immune response could be related to the virulence and *in-vivo* replication rate of the PRRSV strain. Antibody differences could be a reflection of the genetic differences between the PRRSV isolates. It would be interesting to compare the nAb responses between the NVSL and KS06 isolates in the PHGC dataset. Given the trends observed by Johnson et al [83] we could expect to observe a less dominant humoral response in the KS06 infected pigs. However it is important to note that even without the development of nAbs viraemia resolution can be occur in a PRRSV infection [19,21,84]. However during a PRRSV infection the levels of nAbs typically remain low, when compared to other respiratory infections. Hence a strong but inefficient antibody response could be responsible for persistent viraemia profiles, i.e. a longer infection duration[32], which was confirmed by the result of the odds ratios of nAb cross protection and viraemia class. Understanding the host's ability to mount a non-neutralizing PRRSV-specific antibody response could lead to deeper insights related to the non-isolate specific host-response to PRRSV infection. Whilst studying the breadth of the nAb cross-protection could lead to the identification of pigs with desirable immune response traits, particularly for pigs under field conditions where multiple PRRSV strains could be in simultaneous circulation [85].

Suppression of the innate system during a PRRSV infection could be responsible for the persistent or prolonged viraemia profiles. It has been reported that PRRSV can suppress phagocytosing activity and the expression of innate cytokines, and alter the expression patterns of the latter [19,22]. However we found that there were no marked differences between the cytokine expression profiles between persistent and cleared profile; similar cytokine expression led to different trends in viraemia profiles and infection duration.

In conclusion, the associations between viraemia and cytokine indicate that cytokines drive the viraemia profiles from 4dpi onwards. Associations between IFNA, CCL2 and the viraemia profiles were the most consistently significant, with the viraemia rebound trends being captured in these cytokines; however, the cause and effect remains hard to disentangle due to the dynamic nature of the virus and the immune response interactions. Associations between serum cytokines and viraemia rebound could point towards understanding the mechanisms surrounding the variation in viral profiles. The “rebound” in CCL2 could be a driving force in the recruitment of new target cells at the site of infection, whilst the “rebound “ in IFNA could be a consequence of the elevated viraemia levels due to rebound. Future studies are needed to fully determine the underlying factors driving the cytokine or nAb response, the role of CCL2 during infection, and the host genetics association with the nAb response in order to derive vaccine-ready pigs capable of mounting successful responses against a variety of currently circulating PRRSV strains. It would be interesting to assess the relationship between the nAbs and the cytokines to determine whether the strength of cytokine

response and nAb cross-protectivity were related. However the current data on the nAb and cytokine does not overlap and thus we are unable to assess their relationship in the current study.

References for Chapter 4

1. Islam ZU, Bishop SC, Savill NJ, Rowland RR, Lunney JK, et al. (2013) Quantitative Analysis of Porcine Reproductive and Respiratory Syndrome (PRRS) Viremia Profiles from Experimental Infection: A Statistical Modelling Approach. *PloS one* 8: e83567.
2. Boddicker N, Waide EH, Rowland RRR, Lunney JK, Garrick DJ, et al. (2012) Evidence for a major QTL associated with host response to Porcine Reproductive and Respiratory Syndrome Virus challenge. *Journal of Animal Science* 90: 1733-1746.
3. Boddicker NJ, Bjorkquist A, Rowland RRR, Lunney JK, Reecy JM, et al. (2014) Genome-wide association and genomic prediction for host response to porcine reproductive and respiratory syndrome virus infection. *Genetics Selection Evolution* 46.
4. Boddicker NJ, Garrick DJ, Rowland RRR, Lunney JK, Reecy JM, et al. (2014) Validation and further characterization of a major quantitative trait locus associated with host response to experimental infection with porcine reproductive and respiratory syndrome virus. *Animal Genetics* 45: 48-58.
5. Kim J, Ahn H, Woo H-M, Lee E, Lee G-S (2014) Characterization of porcine NLRP3 inflammasome activation and its upstream mechanism. *Veterinary research communications* 38: 193-200.
6. Shenoy AR, Wellington DA, Kumar P, Kassa H, Booth CJ, et al. (2012) GBP5 Promotes NLRP3 Inflammasome Assembly and Immunity in Mammals. *Science* 336: 481-485.
7. Boddicker N, Waide E, Rowland R, Lunney J, Garrick D, et al. (2012) Evidence for a major QTL associated with host response to Porcine Reproductive and Respiratory Syndrome virus challenge. *Journal of Animal Science* 90: 1733-1746.
8. Lunney JK, Fang Y, Ladinig A, Chen N, Li Y, et al. (2015) Porcine Reproductive and Respiratory Syndrome Virus (PRRSV): Pathogenesis and Interaction with the Immune System. *Annual review of animal biosciences* 4 (2016): : 129-154.
9. Gómez-Laguna J, Salguero FJ, De Marco MF, Pallarés FJ, Bernabé A, et al. (2009) Changes in lymphocyte subsets and cytokines during European porcine reproductive and respiratory syndrome: increased expression of IL-12 and IL-10 and proliferation of CD4⁺ CD8^{high}. *Viral immunology* 22: 261-271.
10. Gomez-Laguna J, Salguero F, Barranco I, Pallares F, Rodriguez-Gomez I, et al. (2010) Cytokine expression by macrophages in the lung of pigs infected with the porcine reproductive and respiratory syndrome virus. *Journal of comparative pathology* 142: 51-60.
11. Johnsen C, Bøtner A, Kamstrup S, Lind P, Nielsen J (2002) Cytokine mRNA profiles in bronchoalveolar cells of piglets experimentally infected in utero with porcine reproductive and respiratory syndrome virus: association of sustained expression of IFN- γ and IL-10 after viral clearance. *Viral immunology* 15: 549-556.
12. Ladinig A, Lunney JK, Souza CJ, Ashley C, Plastow G, et al. (2014) Cytokine profiles in pregnant gilts experimentally infected with porcine reproductive and respiratory syndrome virus and relationships with viral load and fetal outcome. *Veterinary research* 45: 113.
13. Van Reeth K, Labarque G, Nauwynck H, Pensaert M (1999) Differential production of proinflammatory cytokines in the pig lung during different respiratory virus infections: correlations with pathogenicity. *Research in veterinary science* 67: 47-52.
14. Thanawongnuwech R, Thacker B, Halbur P, Thacker EL (2004) Increased production of proinflammatory cytokines following infection with porcine reproductive and respiratory syndrome virus and *Mycoplasma hyopneumoniae*. *Clinical and diagnostic laboratory immunology* 11: 901-908.
15. Albina E, Carrat C, Charley B (1998) Short Communication: Interferon- α Response to Swine Arterivirus (PoAV), the Porcine Reproductive and Respiratory Syndrome Virus. *Journal of interferon & cytokine research* 18: 485-490.
16. Lunney JK, Fritz ER, Reecy JM, Kuhar D, Prucnal E, et al. (2010) Interleukin-8, interleukin-1 β , and interferon- γ levels are linked to PRRS virus clearance. *Viral immunology* 23: 127-134.

17. Li X, Galliher-Beckley A, Pappan L, Tribble B, Kerrigan M, et al. (2014) Comparison of host immune responses to homologous and heterologous type II porcine reproductive and respiratory syndrome virus (PRRSV) challenge in vaccinated and unvaccinated pigs. *BioMed research international* 2014.
18. Molitor T, Bautista E, Choi C (1997) Immunity to PRRSV: double-edged sword. *Veterinary microbiology* 55: 265-276.
19. Mateu E, Diaz I (2008) The challenge of PRRS immunology. *The Veterinary Journal* 177: 345-351.
20. Vincent A, Thacker B, Halbur P, Rothschild M, Thacker E (2005) In vitro susceptibility of macrophages to porcine reproductive and respiratory syndrome virus varies between genetically diverse lines of pigs. *Viral immunology* 18: 506-512.
21. Murtaugh MP, Genzow M (2011) Immunological solutions for treatment and prevention of porcine reproductive and respiratory syndrome (PRRS). *Vaccine* 29: 8192-8204.
22. Kimman TG, Cornelissen LA, Moormann RJ, Rebel JMJ, Stockhofe-Zurwieden N (2009) Challenges for porcine reproductive and respiratory syndrome virus (PRRSV) vaccinology. *Vaccine* 27: 3704-3718.
23. Gómez-Laguna J, Salguero FJ, Pallarés FJ, Carrasco L (2013) Immunopathogenesis of porcine reproductive and respiratory syndrome in the respiratory tract of pigs. *The Veterinary Journal* 195: 148-155.
24. Calzada-Nova G, Schnitzlein WM, Husmann RJ, Zuckermann FA (2011) North American porcine reproductive and respiratory syndrome viruses inhibit type I interferon production by plasmacytoid dendritic cells. *Journal of virology* 85: 2703-2713.
25. Lawson S, Lunney J, Zuckermann F, Osorio F, Nelson E, et al. (2010) Development of an 8-plex Luminex assay to detect swine cytokines for vaccine development: assessment of immunity after porcine reproductive and respiratory syndrome virus (PRRSV) vaccination. *Vaccine* 28: 5356-5364.
26. Lee S-M, Schommer SK, Kleiboeker SB (2004) Porcine reproductive and respiratory syndrome virus field isolates differ in in vitro interferon phenotypes. *Veterinary immunology and immunopathology* 102: 217-231.
27. Dwivedi V, Manickam C, Binjawadagi B, Linhares D, Murtaugh MP, et al. (2012) Evaluation of immune responses to porcine reproductive and respiratory syndrome virus in pigs during early stage of infection under farm conditions. *Virology journal* 9: 1.
28. Souza C, Choi I, Araujo K, Abrams S, Kerrigan M, et al. Comparative serum immune responses of pigs after a challenge with porcine reproductive and respiratory syndrome virus (PRRSV); 2013.
29. Darwich L, Gimeno M, Sibila M, Diaz I, De La Torre E, et al. (2011) Genetic and immunobiological diversities of porcine reproductive and respiratory syndrome genotype I strains. *Veterinary microbiology* 150: 49-62.
30. Yoon KJ, Zimmerman JJ, Swenson SL, McGinley MJ, Eernisse KA, et al. (1995) Characterization of the humoral immune response to porcine reproductive and respiratory syndrome (PRRS) virus infection. *Journal of Veterinary Diagnostic Investigation* 7: 305.
31. Diaz I, Darwich L, Pappaterra G, Pujols J, Mateu E (2005) Immune responses of pigs after experimental infection with a European strain of porcine reproductive and respiratory syndrome virus. *Journal of general virology* 86: 1943-1951.
32. Darwich L, Díaz I, Mateu E (2010) Certainties, doubts and hypotheses in porcine reproductive and respiratory syndrome virus immunobiology. *Virus Research* 154: 123-132.
33. Nguyen KB, Salazar-Mather TP, Dalod MY, Van Deusen JB, Wei X-q, et al. (2002) Coordinated and distinct roles for IFN- $\alpha\beta$, IL-12, and IL-15 regulation of NK cell responses to viral infection. *The Journal of Immunology* 169: 4279-4287.
34. Renukaradhya GJ, Alekseev K, Jung K, Fang Y, Saif LJ (2010) Porcine Reproductive and Respiratory Syndrome Virus–Induced Immunosuppression Exacerbates the Inflammatory Response to Porcine Respiratory Coronavirus in Pigs. *Viral immunology* 23: 457-466.

35. Dwivedi V, Manickam C, Patterson R, Dodson K, Weeman M, et al. (2011) Intranasal delivery of whole cell lysate of Mycobacterium tuberculosis induces protective immune responses to a modified live porcine reproductive and respiratory syndrome virus vaccine in pigs. *Vaccine* 29: 4067-4076.
36. Murtaugh MP, Xiao Z, Zuckermann F (2002) Immunological responses of swine to porcine reproductive and respiratory syndrome virus infection. *Viral immunology* 15: 533-547.
37. Rowland RR, Joan Lunney, and Jack Dekkers. (2012) Control of porcine reproductive and respiratory syndrome (PRRS) through genetic improvement in disease resistance and tolerance. *Frontiers of Livestock Genomics*: 3:260.
38. Lunney JK, Steibel JP, Reecy JM, Fritz E, Rothschild MF, et al. Probing genetic control of swine responses to PRRSV infection: current progress of the PRRS host genetics consortium; 2011. BioMed Central Ltd. pp. 30.
39. Fang Y, Schneider P, Zhang W, Faaberg K, Nelson E, et al. (2007) Diversity and evolution of a newly emerged North American Type 1 porcine arterivirus: analysis of isolates collected between 1999 and 2004. *Archives of virology* 152: 1009-1017.
40. Lunney JK, Chen H (2010) Genetic control of host resistance to porcine reproductive and respiratory syndrome virus (PRRSV) infection. *Virus Research* 154: 161-169.
41. Boddicker NJG, Dorian J.; Reecy, James M.; Rowland, Bob; Lunney, Joan K.; and Dekkers, Jack C. M. (2013) Quantitative Trait Locus on Sus scrofa Chromosome 4 Associated with Host Response to Experimental Infection with Porcine

Reproductive and Respiratory Syndrome Virus Animal Industry Report AS 659, ASL R2823.

42. Hess AS, Boddicker N, Rowland B, Lunney J, Plastow G, et al. (2014) Validation of the Effects of a SNP on SSC4 Associated with Viral Load and Weight Gain in Piglets Experimentally Infected with a 2006 PRRS Virus Isolate. *Animal Industry Report* 660: 89.
43. Guide MUs (1998) The mathworks. Inc, Natick, MA 5: 333.
44. Suradhat S, Thanawongnuwech R, Poovorawan Y (2003) Upregulation of IL-10 gene expression in porcine peripheral blood mononuclear cells by porcine reproductive and respiratory syndrome virus. *Journal of general virology* 84: 453-459.
45. Flori L, Gao Y, Oswald IP, Lefevre F, Bouffaud M, et al. Deciphering the genetic control of innate and adaptive immune responses in pig: a combined genetic and genomic study; 2011. BioMed Central. pp. S32.
46. Mach N, Gao Y, Lemonnier G, Lecardonnel J, Oswald IP, et al. (2013) The peripheral blood transcriptome reflects variations in immunity traits in swine: towards the identification of biomarkers. *BMC genomics* 14: 894.
47. Wang J, Wang Y, Wang H, Wang H, Liu J-F, et al. (2016) Transcriptomic Analysis Identifies Candidate Genes and Gene Sets Controlling the Response of Porcine Peripheral Blood Mononuclear Cells to Poly I: C Stimulation. *G3: Genes| Genomes| Genetics* 6: 1267-1275.
48. Niu P, Kim SW, Kim WI, Kim KS (2015) Association analyses of DNA polymorphisms in immune-related candidate genes GBP1, GBP2, CD163, and CD169 with porcine growth and meat quality traits. *Journal of Biomedical Research* 16: 40-46.
49. Royae AR, Husmann RJ, Dawson HD, Calzada-Nova G, Schnitzlein WM, et al. (2004) Deciphering the involvement of innate immune factors in the development of the host response to PRRSV vaccination. *Veterinary immunology and immunopathology* 102: 199-216.
50. Miller L, Laegreid W, Bono J, Chitko-McKown C, Fox J (2004) Interferon type I response in porcine reproductive and respiratory syndrome virus-infected MARC-145 cells. *Archives of virology* 149: 2453-2463.
51. Buddaert W, Van Reeth K, Pensaert M (1998) In vivo and in vitro interferon (IFN) studies with the porcine reproductive and respiratory syndrome virus (PRRSV). *Coronaviruses and Arteriviruses*: Springer. pp. 461-467.

52. Murtaugh MP, Johnson CR, Xiao Z, Scamurra RW, Zhou Y (2009) Species specialization in cytokine biology: Is interleukin-4 central to the T H 1–T H 2 paradigm in swine? *Developmental & Comparative Immunology* 33: 344-352.
53. Janeway C, Murphy KP, Travers P, Walport M (2008) *Janeway's immunobiology*: Garland Science.
54. Petry D, Lunney J, Boyd P, Kuhar D, Blankenship E, et al. (2007) Differential immunity in pigs with high and low responses to porcine reproductive and respiratory syndrome virus infection. *Journal of Animal Science* 85: 2075-2092.
55. Guo B, Lager KM, Henningson JN, Miller LC, Schlink SN, et al. (2013) Experimental infection of United States swine with a Chinese highly pathogenic strain of porcine reproductive and respiratory syndrome virus. *Virology* 435: 372-384.
56. Colonna M, Trinchieri G, Liu Y-J (2004) Plasmacytoid dendritic cells in immunity. *Nature immunology* 5: 1219-1226.
57. Baumann A, Mateu E, Murtaugh MP, Summerfield A (2013) Impact of genotype 1 and 2 of porcine reproductive and respiratory syndrome viruses on interferon-alpha responses by plasmacytoid dendritic cells. *Vet Res* 44: 1186.
58. Chung H-K, Chae C (2003) Expression of interleukin-10 and interleukin-12 in piglets experimentally infected with porcine reproductive and respiratory syndrome virus (PRRSV). *Journal of comparative pathology* 129: 205-212.
59. Carter QL, Curiel RE (2005) Interleukin-12 (IL-12) ameliorates the effects of porcine respiratory and reproductive syndrome virus (PRRSV) infection. *Veterinary immunology and immunopathology* 107: 105-118.
60. Song S, Bi J, Wang D, Fang L, Zhang L, et al. (2013) Porcine reproductive and respiratory syndrome virus infection activates IL-10 production through NF- κ B and p38 MAPK pathways in porcine alveolar macrophages. *Developmental & Comparative Immunology* 39: 265-272.
61. Flores-Mendoza L, Silva-Campa E, Reséndiz M, Osorio FA, Hernández J (2008) Porcine reproductive and respiratory syndrome virus infects mature porcine dendritic cells and up-regulates interleukin-10 production. *Clinical and Vaccine Immunology* 15: 720-725.
62. Wang X, Eaton M, Mayer M, Li H, He D, et al. (2007) Porcine reproductive and respiratory syndrome virus productively infects monocyte-derived dendritic cells and compromises their antigen-presenting ability. *Archives of virology* 152: 289-303.
63. Thanawongnuwech R, Young TF, Thacker BJ, Thacker EL (2001) Differential production of proinflammatory cytokines: in vitro PRRSV and *Mycoplasma hyopneumoniae* co-infection model. *Veterinary immunology and immunopathology* 79: 115-127.
64. Abbas AK, Lichtman AH, Pillai S (2014) *Cellular and Molecular Immunology: with STUDENT CONSULT Online Access*: Elsevier Health Sciences.
65. Peng J, Wang J, Wu J, Du Y, Li J, et al. (2013) Positive inductive effect of swine Interleukin-4 on immune responses elicited by modified live porcine reproductive and respiratory syndrome virus (PRRSV) vaccine. *Viral immunology* 26: 404-414.
66. Rowland R, Robinson B, Stefanick J, Kim T, Guanghua L, et al. (2001) Inhibition of porcine reproductive and respiratory syndrome virus by interferon-gamma and recovery of virus replication with 2-aminopurine. *Archives of virology* 146: 539-555.
67. Choi C, Cho W-S, Kim B, Chae C (2002) Expression of interferon-gamma and tumour necrosis factor-alpha in pigs experimentally infected with porcine reproductive and respiratory syndrome virus (PRRSV). *Journal of comparative pathology* 127: 106-113.
68. Bautista E, Molitor T (1999) IFN γ inhibits porcine reproductive and respiratory syndrome virus replication in macrophages. *Archives of virology* 144: 1191-1200.
69. Lager K, Mengeling W, Brockmeier SL (1997) Duration of homologous porcine reproductive and respiratory syndrome virus immunity in pregnant swine. *Veterinary microbiology* 58: 127-133.

70. Mengeling WL, Lager KM, Vorwald AC, Clouser DF (2003) Comparative safety and efficacy of attenuated single-strain and multi-strain vaccines for porcine reproductive and respiratory syndrome. *Veterinary microbiology* 93: 25-38.
71. Nowak M, May RM (2000) *Virus dynamics: mathematical principles of immunology and virology*: Oxford university press.
72. Kumar R, Clermont G, Vodovotz Y, Chow CC (2004) The dynamics of acute inflammation. *Journal of Theoretical Biology* 230: 145-155.
73. Yoo D, Song C, Sun Y, Du Y, Kim O, et al. (2010) Modulation of host cell responses and evasion strategies for porcine reproductive and respiratory syndrome virus. *Virus Research* 154: 48-60.
74. Pawelek KA, Huynh GT, Quinlivan M, Cullinane A, Rong L, et al. (2012) Modeling within-host dynamics of influenza virus infection including immune responses. *PLoS computational biology* 8: e1002588.
75. Labarque GG, Nauwynck HJ, Van Reeth K, Pensaert MB (2000) Effect of cellular changes and onset of humoral immunity on the replication of porcine reproductive and respiratory syndrome virus in the lungs of pigs. *Journal of general virology* 81: 1327-1334.
76. Xiao Z, Batista L, Dee S, Halbur P, Murtaugh MP (2004) The level of virus-specific T-cell and macrophage recruitment in porcine reproductive and respiratory syndrome virus infection in pigs is independent of virus load. *Journal of virology* 78: 5923-5933.
77. Kurosaki T, Kometani K, Ise W (2015) Memory B cells. *Nature Reviews Immunology* 15: 149-159.
78. Costers S, Lefebvre DJ, Van Doorsselaere J, Vanhee M, Delputte PL, et al. (2010) GP4 of porcine reproductive and respiratory syndrome virus contains a neutralizing epitope that is susceptible to immunoselection in vitro. *Archives of virology* 155: 371-378.
79. Delisle B, Gagnon CA, Lambert M-E, D'Allaire S (2012) Porcine reproductive and respiratory syndrome virus diversity of Eastern Canada swine herds in a large sequence dataset reveals two hypervariable regions under positive selection. *Infection Genetics and Evolution* 12: 1111-1119.
80. Triple BR, Popescu LN, Monday N, Calvert JG, Rowland RRR (2015) A Single Amino Acid Deletion in the Matrix Protein of Porcine Reproductive and Respiratory Syndrome Virus Confers Resistance to a Polyclonal Swine Antibody with Broadly Neutralizing Activity. *Journal of Virology* 89: 6515-6520.
81. Delisle B, Gagnon CA, Lambert M-È, D'Allaire S (2012) Porcine reproductive and respiratory syndrome virus diversity of Eastern Canada swine herds in a large sequence dataset reveals two hypervariable regions under positive selection. *Infection, Genetics and Evolution* 12: 1111-1119.
82. Triple BR, Popescu LN, Monday N, Calvert JG, Rowland RR (2015) A single amino acid deletion in the matrix protein of porcine reproductive and respiratory syndrome virus confers resistance to a polyclonal swine antibody with broadly neutralizing activity. *Journal of virology* 89: 6515-6520.
83. Johnson W, Roof M, Vaughn E, Christopher-Hennings J, Johnson CR, et al. (2004) Pathogenic and humoral immune responses to porcine reproductive and respiratory syndrome virus (PRRSV) are related to viral load in acute infection. *Veterinary immunology and immunopathology* 102: 233-247.
84. Nelson EA, Christopher-Hennings J, Benfield DA (1994) Serum immune responses to the proteins of porcine reproductive and respiratory syndrome (PRRS) virus. *Journal of Veterinary Diagnostic Investigation* 6: 410-415.
85. Goldberg TL, Lowe JF, Milburn SM, Firkins LD (2003) Quasispecies variation of porcine reproductive and respiratory syndrome virus during natural infection. *Virology* 317: 197-207.

Chapter 5. Discussion

5.0 Summary of the novel findings of this thesis and their implications

The overarching aim of this thesis was to gain novel insights into the within host infection dynamics of pigs after an *in vivo* infection challenge, with one of two PRRS virus isolates, using a statistical modelling approach. Empirical models for infection profiles were fitted to virus load and immune response measurements over time and statistical analysis was conducted on longitudinal viraemia, cytokine measures and nAbs cross-protection data. We quantified the inter-host variation, explored the time trends of the longitudinal viraemia and cytokine measures, and determined the influencing factors on them. In total, to date, the PHGC infection trials consist of 15 PRRSV infection trials comprising of one of two PRRSV isolates (NVSL or KS06). In Chapter 2 viraemia data from Trials 1-8, 10-12 and 14-15 were used to explore the influential effects on the PRRS viraemia profiles such as the virus strain, the WUR genotype and the genetic background. Thus, in Chapter 2, Trials 9 and 13 were excluded due to the lack of WUR genotype variation in the pigs, and unusual viraemia profiles due to a likely co-infection, respectively. Chapter 3 focused on capturing the inter-host variation in viraemia profiles using the Wood's and Extended Wood's model. The models were fit individually to all pigs, which contained a minimum of 6 repeated measures, in the PHGC dataset in order to generate new phenotypes for every individual. These new phenotypes have and will be used in subsequent genetic analysis for the selection of pigs with desirable infection traits, such as the study included in Appendix 3 and other ongoing studies carried out by the PHGC. The focus of Chapter 4 was on the immune response and the relationship between the immune response measures and the viraemia profile trends. The longitudinal cytokine response profiles and their time trends, relationships between cytokines, and the associations between the cytokines and the viraemia profiles were explored. However longitudinal cytokine data was only obtained from a subset of pigs from Trials 3, 5 and 7. Categorical data on cytokine responsiveness and the neutralizing antibody (nAb) cross-protection and their association with viraemia class, WUR genotype and the genetic background was also examined in Chapters 3 and 4. The nAb data was obtained from a subset of pigs from Trials 1-3, which did not overlap the cytokine data and hence the associations between the cytokine and nAb responses were not examined.

Novel insights were gained in this thesis on the variation in the host response to an identical infection challenge, represented by the wide variation in the longitudinal repeated viraemia and cytokine measures for large numbers of pigs in the PHGC trials. Viraemia and cytokine trends, as well as nAb cross-protectivity were successfully quantified and pigs were categorised according to their responses across trials, genetic backgrounds and PRRSV isolates in this thesis. This is one of few PRRSV studies that combines the investigation of viraemia with longitudinal cytokine data and nAb cross-

protection data. In the following discussion we present the novel findings of our study, their implications for the PRRSV infection research, and discuss emerging scientific questions to be explored in future studies.

5.0.1 The Wood's model

This thesis, and also the study presented in Appendix 3, has demonstrated the suitability of mathematical functions to assess the impact of various factors including host genetics on PRRS viraemia kinetics. This is the first study to apply the Wood's and Extended Wood's model to PRRS viraemia profiles. The Wood's curve is concisely described by three parameters, a , b , and c , which are related to the magnitude of the values (a), and describe the shape of the curve (b , which is dominant pre-peak, and c , which is dominant post-peak) [1]. While other mathematical functions may more adequately model PRRS viraemia during infection, the number of data points collected during these PHGC trials limited the ability to fit more complex models. Fitting a Wood's curve is a more powerful method for comparing viraemia dynamics than the Loess smoothed fit used in previous analyses of a subset of the PHGC data [2-4]. The Loess smoothed fit uses a parameter indicating the degree of the polynomial to fit to the data and a smoothing parameter for curve fitting [5], with the primary aim of filtering noise. The limitation with the Loess and other polynomial spline functions, however, is that this method does not lend itself to extract fitted parameters that specify particular physical properties of a system which have important implications in understanding the dynamics of PRRSV infection. Although both methods adequately fit the data, the Wood's curve parameters describe both the magnitude and shape of the curve, which can be used to explore different characteristics of the viraemia curves. Exploring Wood's curve characteristics can provide insight into important biological questions, such as which immune responses are associated with the rate of decline (parameter c) or timing of the peak viraemia (T_{max}), which aspects of host response are under strongest genetic control and how selection for one curve characteristic may affect others and, thus, the entire response profile (in Appendix 3). It may also be used to explore the relationship between curve characteristics and other phenotypes, such as weight gain (WG) under infection in accompanying studies (such as Appendix 3 or current studies on disease tolerance in a PRRSV infection).

Fitting a Wood's curve provided reliable estimates for the function parameters while not over-parameterizing the data to explore: the associations between the immune response measures at key profile characteristics such as the time of the peak (T_{max}) and time of maximal viraemia decline (ΔT) and the different aspects of the PRRS viraemia curves for subsequent genetic analysis (see Appendix 3). Furthermore, comparison of the Extended Wood's and Wood's curve functions allowed for an objective classification of viraemia profiles using the full time course of the experiment in Chapter 3.

Limitations of the Wood's model

While the advantages of fitting a Wood's curve to model the dynamics of PRRS viraemia are clear, care needs to be taken in the interpretation of the correlations between curve characteristics because strong correlations between these curve characteristics are likely to arise partly as an artifact of the Wood's function and partly as they reflect true correlations between curve characteristics that are independent of the Wood's function. One example whereby the genetic correlation between traits is likely to be driven by the Wood's function is the high genetic correlation observed between ΔT (time of maximum decline, T_{max} , in Appendix 3) and ΔV (value of viraemia at maximum decline, V_{max} , in Appendix 3) in Appendix 3, because they rely heavily on the b parameter of the Wood's function.

5.0.2 Review and comparison of the statistical modelling and inferences employed

Empirical mathematical models have proven useful for describing the temporal evolution of a response variable and filtering stochastic noise from dynamic biological systems whilst retaining the most fundamental features [6-9]. Linear mixed models are a well-established methodology used to model longitudinal data with the inclusion of both fixed and random effects [8,10-13]. The repeated measures modelling approach was appropriate for the assessment of influential factors on the time trends of viraemia and cytokines in Chapters 2 and 4. The advantage of the repeated measures modelling approach was that temporal correlations could be incorporated into the models without assuming any prior information about the shape of the profiles. They were thus a logical place from which to begin analysing the impact of diverse influencing factors on the longitudinal data [11,13]. Through the repeated measures model, LSMs for viraemia and cytokines were obtained at each observation time and the effects of the influencing factors on these were examined. However the repeated measures modelling approach was limited to the observation times only and could not be used to capture the full non-linear time trends of the individual viraemia profiles across the duration of the experiment. Although the impact of effects on the LSMs can be tested, this method does not result in the generation of biologically interpretable parameter estimates for key profile characteristics, which is key for the selection of individuals with desirable infection phenotypes (i.e. parameters relating to the rate of viraemia clearance).

Cubic spline functions were fit to the cytokines data in Chapter 4 in order to remove noise from the data prior to subsequent analysis. The splines were successful at smoothing profiles and filtering noise. Furthermore spline functions provide estimates for each observation of the experiment, as opposed to the repeated measures models which provide LSM estimates at the observation times only. However it is difficult to extract fitted parameters from splines that specify particular physical properties of a system, which have important implications in understanding the dynamics of PRRSV

infection. Similar to the linear mixed models, a mixed modelling approach could be directly applied to the spline functions [14-19]. However in this thesis splines were used only as a method to filter out noise from the data.

The Wood's model and linearized Wood's model fitting approach was adopted in Chapters 2 and 3 which allowed the construction of viraemia curves for the entire time course of the experiment, and also the examination of the effect of various factors on the model parameter estimates. However the residuals from fitting the final linearized Wood's function in a classical linearized mixed modelling framework revealed that the model was a poor fit to the data and, as with the repeated measures approach, bimodal profiles reduced the model fit to the data. A better fit was needed in order to determine host genetic influence on viraemia profiles (for Appendix 3) and to explore the relationship between viraemia profiles and immune response.

The poor Wood's model's fits in Chapter 2 were a likely manifestation of the linearization process as opposed to a reflection of the suitability of the Wood's function as a candidate model for viraemia profiles. Mixed models can also be implemented in Bayesian framework [20-25]; however this was not explored in this thesis. In Chapter 3 the nonlinear function Wood's function was fit directly to the data using a Bayesian framework. Directly fitting the Wood's model to the log-transformed viraemia data overcame the poor model fits from Chapter 2. However, the Bayesian inference for the Wood's model parameters came at a higher computational cost; taking several months to obtain estimates for all the pigs in the PHGC dataset. The Bayesian inference methodology was more flexible than the linear mixed modelling approach in Chapter 2 and was able to fit a wider range of functions to the data in particular the bimodal Extended Wood's model. In summary, directly fitting the Wood's model and Extended Wood's model using a Bayesian approach in Chapter 3 allowed for: a better fit to the data, and the opportunity to fit a wider range of functions to the data than the linearized Wood's function in the linear mixed models framework of Chapter 2.

The Wood's and Extended Wood's model was used for the modelling of viraemia time trends in this thesis however there are other potential mathematical functions that could have been applied to capture the time trends in the longitudinal viraemia data such as, but not limited to: Legendre polynomials, which have been used to analyse patterns of genetic variation in lactation curves [26], the Ali-Schaeffer curve, which is a well-established parametric function [27], Wilmlink curve, which has an exponential component [28], Lidauer-Mäntysaari function, which also has an exponential component [29], and regression splines [30]. For the purposes of our study the Wood's and Extended Wood's model provided an adequate fit to the data however comparison of the Wood's approaches with other mathematical functions could be pursued in future studies in order to robustly identify the most suitable model; similar comparisons have been conducted for lactation curves in dairy cattle [29,31,32].

5.0.3 Statistical categorization of pigs: viraemia profiles

The longitudinal viraemia measures from the PHGC PRRSV challenge experiment revealed substantial differences in the viraemia profiles between hosts infected with the same PRRSV challenge dose, pointing to considerable variation in the host response to PRRSV infections. The statistical categorization of pigs from the PHGC trials, combined with model fitting, provides a critical basis to generate new phenotypes for the selection of pigs with favourable infection traits. In Chapter 3, viraemia profiles were assigned to one of three groups: cleared (uni-modal resolution of viraemia by 42dpi, persistent (uni-modal detectable viraemia by 42dpi) and rebound (bimodal profiles). This is the first study to fully quantify the wide variation of host response from a PRRSV in vivo challenge. Bimodal viraemia trends within 42dpi had been observed in previous studies [33-35] but were either removed by truncating the data (0-21dpi)[34] or the phenomenon was ignored and left both unexplained and unquantified [33,35]. A key and novel insight from this thesis is that viraemia rebound was observed across all trials, genetic backgrounds and both PRRS virus isolates. Furthermore rebound withstood definition via the robust method using the full duration of the experiment with an objective measure of statistical significance that also took measurement error into account, as opposed to a threshold of differences between observations determined via subjective visual inspection. Thus we can conclude that rebound, or bimodality in viraemia, is a generic phenomenon along with clearance and persistence (or prolonged viraemia) of viraemia profiles resulting from a PRRSV challenge. The key questions to emerge from this finding are: what are the mechanisms, of the host, the virus or both that are behind the observed rebound and what implications, if any, does rebound have in driving the epidemiology of the virus within a herd.

It is interesting that we were able to determine that information derived from the early phase of infection could not be used to predict the serum viraemia characteristics at the later stage of infection i.e. whether a profile would rebound, clear or persist. Specifically the rebound and clearance profiles could not be distinguished based on information from the primary phase of infection (0-21dpi). This result has however important implications with regards to the following hypothesis: considering that serum viraemia data were only collected for 42dpi, one may hypothesise that every pig may eventually experience rebound, provided that the virus has not been completely cleared, and that rebound could only be observed for a subset of pigs in this study due to censoring. However, if this hypothesis was correct, there would be a higher probability of observing rebound in individuals with faster viraemia decline within 21dpi. But, since no statistical difference was observed between rebound and clearance on the truncated dataset, the existing evidence would suggest that only a subset of pigs experiences viraemia rebound. Furthermore, we also observed that none of the pigs with non-detectable viraemia levels for 2 or more weeks experienced viraemia rebound within 42dpi (results not shown), thus indicating that rebound is unlikely to occur if the serum virus has been cleared for a period of several weeks.

Overall this is the first study to fully capture the full range of viraemia profiles obtained from a large scale PRRSV infection experiment. Furthermore the resulting statistical classification of pigs according to viraemia response was used in Chapter 4 to examine their association with the immune response, and in Appendix 3 as well as ongoing studies, to determine the genetic component associated with viraemia profile characteristics and other phenotypes.

Viraemia Rebound

Viraemia rebound was observed across trials, genetic backgrounds and virus isolates. Rebound was observed more frequently when pigs were infected with the NVSL isolate (17% rebound) than with the KS06 isolate (8% rebound). One explanation for this is the presence of quasispecies within a host. PRRSV has a very high mutation rate, estimated at $4.7-9.8 \times 10^{-2}$ nucleotides/year [36]; this causes within animal PRRSV genome variation [37], with each variant labelled a quasispecies. Pigs infected with NVSL have higher viraemia than pigs infected with KS06 throughout most of the primary phased of infection (0-21dpi). Higher viraemia levels correspond to a higher number of virus replications i.e. a higher frequency of events in which virus mutation could occur. It can thus be hypothesized that there would, as a consequence of a higher virus replication rate, be a greater number of quasispecies present within the host of a pig infected with the more virulent NVSL than KS06 infection. A consequence of the higher viral diversity within the host is an increased potential for the emergence of an immune escape-mutant PRRSV strain to emerge, which hypothetically could manifest in the observed viraemia rebound in the serum [38]. Furthermore NVSL infected pigs could also have a greater number of circulating quasispecies, than during a KS06 infection, if NVSL had a higher virus mutation rate; a higher mutation rate would increase the likelihood for the emergence of immune escape-mutants of PRRSV during an infection.

Furthermore from an epidemiological perspective viraemia rebound may be of particular importance for herd level persistence; a mutated virus that escapes the immune response mounted against the homologous strain could be transferred between pigs thus causing reinfection and viral rebound. Cycles of transmission between pigs within the same herd of immune-escape mutants could thus perpetuate cycles of future PRRSV infection within a herd [37]. Indeed if viraemia were measured over a longer duration, than the 42days in this study, perhaps further cycles of damped viraemia oscillations with several waves of rebound would be observed within individual pigs.

Alternately NVSL may partly avoid the host immune response, possibly escaping the humoral immune response by localizing to certain tissues such as the tonsils which have been found to be a source of PRRSV viral persistence in previous studies [39,40]. In the tonsils there is an abundance of memory B-cells but a lack in effector plasma-producing, B-cells [41]. Thus a hypothesized stochastic “out-pouring” from the persistently PRRSV- infected tonsils into the serum provides an alternative explanation for the mechanisms behind the observed viraemia rebound in this thesis. If the ability of

the virus to remain in the tonsils and escape the immune response differed between PRRSV isolates then differences in tonsil viraemia levels would be apparent; serum viraemia differences would be insufficient to test this theory. Hence further studies are underway to address this hypothesis.

The underlying mechanisms behind the observed viral rebound have yet to be fully determined. However the viraemia profile class differences were captured by a higher IFNA and CCL2 expression in the secondary phase of infection for rebound pigs (21-42dpi). More data is needed since there were a limited number of rebound pigs (28 pigs) in the cytokine dataset in the present study. One hypothesis that could be explored in future studies could be that CCL2 up-regulation might be a protective mechanism of the host in response to infection. CCL2 is a ligand for CCR2, a receptor which is expressed on a subset of monocytes in peripheral blood. In a previous study it has been found that the monocyte subset CD14⁺⁺ CD163^{low}/negative expressed much higher levels of CCR2 than the CD14⁺ CD163^{low/high} subset.

5.0.4 Influential effects on the viraemia profiles

Virus Isolate: More virulent PRRSV isolates typically elicit higher viraemia measures [42]. NVSL and KS06 were isolated from different geographic regions approximately ten years apart, and were 89% similar at the GP5 nucleotide sequence level. PRRSV glycoprotein 5 (GP5) is a major envelope protein, important in virion formation and infectivity and harbors a major neutralizing epitope [43]. The corresponding gene is often used to assess genetic differences between PRRSV isolates and is suggestive of differences in virulence between isolates [44]. Variation in GP5 impacts the pig's ability to produce nAbs, which may only be protective against specific, but not all, isolates [44,45]. These two North American strains are clustered distinctly into two branches according to molecular phylogeny [46]. In Chapter 2 we demonstrated that these virus isolates differ in both their virulence and in resulting viraemia profile characteristics. Infection with NVSL is characterized by reaching a high peak viraemia early, followed by a quick clearance of the virus, whereas the KS06 virus accumulates more slowly towards a lower peak viraemia and has a slower rate of viraemia clearance. In Chapter 3 the Wood's and Extended Wood's model provided a good fit for both virus isolates, with fewer rebounding, but higher numbers of persistent profiles for KS06. Given the flexibility of the Wood's function to capture adequately the more rapid, higher peak and more virulent dynamics of the NVSL viraemia and the slower, more prolonged infection of the less virulent dynamics of the KS06 strain we would expect the Wood's function to perform adequately well for further North American strains.

WUR genotype: The WUR genotype, associated with lower cumulative viraemia (i.e. viraemia AUC until 21 dpi) in previous studies of a subset of the PHGC NVSL challenge data [34,47-49], resulted in lower viraemia predictions at all observation times between 0-42 dpi according to the repeated

measures model of Chapter 2. However the linearized Wood's parameters differences between the WUR genotypes were not statistically significant despite slight reductions in the viraemia predictions for the favourable B allele were observed. The impact of the WUR genotype was found to be isolate dependent. In Appendix 3 it was found that pigs with the WUR genotype 1 had a more desirable phenotype than WUR 0 pigs for many of the derived Wood's model traits under NVSL infection, but only for cumulative viraemia (viraemia AUC 0-21dpi) and the peak viraemia load (Vmax) for KS06 with no WUR association for the other traits. Accounting for the WUR genotype had little impact on the genetic correlation between isolates, suggesting that there is a substantial polygenic component to response to PRRSV infection that is common between these two PRRSV isolates. Our results suggest that KS06 is a less virulent PRRSV isolate than NVSL, but, importantly, that genomic selection will be effective for selection for improved weight gain (Appendix 3) and reduced viral load under either PRRSV infection. This thesis affirms the important influence of the genetic marker WUR on host response to PRRSV. The results of the isolate dependent impact of the WUR genotype suggests that the influence of this marker may be dependent on the virulence of the PRRSV isolate.

It is interesting to combine our findings from the viraemia profile isolate differences from Chapters 2 and 3 with the findings relating to weight gain under infection which was also explored in Appendix 3. In the latter study it was found that KS06 infection had less of a negative impact on the growth rate. Thus we could hypothesize that due to the lower viraemia levels and slower dynamics the piglets infected with the KS06 isolate do not need to put as much energy into eliminating the virus, thus allowing them to allocate more energy towards growth than those infected with NVSL according to resource allocation theory [50]. The genetic correlations between viraemia and weight gain varied over time and tended to be more extreme in NVSL infected pigs than KS06 infected pigs, suggesting that more energy is required to fight infection with NVSL, and is supported by the lower weight gain observed in NVSL infected pigs. The effect of WUR genotype on weight gain was not found in pigs infected with KS06. Virus isolate differences were greater than WUR genotype 1 and 2 (refers to the number of the favorable B allele) differences on viraemia profiles magnitude, dynamics and derived phenotypes from the Wood's mode (see summary tables of derived phenotypes in Chapter 4). It has been found that WUR had the strongest effect on the following Wood's parameters and derived traits obtained from this thesis: Vmax (peak viraemia), Tmax (time of peak viraemia), DeltaT (time of maximum viraemia decline) and DeltaV (viraemia at the time of the maximal viraemia decline).

Genetic background: In this thesis the infected pigs were crossbred commercial pigs from 10 genetic backgrounds. Numerous PRRSV *in vivo* and *in vitro* studies have pointed to breed differences in the response to infection; which suggest that there is a host genetic component in the host resistance to infection [3,34,35,48,49,51-58]. Previously breed differences have also been found in serum viraemia [59]. It is thus not surprising that viraemia profile differences were observed between genetic backgrounds in our study. The time trends in viraemia were roughly the same between the genetic

backgrounds within each virus isolate, however genetic line differences within isolates were found in the time of the peak and the rate of viraemia decline. Exploration of trial differences allowed us to partly disentangle the virus and genetic background effect. Pigs of the same genetic background infected with different virus isolates had significant differences in response, which is an indication of the viraemia isolate differences discussed earlier. However significant viraemia differences between pigs of the same background infected with the same virus in the repeated measures approach indicated that the trial could have an impact on the viraemia. These differences are more difficult to interpret, however it is reassuring that these differences were not captured in the model parameter differences of the linearized Wood's modelling approach. We can thus conclude that the within genetic background variation is lower than the between genetic background variation in the PRRS viraemia profiles of this study.

5.0.5 The relationships between the viraemia and the immune response measures

This is the first study to fully categorize pigs using multiple repeated measures across 7 measured serum cytokines following PRRSV infection. In this thesis individual cytokine profiles could be classed as responders or non-responders to PRRSV infection. The percentage of responding pigs differed between cytokines. However, the majority of the pigs responded in the pro-inflammatory and anti-viral cytokines (IL-1b, IL-8, CCL2 and IFNA) and also the immune regulatory cytokine IL-10. In particular, the highest percentage of responders was found for IFNA and CCL2, for which over 95% of pigs elicited a noticeable response. The immune regulatory cytokines IL-4 and IL-12 had the highest percentage of non-responders (71% and 54%, respectively) compared to the other cytokines. The breadth of the cytokine responsiveness was associated with viral profile class and genetic background but not the WUR genotype. Rebounders had a narrower cytokine response than non-rebounders, and pigs from genetic background 1 had a broader response than genetic background 3. The genetic line differences suggest that there is a potential host genetic contribution in the breadth of the cytokine response. However since the WUR genotype was not found to be significant it is likely that the cytokine responsiveness is associated with other host genes which could be explored in future studies.

The rate of viraemia decline, captured by the Wood's parameter c was associated with the strength of response in IL-10, IL-12 and IL-1b; however the final model, including cytokine measures as predictors, was not a significantly better than the null model without cytokine response variables included as predictor. The strength of the early viraemia was correlated with the strength of early IFNA and CCL2; however this correlation decreased over time.

Different genetic backgrounds had different baseline cytokine values and differed in the overall magnitudes of expression (IFNA, CCL2), but broadly similar response patterns. However differences

in the general trend i.e. whether there was a slight increase or decrease following infection was found in IL-1b, IL-12 and IL-10, between genetic backgrounds.

Viraemia class differences were reflected in the profiles of the cytokines CCL2 and IFNA. Rebounders elicited a stronger response in most of the cytokines at the later stages of infection (from 28dpi onwards) than non-rebounders, although the differences were not always statistically significant. Rebound profiles had statistically significant higher levels of IFNA expression at 28-35dpi than cleared profiles and higher IL-8 expression at 35dpi. Differences between pigs with cleared and persistent profiles were small and not statistically significant. Somewhat surprisingly, due to the anti-viral role of the cytokine [60,61], rebound profiles had on average significantly higher baseline levels of IFNA than cleared profiles. Rebound profiles have on average a faster post-peak rate of decline compared to non-rebound viraemia profiles, hence the higher baseline IFNA could, hypothetically, contribute to the fast viraemia decline observed. Furthermore, whilst pigs associated with cleared and persistent viraemia profiles experienced a post-peak decline of CCL2 expression to baseline levels, pigs with rebound viraemia profiles, however, also experienced a “rebound” in CCL2 values at similar times.

The WUR genotypes had little impact on the cytokine profiles. The cytokine predictors significantly improved the models for the majority of the viraemia traits, whereas the viraemia traits were poor predictors of the cytokine measures. These results suggest that the cytokines drive the viraemia rather than vice versa. IFNA and CCL2 in serum were the key cytokines for serum viral dynamics. IFNA was consistently a significant predictor for viraemia characteristics, which is unsurprising due to its already established antiviral role and association with viraemia clearance in previous studies [60,61]. However the role of CCL2 during an *in vivo* PRRSV infection is not fully understood.

Limitations: The distance between the longitudinal measurements of the challenge experiment may be relatively large and hence some informative viraemia or cytokine dynamics may be lost. Given that the majority of the cytokine measures were of the innate immune response the 4 day gap in the observation period could mean that the data failed to capture the early response. The cytokine response is very transient [62], so a weekly window may not capture sharp responses. Cytokines and virus in serum are a ‘spill-over’ from those in the infection target site. This, together with the fact that some cytokines are locally produced may weaken the strength of the true associations that would be found directly at the site of infection.

Implications for future studies: In Chapter 4 we found that the majority of pigs showed responses in IFNA and CCL2. IFNA and CCL2 in serum were the key cytokines for serum viral dynamics. IFNA was consistently a significant predictor for viraemia characteristics, which is unsurprising due to its already established antiviral role [60,61] and association with viraemia clearance in previous studies. PRRSV can inhibit the type 1 interferon production in certain dendritic cells with roles in the innate

immune response [63]. Conversely some PRRSV strains led to little or no suppression of the IFNA expression in the same dendritic cells [64]. Previous studies differ in the nature and magnitude of the IFNA response following a PRRSV infection. The more widely reported result is a lack of significant and comparatively low IFNA response, compared to other infections [65-68]. However this is contrasted by reported increases in serum IFNA levels following PRRSV infection [69-71], which is in line with our results from Chapter 4.

Viraemia class differences were also captured in both IFNA and CCL2 expression profiles. Increased cytokine expression during the secondary phase, when viral rebound would occur, suggests that cytokine expression of IFNA and CCL2 potentially mimic viraemia trends. Higher levels of viraemia were correlated with a higher expression of IFNA. Unlike IFNA the role of the cytokine CCL2 has not been established in previous PRRS studies. The high levels of CCL2 during the secondary phase of infection is interesting from a biological perspective since the role of CCL2 is thought to be that of causing an influx of macrophages to the site of infection [72]. A potential hypothesis that emerges from this study is that the increase in CCL2 could result in an influx of new PRRSV target cells thus driving the rebound in viraemia that we observe [73,74]. Few PRRSV studies have examined the role of CCL2 in PRRSV infection; studying the CCL2 response could be potentially informative for understanding the underlying mechanisms of viral rebound.

An effective cytokine response following infection may be indicative of the immune-competence of a pig which may also have a host genetic component [75]. Identification of pigs with a robust IFNA response from 0- 4dpi could be explored in future studies. The genetic selection of pigs with effective cytokine responses could be used in the search for breeding for higher levels of immune competence during a PRRSV infection, which will be discussed in the following section as an alternative disease control strategy.

5.1 Further Implications

5.1.1 Genetic selection for host resistance to PRRSV infection

This PhD was part of a wider project of the PRRS Host Genetic Consortium called “Application of Genomics to Improve Swine Health and Welfare” (funded by Genome Canada). The overall goal of the PRRS Host Genetics Consortium (PHGC) is to exploit state-of-the art genomic technologies to breed healthier pigs with improved resistance to PRRSV infection. Previous studies have provided evidence for a host-genetic component in the effectiveness of responding to and clearing a PRRSV infection [52-54,76,77]. The data generated from the PHGC PRRSV challenge experiments can be used for identifying the genetic loci and pathways that are responsible for the genetic control of PRRSV infection responses[51]. Prior to this thesis there was strong evidence for a host genetic component to PRRSV infection through the identification of a major QTL on SSC4, i.e. the WUR

genotype, that was found to be associated with reduced cumulative viraemia (viraemia AUC up to 21dpi) [3,4,34,47,49]. The work of this thesis has delivered new phenotypes associated with the dynamic aspects of measured infection traits, and led to the statistical categorization of pigs according to viraemia, cytokine and nAb responses. We found that the viraemia rebound was not heritable ($h^2=0.00000$) and the new viraemia phenotypes derived from this thesis have already been implemented in other studies (see the manuscript of Appendix 3). The results from Chapter 4 indicate that future studies should be conducted with more frequent measures of IFNA and CCL2. Analysis into the host genetic components of their respective expression both at the early and late phase of infection could be key to furthering our understanding of both viral clearance and also viraemia rebound.

Viraemia traits: The Wood's model and Extended Wood's model for viraemia generated new phenotypes for host resistance that have been used in subsequent genetic analyses to assess the effect of previously identified genetic loci (the WUR SNP) on the viraemia profile characteristics and to identify novel genomic regions associated with these for both PRRSV isolates (NVSL and KS06) (see for e.g. Appendix 3). In these studies, the WUR SNP was found to be associated with all curve characteristics (Vmax, Tmax, deltaT, deltaV, I21, T1, V1 as defined in Chapter 4) in the NVSL trials; but only with I21 (AUC of viral load up to 21dpi, VL in Appendix 3) and Vmax (peak viraemia, PV in Appendix 3) in KS06 trials, suggesting the effect of the WUR SNP may depend on the virulence of the PRRSV isolate. The results thus suggest that genetic selection for reduced susceptibility to genetically distinct isolates PRRSV is feasible, but may have different impact on viraemia profiles shapes for different PRRSV isolates. Analysis of the relationship between viraemia and weight gain via genome-wide association studies over the course of infection in future studies, will allow for a more comprehensive understanding of the host genes and genomic regions associated with response to PRRSV infection.

Infection trials involving more isolates of PRRSV are necessary to confirm that genetic factors influencing host response to PRRSV infection are consistent under infection with a range of PRRSV isolates. Quantitative genetic analyses of the relationship between viraemia and weight gain over the course of infection are currently being carried out and will allow for a more comprehensive understanding of the host genes and genomic regions associated with both host resistance and tolerance to PRRSV infections. Studies currently underway as part of the PHGC includes: field trials, infection with a third PRRSV isolate, and the response to vaccination and co-infection with PRRSV and PCV2b. For comparison of the impact of traits and viraemia characteristics from the isolates in this study it would be useful for the Wood's functions to be fit to the viraemia data in subsequent studies. In this thesis the function has proven to be able to capture viraemia differences in the NVSL and KS06 isolates and is thus a potentially good candidate for capturing the viraemia trends of other North American PRRSV infections. The resulting derived phenotypes from the model fitting for new

isolates could result in a useful dataset to assess the variation in viraemia and sources of variation of host responses across a wide range of isolates and infection conditions.

Another potential strategy in livestock disease management consists of focusing on improving the immune-competence of the host. As defined by [78], immuno-competence is the host's ability to mount an immune response of sufficient specificity and magnitude, and therefore represents the effective quality of the host's immune system. It has been proposed that many immune competence parameters including in vitro innate cytokines, adaptive cytokines and the host's IgG response, could be under genetic control and that there may be scope for them to be included in future the selection protocols [75,78-80]. Indeed in a previous study it was found that gene expression profiling in the blood could be used as a phenotype to identify potential biomarkers for the analysis of the host immune response; biomarkers were found for various immune measures including IL-12 [78], which is one of the cytokines measured in Chapter 4 of this thesis. The analysis and statistical characterization of the serum cytokine profiles and nAb responses in Chapters 3 and 4 could potentially be used to better characterize the host's immunity traits in future studies. Thus in the following sub-sections we discuss the nAb and cytokine responses in relation to breeding for improved immune competence against PRRSV infections.

The nAb response: Different PRRSV isolates harbor high levels of genetic and antigenic variability [81]. Antibody responses can be categorized into a neutralizing antibody response, where the antibody directly inhibits the virus function [82] and non-neutralizing antibody response, where the antibody binds to the virus for the identification for viral clearance via other immune mechanisms (e.g. phagocytosis)[83]. Following a PRRSV infection, the earliest and strongest antibody response is a non-neutralizing (IgG) response against the virus nucleocapsid (N) protein [84]. Virus neutralizing antibodies are typically weak and delayed during PRRSV infection however once a nAb is produced the response is effective [82]. This effective nAb response is often only restricted to homologous isolates of PRRSV. Therefore vaccination with modified live virus (MLV) or previous natural infection typically results in only homologous protection against closely related PRRSV isolates [85]. However in addition to the strong homologous response a broader nAb cross-protectivity against different PRRSV strains was also observed in Chapter 3.

As observed in previous studies [86,87] the PRRSV infection elicited a strong homologous antibody response in the majority of pigs in Chapter 3 of this thesis. This is one of only a few studies that explore the nAb cross-protectivity of PRRSV infected pigs. It is particularly interesting that a diversity in the breadth of the nAb cross-protectivity was observed. This is the first study to find a significant association between the viraemia profile class (cleared, persistent or rebound) and the cross-protectivity of the nAb response. Clearance corresponded to a less diverse nAb response than persistence and pigs with persistent viraemia had a more diverse nAb response than those with

rebound profiles. However, there was no statistical significant difference in nAb cross-protectivity between pigs that cleared viraemia within 42dpi and rebounders. The WUR genotype was not significantly associated with the breadth of the nAb response. The novel insights gained from the nAb analysis can be used to develop hypotheses surrounding the observed viraemia variation.

Understanding the host's ability to mount a non-neutralizing PRRSV-specific antibody response could lead to deeper insights related to the non-isolate specific host-response to PRRSV infection. In contrast, studying the breadth of the nAb cross-protection could lead to the identification of pigs with desirable virus neutralizing abilities, particularly for pigs under field conditions where multiple PRRSV strains could be in simultaneous circulation [37].

One hypothesis is that the breadth and magnitude of the nAb response could have a host genetic element. The identification of genomic markers linked to a broad nAb response would be a novel finding with significant implications for the selection of pigs that show improved protection following vaccination; the so-called "vaccine ready" pig [58]. Thus genetic improvement to enhance the response to vaccination could create the opportunity to bring PRRS control closer to achieving an effective vaccine. Development of an effective PRRSV vaccine has been widely unsuccessful because they lack cross protection against different PRRSV strains [81]. Selection of pigs that are resistant to a broad spectrum of currently circulating PRRV field isolates could be a successful disease control measure [75,88,89].

A robust PRRSV-specific non-neutralizing antibody response is observed early and is maintained following infection and even after serum clearance of PRRSV [84]. N-protein specific antibody response in PRRSV has been found to be favorably genetically correlated with sow reproductive performance during a PRRSV outbreak [90]. The development of PRRSV nAb is typically weak and delayed [58]. However, at the population level there is evidence to suggest inter-host variation in the diversity of the nAb response as shown in Chapter 3. One aspect of the strength of the nAb response during infection relates to the genetics of the virus; the removal of glycosylation sites on the virus results in increased susceptibility of the virus to nAb and increased production of nAb by the host [44]. The categorization of pigs according to their antibody response is crucial for determining the host genes associated with the desirable subpopulation of pigs able to produce strong and life-long immunity following a PRRSV infection. The characterization of the nAb response in Chapter 3 could thus be used to determine the association between different nAb responses and the host genes in future studies. The antibody response has the potential to be used as a biomarker for the selection of pigs with improved resistance to PRRS [91], however the WUR genotype was not associated with differences in nAb cross-protection in Chapter 3. This suggests that other genes may be responsible or related to the nAb response. Studies are currently underway exploring the genetic relationships of antibody response, viraemia level and weight gain in pigs experimentally infected with PRRSV. It is

also important to assess the optimal strength of antibody response that would increase resistance to PRRSV, whilst not compromising the host's ability to combat other disease causing pathogens.

Antibody responses could provide insight into the causative immune mechanisms resulting in cleared, persistent and rebound viraemia profiles. Variation in the rate of viraemia reduction may be a function of the host's own immune response, virus mutation mechanisms or the interaction between both processes. In Chapter 3 the moderate negative correlation between the NVSL Wood's parameters c_1 and c_2 (-0.52) indicates that a slow decline in the first cycle corresponds to faster decline in the second cycle and vice versa. This association may be indicative of the temporal evolution of the immune response. A slow immune response in the primary phase may prolong the conditions required to produce neutralising antibodies and thus manifest in a stronger or more diverse nAb at the end of the second phase. Conversely, a fast initial immune response may indicate an effective, but narrow nAb response during the primary phase so that fewer or less diverse nAb are available for the second phase. The identified association between nAb and viraemia categories would support this hypothesis, since persistent profiles have the broadest response of all the profile categories.

If viral rebound was due to immune escape by the virus, which is recognized as re-exposure to the virus by the host then we could hypothesize that rebound pigs would have a greater memory B cell activity of memory B cells resulting in a higher level of antibody than non-rebound [92].

Alternatively, high antibody levels could place selective pressure on the virus which could manifest in an increased likelihood of viral rebound occurring [38,93-96]. Longitudinal antibody response measures would thus be needed to test these hypotheses and further determine the relationships between viraemia profiles and the antibody response.

Cytokine response: As hypothesised for the antibody response, in the subsection above, the effectiveness, strength and breadth of the cytokine response following infection may also have a host-genetic component [57]. The cytokine responsiveness may also be an indication of the immune-competence of a host in dealing with a PRRSV infection. However the WUR genotype was not associated with significant differences in longitudinal cytokine expression profiles or the breadth of the cytokine responsiveness in Chapter 4. This suggests that other genes may be responsible or related to the cytokine responses. Cytokine responses could however provide insight into the causative immune mechanisms resulting in cleared, persistent and rebound viraemia profiles; viraemia profile differences captured in elevated responses in IFNA, CCL2 and IL-8 during the rebound phase (21-42dpi) in Chapter 4, which thus supports this hypothesis.

Previous studies have linked serum cytokines such as IL-8, IFN-gamma and IL-1b to PRRSV clearance [42,97]. In particular IFNA, which has already been established as playing an anti-viral role during a PRRSV infection [60,61], was found as a consistently a significant predictor for viraemia characteristics in Chapter 4. The identification of genomic markers linked to a robust IFNA response,

particularly between 0-4dpi, would be a novel finding with significant implications for the selection of pigs that could effectively clear the virus. In previous studies numerous immune proteins have been identified with roles in viral disease resistance [57]. However future studies could focus on identifying the SNPs for specific candidate genes for the serum cytokines associated to viral clearance (i.e. IFNA and CCL2), viral rebound (i.e. IFNA, CCL2 and IL-8) and the breadth of the cytokine responsiveness across all the measured cytokines. More repeated measures of IFNA and CCL2 need to be collected in future studies in order to determine the host genetic component associated with the immune-competence in relation to resistance to PRRS. It would also be important to ensure improved immune competence in relation to PRRS was not at the detriment of other desirable production traits. Furthermore it would be important to simultaneously consider immune-competence not only to a PRRSV infection but also in relation to other pathogens since it would not be of benefit to breed specifically for resistance to PRRS at the expense of significantly improved vulnerability to other costly disease causing pathogens.

5.1.2 Process based mathematical modelling of PRRSV infection

Process based mathematical modelling is an alternative approach to exploring hypotheses surrounding the within host dynamics of viral infections. Systems of ODEs (ordinary differential equations) have been used to represent the various components of within host dynamics of virus infections such as HIV [98-103], influenza [104-106] and more recently PRRSV [107,108]. Parallels can be drawn between HIV and PRRSV, in terms of high mutation rates and immune escape mechanisms, and thus gaining insights into modelling approaches that have been used for HIV could aid the development of new models for PRRS. Furthermore in equine influenza infection bimodal virus titre curves were also observed, for about 50% of the cases, which were modelled through the incorporation of antiviral effects of interferon [109].

The most recent process-based model for PRRSV [107,110] includes a detailed description of the host's immune response. The model describes the evolution over time the PRRSV infection in the lung. Briefly, in the model the interactions between the macrophages and the pathogen, the orientation of the adaptive response and the cytokine regulations are defined in a system of ODEs with 18 state variables. The viral particles, macrophage states during infection (susceptible, latent, viral excreting) and the adaptive and innate immune response are represented. Direct comparison between the results from this thesis with the predictions of the process based model would need to be adjusted since in this study inferences have been made from the serum measurements whilst the process-based model is defined for the site of infection. However the emergence of the distinct types of viraemia responses in this thesis could be used to modify, validate and inform the input parameters of the PRRSV process based model [107]. A key question to be explored using the current process based model for PRRSV infection is what model parameter combinations and key immune components in the model result in

the three types of viral profiles observed in this thesis? The answers to which should be tested in subsequent experimental studies. Furthermore, the process based model could provide valuable information on the expected relationship between immune response components (e.g. cytokine or nAb response) and virus load over time, which would be useful for evaluating the direction and strength of relationships observed in this study.

5.1.3 Epidemiological consequences of infection

Our focus in this PhD has been on the within-host aspect of a PRRSV infection; however, the epidemiological consequences of PRRSV infection are also of concern to the industry. The variation in viraemia profiles may have important epidemiological consequences. Individuals with persistent viraemia profiles are likely to be infectious for longer. From an epidemiological perspective, viraemia rebound may constitute a problem as pigs diagnosed as cleared may have high levels of infectious virus a few days later. In particular, it would be useful to know whether virus rebound, or persistence, was associated with higher levels of infectiousness in future studies.

From the current study we cannot affirm that there would be infectious and epidemiological consequences in the secondary phase of rebound profiles. Inferences made on infectiousness and epidemiological consequences using the data obtained via quantitative RT-PCR may be limited due to the potential discrepancy between the measured viral genome load and the non-measured true infectious viral load. Thus, the observed secondary phase of rebound may be the result of detecting circulating junk genomes (i.e. non-functional genomes that do not play a role in the infection dynamics) rather than genomes of infectious particles and may thus have no significant epidemiological consequence. However, previous studies have explored the relationship between diverse viraemia measurements and infectiousness of pigs infected with PRRSV [111-113]. For example, Charpin et al. [111] detected viral genome in the blood of inoculated pigs from 7-77dpi using RT-PCR, whereas viral genome shedding was detectable from nasal swabs from 2-48dpi. Furthermore their study concluded that infectiousness was indeed correlated with the time course of viral-genome in the blood measured by RT-PCR and that the decrease in infectiousness was related to the increase in antibodies [111]. A North American PRRSV study observed that even when there were low levels of the virus replication the virus was easily transmitted and it was only by 260dpi that pigs were no longer able to transmit the virus to sentinel pigs [112]. Thus it has been established that some PRRSV-infected pigs can support virus replication and transmit infection for an extended period far beyond the duration of the secondary phase of the profiles in our study. By this logic one may argue that the observed rebound in viral genome load may indeed have biological consequences in terms of viral shedding and transmission to susceptible animals.

5.1.4 Sequencing the virus from rebound, persistent and cleared pigs to understand viraemia profile variation

To explore the hypothesis of virus mutation driving the variation in viraemia profiles it could be informative to sequence the virus taken from pigs from the different viraemia classifications to determine which specific viral regions, if any, that under-go change are associated to the observed viraemia trends in future studies: knowledge that could help us understand the causes behind the observed variation in viraemia profiles. There are plans to sequence the virus from the PHGC infected pigs in future studies.

5.2 Limitations

5.2.1 Viraemia and the immune responses: could different underlying immune responses result in similar observed viraemia?

The role of cytokines such as CCL2 and the orientation of the adaptive immune response needs to be determined in future studies since the mechanisms associated with a prolonged infection or persistent viraemia profile have not yet been fully determined [114]. It is possible that pigs could differ quite considerably in their underlying *in vivo* immune responses to PRRSV challenge and yet have the same infection duration and observed viraemia profiles. A recent process based modelling study [110] and a review of the PRRSV literature [42,59,69,115] indicates that some of the key mechanisms assumed to determine the infection duration appear to be contradictory. In previous PRRSV infection studies high viraemia, infection duration and host susceptibility has been found to be associated to numerous factors, which will be discussed below.

The magnitude of the immune response could be related to the virulence and *in vivo* replication rate of the PRRSV strain [116,117]. PRRSV virus isolates differ in their virulence levels as indicated by the effect of isolate on the viraemia profiles in Chapter 2. The results from the study by Petry et al.[42] indicate that a more virulent PRRSV infection could result in both higher viraemia and higher expression of immune function genes. Virulent field isolates exhibit longer and more elevated viraemia profiles, and can induce a faster and more intense humoral response [118]. In the study by Johnson et al. [118] highly virulent PRRSV field isolates replicated to a substantially higher *in vivo* titre than attenuated or lower virulent isolates.

Antibody differences could be a reflection of the genetic differences between the PRRSV isolates. N-protein antibody responses have been found to be higher in pigs infected with more virulent isolates, as were their viraemia measures [118]. The antibody trends were similar between the isolates but differed in magnitude; thus providing evidence for a strong association between the humoral response

and the serum viraemia load [118]. Indeed, it would be interesting to compare and contrast the same immune measures from Chapter 4 obtained for the NVSL infection for the KS06 isolate. Although several more recent studies than [118] have explored antibody responses to PRRSV [119-121] they have not combined their analysis of the antibody responses directly with the viraemia profiles. Given the trends observed by Johnson et al, (2004) [118] and the more recent study using highly pathogenic PRRS strains by Wang et al, (2016) [117] we could expect to observe a less dominant humoral response for the less virulently KS06 infected pigs. However it is important to note that even without the development of nAbs viraemia resolution can occur in a PRRSV infection [67,114,122]. However during a PRRSV infection the levels of nAbs typically remain low, when compared to other respiratory infections. Hence a strong but ineffective antibody response could be responsible for persistent viraemia profiles, i.e. a longer infection duration[81], indeed persistent profiles had a higher nAb cross-protectivity in Chapter 3.

The antiviral cytokine IFNA appears to play a significant role during the PRRSV infection in this thesis and was found to be associated with viraemia measures through the course of infection and also captured differences between rebound and non-rebound pigs in Chapter 4. Previous PRRSV studies typically report a down-regulation of this anti-viral cytokine in vitro [68,123]. However the more recent in vivo study using the NVSL strain in pregnant gilts, observed similar trends in IFNA response to the IFNA profiles typically observed in Chapter 4 of this thesis [69].

In the PRRSV literature it has been reported that infection often leads to a low cellular and anti-viral cytokine responses, for both the North American and European PRRSV strains [42,57,124-126], however there appear to be contradictory reports. A strong cellular response does not always result in a short infection duration [127]. Hence we can hypothesise that differing immune responses could potentially result in the same infection duration and viraemia trends or profiles.

Suppression of the innate system during a PRRSV infection could be responsible for the persistent or prolonged viraemia profiles. It has been reported that PRRSV can suppress phagocytosing activity, the expression of innate cytokines and alter their expression patterns [67,124]. However in Chapter 4 we found that there were no marked differences between the cytokine expression profiles between persistent and cleared profile for all the cytokines except IFNA; similar cytokine expression, with the exclusion of IFNA, led to different trends in viraemia profiles and infection duration. The underlying mechanism behind the variation in observed viraemia profiles is not yet completely understood. However since viraemia class differences were reflected in the anti-viral cytokine IFNA (Chapter 4) we could hypothesise that higher viraemia drives a stronger expression of IFNA. Higher IFNA expression was associated to persistent profiles between 7-21dpi and rebound profiles between 21-35dpi. High levels of CCL2 from 21dpi suggest that rebound could be driven by the recruitment of

new susceptible cells to the site of infection [69]. We have found that the strain, and its virulence, also impacts upon the viraemia profiles in Chapter 2. It would be interesting to assess antibody and cytokine differences between strains and see where the time trends differed in the timings and magnitude of the immune measures in future studies.

5.2.2 Challenge and strain specific conditions

The PRRSV isolates used in this thesis are all North American strains; the results from the European strain are likely to differ quite considerably due to the differences in the severity, virulence and immune responses elicited between the virus types [115]. Longitudinal data can allow us to explore temporal evolution within a host. There exist three main types of PRRSV infection data explored in previous studies: field data, *in vitro* infection data, and *in vivo* challenge data. We were ultimately concerned with the *in vivo* PRRSV challenge infection data in this thesis. It may be hard to disentangle cause and effect using data from field studies due to the likelihood of co-infections making the data incredibly noisy. Furthermore in field conditions it is typical that PRRS exists as waves of subclinical infection over several weeks in non-adult pigs [128]. The results and trends observed *in vitro* may not always be representative of what occurs during *in vivo* infection due to complex *in vivo* dynamics that would not be captured [68]. However *in vivo* studies with large numbers of replicates can be expensive requiring a large number of resources, and be relatively time consuming to conduct. The challenge conditions however are useful for limiting the impact of other disease causing pathogens, however it may not be fully representative of what we observe in the field; thus we need to validate our findings using data taken from field conditions in future studies.

5.2.3 Weight gain and tolerance to infection

There are three broad areas for potential improvement in pigs following a PRRSV challenge: resilience, resistance and tolerance [129]. Resilience can be defined as the ability of animals to maintain relatively undiminished performance levels whilst subjected to a pathogen challenge, resistance can be defined as the ability to reduce pathogen establishment, and tolerance can be defined as the ability to maintain performance by counteracting the pathogen causing damage [129]. It has been proposed that selection for the improved health of pigs should include disease resistance and disease resilience, the latter traits could be based on immune measures, disease incidence or the survival rates of pigs [129,130]. Weight gain under infection and tolerance to infection are also important traits for livestock production, which play a part in the control of a disease and reflect the impact of infection on health and production that have not been explored in this thesis. For growing piglets infected with PRRSV an important performance trait would be weight gain under infection [131]. The classification of the PHGC infected pigs by the combined virus load and weight gain responses under infection indicates that some pigs were “tolerant” to infection; for a subset of pigs weight gain was relatively high despite infection[58]. The identification of tolerance genomic markers may be challenging due to the complex statistical models required for obtaining tolerance estimates [132].

The relationship between viraemia and weight gain is likely to depend partly on the viral strain. In Appendix 3 it was found that pig growth tended to be less stunted when pigs were infected with the KS06 isolate compared to the NVSL isolate. This may be because piglets infected with the KS06 isolate do not need to put as much energy into eliminating the virus, thus allowing them to place more emphasis on growth. These results are consistent with the resource allocation theory, which hypothesizes that trade-offs between competing traits (e.g. health and growth) are a consequence of limited resources (i.e. energy availability) [50]. The genetic correlations between viraemia and weight gain varied over time and tended to be more extreme in NVSL infected pigs than KS06 infected pigs, suggesting that more energy is required to fight infection with NVSL, and is supported by the lower weight gain observed during an NVSL infection.

5.3 Conclusions

In conclusion following an in vivo PRRSV challenge we observe a wide variation in the viraemia profiles with: cleared (uni-modal resolution of viraemia by 42dpi), persistent (uni-modal detectable viraemia by 42dpi) and rebound (bimodal profiles) being observed. Identification of the viraemia classes can be used in the selection of candidate pigs from which the virus is sequenced, in future studies, in order to determine which specific viral regions, if any, under-go change are associated to viraemia trends, and if indeed the quasispecies hypothesis for rebound is correct. The Wood’s and

Extended Wood's model analysis allowed for the characterisation of the viraemia curve characteristics and has generated valuable new phenotypes for subsequent genetic analysis for the selection of pigs with desirable infection traits. However our findings need to be validated in field conditions, across further PRRSV isolates and the epidemiological consequences of rebound need to be determined. The viraemia trends were captured in immune measures of the longitudinal serum cytokine profiles for IFNA, CCL2 and the breadth of the nAb cross-protection; associations which generate new hypothesis of the causative immune mechanisms for the observed viraemia variation to be tested in future experimental studies. Future studies measuring the serum cytokine levels should use smaller intervals between observations to allow for the innate dynamics to be captured. Inter-host differences in cytokine responsiveness, and breed differences in certain cytokine time-trends, indicate that the role of the measured immune response in serum is highly variable, complex and yet can lead to similar viraemia trends. Ultimately the statistical characterisation of pigs according to viraemia response, cytokine response and nAb cross-protection could be used in the identification of desirable traits for commercial pigs in future quantitative genetic studies. Furthermore the identification of broad nAb cross-protective pigs, could be used to breed for a "vaccine-ready" pig if future quantitative genetic studies found strong genomic associations to the breadth of nAb response. It is interesting that there was variation in the responsiveness in certain cytokines; with pigs being defined as responders or non-responders according to each cytokine profile. The statistical categorization of pigs according to immune responses in this thesis could be used in future studies exploring immune-competence of the host during PRRSV infection. However it remains a biological enigma as to why the cytokine responsiveness was not a strong predictor and was poorly reflected in the viraemia profile trends; in future studies it would be interesting to determine what measures during infection the cytokine responsiveness is related to. The answer could lie in the fact that in this thesis we are analysing measurements taken from the serum, hence it would be useful to contrast the associations found in this thesis with the associations found for comparable measures but taken at the site of infection. The methods of parameterising the host response to a PRRSV infection used in this thesis including analysis via the Woods model for viraemia and the assessment of the change in cytokine baseline levels using cubic splines have the potential to be used on data from other PRRSV challenge trials and for other infectious disease data. Indeed subsequent studies have already utilised the models developed in this thesis thus pointing to the impact of the work in this thesis for the development of enhancing our understanding of a PRRSV infection [49,133]. Ultimately we have identified new key questions that could be explored in future studies such as: what immune processes cause the variation in observed viraemia, and what is the role of CCL2 in a PRRSV infection?

A summary of the answers to the scientific questions raised in the introduction of this thesis:

From Chapter 2 we apply the linear mixed model framework to analyse viraemia time trends and the corresponding influencing factors:

- The PHGC viraemia follows the time trend of rise to a peak by 7dpi followed by a decline to viraemia clearance.
- Inter-host variation increases over time and there are a subset of viraemia profiles that exhibit bimodal behaviour in the viraemia after the initial peak.
 - The time trends of the viraemia are influenced by the virus isolate, genetic background, PHGC trial and WUR genotype.
 - NVSL viraemia profiles have a higher peak, faster rate of decline than KS06 infected pigs.
- The bimodal viraemia profiles could not be adequately captured in the linear mixed models framework.
- The presence of bimodal viraemia profiles reduce the model fit to the data but do not impact upon the significance of the significant fixed effects.

The limitations in the ability to fit bimodal functions and the poor fit of the linearized approach in Chapter 2 led to a Bayesian model fitting approach being adopted in Chapter 3:

- Viraemia rebound (or bimodal viraemia profile) phenomenon occurred across all trials and viraemia isolates (NVSL and KS06).
- Information derived from the early stage of infection could not be used to predict viraemia rebound.
- The Woods model and the extended Woods model successfully quantified the inter-host variation from all types of viraemia profiles.
- An objective method of classifying viraemia profiles using the model fits was derived.
- The Woods model adequately represented the full range of viraemia profiles obtained from this large scale PRRSV infection experiment, and was used these to determine quantitative characteristics of infection dynamics.
 - Derived parameters of the model represented the peak viraemia, time to the peak etc.
- There was a strong homologous nAb response
 - Clearance profiles had a less diverse nAb response than persistent profiles
 - Persistent profiles had a more diverse response than rebound profiles
 - There was no significant difference between clearance and rebound nAb response
 - WUR genotype did not have a significant effect on the nAb response

In Chapter 4 we combined the viraemia profiles with measures of the immune response in the form of longitudinal cytokine profiles:

- Distinct time trends following infection were observed in IFNA and CCL2
- There was variation in the responsiveness in the measured cytokines
 - The time trends for IFNA, CCL2 and IL-8 captured the viraemia profile class rebound
 - Persistence and cleared profiles were not distinguishable from the cytokine expression profiles
 - The genetic background differences were captured in different baseline levels of expression (0dpi) but the general time trends remained the same across the genetic backgrounds.
 - The WUR genotype had little impact on the expression of the majority of the measured cytokines
 - Higher IFNA was observed for the WUR 2 genotype at 4dpi indicates the more resistant WUR 2 pigs could be due to a stronger early anti-viral response.
- CCL2 was a significant predictor of early IFNA expression and vice versa
- The majority of pigs were responders in IFNA and CCL2
- Rebound pigs had a narrower cytokine response
- Genetic background 1 had a broader response than genetic background 3
- The WUR genotype was not associated with the responsiveness in the cytokines
- The cytokines CCL2 and IFNA driving viraemia is a stronger relationship then vice versa
- CCL2 has slower dynamics than IFNA
- Rebound in CCL2 could be related to an influx of macrophages at the site of infection thus driving the rebound infection dynamics

References for Chapter 5

1. Wood PDP (1967) ALGEBRAIC MODEL OF LACTATION CURVE IN CATTLE. *Nature* 216: 164-8.
2. Boddicker N, Waide EH, Rowland RRR, Lunney JK, Garrick DJ, et al. (2012) Evidence for a major QTL associated with host response to Porcine Reproductive and Respiratory Syndrome Virus challenge. *Journal of Animal Science* 90: 1733-1746.
3. Boddicker NJ, Bjorkquist A, Rowland RRR, Lunney JK, Reecy JM, et al. (2014) Genome-wide association and genomic prediction for host response to porcine reproductive and respiratory syndrome virus infection. *Genetics Selection Evolution* 46.
4. Boddicker NJ, Garrick DJ, Rowland RRR, Lunney JK, Reecy JM, et al. (2014) Validation and further characterization of a major quantitative trait locus associated with host response to experimental infection with porcine reproductive and respiratory syndrome virus. *Animal Genetics* 45: 48-58.
5. Jacoby WG (2000) Loess: a nonparametric, graphical tool for depicting relationships between variables. *Electoral Studies* 19: 577-613.
6. Trefan L, Bünger L, Bloom-Hansen J, Rooke J, Salmi B, et al. (2011) Meta-analysis of the effects of dietary vitamin E supplementation on α -tocopherol concentration and lipid oxidation in pork. *Meat Science* 87: 305-314.
7. English S, Bateman AW, Clutton-Brock TH (2012) Lifetime growth in wild meerkats: incorporating life history and environmental factors into a standard growth model. *Oecologia* 169: 143-153.
8. Brown H, Prescott R (2006) *Applied mixed models in medicine*: John Wiley West SussexUK.
9. Grossman M, Koops W (2003) Modeling extended lactation curves of dairy cattle: a biological basis for the multiphasic approach. *Journal of dairy science* 86: 988-998.
10. Wolfinger RD (1997) An example of using mixed models and PROC MIXED for longitudinal data. *Journal of Biopharmaceutical statistics* 7: 481-500.
11. Verbeke G, Molenberghs G (1997) *Linear mixed models in practice: a SAS oriented approach*. New York: Springer-Verlag
12. Meetings A-A-CN (2002) *Mixed Model Workshop*. Canada.
13. Littell R, Henry P, Ammerman C (1998) Statistical analysis of repeated measures data using SAS procedures. *Journal of Animal Science* 76: 1216-1231.
14. Schaeffer L (2004) Application of random regression models in animal breeding. *Livestock Production Science* 86: 35-45.
15. Durrleman S, Simon R (1989) Flexible regression models with cubic splines. *Statistics in medicine* 8: 551-561.
16. Friedman JH (1991) Multivariate adaptive regression splines. *The annals of statistics*: 1-67.
17. Huisman A, Veerkamp R, Van Arendonk J (2002) Genetic parameters for various random regression models to describe the weight data of pigs. *Journal of Animal Science* 80: 575-582.
18. Royston P, Sauerbrei W (2007) Multivariable modeling with cubic regression splines: a principled approach. *Stata Journal* 7: 45.
19. Sleeper LA, Harrington DP (1990) Regression splines in the Cox model with application to covariate effects in liver disease. *Journal of the American Statistical Association* 85: 941-949.
20. Institute S (1985) *SAS user's guide: statistics*: Sas Inst.
21. Fong Y, Rue H, Wakefield J (2009) Bayesian inference for generalized linear mixed models. *Biostatistics*: kxp053.
22. Liang F, Wong WH (2001) Real-parameter evolutionary Monte Carlo with applications to Bayesian mixture models. *Journal of the American Statistical Association* 96: 653-666.

23. Natarajan R, Kass RE (2000) Reference Bayesian methods for generalized linear mixed models. *Journal of the American Statistical Association* 95: 227-237.
24. Ronquist F, Huelsenbeck JP (2003) MrBayes 3: Bayesian phylogenetic inference under mixed models. *Bioinformatics* 19: 1572-1574.
25. Bolker BM, Brooks ME, Clark CJ, Geange SW, Poulsen JR, et al. (2009) Generalized linear mixed models: a practical guide for ecology and evolution. *Trends in ecology & evolution* 24: 127-135.
26. Pool M, Janss L, Meuwissen T (2000) Genetic parameters of Legendre polynomials for first parity lactation curves. *Journal of dairy science* 83: 2640-2649.
27. Buttchereit N, Stamer E, Junge W, Thaller G (2010) Evaluation of five lactation curve models fitted for fat: protein ratio of milk and daily energy balance. *Journal of dairy science* 93: 1702-1712.
28. Torshizi ME, Aslamenejad A, Nassiri M, Farhangfar H (2011) Comparison and evaluation of mathematical lactation curve functions of Iranian primiparous Holsteins. *South African Journal of Animal Science* 41: 104-115.
29. Kheirabadi K, Rashidi A, Alijani S, Imumorin I (2014) Modeling lactation curves and estimation of genetic parameters in Holstein cows using multiple-trait random regression models. *Animal Science Journal* 85: 925-934.
30. Meyer K (2005) Random regression analyses using B-splines to model growth of Australian Angus cattle. *Genetics Selection Evolution* 37: 473-500.
31. Beever D, Rook A, France J, Dhanoa M, Gill M (1991) A review of empirical and mechanistic models of lactational performance by the dairy cow. *Livestock Production Science* 29: 115-130.
32. Druet T, Jaffrézic F, Boichard D, Ducrocq V (2003) Modeling lactation curves and estimation of genetic parameters for first lactation test-day records of French Holstein cows. *Journal of dairy science* 86: 2480-2490.
33. Mulupuri P, Zimmerman JJ, Hermann J, Johnson CR, Cano JP, et al. (2008) Antigen-specific B-cell responses to porcine reproductive and respiratory syndrome virus infection. *Journal of virology* 82: 358-370.
34. Boddicker N, Waide E, Rowland R, Lunney J, Garrick D, et al. (2012) Evidence for a major QTL associated with host response to Porcine Reproductive and Respiratory Syndrome virus challenge. *Journal of Animal Science* 90: 1733-1746.
35. Reiner G, Willems H, Pesch S, Ohlinger V (2009) Variation in resistance to the porcine reproductive and respiratory syndrome virus (PRRSV) in Pietrain and Miniature pigs. *Journal of Animal Breeding and Genetics* 127: 100-106.
36. Murtaugh MP, Stadejek T, Abrahante JE, Lam TTY, Leung FCC (2010) The ever-expanding diversity of porcine reproductive and respiratory syndrome virus. *Virus Research* 154: 18-30.
37. Goldberg TL, Lowe JF, Milburn SM, Firkins LD (2003) Quasispecies variation of porcine reproductive and respiratory syndrome virus during natural infection. *Virology* 317: 197-207.
38. Costers S, Lefebvre DJ, Van Doorsselaere J, Vanhee M, Delputte PL, et al. (2010) GP4 of porcine reproductive and respiratory syndrome virus contains a neutralizing epitope that is susceptible to immunoselection in vitro. *Archives of virology* 155: 371-378.
39. Wills RW, Zimmerman JJ, Yoon KJ, McGinley MJ, Hill HT, et al. (1997) Porcine reproductive and respiratory syndrome virus: A persistent infection. *Veterinary Microbiology* 55: 231-240.
40. Wills RW, Doster AR, Galeota JA, Sur JH, Osorio FA (2003) Duration of infection and proportion of pigs persistently infected with porcine reproductive and respiratory syndrome virus. *Journal of Clinical Microbiology* 41: 58-62.
41. Mulupuri P, Zimmerman JJ, Hermann J, Johnson CR, Cano JP, et al. (2008) Antigen-specific B-cell responses to porcine reproductive and respiratory-syndrome-virus infection. *Journal of Virology* 82: 358-370.

42. Petry D, Lunney J, Boyd P, Kuhar D, Blankenship E, et al. (2007) Differential immunity in pigs with high and low responses to porcine reproductive and respiratory syndrome virus infection. *Journal of Animal Science* 85: 2075-2092.
43. Ostrowski M, Galeota JA, Jar AM, Platt KB, Osorio FA, et al. (2002) Identification of neutralizing and nonneutralizing epitopes in the porcine reproductive and respiratory syndrome virus GP5 ectodomain. *Journal of Virology* 76: 4241-4250.
44. Ansari IH, Kwon B, Osorio FA, Pattnaik AK (2006) Influence of N-linked glycosylation of porcine reproductive and respiratory syndrome virus GP5 on virus infectivity, antigenicity, and ability to induce neutralizing antibodies. *Journal of Virology* 80: 3994-4004.
45. Pirzadeh B, Gagnon CA, Dea S (1998) Genomic and antigenic variations of porcine reproductive and respiratory syndrome virus major envelope GP(5) glycoprotein. *Canadian Journal of Veterinary Research-Revue Canadienne De Recherche Veterinaire* 62: 170-177.
46. Ladinig A, Detmer SE, Clarke K, Ashley C, Rowland RRR, et al. (2015) Pathogenicity of three type 2 porcine reproductive and respiratory syndrome virus strains in experimentally inoculated pregnant gilts. *Virus Research* 203: 24-35.
47. Boddicker NJG, Dorian J.; Reecy, James M.; Rowland, Bob; Lunney, Joan K.; and Dekkers, Jack C. M. (2013) Quantitative Trait Locus on *Sus scrofa* Chromosome 4 Associated with Host Response to Experimental Infection with Porcine

Reproductive and Respiratory Syndrome Virus Animal Industry Report AS 659, ASL R2823.

48. Boddicker NJ, Garrick DJ, Rowland RRR, Lunney JK, Reecy JM, et al. (2013) Validation and further characterization of a major quantitative trait locus associated with host response to experimental infection with porcine reproductive and respiratory syndrome virus. *Animal Genetics*: n/a-n/a.
49. Hess AS, Boddicker N, Rowland B, Lunney J, Plastow G, et al. (2014) Validation of the Effects of a SNP on SSC4 Associated with Viral Load and Weight Gain in Piglets Experimentally Infected with a 2006 PRRS Virus Isolate. *Animal Industry Report* 660: 89.
50. Rauw WM (2008) Resource allocation theory applied to farm animal production. *Resource allocation theory applied to farm animal production*: 320 pp.-320 pp.
51. Lunney JK, Steibel JP, Reecy JM, Fritz E, Rothschild MF, et al. Probing genetic control of swine responses to PRRSV infection: current progress of the PRRS host genetics consortium; 2011. BioMed Central Ltd. pp. 30.
52. Vincent A, Thacker B, Halbur P, Rothschild M, Thacker E (2005) In vitro susceptibility of macrophages to porcine reproductive and respiratory syndrome virus varies between genetically diverse lines of pigs. *Viral immunology* 18: 506-512.
53. Vincent A, Thacker B, Halbur P, Rothschild M, Thacker E (2006) An investigation of susceptibility to porcine reproductive and respiratory syndrome virus between two genetically diverse commercial lines of pigs. *Journal of Animal Science* 84: 49-57.
54. Halbur P, Rothschild M, Thacker B, Meng XJ, Paul P, et al. (1998) Differences in susceptibility of Duroc, Hampshire, and Meishan pigs to infection with a high virulence strain (VR2385) of porcine reproductive and respiratory syndrome virus (PRRSV). *Journal of Animal Breeding and Genetics* 115: 181-189.
55. Lowe JF, Husmann R, Firkins LD, Zuckermann FA, Goldberg TL (2005) Correlation of cell-mediated immunity against porcine reproductive and respiratory syndrome virus with protection against reproductive failure in sows during outbreaks of porcine reproductive and respiratory syndrome in commercial herds. *Journal of the American Veterinary Medical Association* 226: 1707-1711.
56. Ait-Ali T, Wilson AD, Westcott DG, Clapperton M, Waterfall M, et al. (2007) Innate immune responses to replication of porcine reproductive and respiratory syndrome virus in isolated Swine alveolar macrophages. *Viral immunology* 20: 105-118.
57. Lunney JK, Chen H (2010) Genetic control of host resistance to porcine reproductive and respiratory syndrome virus (PRRSV) infection. *Virus Research* 154: 161-169.

58. Rowland RR, Joan Lunney, and Jack Dekkers. (2012) Control of porcine reproductive and respiratory syndrome (PRRS) through genetic improvement in disease resistance and tolerance. *Frontiers of Livestock Genomics*: 3:260.
59. Petry D, Holl J, Weber J, Doster AR, Osorio FA, et al. (2005) Biological responses to porcine respiratory and reproductive syndrome virus in pigs of two genetic populations. *Journal of Animal Science* 83: 1494-1502.
60. Royae AR, Husmann RJ, Dawson HD, Calzada-Nova G, Schnitzlein WM, et al. (2004) Deciphering the involvement of innate immune factors in the development of the host response to PRRSV vaccination. *Veterinary immunology and immunopathology* 102: 199-216.
61. Miller L, Laegreid W, Bono J, Chitko-McKown C, Fox J (2004) Interferon type I response in porcine reproductive and respiratory syndrome virus-infected MARC-145 cells. *Archives of virology* 149: 2453-2463.
62. Murtaugh MP, Xiao Z, Zuckermann F (2002) Immunological responses of swine to porcine reproductive and respiratory syndrome virus infection. *Viral immunology* 15: 533-547.
63. Calzada-Nova G, Schnitzlein WM, Husmann RJ, Zuckermann FA (2011) North American porcine reproductive and respiratory syndrome viruses inhibit type I interferon production by plasmacytoid dendritic cells. *Journal of virology* 85: 2703-2713.
64. Baumann A, Mateu E, Murtaugh MP, Summerfield A (2013) Impact of genotype 1 and 2 of porcine reproductive and respiratory syndrome viruses on interferon-alpha responses by plasmacytoid dendritic cells. *Vet Res* 44: 1186.
65. Lawson S, Lunney J, Zuckermann F, Osorio F, Nelson E, et al. (2010) Development of an 8-plex Luminex assay to detect swine cytokines for vaccine development: assessment of immunity after porcine reproductive and respiratory syndrome virus (PRRSV) vaccination. *Vaccine* 28: 5356-5364.
66. Gómez-Laguna J, Salguero FJ, De Marco MF, Pallarés FJ, Bernabé A, et al. (2009) Changes in lymphocyte subsets and cytokines during European porcine reproductive and respiratory syndrome: increased expression of IL-12 and IL-10 and proliferation of CD4⁺ CD8^{high}. *Viral immunology* 22: 261-271.
67. Mateu E, Diaz I (2008) The challenge of PRRS immunology. *The Veterinary Journal* 177: 345-351.
68. Buddaert W, Van Reeth K, Pensaert M (1998) In vivo and in vitro interferon (IFN) studies with the porcine reproductive and respiratory syndrome virus (PRRSV). *Coronaviruses and Arteriviruses*: Springer. pp. 461-467.
69. Ladinig A, Lunney JK, Souza CJ, Ashley C, Plastow G, et al. (2014) Cytokine profiles in pregnant gilts experimentally infected with porcine reproductive and respiratory syndrome virus and relationships with viral load and fetal outcome. *Veterinary research* 45: 113.
70. Dwivedi V, Manickam C, Binjawadagi B, Linhares D, Murtaugh MP, et al. (2012) Evaluation of immune responses to porcine reproductive and respiratory syndrome virus in pigs during early stage of infection under farm conditions. *Virology journal* 9: 1.
71. Guo B, Lager KM, Henningson JN, Miller LC, Schlink SN, et al. (2013) Experimental infection of United States swine with a Chinese highly pathogenic strain of porcine reproductive and respiratory syndrome virus. *Virology* 435: 372-384.
72. Janeway C, Murphy KP, Travers P, Walport M (2008) *Janeway's immunobiology*: Garland Science.
73. Labarque GG, Nauwynck HJ, Van Reeth K, Pensaert MB (2000) Effect of cellular changes and onset of humoral immunity on the replication of porcine reproductive and respiratory syndrome virus in the lungs of pigs. *Journal of general virology* 81: 1327-1334.
74. Xiao Z, Batista L, Dee S, Halbur P, Murtaugh MP (2004) The level of virus-specific T-cell and macrophage recruitment in porcine reproductive and respiratory syndrome virus infection in pigs is independent of virus load. *Journal of virology* 78: 5923-5933.
75. Flori L, Gao Y, Oswald IP, Lefevre F, Bouffaud M, et al. Deciphering the genetic control of innate and adaptive immune responses in pig: a combined genetic and genomic study; 2011. *BioMed Central*. pp. S32.

76. Lewis CRG, Ait-Ali T, Clapperton M, Archibald AL, Bishop S (2007) Genetic perspectives on host responses to porcine reproductive and respiratory syndrome (PRRS). *Viral immunology* 20: 343-358.
77. Lewis C, Torremorell M, Bishop S (2009) Effects of porcine reproductive and respiratory syndrome virus infection on the performance of commercial sows and gilts of different parities and genetic lines. *J Swine Health Prod* 17: 140-147.
78. Mach N, Gao Y, Lemonnier G, Lecardonnel J, Oswald IP, et al. (2013) The peripheral blood transcriptome reflects variations in immunity traits in swine: towards the identification of biomarkers. *BMC genomics* 14: 894.
79. Wang J, Wang Y, Wang H, Wang H, Liu J-F, et al. (2016) Transcriptomic Analysis Identifies Candidate Genes and Gene Sets Controlling the Response of Porcine Peripheral Blood Mononuclear Cells to Poly I: C Stimulation. *G3: Genes| Genomes| Genetics* 6: 1267-1275.
80. Niu P, Kim SW, Kim WI, Kim KS (2015) Association analyses of DNA polymorphisms in immune-related candidate genes GBP1, GBP2, CD163, and CD169 with porcine growth and meat quality traits. *Journal of Biomedical Research* 16: 40-46.
81. Darwich L, Díaz I, Mateu E (2010) Certainties, doubts and hypotheses in porcine reproductive and respiratory syndrome virus immunobiology. *Virus Research* 154: 123-132.
82. Lopez OJ, Osorio FA (2004) Role of neutralizing antibodies in PRRSV protective immunity. *Veterinary Immunology and Immunopathology* 102: 155-163.
83. Burton DR (2002) Antibodies, viruses and vaccines. *Nature Reviews Immunology* 2: 706-713.
84. Chand RJ, Tribble BR, Rowland RRR (2012) Pathogenesis of porcine reproductive and respiratory syndrome virus. *Current Opinion in Virology* 2: 256-263.
85. Huang YW, Meng XJ (2010) Novel strategies and approaches to develop the next generation of vaccines against porcine reproductive and respiratory syndrome virus (PRRSV). *Virus Research* 154: 141-149.
86. Vu HL, Kwon B, Yoon K-J, Laegreid WW, Pattnaik AK, et al. (2011) Immune evasion of porcine reproductive and respiratory syndrome virus through glycan shielding involves both glycoprotein 5 as well as glycoprotein 3. *Journal of virology* 85: 5555-5564.
87. Zhou L, Ni Y-Y, Piñeyro P, Sanford BJ, Cossaboom CM, et al. (2012) DNA shuffling of the GP3 genes of porcine reproductive and respiratory syndrome virus (PRRSV) produces a chimeric virus with an improved cross-neutralizing ability against a heterologous PRRSV strain. *Virology* 434: 96-109.
88. Lewis CRG, Ait-Ali T, Clapperton M, Archibald AL, Bishop SC (2007) Genetic perspectives on host responses to porcine reproductive and respiratory syndrome (PRRS). *Viral Immunology* 20: 343-357.
89. Hess A, Islam Z, Hess MK, Rowland RRR, Lunney JK, et al. (2016) Comparison of Host Genetic Factors Influencing Piglet Response to Infection with Two Isolates of Porcine Reproductive and Respiratory Syndrome Virus. Submitted to *Genet Sel Evol*.
90. Serao NVL, Matika O, Kemp RA, Harding JCS, Bishop SC, et al. (2014) Genetic analysis of reproductive traits and antibody response in a PRRS outbreak herd. *Journal of Animal Science* 92: 2905-2921.
91. Hess AS, Tribble B, Wang Y, Rowland B, Lunney J, et al. (2014) Factors Associated with N-specific IgG Response in Piglets Experimentally Infected with Porcine Reproductive and Respiratory Syndrome Virus. *Animal Industry Report* 660: 90.
92. Kurosaki T, Kometani K, Ise W (2015) Memory B cells. *Nature Reviews Immunology* 15: 149-159.
93. Delisle B, Gagnon CA, Lambert M-E, D'Allaire S (2012) Porcine reproductive and respiratory syndrome virus diversity of Eastern Canada swine herds in a large sequence dataset reveals two hypervariable regions under positive selection. *Infection Genetics and Evolution* 12: 1111-1119.
94. Tribble BR, Popescu LN, Monday N, Calvert JG, Rowland RRR (2015) A Single Amino Acid Deletion in the Matrix Protein of Porcine Reproductive and Respiratory Syndrome Virus Confers

- Resistance to a Polyclonal Swine Antibody with Broadly Neutralizing Activity. *Journal of Virology* 89: 6515-6520.
95. Delisle B, Gagnon CA, Lambert M-È, D'Allaire S (2012) Porcine reproductive and respiratory syndrome virus diversity of Eastern Canada swine herds in a large sequence dataset reveals two hypervariable regions under positive selection. *Infection, Genetics and Evolution* 12: 1111-1119.
 96. Tribble BR, Popescu LN, Monday N, Calvert JG, Rowland RR (2015) A single amino acid deletion in the matrix protein of porcine reproductive and respiratory syndrome virus confers resistance to a polyclonal swine antibody with broadly neutralizing activity. *Journal of virology* 89: 6515-6520.
 97. Lunney JK, Fritz ER, Reecy JM, Kuhar D, Prucnal E, et al. (2010) Interleukin-8, interleukin-1 β , and interferon- γ levels are linked to PRRS virus clearance. *Viral immunology* 23: 127-134.
 98. Perelson AS, Kirschner DE, De Boer R (1993) Dynamics of HIV infection of CD4+ T cells. *Mathematical biosciences* 114: 81-125.
 99. Dominik Wodarz ALL, Vincent A. A. Jansen And Martin A. Nowak (1999) Dynamics of Macrophage and T cell infection by HIV. *Journal of Theoretical Biology* 196: 101-113.
 100. Perelson AS, Neumann AU, Markowitz M, Leonard JM, Ho DD (1996) HIV-1 dynamics in vivo: virion clearance rate, infected cell life-span, and viral generation time. *Science* 271: 1582-1586.
 101. Leslie A, Pfafferoth K, Chetty P, Draenert R, Addo M, et al. (2004) HIV evolution: CTL escape mutation and reversion after transmission. *Nature medicine* 10: 282-289.
 102. Wodarz D, Nowak MA (2002) Mathematical models of HIV pathogenesis and treatment. *BioEssays* 24: 1178-1187.
 103. Wei XP, Ghosh SK, Taylor ME, Johnson VA, Emini EA, et al. (1995) Viral Dynamics In Human-Immunodeficiency-Virus Type-1 Infection. *Nature* 373: 117-122.
 104. Saenz RA, Quinlivan M, Elton D, MacRae S, Blunden AS, et al. (2010) Dynamics of influenza virus infection and pathology. *Journal of virology* 84: 3974-3983.
 105. Pawelek KA, Huynh GT, Quinlivan M, Cullinane A, Rong L, et al. (2012) Modeling within-host dynamics of influenza virus infection including immune responses. *PLoS computational biology* 8: e1002588.
 106. Beauchemin C, Samuel J, Tuszynski J (2005) A simple cellular automaton model for influenza A viral infections. *Journal of Theoretical Biology* 232: 223-234.
 107. Go N (2014) Modelling the immune response to the Porcine Reproductive and Respiratory Syndrome virus: AgroParisTech.
 108. Doeschl-Wilson A, Galina-Pantoja L (2010) Using Mathematical Models to Gain Insight into Host-Pathogen Interaction in Mammals: Porcine Reproductive and Respiratory Syndrome. *Host-Pathogen Interactions: Genetics, Immunology, Physiology* Nova Science Publishers Inc, New York
- 109-131
109. Baccam P, Beauchemin C, Macken CA, Hayden FG, Perelson AS (2006) Kinetics of influenza A virus infection in humans. *Journal of virology* 80: 7590-7599.
 110. Go N, Bidot C, Belloc C, Touzeau S (2014) Integrative model of the immune response to a pulmonary macrophage infection: what determines the infection duration? *PloS one* 9: e107818.
 111. Charpin C, Mahe S, Keranflec'h A, Madec F, Belloc C, et al. Estimation of time-dependent infectiousness of pigs infected by the Porcine Reproductive and Respiratory Syndrome virus (PRRSV): correlation with the viral genome load in blood, nasal swabs and the serological response; 2012. Institut du Porc. pp. 67-72.

112. Rowland R, S Lawson, K Rossow, DA Benfield (2003) Lymphotropism of porcine reproductive and respiratory syndrome virus replication during persistent infection of pigs originally exposed to virus in utero. *Vet Micro* 96: 219-235.
113. Rowland RR, Steffen M, Ackerman T, Benfield DA (1999) The evolution of porcine reproductive and respiratory syndrome virus: quasispecies and emergence of a virus subpopulation during infection of pigs with VR-2332. *Virology* 259: 262-266.
114. Murtaugh MP, Genzow M (2011) Immunological solutions for treatment and prevention of porcine reproductive and respiratory syndrome (PRRS). *Vaccine* 29: 8192-8204.
115. Lunney JK, Fang Y, Ladinig A, Chen N, Li Y, et al. (2015) Porcine Reproductive and Respiratory Syndrome Virus (PRRSV): Pathogenesis and Interaction with the Immune System. *Annual review of animal biosciences* 4 (2016): : 129-154.
116. Hu S, Zhang Z, Liu Y, Tian Z, Wu D, et al. (2013) Pathogenicity and distribution of highly pathogenic porcine reproductive and respiratory syndrome virus in pigs. *Transboundary and emerging diseases* 60: 351-359.
117. Wang G, Yu Y, Zhang C, Tu Y, Tong J, et al. (2016) Immune responses to modified live virus vaccines developed from classical or highly pathogenic PRRSV following challenge with a highly pathogenic PRRSV strain. *Developmental & Comparative Immunology* 62: 1-7.
118. Johnson W, Roof M, Vaughn E, Christopher-Hennings J, Johnson CR, et al. (2004) Pathogenic and humoral immune responses to porcine reproductive and respiratory syndrome virus (PRRSV) are related to viral load in acute infection. *Veterinary immunology and immunopathology* 102: 233-247.
119. Serão N, Matika O, Kemp R, Harding J, Bishop S, et al. (2014) Genetic analysis of reproductive traits and antibody response in a PRRS outbreak herd. *Journal of Animal Science* 92: 2905-2921.
120. Brown E, Lawson S, Welbon C, Gnanandarajah J, Li J, et al. (2009) Antibody response to porcine reproductive and respiratory syndrome virus (PRRSV) nonstructural proteins and implications for diagnostic detection and differentiation of PRRSV types I and II. *Clinical and Vaccine Immunology* 16: 628-635.
121. Gao J, Xiao S, Xiao Y, Wang X, Zhang C, et al. (2016) MYH9 is an Essential Factor for Porcine Reproductive and Respiratory Syndrome Virus Infection. *Scientific Reports* 6.
122. Nelson EA, Christopher-Hennings J, Benfield DA (1994) Serum immune responses to the proteins of porcine reproductive and respiratory syndrome (PRRS) virus. *Journal of Veterinary Diagnostic Investigation* 6: 410-415.
123. Genini S, Delputte PL, Malinverni R, Cecere M, Stella A, et al. (2008) Genome-wide transcriptional response of primary alveolar macrophages following infection with porcine reproductive and respiratory syndrome virus. *Journal of general virology* 89: 2550-2564.
124. Kimman TG, Cornelissen LA, Moormann RJ, Rebel JMJ, Stockhofe-Zurwieden N (2009) Challenges for porcine reproductive and respiratory syndrome virus (PRRSV) vaccinology. *Vaccine* 27: 3704-3718.
125. Díaz I, Gimeno M, Darwich L, Navarro N, Kuzemtseva L, et al. (2012) Characterization of homologous and heterologous adaptive immune responses in porcine reproductive and respiratory syndrome virus infection. *Vet Res* 43: 1186.
126. Weesendorp E, Morgan S, Stockhofe-Zurwieden N, Popma-De Graaf DJ, Graham SP, et al. (2013) Comparative analysis of immune responses following experimental infection of pigs with European porcine reproductive and respiratory syndrome virus strains of differing virulence. *Veterinary microbiology* 163: 1-12.
127. Murtaugh MP (2005) PRRS immunology: what are we missing. Presentation in Nanjing.
128. Amadori M, Razzuoli E (2014) Immune control of PRRS: lessons to be learned and possible ways forward. *Frontiers in Veterinary Science* 1.
129. Andrea B. Doeschl-Wilson GL (2014) Inferring genetic resilience of animals to infectious pathogens— opportunities and pitfalls. *Breeding Focus 2014 – Improving Resilience*.

130. S. Hermes LL, A. B. Doeschl-Wilson, H. Gilbert (2015) Selection for productivity and robustness traits in pigs. *Animal Production Science* 55: 1437–1447.
131. Doeschl-Wilson AB, Kyriazakis I (2012) Should we aim for genetic improvement in host resistance or tolerance to infectious pathogens? *Frontiers in Genetics* 3: 5.
132. Doeschl-Wilson AB, Villanueva B, Kyriazakis I (2012) The first step toward genetic selection for host tolerance to infectious pathogens: obtaining the tolerance phenotype through group estimates. Should we aim for genetic improvement in host resistance or tolerance to infectious disease? 3: 7-18.
133. Hess AS, Islam Z, Hess MK, Rowland RR, Lunney JK, et al. (2016) Comparison of host genetic factors influencing pig response to infection with two North American isolates of porcine reproductive and respiratory syndrome virus. *Genetics Selection Evolution* 48: 43.

Appendix 1

The effect of the removal of bimodal profiles on the linearized Woods model curves from Chapter 3

1. Virus differences: removing the bimodal profiles

The removal of the bimodal profiles (i.e. model fitting to dataset 2) results in the same significant fixed and random effects in the final linearized Wood's model and parameter differences.

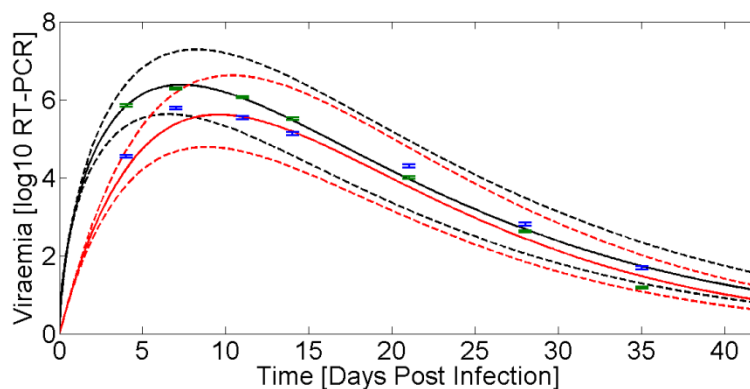


Figure S1 Wood's model for dataset 2: Virus 1(NVSL) in black and Virus 2(KS06) in red. The dashed lines delimit the respective confidence intervals constructed by the model predictions from the upper and lower parameter estimates determined by: $LSM(\text{model parameter}) \pm 1.96 SE(\text{model parameter})$. Repeated measures model with bimodal removed: Virus 1 (NVSL) in green and Virus 2 (KS06) in blue.

2. WUR genotype differences: removing the bimodal profiles

The removal of the bimodal profiles (fitting the model to dataset 2) results in the same significant fixed and random effects in the final linearized Wood's model and significant parameter differences.

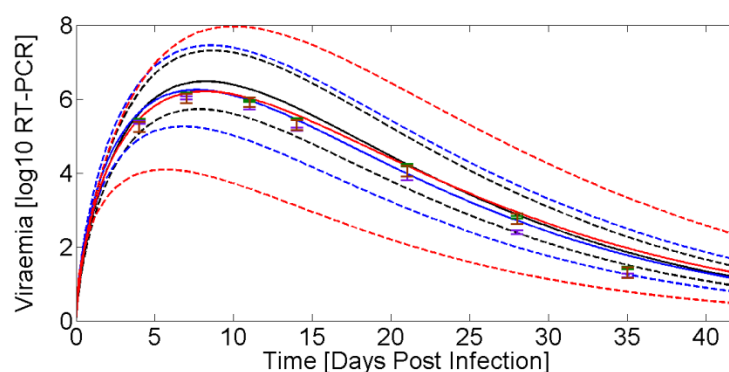


Figure S2 Wood's model predictions for WUR genotype 0(black), 1(blue), 2(red). The WUR genotype 0 has the highest level of peak viraemia compared to WUR 1 and 2. The dashed lines delimit the respective confidence intervals constructed by the model predictions from the upper and lower parameter estimates determined by: $LSM(\text{model parameter}) \pm 1.96 SE(\text{model parameter})$.

3. Genetic background differences: removing the bimodal profiles

The removal of the bimodal profiles results in the same significant fixed and random effects in the final linearized Wood's model for the genetic groups.

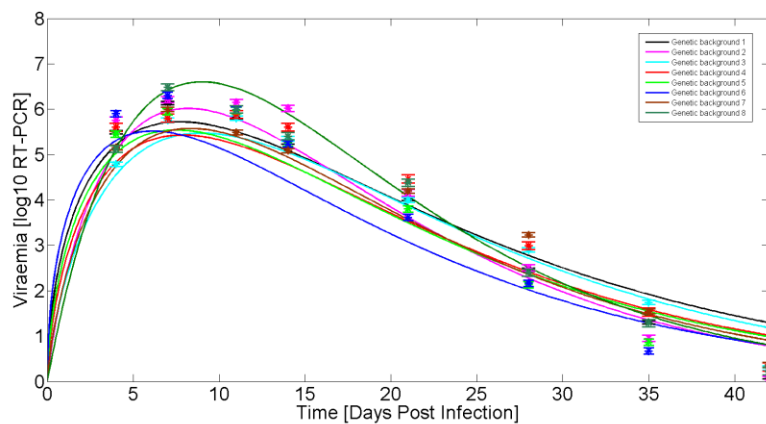


Figure S3 Wood's model predictions for each genetic background (lines) and the repeated measure model LSMs for each genetic group (asterisks) from dataset 2.

4.The PHGC trial

The Woods models and repeated measures approach yield similar results for dataset 2, when bimodal profiles are removed as shown in **Figure S4**.

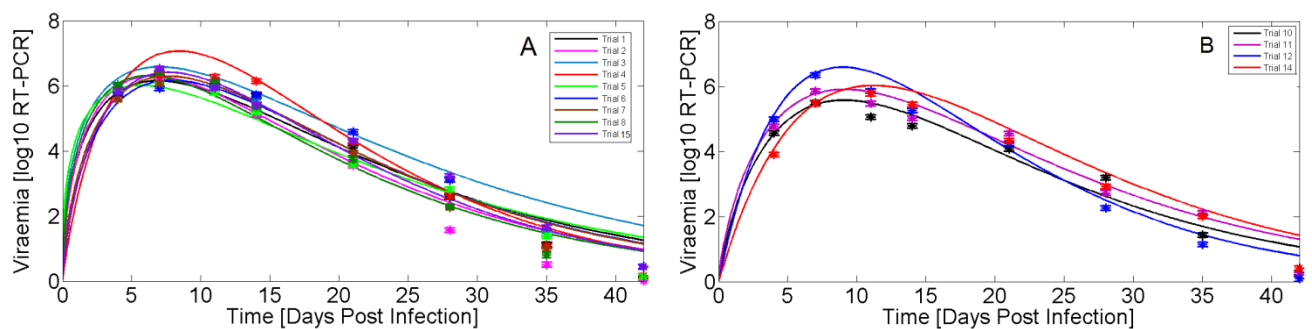


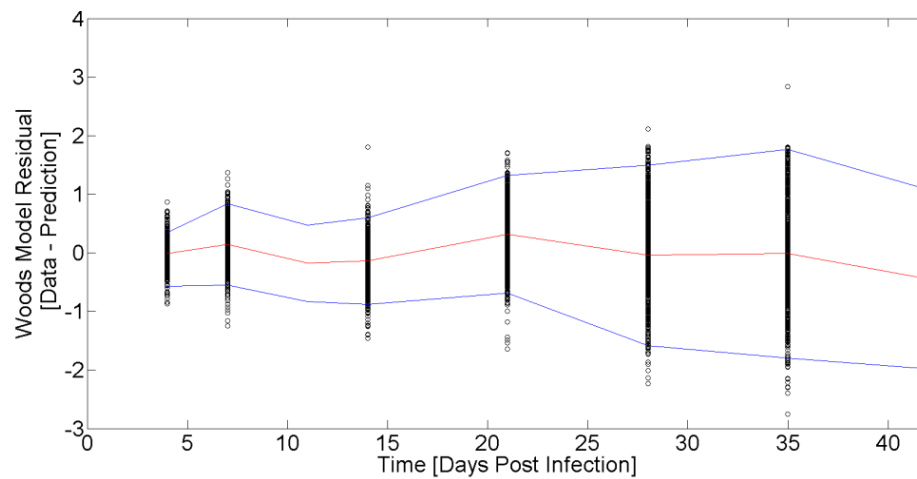
Figure S4 Wood's model for each trial (lines) and the repeated measures LSMs (asterisks). **Figure S4A** are the trials infected with virus 1(NVSL), and **Figure S4B** are the trials infected with virus 2(KS06).

Appendix 2

KS06 Wood's and Extended Wood's model residuals

The model residuals for the KS06 infected pigs followed similar trends to NVSL infected pigs. In this Appendix the model residual plots for KS06 pigs are shown.

A



B

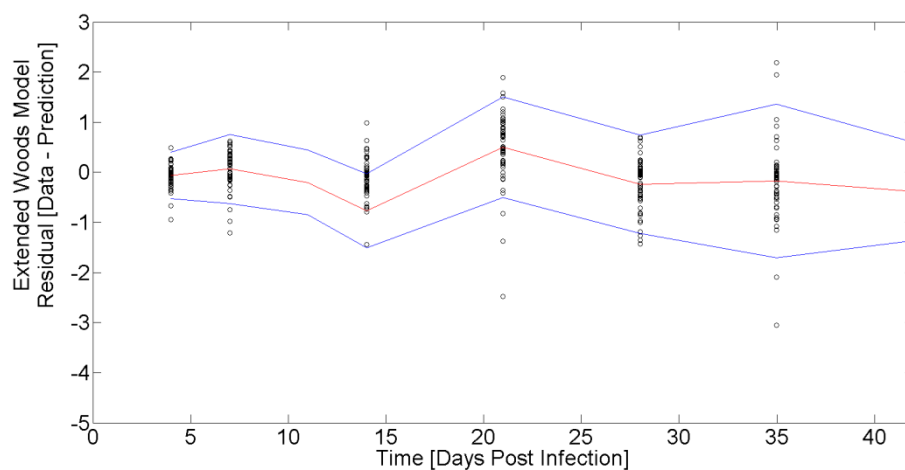


Figure S5 The Wood's model residuals (A) and the Extended Wood's model residuals (B) for the KS06 isolate. The red lines show the residual mean and the blue lines delimit two standard deviations from the mean.

Appendix 2b

The breadth of nAb cross-protectivity was distributed similarly across the WUR genotypes as shown in Table 4.9. Given that the allele acts in a dominant manner the WUR classes 1 and 2 were pooled (WUR Y) and further odds ratios were obtained to compare differences between the WUR 0 and pigs with the favourable B allele. There were not any statistically significant associations (at the 95% significance level) between the WUR genotype and the nAb cross-protectivity as shown in Table 4.10.

WUR genotype	No cross protection (% within WUR class)	Cross protection (% within WUR class)
0	188 (59)	131 (41)
1	67 (61)	42 (39)
2	8 (73)	3 (27)
Y (Pooled WUR 1 & 2)	75 (62.5)	45 (37.5)

Table 4.9 The distribution of the nAb cross-protectivity by WUR genotype.

Class 1	Class 2	Odds ratio (95% Confidence interval)	P- value
Clearance	Persistence	0.61 (0.38, 0.98)	0.04
Clearance	Rebound	0.86 (0.53, 1.38)	0.53
Persistence	Rebound	1.40 (0.80, 2.45)	0.24
Class 1	Class 2	Odds ratio (95% Confidence interval)	P- value
WUR 0	WUR 1	1.06 (0.68, 1.68)	0.79
WUR 0	WUR 2	1.72 (0.43, 6.81)	0.44
WUR 1	WUR 2	1.62 (0.39, 6.64)	0.51
Class 1	Class 2	Odds ratio (95% Confidence interval)	P- value
WUR 0	WUR Y	1.107 (0.71, 1.72)	0.65

Table 4.10 Odds ratios for the nAb cross protection. Odds ratios of the cross protectivity of neutralising antibodies (nAbs) from individuals from Class 1 relative to that of Class 2. The nAb class was pooled into the binary trait: cross-protective (nAb class 1-2) or not cross-protective (nAb class 3-5). The 95% significance level was used ($p < 0.05$).

The breadth of nAb cross-protectivity was distributed similarly across the WUR genotypes as shown in Table 4.9. Given that the allele acts in a dominant manner the WUR classes 1 and 2 were pooled (WUR Y) and further odds ratios were obtained to compare differences between the WUR 0 and pigs with the favourable B allele. There were not any statistically significant associations (at the 95% significance level) between the WUR genotype and the nAb cross-protectivity as shown in Table 4.10.

WUR genotype	No cross protection (% within WUR class)	Cross protection (% within WUR class)
0	188 (59)	131 (41)
1	67 (61)	42 (39)
2	8 (73)	3 (27)
Y (Pooled WUR 1 & 2)	75 (62.5)	45 (37.5)

Table 4.9 The distribution of the nAb cross-protectivity by WUR genotype.

Class 1	Class 2	Odds ratio (95% Confidence interval)	P- value
Clearance	Persistence	0.61 (0.38, 0.98)	0.04
Clearance	Rebound	0.86 (0.53, 1.38)	0.53
Persistence	Rebound	1.40 (0.80, 2.45)	0.24
Class 1	Class 2	Odds ratio (95% Confidence interval)	P- value
WUR 0	WUR 1	1.06 (0.68, 1.68)	0.79
WUR 0	WUR 2	1.72 (0.43, 6.81)	0.44
WUR 1	WUR 2	1.62 (0.39, 6.64)	0.51
Class 1	Class 2	Odds ratio (95% Confidence interval)	P- value
WUR 0	WUR Y	1.107 (0.71, 1.72)	0.65

Table 4.10 Odds ratios for the nAb cross protection. Odds ratios of the cross protectivity of neutralising antibodies (nAbs) from individuals from Class 1 relative to that of Class 2. The nAb class was pooled into the binary trait: cross-protective (nAb class 1-2) or not cross-protective (nAb class 3-5). The 95% significance level was used ($p < 0.05$).

Appendix 3

The following manuscript has been submitted to the Journal of Animal Science:

COMPARISON OF HOST GENETIC FACTORS INFLUENCING PIGLET RESPONSE TO INFECTION WITH TWO DIFFERENT ISOLATES OF PORCINE REPRODUCTIVE AND RESPIRATORY SYNDROME VIRUS SUGGESTS SELECTION FOR REDUCED SUSCEPTIBILITY TO PRRSV INFECTION IS FEASIBLE ACROSS ISOLATES

Hess, A.S., Islam, Z., Hess, M.K., Rowland, R.R.R, Lunney, J.K., Doeschl-Wilson, A., Bishop, S., Plastow, G.S, Dekkers, J.C.M

ABSTRACT

Porcine Reproductive and Respiratory Syndrome (PRRS) is one of the most important swine diseases in the world and genetic selection of pigs that are less susceptible to PRRS is an attractive method to improve swine herd health status. Pigs were infected with one of two genetically distinct PRRSV isolates: NVSL-97-7895 (NVSL; ~1500 pigs) and KS-2006-72109 (KS06; ~700 pigs). The Wood's curve was fitted to repeated viraemia measurements during the first 42 days post infection (dpi) and five curve characteristics were derived. The goal of this study was to compare genetic and phenotypic response to infection with either NVSL or KS06 PRRSV isolates and evaluate whether a genetic marker (WUR10000125), associated with viral load and weight gain under infection with NVSL, has an effect on response to infection across PRRSV isolates. Infection with NVSL was characterized by reaching a $14 \pm 2\%$ higher peak viraemia (PV) 2.5 ± 0.6 days earlier than KS06 (TP), followed by $36 \pm 14\%$ faster virus clearance (V_{max}) which occurred 3.9 ± 0.7 days sooner (T_{max}). Weight gain from 0-42 dpi (WG) tended to be higher under infection with KS06 than NVSL (3.7 ± 1.5 kg). Viral Load from 0-21dpi (VL) (NVSL: 0.31 ± 0.06 ; KS06: 0.51 ± 0.09) and WG (NVSL: 0.33 ± 0.06 ; KS06: 0.31 ± 0.09) were shown to have moderate heritabilities for both PRRSV isolates. Strong negative genetic correlations were observed between VL and WG for both NVSL (-0.74 ± 0.10) and KS06 (-

0.52±0.17) infected pigs. Pigs with the AB WUR genotype had a more desirable phenotype than AA pigs for all traits under NVSL infection ($VL_{AA}-VL_{AB}=4.5\pm0.4\%$; $WG_{AA}-WG_{AB}=-2.0\pm0.2$ kg; $PV_{AA}-PV_{AB}=2.8\pm0.4\%$; $TP_{AA}-TP_{AB}=0.20\pm0.09$ days; $Tmax_{AA}-Tmax_{AB}=0.68\pm0.16$; $Vmax_{AA}-Vmax_{AB}=-3.8\pm1.5\%$), but only for VL and PV for KS06 ($VL_{AA}-VL_{AB}=4.2\pm0.9\%$; $PV_{AA}-PV_{AB}=3.4\pm0.7\%$), with no WUR association for the other traits. Genetic correlations of host response between isolates were high for VL (0.86 ± 0.19), WG (0.86 ± 0.27), and PV (0.94 ± 0.28). Accounting for WUR genotype had little impact on the genetic correlation between isolates, suggesting that there is a substantial polygenic component to response to PRRSV infection that is common between these two PRRSV isolates. These results suggest that KS06 is a less virulent PRRSV isolate than NVSL however, importantly genetic selection for reduced susceptibility to either of these genetically distinct isolates will reduce susceptibility to the other.

INTRODUCTION

Porcine Reproductive and Respiratory Syndrome (PRRS) costs the U.S. swine industry \$664 million per year [1]. Past efforts to contain PRRS have had limited success, in large part due to the rapid mutation rates and antigenic variability of PRRS virus (PRRSV), which have encumbered efforts to produce vaccines that are cross-protective to different PRRSV isolates [2].

Genetic selection of pigs that are less susceptible to PRRS is an attractive method to improve the swine herd health status [3]. The goal of the PRRS Host Genetics Consortium (PHGC) is to identify host genes or genomic regions associated with reduced susceptibility of pigs to PRRSV infection [4]. Previous studies using multiple contemporary North American crossbred weaner pigs experimentally infected with the NVSL-97-7895 (NVSL) isolate of PRRSV identified heritable genetic components to viral load and weight gain, and found an association between the single nucleotide polymorphism (SNP) WUR10000125 (WUR) on chromosome 4 and these two

host response traits [5-7]. A putative gene in high LD with WUR, *GBP5*, was identified by Koltes et al. [8] that plays a crucial role in the NLRP3-mediated formation of the inflammasome, which is involved with inflammatory response [9]. It is currently unknown whether the host genetics influencing response to PRRSV infection is consistent across PRRSV isolates.

The objectives of this study were to 1) compare responses to infection with NVSL and the genetically distinct PRRSV isolate KS-2006-72109 (KS06); 2) estimate the genetic parameters of response to infection when pigs are infected with either NVSL or KS06; and 3) estimate the associations of the WUR SNP with response following infection with NVSL or KS06. It was hypothesized that the host genetics influencing response to infection would be highly correlated between the two virus isolates and that associations of the WUR SNP with response would be similar. The Wood's function has previously been shown to appropriately model PRRS serum viraemia following experimental infection [10]. Thus, curve characteristics of the fitted viraemia profiles derived from the Wood's curve parameters were used to quantify different aspects of the dynamics of host response to PRRSV infection with these two isolates.

MATERIALS AND METHODS

Study Design

A detailed description of the design, data collection and molecular techniques used in PHGC trials is in [4]. The Kansas State University Institutional Animal Care and Use Committee approved all experimental protocols for these trials. Pigs used for this study were from 14 PHGC trials of ~200 weaner pigs (Table 1). Pigs were provided from commercial breeding programs in the United States and Canada. Four breeding companies supplied pigs of the same breed cross for more than one trial, with pigs from one trial infected with KS06 and one or more trials with

NVSL (Table 1). Pigs from the same breeding company and the same breed cross were from the same genetic background. Within each challenge trial, pigs were from a single high health farm and genetic background, except for trials 5, 8 and 12, which each included pigs from one genetic background but two farms. All source farms were free of PRRS, *Mycoplasma hyopneumoniae*, and swine influenza. Animals were transported at weaning (average age of 21 days) to Kansas State University and randomly placed into pens of 10 to 15 pigs. After a 7-day acclimation period, pigs were experimentally infected, both intramuscularly and intranasally, with 10^5 (TCID₅₀) of either NVSL-97-7985, a highly virulent PRRSV isolate [11] for trials 1-8 and 15; or with KS-2006-72109, a more contemporary PRRSV isolate, for trials 10-14. NVSL and KS06 are 89% similar at the GP5 nucleotide sequence level [12]. Blood samples were collected at -6, 0, 4, 7, 11, 14, 21, 28, 35, and 42 days post-infection (dpi). Body weight was measured at 0, 7, 14, 21, 28, 35, and 42 dpi. Pigs were euthanized at 42 dpi. Trials 7 and 8 were stopped at 35 dpi due to facility unavailability.

Serum viraemia was measured using a semi-quantitative TaqMan PCR assay for PRRSV RNA, as described in Boddicker et al. [5-7] and Ladinig et al. (2015). Assay results were reported as the log₁₀ of PRRSV RNA copies per mL of serum. A time course of viraemia levels for each animal within a trial was plotted in order to provide an initial assessment of the response to infection and to confirm all animals were initially infected (Supplemental Figure 1). Trial 13 was excluded from further analysis due to unusual viraemia profiles not observed in any other PHGC infection trial: some trial 13 animals showed delayed presence of serum viraemia, and all individuals had low, noisy viraemia levels compared to individuals in other trials, suggesting the virus was attenuated or the pigs were not naïve. If the pigs were not naïve it could be due to the

presence of maternal antibodies as a result of previous infection or vaccination in the herd from which they were sourced [13].

Ear tissue was collected from all pigs for DNA isolation. Tissues or DNA samples for trials 1-10 were genotyped with Illumina's Porcine SNP60 Beadchip v1 (San Diego, California) at GeneSeek Inc. (Lincoln, Nebraska) and samples from trials 11-15 were genotyped with Illumina's Porcine SNP60 Beadchip v2 (San Diego, California) at Delta Genomics (Edmonton, Alberta). Only SNPs that were included on both versions of the Illumina's Porcine SNP60 Beadchip were used in this study. SNPs were removed if they were fixed within a breed, or if they were unmapped or mapped to a sex chromosome in build 10.2 of the swine genome (<http://www.ncbi.nlm.nih.gov/genome/guide/pig/>, accessed August 13, 2015); this left 48,164 SNPs. Missing genotypes were assigned the average genotype (on 0,1,2 scale) for animals in that trial for that SNP. This set of SNPs will be referred to as 60k SNPs.

Across all nine trials infected with NVSL, 12% of pigs died or were euthanized for humane reasons before 42 dpi. Mortality rate was similar in the KS06 trials, with 9% pigs dying or euthanized before 42 dpi across the five trials. Dead pigs were necropsied and subsequent gross and microscopic pathology by a board-certified pathologist identified PRRS associated disease as the major source of mortality, except for trial 6. Death loss was high in trial 6 (46% by day 42), due to secondary bacterial infections, as identified by pathology, including *Escherichia coli*, *Streptococcus suis*, *Staphylococcus aureus*, and *Mycoplasma hyopneumoniae*.

Modelling viraemia profiles with the Wood's function

The Wood's curve, an incomplete gamma function often used to model lactation yield in dairy cattle [14-16], was shown to appropriately model viraemia profiles in PHGC trials 1-8 [10].

$$V(t) = a_1 t^{b_1} e^{-c_1 t}$$

where $V(t)$ is serum viraemia on the \log_{10} scale at time t dpi, a_1 impacts the magnitude of all points on the curve, b_1 is an indicator of the initial rate of increase to peak viraemia, c_1 is an indicator of the rate of decline after the peak and dominates the viraemia profile at the later stages of infection. The three function parameters were estimated for each individual that had at least five time points measured using Bayesian inference with a likelihood framework, implemented using a Markov chain Monte Carlo method [10].

The raw viraemia profiles of some pigs appeared bi-modal, so an extended Wood's curve was also fitted for each piglet using the same methodology above:

$$V(t) = a_1 t^{b_1} e^{-c_1 t} + \max(0, a_2 (t - t_0)^{b_2} e^{-c_2 (t - t_0)})$$

whereby t_0 denotes the onset of the second phase of the profile, which is assumed to follow the same Wood's shape as the primary phase and is thus defined by a second set of Wood's model parameters. A piglet was classified as experiencing viraemia rebound based on the Akaike's Information Criterion (AIC) if $AIC_{\text{WOOD'S}} - AIC_{\text{EXTENDEDWOOD'S}}$ was greater than 1.488, corresponding to the 95% significance level of the likelihood ratio test between these models [10]. A total of 16% of NVSL pigs and 6% of KS06 pigs were classified as rebound pigs.

Using the piglet specific curve parameters estimates, \hat{a}_1 , \hat{b}_1 , and \hat{c}_1 , a fitted viraemia value can be estimated for each piglet for each time point ($\widehat{V(t)}$).

Viraemia curve characteristics

In previous studies, Boddicker et al. [5-7] used area under the viraemia curve (AUC) or viral load (VL) from 0-21 dpi as a measurement of response to PRRSV infection. Area under the

curve is a summary phenotype of the viral burden but it does not explicitly capture the dynamics of an individual animal's curve that can influence this viral burden; two animals that have different viraemia curves can have the same VL. Analysis of different aspects of the viraemia curve may aid in the understanding of differences in virulence in the two virus isolates, as well as insight into the role host genetics plays in response to infection [10]. The genetic mechanisms for one curve characteristic may be highly conserved across isolates, while highly variable across isolates for another curve characteristic.

Five curve characteristics were derived to describe individual viraemia profiles using the estimates of the curve parameters $(\hat{a}_1, \hat{b}_1, \hat{c}_1)$ of the single or the extended Wood's curve. The primary phase was chosen for this study because this phase has previously been shown to have a heritable genetic component, while heritability for rebound was previously estimated to be 0.03, suggesting that this phase is largely governed either by viral escape or other environmental factors [10].

The first characteristic evaluated, area under the Wood's curve, hereafter referred to as viral load (VL), was given by the definite integral:

$$VL = \int_0^{21} \hat{a}_1 t^{\hat{b}_1} e^{-\hat{c}_1 t} dt$$

VL is a measure of both the level of viraemia and the extent to which viraemia is maintained. The range 0-21 dpi were chosen to capture the uni-modal phase of infection common to all pigs. Previous analyses on trials 1-8 fitted a Loess curve through viraemia and integrated to get area under the curve from 0-21 dpi [5-7], which will be denoted by VL_B . It was unknown how similar VL_B and VL were to each other, which may impact the interpretation of the results and comparisons that are drawn between this study and previous studies. Therefore, the pedigree

relationship matrix was constructed in ASReml 3.0 [17] for all animals used in the analysis. Pedigree information was available for all pigs in all trials. Trials 1-3 had the most extensive pedigree information, with records up to two generations back, while the rest of the trials only had sire and dam recorded. As such, there were no relationships between animals in different trials, except for trials 1-3 which consisted of animals from the same breeding company in consecutive parities. Pedigree was corrected using parental genotypes for trials 1 through 8, as described by Boddicker et al. [7]. The 1250 highest quality 60k SNPs, based on GC score and call rate, were used in Cervus 3.0 [18] to verify pedigree information for trials 11 and 15, and assign sire for trials 12 and 13, because pooled semen was used in these two trials. Parental genotypes were unavailable for trials 10 and 14. A bivariate model using pedigree information for VL and VL_B was fitted separately for the KS06 and NVSL trials, using ASReml 3.0. It was concluded that VL based on the Wood's curve describes the same biological trait as VL_B due to similar heritabilities and high genetic and phenotypic correlations (Table 2); therefore VL derived based on the Wood's curve was used for all remaining analyses.

The second curve characteristic evaluated was time to peak viraemia (TP), derived by setting the first derivative of the Wood's equation to zero and solving for t, resulting in:

$$TP = \frac{\widehat{b}_1}{\widehat{c}_1}$$

The third curve characteristic was peak viraemia (PV), which was calculated by setting $t = TP$ in the Wood's equation:

$$PV = \widehat{a}_1 \left(\frac{\widehat{b}_1}{\widehat{c}_1} \right)^{\widehat{b}_1} e^{-\widehat{b}_1}$$

TP and PV are related to the host's ability to respond during the replication-dominant phase of early PRRSV infection [19]. PV is reached when the rate of virus clearance from serum is equal to the number of virus particles released into the blood stream. TP is the time it takes to reach PV, with animals that can mount a response early in infection expected to have a shorter TP.

Curve characteristics that relate to the host's response to the post-peak, clearance-dominant phase of PRRSV infection were also evaluated. The maximal decay rate (Vmax) is reached when the rate of viral clearance from serum is highest compared to the rate of viral replication. Time to maximal decay (Tmax) was derived by setting the second derivative of the Wood's equation to zero and solving for t:

$$T_{\max} = \frac{\hat{b} + \sqrt{\hat{b}}}{\hat{c}}$$

Plugging this value in for t in the first derivative and taking the absolute value gave Vmax:

$$V_{\max} = \left| -\hat{a}\sqrt{\hat{b}} \left(\frac{\hat{b} + \sqrt{\hat{b}}}{\hat{c}} \right)^{\hat{b}-1} e^{-(\hat{b}+\sqrt{\hat{b}})} \right|$$

Vmax was defined as the absolute value of the first derivative for ease of interpretation, whereby an animal with a larger Vmax cleared viraemia from the serum more quickly.

Fitting Daily Weights

Raw weights were collected weekly and used to interpolate daily weights. In ASReml, a random regression model was fitted to each individual's weight data using second order Legendre polynomials in the following model:

$$W(t) = \sum_{n=0}^2 L_n(t) + P + A + S + \sum_{n=0}^2 L_n(t) * R + \sum_{n=0}^2 L_n(t) * An + Tr + Pen(Tr) + \varepsilon$$

where $L_n(t)$ denotes the n th order Legendre polynomial at t dpi. $L_n(t)$, P , A , S and $L_n(t)*R$ were fitted as fixed effects. $L_n(t)$ was fitted as a covariate, whereby t ranged from 0-42 dpi, P was the parity of dam, classified as first, second, or later parities, A was the age of the individual at inoculation, S was the sex of the individual and $L_n(t)*R$ was the interaction between the n th order Legendre polynomial at t dpi and rebound status. This model was fitted separately for animals infected with NVSL and KS06. $L_n(t)*An$, Tr , and $Pen(Tr)$ were included as random effects and denoted the interaction between the n th order Legendre polynomial at t dpi and Animal, trial and the interaction between trial and pen, respectively. $L_n(t)*An$ modeled an individual's weight at each time point, and captured both genetic and permanent environmental effects, and used an unstructured variance-covariance structure. Residual variances were modeled separately for each t dpi, in order to allow for an increase in variance over time. Trial and Trial*Pen were included to capture environmental effects. This model was then used to obtain fitted values of each pig's weight for each dpi (0-42) ($\widehat{W}(t)$), using all coefficients estimated from the above model.

Genomic Relationship Matrices

Due to the limited pedigree information and availability of genotypes on almost all animals, a genomic relationship matrix (G-matrix) among all animals was constructed from the 60k SNP genotype data, using the VanRaden method [20]. The G-matrix (G) included relationships between animals in different trials. In some cases, fitting relationships between breeds can absorb between-breed differences that could be due to selection, this can overestimate the genetic variance because the “base population” is the population from which the breeds subsequently

diverged [21]. A block diagonal G-matrix was also constructed (G_B -matrix) that only took relationships between animals from the same genetic background into account, with zero relationships between animals from different companies. Results from analyses with the G_B -matrix are expected to be similar to what would be found from a pedigree-based analysis of these data if the pedigree was more extensive. A third G-matrix was constructed that was the block diagonal matrix G_B but only consisted of animals from trials that were paired across isolates (G_P -matrix), to assess whether the estimated correlations between NVSL and KS06 could be biased due to different breed crosses being evaluated for each isolate. In order to further assess the impact of the WUR region on each trait, the G , G_B and G_P -matrices were also constructed excluding the 118 SNPs in the 5Mb region surrounding the WUR SNP previously identified to be associated with VL and WG in pigs infected with the NVSL PRRSV isolate [5-7]; these new matrices are designated G_{-W} , G_{B-W} and G_{P-W} , respectively and were used to estimate the genetic correlation between NVSL and KS06 of response traits for the rest of the genome.

Statistical Models

All analyses were conducted using an animal model in ASReml 3.0 [17]. The model was:

$$Y = \mu + P + A + W + S + R + An + Li + Tr + Pen(Tr) + error?$$

Y is the dependent variable of daily fitted viraemia values, weekly weights, VL, TP, PV, Tmax, Vmax, weight gain from 0-42 dpi (WG). Parity of the dam (P), classified as first, second, or later parity, and sex of the piglet (S) were fitted as a fixed class effects. To account for potential model differences in curve fittings between rebound and non-rebound pigs, a fixed class effect of rebound (R) was included in the model. Age (A) and weight (W) of the piglet at infection were fitted as linear covariates. Random effects included animal genetic effects (An ; using the full G -matrix), litter (Li), trial (Tr), and Pen nested within trial ($Pen(Tr)$).

Comparison of NVSL and KS06 Viraemia Profiles and Pig Weight Gain during Infection

Data from paired trials (Table 1) and the full G-matrix were used to estimate daily fitted viraemia values, weekly weights, VL, TP, PV, Tmax, Vmax or WG for each isolate by including isolate as a fixed class effect into the above model. Phenotypic differences between virus isolates were assessed using the t-statistic reported by ASReml 3.0, with a significance cutoff of $\alpha=0.05$.

Within Isolate Genetic Parameters

Within-isolate heritabilities, and phenotypic and genetic correlations were estimated for VL, WG, TP, PV, Tmax or Vmax using the full G-matrix in order to quantify the relationships between the response traits. Heritabilities and litter effects were estimated using a univariate model. A multivariate model using all traits was attempted for genetic and phenotypic correlations between traits but this model did not achieve convergence, so bivariate models were used to get phenotypic and genetic correlations between traits. Estimates of correlations were considered statistically significant based on a t-test with 1496 degrees of freedom for NVSL and 670 degrees of freedom for KS06.

The genetic correlation between viraemia and weight gain was expected to change throughout the experiment due to different host genetic control of these traits during different phases of infection. To assess how the relationship between viraemia and weight gain change over time, the genetic correlation between the fitted viraemia values ($\widehat{V(t)}$) and three-day weight gains from the fitted weight values ($\widehat{W(t)}$) were estimated. Correlations between ($\widehat{V(t)}$) at every other dpi (i.e. 1, 3, 5, ..., 41) and three-day weight gain at 42 dpi were estimated by replacing W in the above model with the weight 3 dpi prior (with the exception of weight at 1 dpi, which was adjusted for weight at infection). Viraemia at each time point was adjusted for weight at 0 dpi. Correlations between these weight gains (WG) and viraemia were also assessed every other day

(i.e. WG0-1, WG0-3, WG2-5...WG38-41). These correlations were calculated for NVSL and KS06 separately. This resulted in two 21x21 matrices of genetic correlations between viraemia and three-day weight gain, which was visualized in a heat map (Figure 4).

Associations of WUR Genotypes with response to NVSL and KS06 Infection

The association of the WUR genotype with VL, WG, TP, PV, Tmax and Vmax were estimated for infection with NVSL and KS06 by including the interaction of isolate with WUR genotype into the above model, with the full G-matrix representing the relationship between animals. This model was also fitted to daily fitted viraemia values and weekly weights to generate viraemia and weight curves for each isolate by WUR genotype combination. Statistical differences between each isolate by WUR combination were assessed using the t-statistic reported in ASReml and the residual degrees of freedom from the model, with a significance cutoff of $\alpha=0.05$.

Genetic Parameters of Response between Isolates

The G-matrices described above were used to estimate genetic correlations between virus isolates for VL, WG, TP, PV, Tmax or Vmax using a bivariate model. Genetic correlations were considered statistically significant using a t-test with 2168 degrees of freedom when using G, G_w, G_B and G_{B-w}, and 1378 degrees of freedom when using only paired trials (G_P and G_{P-w}).

RESULTS

Comparison of NVSL and KS06 Viraemia Profiles and Pig Weight Gain during Infection

Raw viraemia profiles suggested differences in pig response to infection with the NVSL versus the KS06 PRRSV isolate (Figure S1). To statistically quantify these differences, a selection of curve characteristics were derived from the Wood's function parameters and compared between

isolates using data from trials that were paired by genetic background to remove confounding between isolate and genetic background (Table 1). Pigs infected with NVSL had $16\pm 2\%$ higher VL than pigs infected with KS06 (Table 3, Figure 1). Both TP and PV are related to the host's ability to respond during the replication-dominant phase of PRRSV infection. Pigs infected with NVSL had $14\pm 2\%$ higher PV and reached PV 2.5 ± 0.6 days earlier than pigs infected with KS06 (Table 3, Figure 1). Tmax and Vmax are related to the host's ability to clear PRRSV. Compared to pigs infected with KS06, NVSL infected animals reached maximal PRRSV clearance 3.9 ± 0.7 days earlier and cleared at a $36\pm 14\%$ faster maximal rate than their KS06 counterparts (Table 3, Figure 1). When comparing the impact that infection had on weight gain, pigs infected with the NVSL isolate had a tendency to grow more slowly than their KS06 counterparts (Table 3, Figure 1). Taken together, these results indicate that NVSL is more virulent than KS06 because it reached a higher PV more rapidly and resulted in higher overall VL and lower growth rate. KS06 appears to be more persistent than NVSL as shown by a longer time to maximal decay rate, lower maximal decay, and a larger percentage of pigs classified as persistently infected, defined as a non-rebound pig with a fitted log₁₀ serum viraemia value greater than 1 at 42 dpi (56% in KS06 vs 40% in NVSL).

Heritability Estimates

Heritability estimates were similar between NVSL and KS06 for WG, TP, and Tmax. These traits also had similar estimates of the litter components between NVSL and KS06. VL, PV, and Vmax all had lower heritabilities and larger litter components in NVSL compared to KS06. Summing the heritability and litter components for each of VL and PV gave similar results in each isolate even though the heritabilities were quite different between isolates (Table 3). The

larger number of animals infected with the NVSL isolate compared to KS06 may mean the heritability and litter component are more accurately separated by the model.

All traits were estimated to be moderately to highly heritable except for Vmax under infection with NVSL. The traits with the highest estimated heritability under infection with NVSL were VL and WG and these traits also had high heritability estimates under infection with KS06. Vmax had the lowest estimated heritability under infection with NVSL, but a moderate heritability under infection with KS06 (Table 3). The estimated genetic variance of Vmax is similar under infection with NVSL or KS06 (0.00053 vs. 0.00072) so the difference in heritability is driven by a larger estimated environmental variance under infection with NVSL compared to KS06 (0.0057 vs. 0.0027).

Estimates of heritability of VL and WG during NVSL infection were similar to previously reported estimates (VL: 0.31 ± 0.06 vs 0.44 ± 0.13 ; WG: 0.33 ± 0.06 vs 0.29 ± 0.11) (Table 3; [7]. The differences between the estimates can be attributed to the use of the G-matrix rather than the A-matrix, the inclusion of trial 15, and the inclusion of age and weight at infection in the model used in this study but not in the Boddicker et al. (2014b). Age and weight at infection are important to include in the analysis because pigs that are older or heavier at infection tend to be able to mount a stronger immune response, independent of the host's genetic ability to combat the virus [22,23]. The use of the G-matrix halved the standard errors of estimates compared to using the A-matrix because the G matrix more accurately captures the true relationship between animals, especially because there was limited pedigree information available on the pigs used in these trials.

Viral Load and Weight Gain

The genetic and phenotypic correlations between VL and WG were negative and of similar magnitude across isolates (Tables 4 & 5). The genetic correlation estimate was more negative for the NVSL infected pigs than previously reported (r_g : -0.74 ± 0.10 vs -0.46 ± 0.20 ; r_p : -0.33 ± 0.03 vs -0.29 ± 0.03) [5-7] which can be attributed to the combination of using the G-matrix rather than the A-matrix, the addition of trial 15, and the inclusion of age and weight at infection. Strong genetic correlations between VL and WG suggest that there may be common genes or pathways that affect these two traits. WUR is a SNP that has been shown to be associated with both VL and WG in pigs infected with NVSL [5-7]. The genetic correlations between isolate for VL and WG are strong and not significantly different from one (Table 6), indicating that the host genetic control of VL and WG is very similar under infection with either the NVSL or KS06 isolate.

Viral Load and Viraemia Curve Characteristics

VL, defined as area under the Wood's curve from 0-21 dpi, was largely driven by PV as shown by the high genetic and phenotypic correlations between these two traits within isolate (Tables 4 & 5). PV had the highest genetic correlation between PRRSV isolates, suggesting that the correlation for VL is primarily due to their genetic correlation for PV, as no other curve characteristic had a between virus isolate genetic correlation estimate that was significantly different from zero while the genetic correlation between virus isolates for PV was not significantly different from one (Table 6).

Tmax and Vmax had strong negative correlations with each other for both isolates; however, they were only highly correlated with VL for NVSL (Tables 4 & 5). Time to maximal decay rate (Tmax) was approximately 19.3 dpi for KS06 but at 15.4 dpi for NVSL (Table 3), therefore Vmax is expected to play a bigger role in VL for NVSL than for KS06, because VL was calculated from 0-21 dpi in this study. No conclusions can be drawn about the genetic

correlations between isolate for either Tmax or Vmax because the estimates are not significantly different from zero or one due to large standard errors (Table 6).

The two time-related traits (TP and Tmax) had strong, positive genetic and phenotypic correlations in both isolates (Tables 4 & 5) because TP ($\frac{b}{c}$) is a component of Tmax ($T_{max} = TP + \frac{\sqrt{TP}}{\sqrt{c}}$). The genetic correlation between isolates for TP was significantly different to one (Table 6), indicating that host genetic control of the time until maximal virus decay rate may differ between virus isolates.

Weight Gain and Viraemia Curve Characteristics

PV had a moderate negative genetic correlation with WG for NVSL (Table 4) infected pigs but this genetic correlation was not significantly different from zero for KS06 infected pigs (Table 5), due to a larger standard error and a less negative estimate. Vmax also had a significant genetic correlation with WG. These results suggest that the reduction in growth is caused by an overall high viraemia level over a prolonged period of time, which is further supported by the highest observed genetic and phenotypic correlations being between WG and VL (Tables 4 & 5).

Genetic Correlations between VL and WG across Time

A more thorough exploration of the relationship between PRRS viraemia and weight gain was accomplished through the estimation of genetic correlations between fitted viraemia and three-day weight gain values (Figure 4). In animals infected with NVSL, animals that had high viraemia from 0-7dpi tended to have high WG later on in the trial but low WG early on. During the early stages of infection, pigs with high viraemia may need to allocate more energy to fighting the infection than growing, resulting in a negative genetic correlation between early

viraemia and early weight gain. It appears that under infection with NVSL, pigs that have higher viraemia and lower weight gain early in infection may reap the benefits later in infection with higher weight gain. Therefore, animals with higher early viraemia divert more resources to fighting infection early on, which pays off in the long run with higher weight gain at the end of the trial. This notion is supported by the weaker genetic correlations between early viraemia and weight gain under infection with the less virulent isolate, KS06 (Figure 4B), which has lower pre-peak viraemia (Figure 1). It is also likely that pigs with high early viraemia also suffer a loss in appetite [24], which may further reduce weight gain in these animals. The positive correlation between early viraemia and late weight gain could reflect a return to homeostasis after infection in these pigs [25].

While the relationship between weight gain and early viraemia may differ between isolates, the ability of the animal to effectively clear the virus from serum is crucial for maintaining growth. This is made evident by a block of highly negative correlations between viraemia 15-28 dpi and from 22 dpi onward in pigs infected with NVSL. The time period 15-28 dpi corresponds to the time in which pigs are clearing PRRSV from serum the most rapidly. There also appears to be a relationship between viraemia after 28 dpi and later weight gain, in particular viraemia at 33 dpi. This negative correlation is likely observed due to rebound pigs, as this time point corresponds with the average time that rebound pigs reach a secondary peak viraemia.

Similar to NVSL, KS06 infected pigs showed strong negative correlations between viraemia and weight gain that corresponded to viral clearance. In KS06 infected pigs, this critical period seemed to be viraemia after 17-28 dpi and weight gain after 17 dpi. This time period corresponds to the time in which antibodies, specifically IgG, are being produced at the highest rates,

suggesting that the ability to clear the virus effectively may be dependent on the pig's ability to mount a successful adaptive immune response [26].

These genetic correlations provide insight into how host genetic control of Viraemia and WG changes throughout the trial. In order to further elucidate the host genetic mechanisms that are in common between viraemia and weight gain, it would be beneficial to conduct a genome wide association study of these traits at different time points to reveal which regions of the genome have an effect at each stage. This has the potential to identify further loci that would improve host response to PRRSV infection across isolates if selected upon.

Associations of WUR Genotypes under NVSL and KS06 Infection

The least square means of the WUR genotype were estimated by fitting the interaction between isolate and WUR genotype for all trials simultaneously. There were very few pigs with the BB genotype at the WUR locus, and therefore estimates of the least square means for the BB genotype had high standard errors. Furthermore, BB animals were not significantly different from AB animals while significantly differing from AA animals, when AA and AB animals were significantly different, suggesting complete dominance, as previously reported by Boddicker et al. (2012, 2014a, 2014b). Results for BB animals will not be discussed further for these two reasons.

Pigs with the AA WUR genotype had $4.5 \pm 0.4\%$ higher VL ($P < 0.001$) and grew 2.0 ± 0.2 kg less than pigs with the AB genotype after infection with NVSL ($P < 0.001$). These estimates are consistent with previous estimates of the association of WUR under infection with NVSL (Boddicker et al. 2014b). WUR genotype was also found to be associated with VL under infection with KS06, whereby VL was $4.2 \pm 0.9\%$ higher in AA animals than AB animals

($P<0.001$). In contrast to infection with NVSL, no association was found between WUR genotype and WG ($P=0.32$).

The WUR genotype was associated with all curve characteristics in pigs infected with NVSL (Figure 2). Compared to AA animals, AB animals had $2.8\pm0.4\%$ lower PV ($P<0.001$), which was reached 0.20 ± 0.09 days earlier ($P<0.02$); AB animals also had a $3.8\pm1.5\%$ faster maximal decay rate ($P<0.02$) which was reached 0.68 ± 0.16 days sooner ($P<0.001$). In KS06 trials, WUR was associated with $3.4\pm0.7\%$ higher PV in AA animals compared to AB animals ($P<0.001$) but no association was found for Vmax ($P=0.36$) (Figure 2). Compared to AA animals, AB animals tended to reach peak viraemia 0.30 ± 0.16 ($P=0.052$) days sooner and maximal decay rate 0.47 ± 0.29 ($P=0.078$) days later.

Plotting viraemia and weight curves for AA and AB WUR genotype pigs, by isolate (Figure 3), provided results that were consistent with regards to the estimated effects of WUR on WG, VL, and the curve characteristics. For KS06, the effect of WUR on VL was mainly driven by differences in PV but the difference in viraemia level between AA and AB was not maintained due to a slightly lower rate of clearance in AB compared to AA animals, resulting in similar viraemia levels at the end of the trial (42 dpi). Conversely, for NVSL, the difference in viraemia levels between AA and AB animals first appeared around peak viraemia and became larger during the primary stages of infection due to a faster clearance rate for AB animals.

The effect of WUR genotype was significantly different between the NVSL and KS06 isolates for both WG ($P=0.001$) and Vmax ($P=0.041$) (Figure 2). These effects were observed due to large effects of WUR genotype on WG and Vmax in the NVSL trials that were not detected in the KS06 trials. The effect of WUR genotype on Vmax after infection with KS06, though not

significantly different from zero, was in the opposite direction to the WUR genotype effect after infection with NVSL (Figure 2).

The WUR genotype had an effect on all shape characteristics of the Wood's viraemia curve for NVSL, which contributed to the large effect observed for VL in the NVSL trials (Figure 2). In general, the WUR genotype had a lower association with response to infection in pigs infected with KS06 than pigs infected with NVSL; suggesting that the magnitude of the effect of the QTL in high LD with WUR may be dependent on the virulence of the PRRSV isolate.

Impact of the WUR Region on Heritabilities and Genetic Correlations

Heritabilities of response traits were estimated including all SNPs in the full G-matrix (Table 6) and also including all SNPs except the 5Mb region surrounding the WUR locus (G_w ; Table 7). In the NVSL trials, estimated heritabilities were lower for all traits when the G_w -matrix was used, except V_{max} , which remained the same. Estimated heritabilities for WG and T_{max} were the same whether the G-matrix or G_w -matrix was used, while the estimated heritabilities for all other traits dropped when the G_w -matrix was used, with the largest drops in PV and VL.

Genetic correlations between isolates were also estimated for the response traits using both the full G-matrix (Table 6) and the G_w -matrix (Table 7). The estimated genetic correlations between isolates for WG and V_{max} were slightly higher when using the G_w -matrix compared to the full G-matrix, while the estimated genetic correlations between isolates for all other response traits decreases, with the largest decreases in PV and VL.

Genetic correlation estimates for VL, WG and PV were significantly different from zero and not significantly different from one when using both the full G-matrix and the G_w -matrix. This indicates that host genetic control of response to infection is highly conserved across isolate for

these three traits. The high genetic correlation estimates for these traits when using the G_W -matrix indicate the conserved host genetic response between isolate for VL and PV is not solely dependent on WUR genotype, but likely has a large polygenic component. The increase in genetic correlation between isolates for WG when using the G_W -matrix compared to the full G-matrix is consistent with the observed effect of WUR in pigs infected with NVSL but lack of effect in pigs infected with KS06. Estimated genetic correlations between isolates for Tmax and Vmax have large standard errors when using both the full G-matrix and G_W -matrix, therefore no conclusions can be drawn because these estimates are not significantly different from zero or one. Estimated genetic correlations for TP were significantly different from one but not significantly different from zero for both the full G-matrix and G-W-matrix, indicating that host genetic control of TP is not highly conserved across isolate.

Genetic Parameter Estimates Using Different G Matrices

Three different types of G matrices were constructed for both the full G-matrix and the G_W -matrix that were based on different types of information. The G_B matrix only contained the relationships between animals from the same genetic background, with zeros for the relationships between animals of different backgrounds. The full G-matrix contains information about both the within-genetic background and between-genetic background genetic variance when calculating the heritabilities and genetic correlations for the response traits, while the G_B -matrix only contains information about the within-genetic background genetic variance. The G_B -matrix is more similar to the A-matrix than the G-matrix is, because there is usually no pedigree information between animals from different genetic backgrounds so the relationship between animals from different genetic backgrounds is zero. The G_P -matrix is a block diagonal matrix using only pigs from the same genetic background that were paired across isolates and was used

to avoid biases in estimates that were due to including different breeds in the analyses for each isolate. In general, the estimates using the G_P -matrix were consistent with estimates using the G_B -matrix.

Estimates of genetic correlation between isolates for PV are very similar for the full G-matrix and G_B -matrix (Table 6), indicating that host genetic control of PV is conserved across genetic backgrounds. The genetic correlation between isolates for WG was slightly higher using the G_B -matrix compared to the full G-matrix (Table 6), suggesting that pigs from the same genetic background have similar host genetic control of WG during infection with NVSL and KS06 and there are some differences in host genetic control of WG between genetic backgrounds.

The genetic correlation estimate for VL dropped substantially when the G_B -matrix is used, compared to the full G-matrix (Table 6); this suggests that while the genetic correlation between isolates for VL may be moderate within genetic backgrounds, some genetic backgrounds have high VL under infection with both NVSL and KS06 while some genetic backgrounds have low VL under infection with both NVSL and KS06, so when the relationships between genetic backgrounds are considered (using the full G-matrix), the genetic correlation between isolates for VL is high. This suggests that as a whole, selecting for improved VL during infection with one PRRSV isolate is likely to improve VL during infection with another PRRSV isolate, but the extent to which selection is successful across-isolate is likely to vary based on genetic background.

The estimate of genetic correlation between isolates for TP increased when the G_B -matrix was used rather than the full G-matrix (Table 6), such that the estimate from the G_B -matrix was no longer significantly different from one, but still not significantly different from zero, as with the estimate using the full G-matrix. Genetic correlation estimates between isolate for Tmax and

V_{max} remain not significantly different from zero or one when using the G_B-matrix compared to the full G-matrix (Table 6).

The G_B and G_P-matrices were also constructed without the 5Mb WUR region (G_{B-W} and G_{P-W}, respectively) and these results were as expected based on the differences between the full G-matrix and G_W-matrix, and also the G_B and G_P matrices compared to the full G-matrix (Tables 6 & 7).

DISCUSSION

Our results suggest that KS06 is a less virulent PRRSV isolate than NVSL, but, importantly, that genomic selection will be effective for selection for improved weight gain and reduced viral load under either PRRSV infection. This study affirms the important influence of alleles at the genetic marker WUR10000125 on host response to PRRSV. The effect of genotype at this locus was consistent between isolates for traits associated with serum viraemia, but a significant impact was only observed in NVSL for weight gain, suggesting that the influence of this marker on weight gain may be dependent on the virulence of the PRRSV isolate.

Modelling Viraemia using the Wood's Curve

Advantages

This study has demonstrated the utility of mathematical functions to assess the impact of host genetics and virus isolate on PRRS viraemia kinetics. The Wood's curve uses three parameters, a, b, and c, which are related to the magnitude of the values (a), and describe the shape of the curve (b, which is dominant pre-peak, and c, which is dominant post-peak) [14]. While other mathematical functions may more adequately model PRRS viraemia during infection, the number of data points collected during these trials limited the ability to fit more complex models. Fitting a Wood's curve is a more powerful method for comparing viraemia kinetics than the

Loess smoothed fit used in previous analyses of these data [5-7]. The Loess smoothed fit uses a parameter indicating the degree of polynomial to fit to the data and a smoothing parameter for curve fitting [27], with the primary intent of filtering out the noise from the data. The limitation, however, is that this method doesn't lend itself to extract fitted parameters that specify particular physical properties of a system, which have important implications in understanding the dynamics of PRRSV infection. Although both methods adequately fitted the data, Wood's curve parameters describe both the magnitude and shape of the curve, which can be used to explore different characteristics of the viraemia curves. Exploring Wood's curve characteristics can provide insight into important biological questions, such as which aspects of host response are under strongest genetic control, and how selection for one curve characteristic may affect others and thus the entire profile. It may also be used to explore the relationship between curve characteristics and other interesting phenotypes, such as WG under infection. Fitting a Wood's curve provided the necessary parameters to explore different aspects of the PRRS viraemia curves while not over-parameterizing the data. Furthermore, comparison of the extended Wood's and Wood's curve functions allowed for an objective method for separating primary infection from rebound infection viraemia curves (Islam et al. 2013).

Limitations

While the advantages of fitting a Wood's curve to model the dynamics of PRRS viraemia are clear, care needs to be taken in the interpretation of the correlations between curve characteristics because strong correlations between these curve characteristics are likely to arise partly as an artifact of the Wood's function and partly as they reflect true correlations between curve characteristics that are independent of the Wood's function. One example whereby the genetic correlation between traits is likely to be driven by the Wood's function is the high genetic

correlation observed between Tmax and Vmax, because they rely heavily on the b parameter of the Wood's function.

The Impact of PRRSV Genetic Diversity on Host Response to PRRSV Infection

Differences in Viraemia and Weight Gain during infection with NVSL and KS06

PRRSV glycoprotein 5 (GP5) is a major envelope protein, that plays a vital role in the virion's formation and infectivity, and harbors a major neutralizing epitope [28]. This gene is often used to assess genetic differences between PRRSV isolates and is suggestive of differences in virulence between isolates [29]. Variation in GP5 impacts the pig's ability to produce neutralizing antibodies, which may not be protective against different isolates [29,30]. NVSL and KS06 were isolated from different geographic regions nearly ten years apart, and are 89% similar at the GP5 nucleotide sequence level. Molecular phylogeny clustered these viruses into two distinct branches [12]. Forsberg et al. [31] found that, on average, PRRSV isolates have a substitution rate of 0.073 per nucleotide across isolates at ORF5, while the maximum substitution rate between two isolates was 0.153 substitutions per nucleotide; NVSL and KS06 have a substitution rate of 0.11 per nucleotide at the GP5 level [12].

This study has demonstrated that these virus isolates differ in both their virulence and in resulting viraemia profile characteristics. Infection with NVSL is characterized by reaching a high peak viraemia early, followed by a quick clearance of the virus, whereas the KS06 virus accumulates more slowly towards a lower peak viraemia and takes longer to clear from serum. Pig growth tended to be less stunted when pigs are infected with the KS06 isolate compared to the NVSL isolate (Table 3). This may be because piglets infected with the KS06 isolate do not need to put as much energy into eliminating the virus, thus allowing them to place more emphasis on growth. These results are consistent with the resource allocation theory, which

hypothesizes that trade-offs between competing traits (e.g. health and growth) are a consequence of limited resources (i.e. energy availability) [32]. The genetic correlations between viraemia and weight gain varied over time and tended to be more extreme in NVSL infected pigs than KS06 infected pigs, suggesting that more energy is required to fight infection with NVSL (Figure 4), and is supported by the lower weight gain observed in NVSL infected pigs (Figure 1).

Viral Rebound

Rebound (i.e. a bi-modal viraemia profile) was observed more frequently when pigs were infected with the NVSL isolate than with the KS06 isolate. One explanation for this is the presence of quasispecies within a host. PRRSV has a very high mutation rate, estimated at $4.7\text{--}9.8 \times 10^{-2}$ nucleotides/year which was the highest reported for an RNA virus in 2010 [33]. This high mutation rate causes within-animal variation in the PRRSV genome [34], with each variant termed a quasispecies. Pigs infected with NVSL have higher viraemia than pigs infected with KS06 throughout most of the pre-rebound phase (Figure 1). This increased level of viraemia means that more replications, and therefore mutations, have occurred, so there is likely a greater number of quasispecies present in animals infected with NVSL than KS06. The greater the number of quasispecies, the greater the chance that a variant is able to escape host immune response and cause viral rebound [35]. NVSL could also have a greater number of quasispecies if the mutation rate is higher in NVSL than KS06. Animals in the same pen could also transfer quasispecies between each other, whereby a quasispecies from one pig could be transferred to another pig and cause reinfection and viral rebound [34].

Alternately, NVSL may avoid the host immune response, possibly escaping humoral immune response by localizing to certain tissues. Previous research has identified that the tonsils are a primary source of viral persistence [36,37]. This may be due to an abundance of memory B-cells

in the tonsil, but the lack of effector, plasma-producing, B-cells [38]. An abundance of PRRSV in tonsils may result in a cyclical reappearance of circulating virus. If the ability of the virus to localize to tissue to escape immune response differs between isolates, this will be reflected in the tonsil viraemia levels. Studies are underway to address this possibility.

Impact of WUR10000125 on PRRS Disease Resistance

Consistent with previous reports, WUR was significantly associated with VL during PRRSV infection, whereby animals carrying a B allele had lower VL [5-7]. The effect of WUR on VL appears to be primarily driven by the pig's ability to control the level of virus replication, as made evident by the large effect the marker had on PV. This was the only curve characteristic that was significant for both NVSL and KS06 infected pigs (Figure 2), which is likely due to the role the putative gene plays in the host's immune response. The putative gene responsible for the observed WUR effect has been identified to be *GBP5*. *GBP5* showed allele specific expression based on WUR genotype, and animals that have the AA genotype do not produce functional *GBP5* [8]. *GBP5* plays a role in the innate immune response during infection. Specifically, NLRP3 interacts with tetrameric *GBP5* to promote inflammasome assembly with apoptosis-associated speck-like protein containing a caspase activation and recruitment domain protein [9]. While WUR genotype does appear to play a significant role in host response to PRRSV infection, there are a substantial polygenic effects on VL and PV. WUR genotype explained 13% of the total genetic variance for VL [5-7]. Consistent with this finding, accounting for WUR genotype did not account for all of the heritability, and the genetic correlation between isolates dropped, but still remained high and not significantly different from one (Table 7).

Interestingly, an effect of WUR genotype on WG was not found in pigs infected with KS06. The difference in VL between isolates was greater than the difference in VL between AA and AB

genotypes, therefore individuals infected with KS06 with the AA genotype had lower VL than individuals infected with NVSL with the AB genotype. This may mean a lower amount of energy is needed to fight the virus during infection with the KS06 isolate of PRRSV, and weight gain is not as affected, as evidenced by the higher weight gain during infection observed when pigs were infected with KS06. Thus, the effect of WUR on WG may only be present during infections with more virulent isolates of PRRSV due to the increased severity of infection. Isolate-specific QTL have been identified in a number of infection (fungal, bacterial, and viral) studies in plants [39-41] and in a study on Dengue Virus in mosquitoes [42].

It is likely that WUR affects the severity of infection, and its effect on WG is through the increased resources that have to be allocated to fighting the infection when viraemia is higher. The relationship between VL and reduction in WG is likely to be non-linear, which may explain why the direction of the WUR effect on WG is the same for both PRRSV isolates, but the magnitude of the effect differs. A high genetic correlation for WG between isolates was observed, despite the lack of a significant WUR effect for KS06 (Table 7). Given the number of genetic factors that can influence WG, it is likely that what is in common for WG between these two isolates are the polygenic effects, which would explain the high genetic correlation between isolates despite the lack of a QTL in the WUR region in the KS06 trials. The WUR region explained 9% of the total genetic variance for weight gain for the NVSL trials, while few other genomic regions explained greater than 1% of the total genetic variance [6].

Potential Avenues of Selection for Increased Resistance to PRRS

Potential for Selection on WUR Genotype

This study has shown that the WUR genotype has an effect on VL and PV (Figure 2A,D) across two distinct PRRSV isolates, indicating that selection for the B resistance allele may help with

reducing PRRS VL across isolates. Reducing viral burden has the potential to decrease the costs associated with PRRS through reducing PRRS incidence because a lower viral burden is associated with reduced virus shedding [43], which reduces the chance that PRRS will infect other pigs. Even though WUR did not have a significant effect on WG under infection with KS06, the direction of the effect was the same, therefore selection for the WUR B allele is likely to improve WG under infection with more virulent isolates of the virus, and is unlikely to have a negative effect on WG under less virulent isolates (Figure 2B).

Selecting for WUR has the potential to reduce VL and PV across breeds and isolates, however the extent to which it can do this is limited by it being a single locus. As the B allele approaches fixation, selection for the WUR B allele will not have much of an effect on decreasing the VL under PRRSV infection in that population. VL and PV have large polygenic effects that are conserved across isolates and breeds and independent of WUR (Table 6 & 7), therefore genomic selection for VL or PV in combination with marker assisted selection on WUR may hold the highest potential for improved resistance to PRRS.

Potential for Genomic Selection

Genomic selection uses markers spaced throughout the whole genome to predict the genetic merit of an individual. All traits had a moderate-to-high heritable genetic component (Table 3), suggesting that genomic selection for different aspects of host response to PRRSV infection is feasible. There are high genetic correlations between VL, WG and PV in both isolates, except for PV and WG in KS06 (Tables 4 & 5), suggesting that genomic selection for one trait is likely to improve response in the other two. There are also high genetic correlations between isolates for VL, WG and PV (Table 6), suggesting that genomic selection for response under one isolate is likely to result in improvement across isolates.

A limitation of genomic selection is the size of the data that will need to be generated on a continual basis in order to ensure the accurate prediction of breeding values. Genomic predictions tend to be more accurate the more animals are in the training set. It has been shown that the greater the number of generations between the training and prediction sets, the lower the prediction accuracy [44], so periodic re-training on new phenotypes and genotypes will be necessary.

Potential for Selection on Response to Vaccination

While genomic selection for response to PRRSV sounds appealing, one issue is that in order to get accurate predictions, you need quality infection data on many animals. Information on naturally infected commercial pigs can feed back into the nucleus in order to make selection decisions based on the commercial pigs' response. However there are several factors that cannot be controlled in a natural infection setting such as virus dosage, time since infection, and the age and weight of the pig at infection, with all of these having an effect on how the pig responds to infection.

A major current PRRS vaccine is a modified live virus which has reduced virulence compared to commonly occurring wild type isolates [45], so vaccinated pigs will have circulating viraemia which can be measured as with infection with any natural PRRSV isolate. Measuring response to vaccination overcomes the limitations of natural infections because it is a controlled infection. Before this can be implemented in industry, it is necessary to evaluate the genetic correlation between response to vaccination and response to natural infection with a variety of isolates.

Response to vaccination could be evaluated using PV, which has the benefit of needing only a single serum sample, rather than multiple samples throughout the course of infection as is needed for VL. Host genetic response to PV is expected to be highly conserved between isolates, both

within-breed and across the North American pig population (Table 6), and is highly correlated with VL under infection with both NVSL and KS06 (Tables 4 & 5). To be most effective, the timing of PV and correlation between PV and VL after vaccination will need to be evaluated.

Conclusions

Despite pronounced differences in viraemia profiles between NVSL and KS06, the underlying genetic factors influencing host response to infection are largely the same for VL, PV, and WG across these two PRRSV isolates. NVSL and KS06 are diverse isolates, therefore these results suggest that genomic selection for VL, PV, or WG during infection with one isolate would improve these traits when infected with another virus isolate. The WUR SNP, previously identified to be associated with VL and WG under infection with NVSL, was also found to be associated with all curve characteristics in NVSL trials; but only with VL and PV in KS06 trials, suggesting the effect of WUR may depend on the virulence of the PRRSV isolate. Infection trials involving more isolates of PRRSV are necessary to confirm that genetic factors influencing host response to PRRSV infection are consistent under infection with a range of PRRSV isolates. Analysis of the relationship between viraemia and weight gain via genome-wide association studies over the course of infection will allow for a more comprehensive understanding of the host genes and genomic regions associated with response to PRRSV infection. Studies currently underway as part of the PHGC include field trials, infection with a third PRRSV isolate, response to vaccination and coinfection with PRRSV and PCV2b.

TABLES AND FIGURES

Table 1. Animal Composition of the PHGC Trials

PRRS Virus Isolate	Trial Number	Number of Animals	Breed Cross ¹	Genetic Background ²
NVSL-97-7895	1-3	507	LW x LR	A
	4	191	Duroc x LW/LR	B
	5	182	Duroc x LR/LW	C
	6	109	LR x LR	D
	7	186	Pietran x LW/LR	E
	8	158	Duroc x LW/LR	F
	15	166	Pietran x LW	G
KS-2006-72109	10	184	Pietran x LW	G
	11	177	LW x LR	A
	12	146	LR x LW	H
	13 ³	173	Duroc x LW/LR	F
	14	165	Duroc x LR/LW	C

1. LW = Large White; LR = Landrace
2. Genetic background is defined as pigs from the same breeding company and the same breed cross.
3. Trial 13 was excluded from analyses due to unusual viraemia profiles as seen in Figure S1.

Table 2. Comparison of Boddicker Viral Load and Wood's Curve 0-21 dpi Viral Load using the Numerator Relationship matrix (A-matrix)

VL _B vs VL ¹	h ²	r _g	r _p
NVSL VL _B	0.23 (0.10)	0.98 (0.03)	0.90 (0.01)
NVSL VL	0.22 (0.10)		
KS06 VL _B	0.35 (0.09)	0.98 (0.02)	0.90 (0.01)
KS06 VL	0.35 (0.09)		

- 1.) All trials except trial 13 were used in the analysis. NVSL and KS06 were analyzed separately.

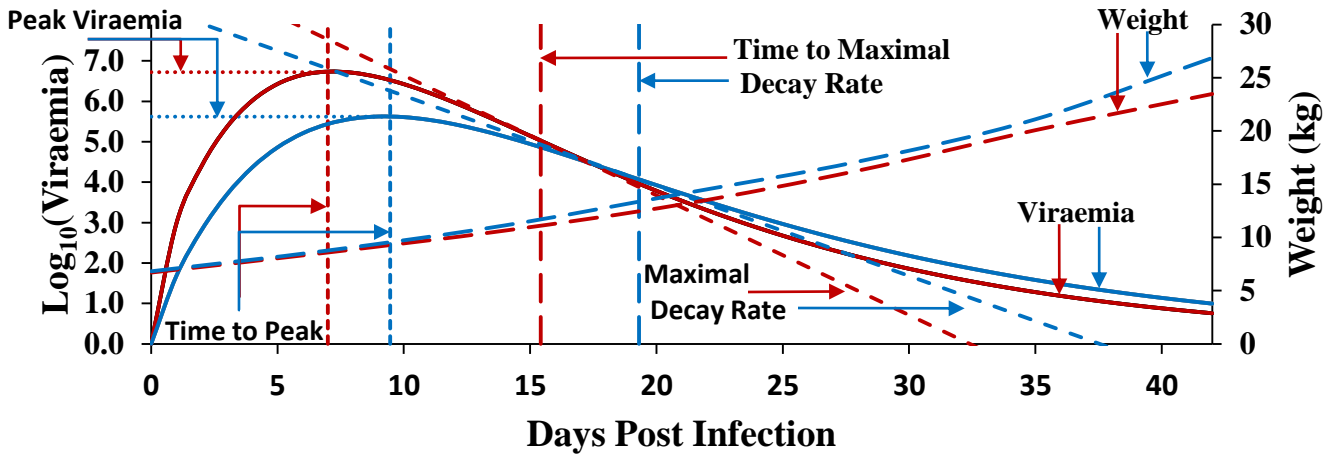


Figure 1. Comparison of Response to Selection when Pigs are infected with NVSL (red) or KS06 (blue) PRRSV isolates. For comparison between viruses, trials were matched based on genetic background. Least Square Means of daily viraemia, predicted using the monophasic Wood's curve parameters, and weights were estimated using ASReml with the full G-matrix. Viraemia, Weight, Time to Peak, Peak Viraemia, Time to Maximal Decay, and Maximal Decay were compared when pigs were infected with either NVSL or KS06 PRRSV isolate.

Table 3. Least Square Means, Heritabilities, Litter Effects, and Phenotypic Standard Deviations of Responses to Infection.

Trait (Units)	LSMeans ^{1,2}		P-value	Heritability ^{2,3}		Litter ^{2,3}		Phen. s.d. ^{2,3}	
	NVSL (s.e.)	KS06 (s.e.)		NVSL (s.e.)	KS06 (s.e.)	NVSL (s.e.)	KS06 (s.e.)	NVSL	KS06
WG (kg)	15.8 (1.1)	19.5 (1.4)	0.076	0.33 (0.06)	0.31 (0.09)	0.07 (0.03)	0.03 (0.04)	3.90	3.91
VL (Viraemia *Days)	110.5 (1.4)	95.0 (1.6)	<0.001	0.31 (0.06)	0.51 (0.09)	0.24 (0.03)	0.01 (0.04)	7.90	7.46
TP (Days)	7.0 (0.4)	9.5 (0.4)	0.004	0.22 (0.05)	0.20 (0.09)	0.16 (0.03)	0.10 (0.05)	1.36	1.54
PV (Viraemia)	6.6 (0.1)	5.8 (0.1)	<0.001	0.17 (0.05)	0.45 (0.08)	0.27 (0.04)	0.00 (0.00)	0.40	0.41
Tmax (Days)	15.4 (0.5)	19.3 (0.6)	0.002	0.21 (0.05)	0.16 (0.09)	0.15 (0.03)	0.14 (0.05)	2.38	2.73
Vmax (Viraemia /Day)	0.30 (0.02)	0.22 (0.02)	0.033	0.09 (0.05)	0.26 (0.09)	0.08 (0.03)	0.01 (0.04)	0.08	0.05

1.) Full G-matrix used

2.) Estimates were obtained by fitting isolate into the model, and only included trials paired with NVSL and KS06

3.) Estimates were obtained by using the full G-matrix. NVSL and KS06 estimates were estimated separately, and included all animals infected with that isolate, except trial 13.

Table 4. Correlations of Response to infection with PRRSV Isolate NVSL using the Full G-matrix

Trait ¹	VL	WG	TP	PV	Tmax	Vmax
VL		-0.33 (0.03)	0.10 (0.03)	0.66 (0.02)	0.36 (0.03)	-0.27 (0.03)
WG	-0.74 (0.10)		-0.02 (0.03)	-0.22 (0.03)	-0.16 (0.03)	0.12 (0.03)
TP	0.31 (0.15)	0.27 (0.16)		-0.09 (0.03)	0.72 (0.01)	0.12 (0.03)
PV	0.85 (0.07)	-0.73 (0.13)	0.05 (0.19)		-0.23 (0.03)	0.40 (0.03)
Tmax	0.81 (0.10)	-0.11 (0.16)	0.83 (0.07)	0.50 (0.21)		-0.51 (0.02)
Vmax	-0.72 (0.21)	0.45 (0.22)	-0.11 (0.26)	-0.27 (0.33)	-0.57 (0.19)	

¹Phenotypic correlations (above diagonal), Genetic correlations (below diagonal) were estimated using an Animal model in ASReml.

Table 5. Correlations of Response to infection with PRRSV Isolate KS06 using the Full G-matrix

Trait ¹	VL	WG	TP	PV	Tmax	Vmax
VL		-0.23 (0.05)	-0.06 (0.05)	0.76 (0.02)	0.13 (0.05)	-0.16 (0.05)
WG	-0.52 (0.17)		-0.05 (0.05)	-0.13 (0.05)	-0.06 (0.06)	0.13 (0.05)
TP	-0.08 (0.22)	-0.10 (0.24)		0.02 (0.05)	0.80 (0.02)	0.02 (0.05)
PV	0.91 (0.05)	-0.30 (0.18)	-0.08 (0.25)		-0.19 (0.05)	0.52 (0.04)
Tmax	0.19 (0.23)	-0.42 (0.23)	0.69 (0.19)	-0.24 (0.28)		-0.52 (0.04)
Vmax	-0.01 (0.20)	0.42 (0.21)	-0.12 (0.28)	0.51 (0.13)	-0.75 (0.18)	

¹Phenotypic correlations (above diagonal), Genetic correlations (below diagonal) and heritabilities (along diagonal) were estimated using an Animal model in ASReml.

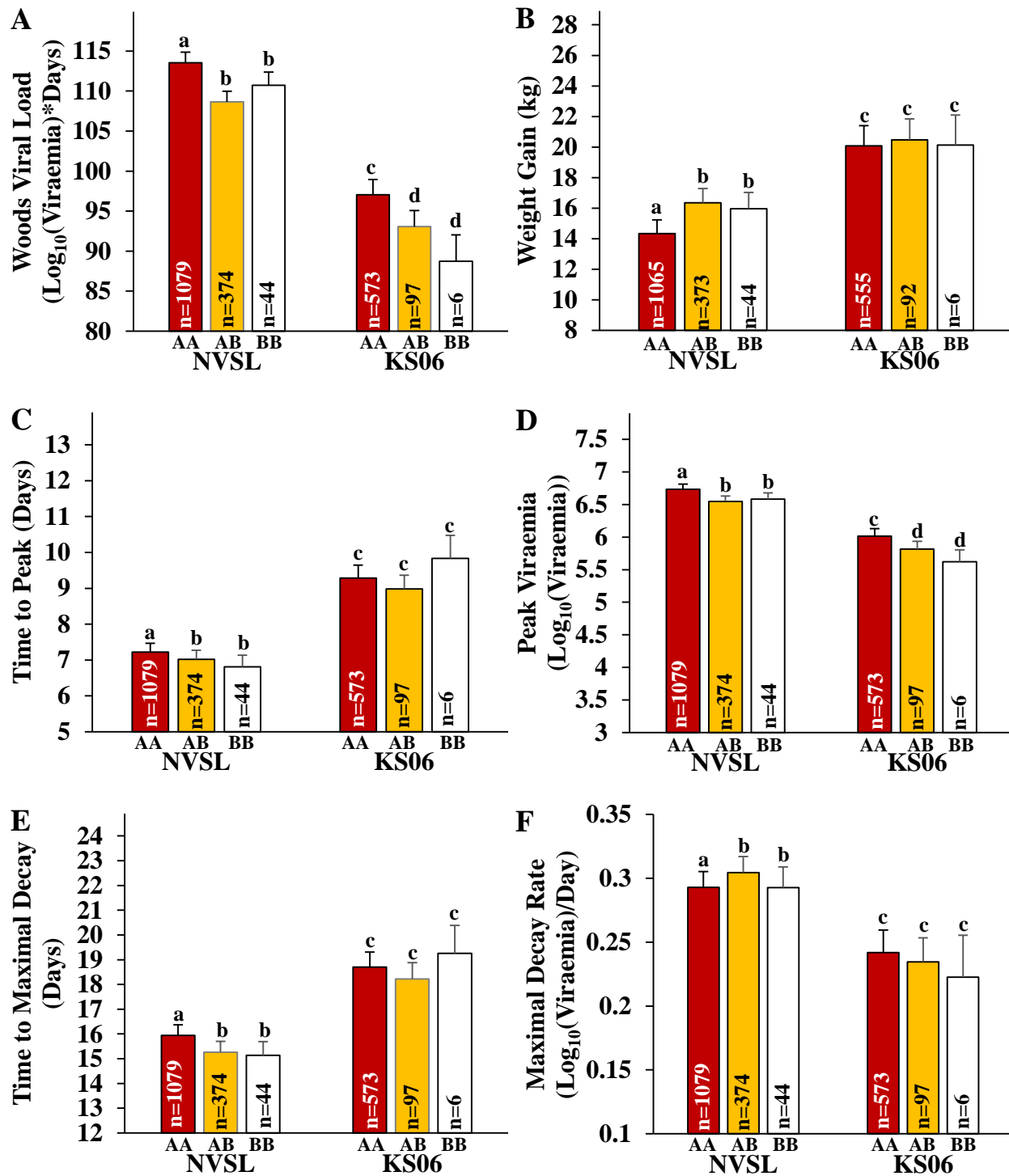


Figure 2. Least Square Means of WUR genotype effects in pigs infected with either the NVSL or KS06 PRRSV isolate. Least Square Means of the WUR genotype for VL (A), WG42 (B), TP (C), PV (D), Tmax (E), and Vmax (F) when fitting the Isolate*WUR interaction into the Animal model in ASReml using the full G-matrix. All trials, except trial 13, were used for the analysis. Estimates with different letter assignments are significantly different ($P \leq 0.05$).

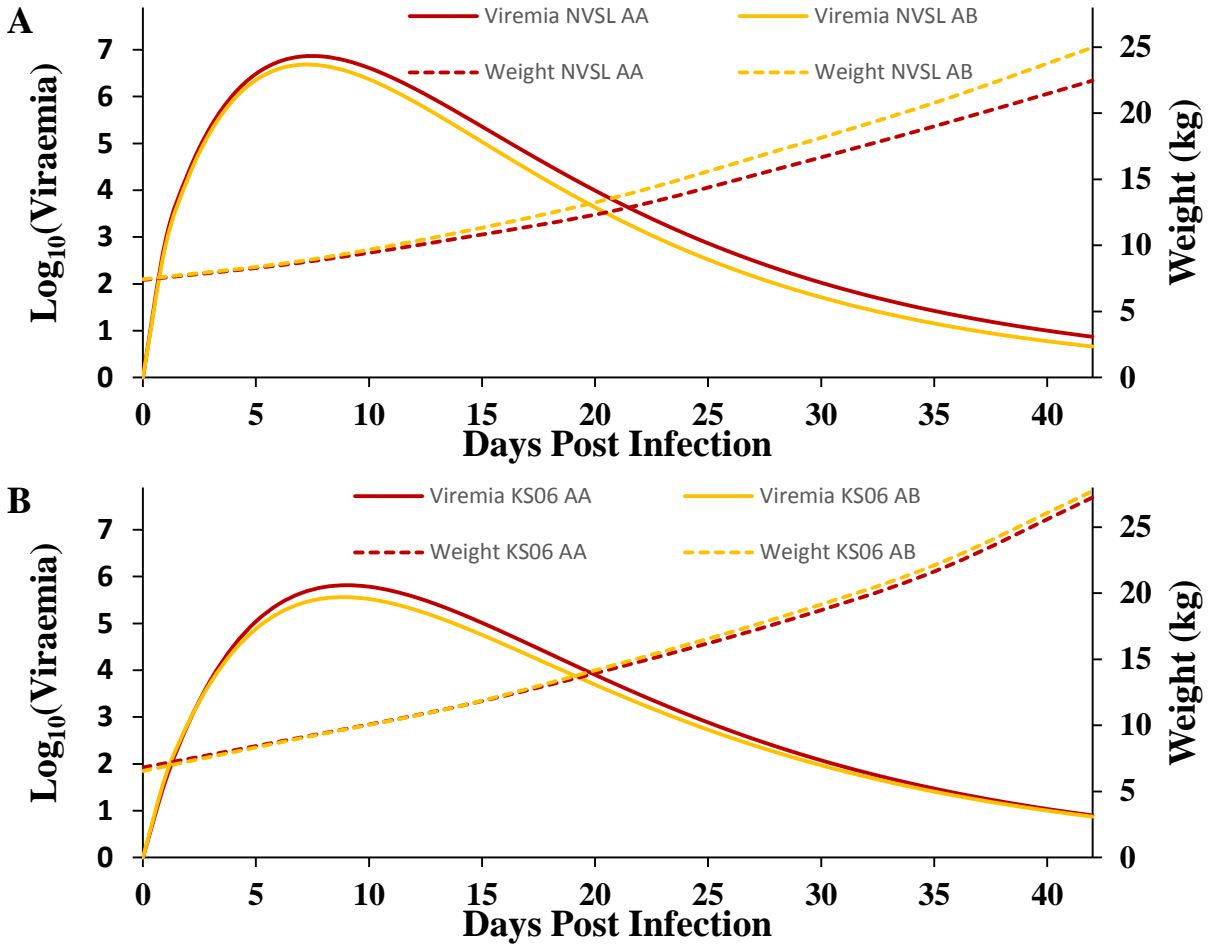


Figure 3. Least Square Means of WUR genotype effects of predicted viraemia and weight in pigs infected with either the NVSL or KS06 PRRSV isolate. Least Square Means of the WUR genotype for predicted viraemia and weight for NVSL (A) and KS06 (B) when fitting the Isolate*WUR interaction into the Animal model in ASReml using the full G-matrix. All trials, except trial 13, were used for the analysis.

Table 6. Genetic Correlations of Response to infection between PRRSV Isolates

Trait	Full (G)			Block Diagonal (G _B)			Paired Block Diagonal (G _P)		
	Heritability		Genetic Corr.	Heritability		Genetic Corr.	Heritability		Genetic Corr.
	NVSL	KS06		NVSL	KS06		NVSL	KS06	
VL	0.32 (0.06)	0.53 (0.07)	0.86 (0.19)	0.40 (0.06)	0.53 (0.08)	0.51 (0.24)	0.51 (0.08)	0.54 (0.09)	0.57 (0.22)
WG	0.33 (0.05)	0.30 (0.09)	0.86 (0.27)	0.37 (0.06)	0.32 (0.10)	0.96 (0.34)	0.41 (0.08)	0.38 (0.11)	0.90 (0.31)
TP	0.22 (0.05)	0.21 (0.09)	0.25 (0.33)	0.28 (0.06)	0.28 (0.10)	0.40 (0.36)	0.32 (0.08)	0.30 (0.12)	0.43 (0.36)
PV	0.17 (0.05)	0.46 (0.07)	0.94 (0.28)	0.23 (0.06)	0.43 (0.08)	0.94 (0.33)	0.29 (0.07)	0.42 (0.09)	0.91 (0.30)
Tmax	0.21 (0.05)	0.14 (0.09)	0.82 (0.53)	0.26 (0.06)	0.16 (0.10)	0.86 (0.59)	NE	NE	NE
Vmax	0.10 (0.05)	0.25 (0.09)	0.63 (0.51)	0.13 (0.05)	0.22 (0.10)	0.32 (0.67)	0.06 (0.06)	0.23 (0.12)	0.41 (0.92)

Table 7. Genetic Correlations of Response to infection between PRRSV Isolates when Excluding the 5 Mb WUR Region from the G Matrix

Trait	Full (G _w)			Block Diagonal (G _{B-w})			Paired Block Diagonal (G _{P-w})		
	Heritability		Genetic Corr.	Heritability		Genetic Corr.	Heritability		Genetic Corr.
	NVSL	KS06		NVSL	KS06		NVSL	KS06	
VL	0.25 (0.06)	0.49 (0.09)	0.76 (0.22)	0.34 (0.06)	0.49 (0.08)	0.44 (0.26)	0.45 (0.08)	0.49 (0.09)	0.51 (0.24)
WG	0.28 (0.06)	0.30 (0.09)	0.89 (0.29)	0.33 (0.06)	0.31 (0.07)	0.93 (0.35)	0.36 (0.08)	0.38 (0.11)	0.90 (0.32)
TP	0.21 (0.05)	0.20 (0.09)	0.18 (0.34)	0.27 (0.06)	0.28 (0.10)	0.36 (0.37)	0.31 (0.08)	0.29 (0.12)	0.37 (0.37)
PV	0.13 (0.05)	0.40 (0.08)	0.79 (0.34)	0.22 (0.06)	0.39 (0.08)	0.81 (0.37)	0.51 (0.10)	0.55 (0.36)	0.77 (0.36)
Tmax	0.19 (0.05)	0.14 (0.09)	0.80 (0.54)	0.24 (0.06)	0.16 (0.10)	0.90 (0.62)	NE	NE	NE

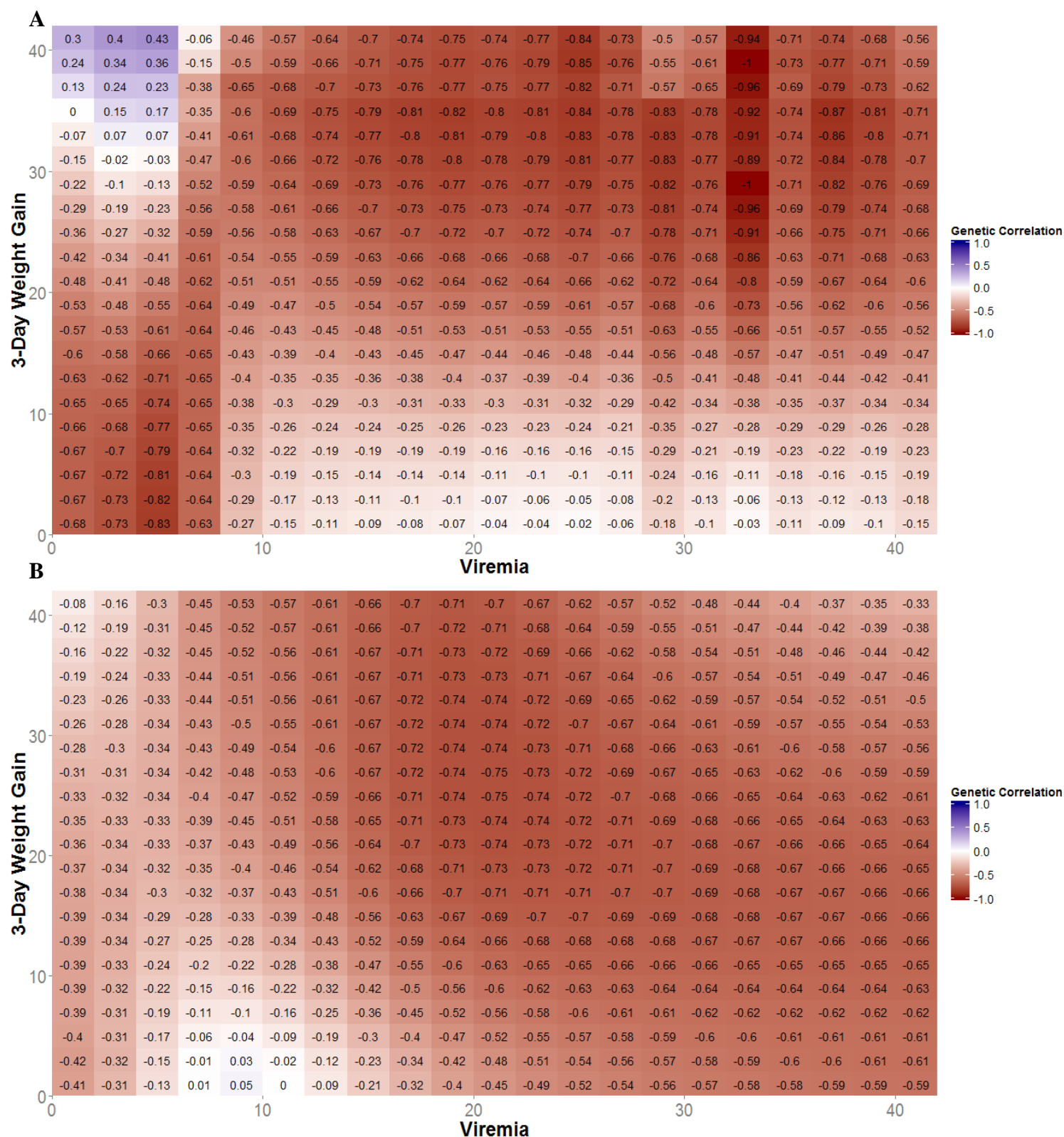
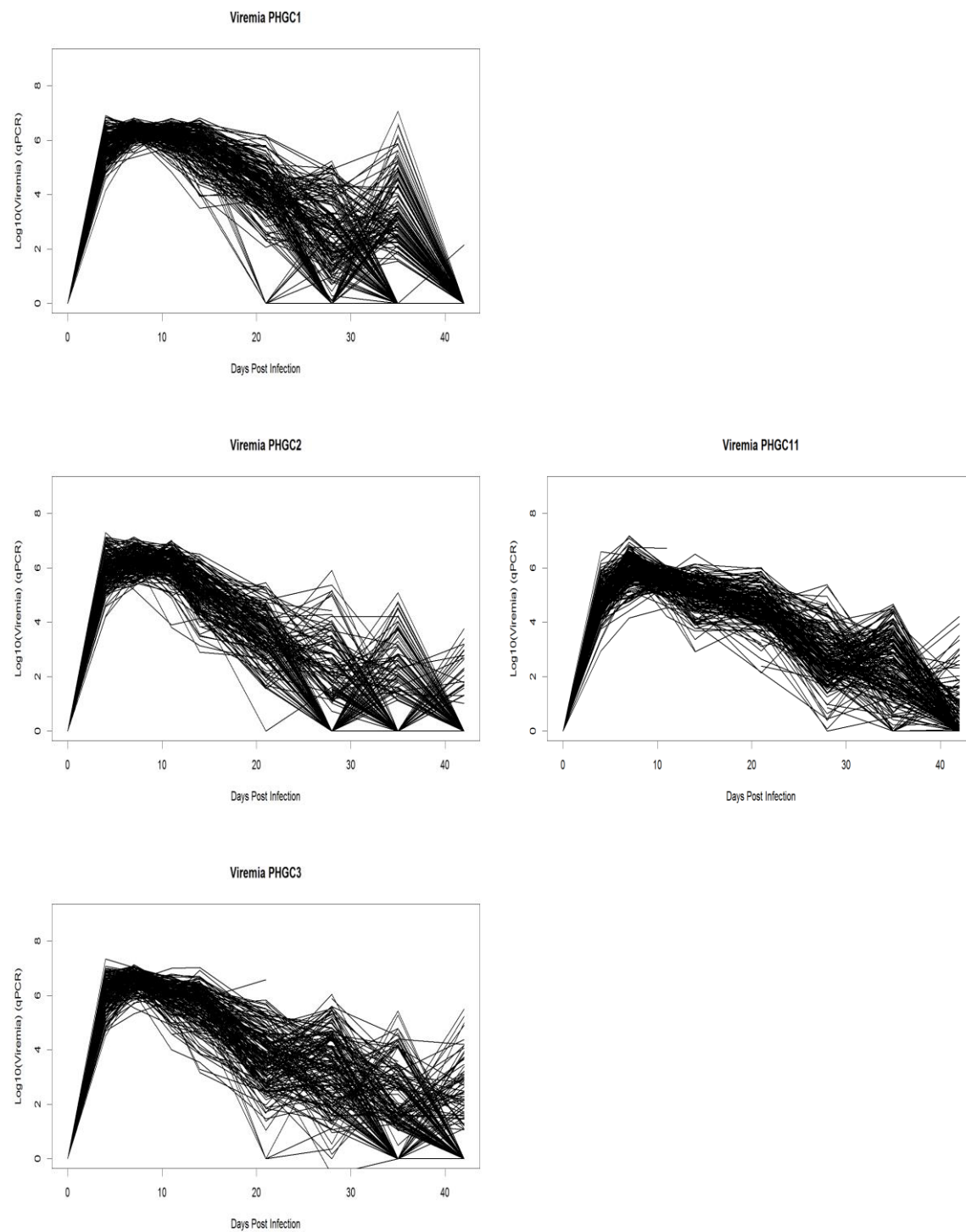
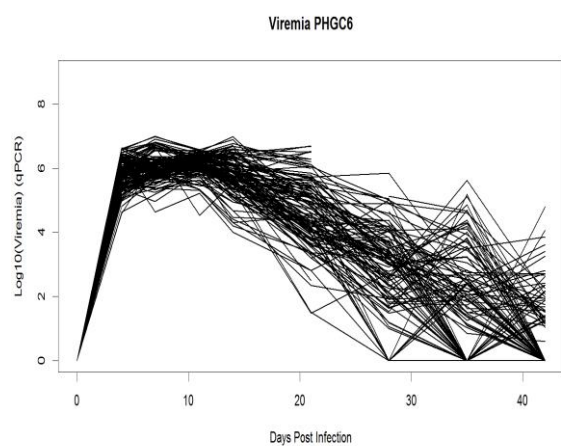
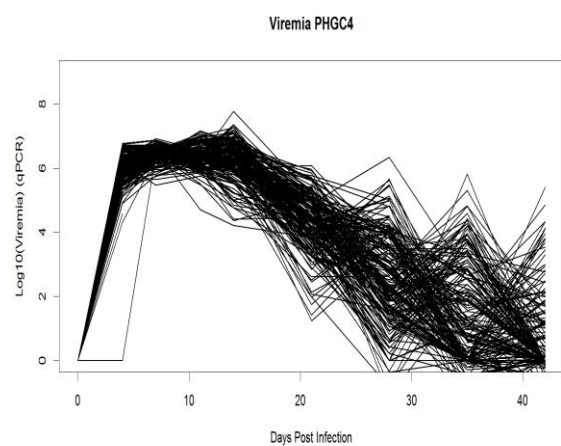
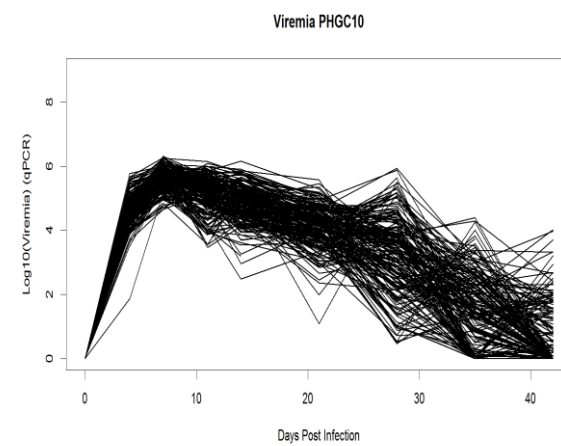
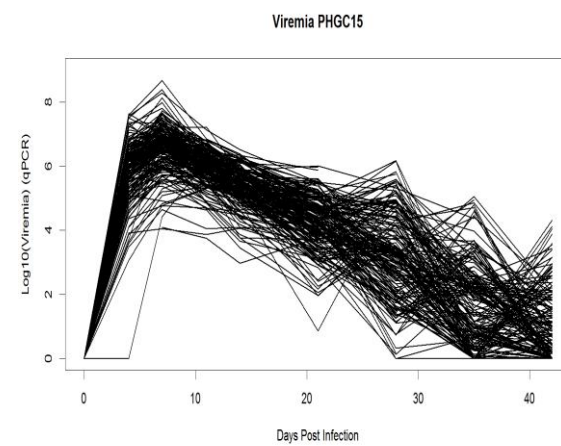
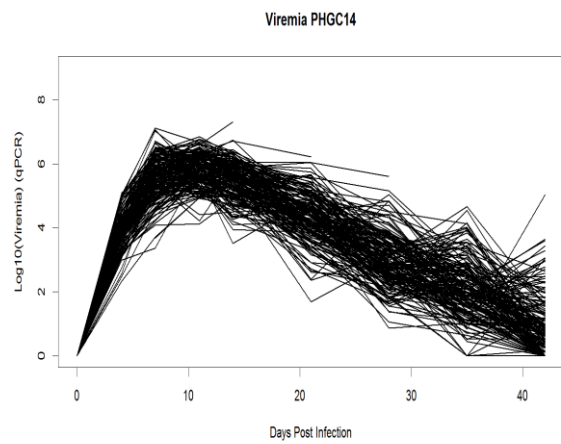
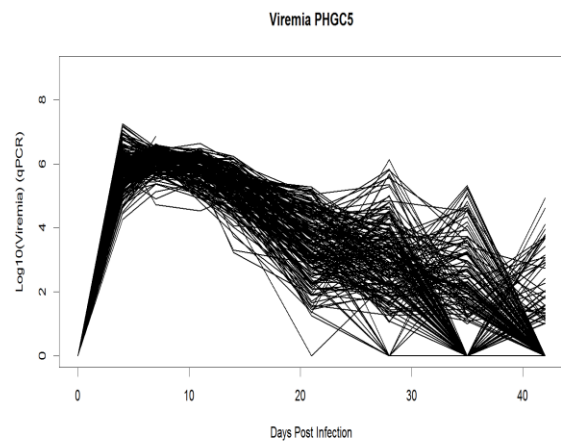
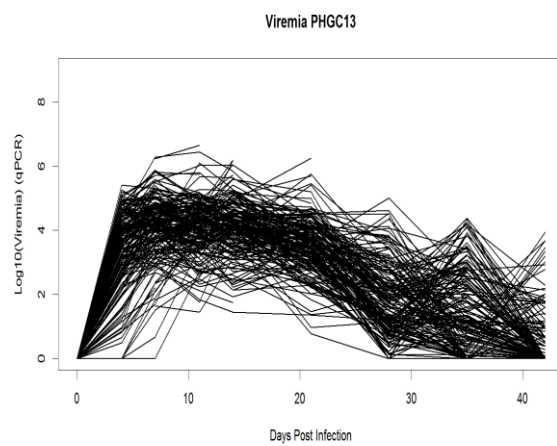
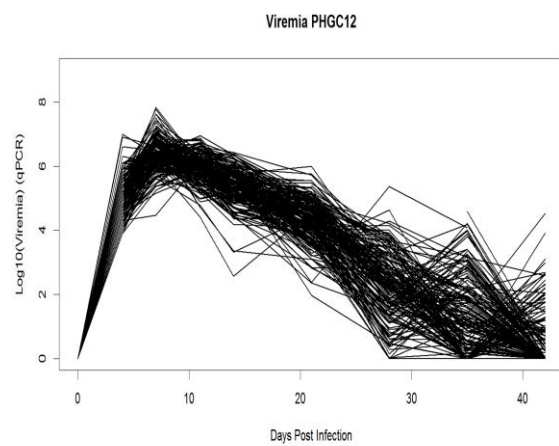
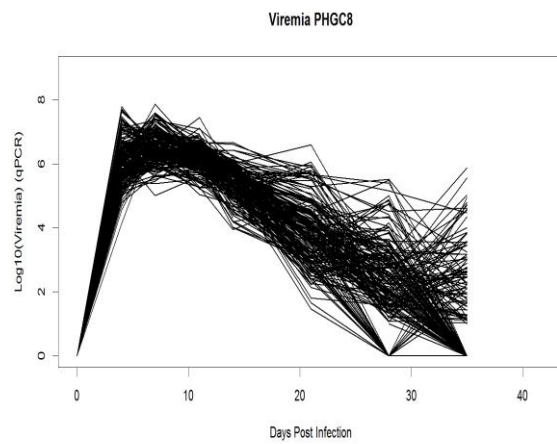
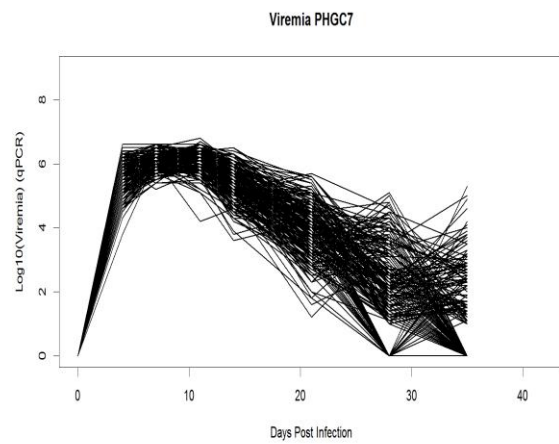


Figure 4. Time course genetic correlation between viraemia and weight gain in pigs infected with either the (A) NVSL or (B) KS06 PRRSV isolate. Genetic correlations from fitting a bivariate animal model in ASReml using the full G-matrix. NVSL and KS06 were analyzed separately. All trials, except trial 13, were used in the analysis

Figure S1. Raw Viraemia Curves for all Trials







LITERATURE CITED

1. Holtkamp DJ, Kliebenstein JB, Neumann EJ, Zimmerman JJ, Rotto HF, et al. (2013) Assessment of the economic impact of porcine reproductive and respiratory syndrome virus on United States pork producers. *Journal of Swine Health and Production* 21: 72-84.
2. Darwich L, Díaz I, Mateu E (2010) Certainties, doubts and hypotheses in porcine reproductive and respiratory syndrome virus immunobiology. *Virus Research* 154: 123-132.
3. Lewis CRG, Ait-Ali T, Clapperton M, Archibald AL, Bishop SC (2007) Genetic perspectives on host responses to porcine reproductive and respiratory syndrome (PRRS). *Viral Immunology* 20: 343-357.
4. Lunney JK, Steibel JP, Reecy JM, Fritz E, Rothschild MF, et al. (2011) Probing genetic control of swine responses to PRRSV infection: current progress of the PRRS host genetics consortium. *BMC proceedings* 5 Suppl 4: S30-S30.
5. Boddicker N, Waide EH, Rowland RRR, Lunney JK, Garrick DJ, et al. (2012) Evidence for a major QTL associated with host response to Porcine Reproductive and Respiratory Syndrome Virus challenge. *Journal of Animal Science* 90: 1733-1746.
6. Boddicker NJ, Bjorkquist A, Rowland RRR, Lunney JK, Reecy JM, et al. (2014) Genome-wide association and genomic prediction for host response to porcine reproductive and respiratory syndrome virus infection. *Genetics Selection Evolution* 46.
7. Boddicker NJ, Garrick DJ, Rowland RRR, Lunney JK, Reecy JM, et al. (2014) Validation and further characterization of a major quantitative trait locus associated with host response to experimental infection with porcine reproductive and respiratory syndrome virus. *Animal Genetics* 45: 48-58.
8. Koltes JE, Fritz-Waters E, Eisley CJ, Choi IS, Bao H, et al. (2015) Identification of a putative quantitative trait nucleotide in guanylate binding protein 5 for host response to PRRS virus infection. *BMC Genomics* 16: (28 May 2015)-(2028 May 2015).
9. Shenoy AR, Wellington DA, Kumar P, Kassa H, Booth CJ, et al. (2012) GBP5 Promotes NLRP3 Inflammasome Assembly and Immunity in Mammals. *Science* 336: 481-485.
10. Islam ZU, Bishop SC, Savill NJ, Rowland RRR, Lunney JK, et al. (2013) Quantitative Analysis of Porcine Reproductive and Respiratory Syndrome (PRRS) Viraemia Profiles from Experimental Infection: A Statistical Modelling Approach. *Plos One* 8.
11. Truong HM, Lu Z, Kutish GF, Galeota J, Osorio FA, et al. (2004) A highly pathogenic porcine reproductive and respiratory syndrome virus generated from an infectious cDNA clone retains the in vivo virulence and transmissibility properties of the parental virus. *Virology* 325: 308-319.
12. Ladinig A, Detmer SE, Clarke K, Ashley C, Rowland RRR, et al. (2015) Pathogenicity of three type 2 porcine reproductive and respiratory syndrome virus strains in experimentally inoculated pregnant gilts. *Virus Research* 203: 24-35.
13. Geldhof MF, Van Breedam W, De Jong E, Rodriguez AL, Karniychuk UU, et al. (2013) Antibody response and maternal immunity upon boosting PRRSV-immune sows with experimental farm-specific and commercial PRRSV vaccines. *Veterinary Microbiology* 167: 260-271.
14. Wood PDP (1967) ALGEBRAIC MODEL OF LACTATION CURVE IN CATTLE. *Nature* 216: 164-&.
15. Boujenane I, Hilal B (2012) Genetic and non genetic effects for lactation curve traits in Holstein-Friesian cows. *Archiv Fur Tierzucht-Archives of Animal Breeding* 55: 450-457.
16. Maiwashe A, Nengovhela NB, Nephawe KA, Sebei J, Netshilema T, et al. (2013) Estimates of lactation curve parameters for Bonsmara and Nguni cattle using the weigh-suckle-weigh technique. *South African Journal of Animal Science* 43: S12-S16.
17. Gilmour AR, Gogel B, Cullis B, Thompson R (2009) ASReml user guide release 3.0. VSN International Ltd, Hemel Hempstead, UK.

18. Marshall TC, Slate J, Kruuk LEB, Pemberton JM (1998) Statistical confidence for likelihood-based paternity inference in natural populations. *Molecular Ecology* 7: 639-655.
19. Beyer J, Fichtner D, Schirrmeier H, Polster U, Weiland E, et al. (2000) Porcine reproductive and respiratory syndrome virus (PRRSV): Kinetics of infection in lymphatic organs and lung. *Journal of Veterinary Medicine Series B-Infectious Diseases and Veterinary Public Health* 47: 9-25.
20. VanRaden PM (2008) Efficient Methods to Compute Genomic Predictions. *Journal of Dairy Science* 91: 4414-4423.
21. Hayes BJ, Bowman PJ, Chamberlain AC, Verbyla K, Goddard ME (2009) Accuracy of genomic breeding values in multi-breed dairy cattle populations. *Genetics Selection Evolution* 41.
22. Thanawongnuwech R, Thacker EL, Halbur PG (1998) Influence of pig age on virus titer and bactericidal activity of porcine reproductive and respiratory syndrome virus (PRRSV)-infected pulmonary intravascular macrophages (PIMs). *Veterinary Microbiology* 63: 177-187.
23. Klinge KL, Vaughn EM, Roof MB, Bautista EM, Murtaugh MP (2009) Age-dependent resistance to Porcine reproductive and respiratory syndrome virus replication in swine. *Virology Journal* 6.
24. Xiao S, Jia J, Mo D, Wang Q, Qin L, et al. (2010) Understanding PRRSV Infection in Porcine Lung Based on Genome-Wide Transcriptome Response Identified by Deep Sequencing. *Plos One* 5.
25. Exton MS (1997) Infection-induced anorexia: Active host defence strategy. *Appetite* 29: 369-383.
26. Lopez OJ, Osorio FA (2004) Role of neutralizing antibodies in PRRSV protective immunity. *Veterinary Immunology and Immunopathology* 102: 155-163.
27. Jacoby WG (2000) Loess: a nonparametric, graphical tool for depicting relationships between variables. *Electoral Studies* 19: 577-613.
28. Ostrowski M, Galeota JA, Jar AM, Platt KB, Osorio FA, et al. (2002) Identification of neutralizing and nonneutralizing epitopes in the porcine reproductive and respiratory syndrome virus GP5 ectodomain. *Journal of Virology* 76: 4241-4250.
29. Ansari IH, Kwon B, Osorio FA, Pattnaik AK (2006) Influence of N-linked glycosylation of porcine reproductive and respiratory syndrome virus GP5 on virus infectivity, antigenicity, and ability to induce neutralizing antibodies. *Journal of Virology* 80: 3994-4004.
30. Pirzadeh B, Gagnon CA, Dea S (1998) Genomic and antigenic variations of porcine reproductive and respiratory syndrome virus major envelope GP(5) glycoprotein. *Canadian Journal of Veterinary Research-Revue Canadienne De Recherche Veterinaire* 62: 170-177.
31. Forsberg R, Storgaard T, Nielsen HS, Oleksiewicz MB, Cordioli P, et al. (2002) The genetic diversity of European type PRRSV is similar to that of the North American type but is geographically skewed within Europe. *Virology* 299: 38-47.
32. Rauw WM (2008) Resource allocation theory applied to farm animal production. *Resource allocation theory applied to farm animal production*: 320 pp.-320 pp.
33. Murtaugh MP, Stadejek T, Abrahante JE, Lam TTY, Leung FCC (2010) The ever-expanding diversity of porcine reproductive and respiratory syndrome virus. *Virus Research* 154: 18-30.
34. Goldberg TL, Lowe JF, Milburn SM, Firkins LD (2003) Quasispecies variation of porcine reproductive and respiratory syndrome virus during natural infection. *Virology* 317: 197-207.
35. Costers S, Lefebvre DJ, Van Doorselaere J, Vanhee M, Delputte PL, et al. (2010) GP4 of porcine reproductive and respiratory syndrome virus contains a neutralizing epitope that is susceptible to immunoselection in vitro. *Archives of Virology* 155: 371-378.
36. Wills RW, Zimmerman JJ, Yoon KJ, McGinley MJ, Hill HT, et al. (1997) Porcine reproductive and respiratory syndrome virus: A persistent infection. *Veterinary Microbiology* 55: 231-240.
37. Wills RW, Doster AR, Galeota JA, Sur JH, Osorio FA (2003) Duration of infection and proportion of pigs persistently infected with porcine reproductive and respiratory syndrome virus. *Journal of Clinical Microbiology* 41: 58-62.

38. Mulupuri P, Zimmerman JJ, Hermann J, Johnson CR, Cano JP, et al. (2008) Antigen-specific B-cell responses to porcine reproductive and respiratory-syndrome-virus infection. *Journal of Virology* 82: 358-370.
39. Leonardsschippers C, Gieffers W, Schaferpregl R, Ritter E, Knapp SJ, et al. (1994) QUANTITATIVE RESISTANCE TO PHYTOPHTHORA-INFESTANS IN POTATO - A CASE-STUDY FOR QTL MAPPING IN AN ALLOGAMOUS PLANT-SPECIES. *Genetics* 137: 67-77.
40. Liu QS, Yuan M, Zhou Y, Li XH, Xiao JH, et al. (2011) A paralog of the MtN3/saliva family recessively confers race-specific resistance to *Xanthomonas oryzae* in rice. *Plant Cell and Environment* 34: 1958-1969.
41. Caranta C, Lefebvre V, Palloix A (1997) Polygenic resistance of pepper to potyviruses consists of a combination of isolate-specific and broad-spectrum quantitative trait loci. *Molecular Plant-Microbe Interactions* 10: 872-878.
42. Fansiri T, Fontaine A, Diancourt L, Caro V, Thaisomboonsuk B, et al. (2013) Genetic Mapping of Specific Interactions between *Aedes aegypti* Mosquitoes and Dengue Viruses. *Plos Genetics* 9.
43. Alberti KA, Estienne MJ, Meng XJ (2011) Effect of vaccination of boars against porcine circovirus type 2 on ejaculate characteristics, serum antibody titers, viraemia, and semen virus shedding. *Journal of Animal Science* 89: 1581-1587.
44. Wolc A, Arango J, Settar P, Fulton JE, O'Sullivan NP, et al. (2011) Persistence of accuracy of genomic estimated breeding values over generations in layer chickens. *Genetics Selection Evolution* 43.
45. Cano JP, Dee SA, Murtaugh MP, Trincado CA, Pijoan CB (2007) Effect of vaccination with a modified-live porcine reproductive and respiratory syndrome virus vaccine on dynamics of homologous viral infection in pigs. *American Journal of Veterinary Research* 68: 565-571.